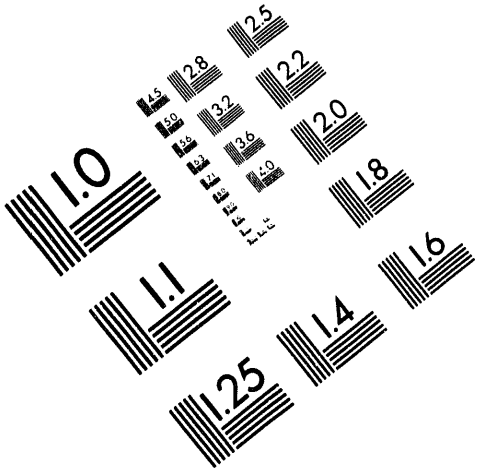

Association for Information and Image Management

1100 Wayne Avenue, Suite 1100
Silver Spring, Maryland 20910

301/587-8202

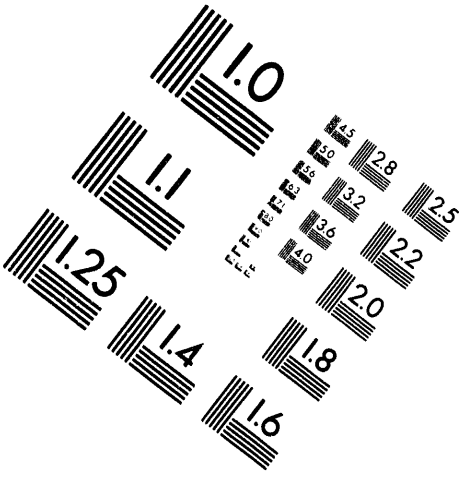

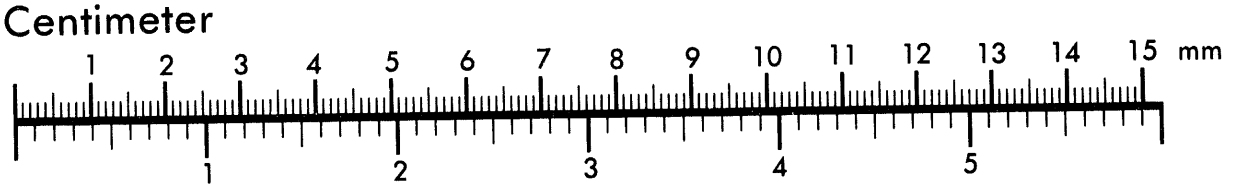

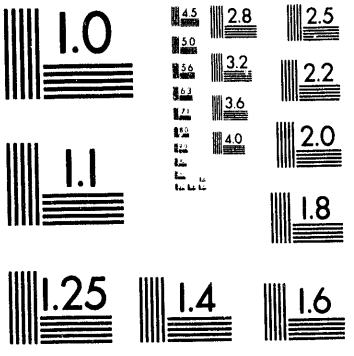

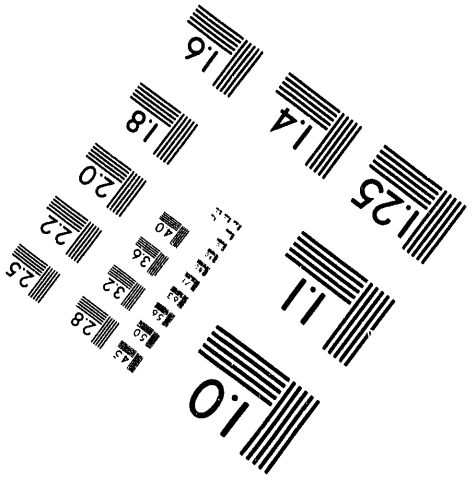

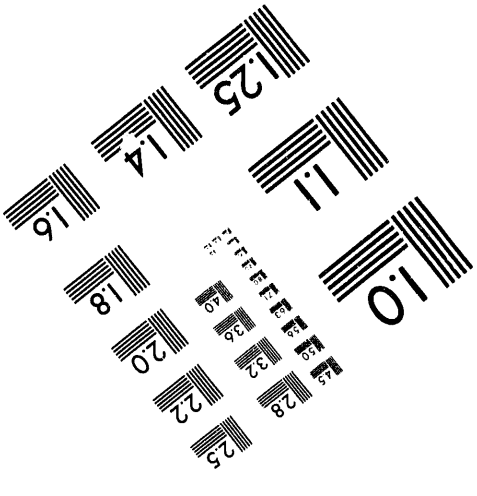

MANUFACTURED TO AIIM STANDARDS
BY APPLIED IMAGE, INC.

1 of 3

DOE/BC/14961-3

Department Of Energy

Quarterly Technical

Report

4/15/94

Roger N. Anderson

Lamont-Doherty
Earth Observatory

Reporting Period: 1/94- 3/94
DE-FC22-93BC14961
Award Date: July 15, 1993
Completion Date: 6/30/94
Government Award for Phase I: [redacted]
COR: James P. Lewis
Columbia University

Lamont-Doherty Earth Observatory

GBRN/DOE Project
"Dynamic Enhanced Recovery Technologies"

DOE Contract #:DE-FC22-93BC14961

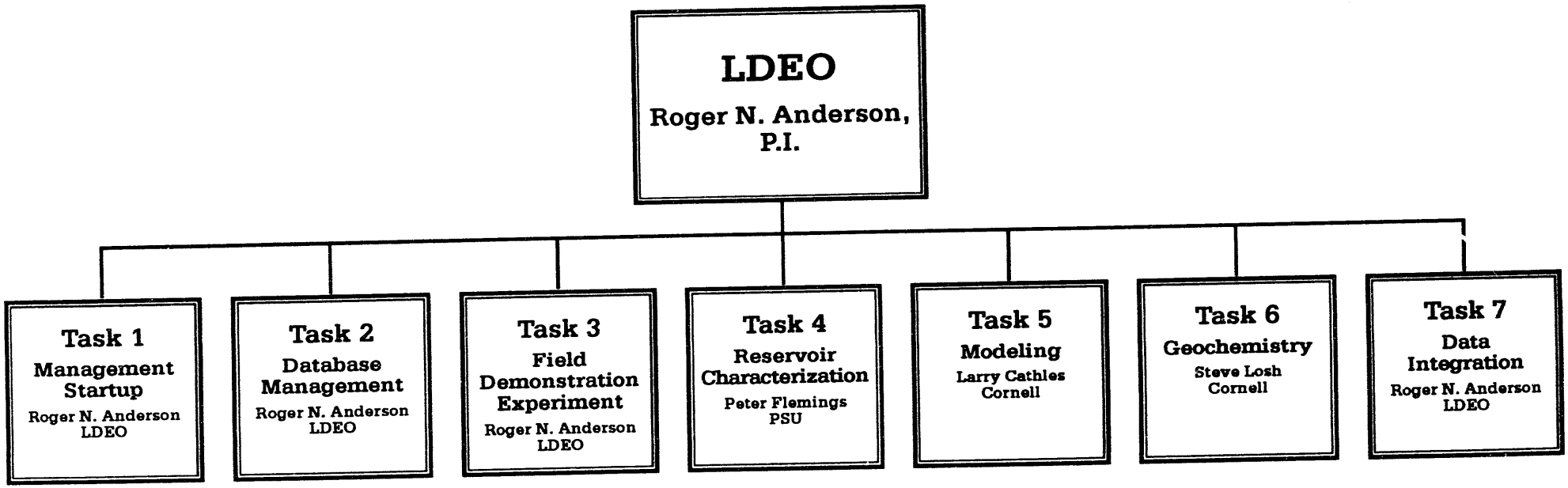

*** designates primary file location**

TASK ONE

MANAGEMENT

START-UP

Roger N.Anderson
LDEO

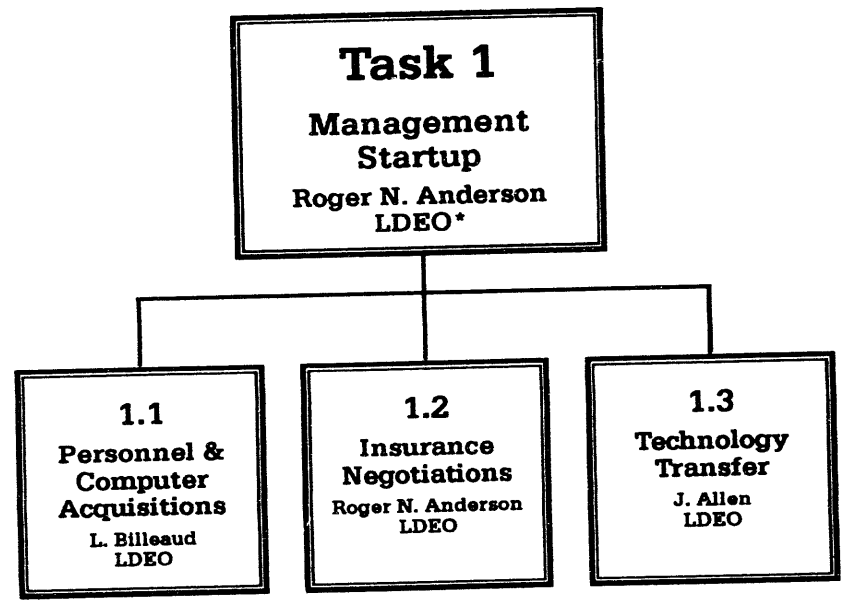
Task 1
Management Startup
Roger N. Anderson
LDEO*
1.1
Personnel & Computer Acquisitions
L. Billeaud
LDEO
1.2
Insurance Negotiations
Roger N. Anderson
LDEO
1.3
Technology Transfer
J. Allen
LDEO

Task One - Management Start-Up
Roger N. Anderson - Task Manager

OBJECTIVES: The purpose of this task to was equip the project with staff and resources (computer and otherwise) to accomplish the other 6 tasks of this project; to negotiate contracts with several industry and university subcontractors to achieve the task objectives; and to initiate the technology transfer to industry and the public from the very beginning of this project.

SUMMARY OF TECHNICAL PROGRESS:

1.1 Personnel and Computer Acquisitions: Liqing Xu was hired to replace Robin Reynolds as AVS operator.

1.2 Contract and Insurance Negotiations: Advanced Visual Systems contract was signed on 3/14/94 and Louisiana State University contract was signed on 1/4/94. Subcontracts with Sarah Tebbens at University of South Florida and Pavel Peska, consultant, are currently being negotiated to complete sub-tasks in Task 7 and Task 4, respectively. Sarah Tebbens will be completing the Sub-Task 7.3, U.S. Reserves Re-evaluation. Pavel Peska will generate a 3-D picture of the complete stress tensor of the Eugene Island 330 area to incorporate into the reservoir characterization model.

1.3 Technology Transfer: Since the field demonstration experiment, technology transfer has been evidenced by the following events:

a. At the GBRN meeting held Jan. 31- Feb. 1, 1994, the results of the field demonstration experiments were presented. All GBRN-member oil companies gave positive feed-back about the field demonstration experiment, and some are considering the possibility of offering scientific leg-extensions on future wells. Minutes of the meeting are included in Task 1 - Attachment A.

b. Pennzoil and partners are considering drilling, and totally funding, a fault zone amplitude anomaly well that we are recommending be drilled from the EI 330 D platform this summer. An isolated sand smear, with no other mechanism for hydrocarbon filling but from the fault, is the target. The decision will be based on the risk assessment, with the normal Pennzoil size criteria of 2500 acre-feet of likely pay in force. We are waiting for delivery of the Shell/Exxon 3-D seismic data, due to us in mid-April 1994, to estimate the volumetrics of this target for this next fault zone conduit test well.

c. Pennzoil has used our new shale coring techniques (developed with Baker Hughes Inteq, MI Drilling Fluids, and industry coring experts) as a basis for coring low-resistivity pay in Eugene Island Block 316. The coring was totally funded by Pennzoil. Our project directly influenced Pennzoil's decision to whole core in this block, and their technical people are closely following our planning and methodology procedures. Dick Ellis, engineering advisor with Pennzoil, stated that we may have revolutionized the concept of whole coring in the Gulf of Mexico (at least within Pennzoil). Using the anti-whirl bit only (without the synthetic mud additive), Pennzoil was only able to get 5'/hour penetration rates, whereas, we were getting up to 150'/hour.

d. Currently, Texaco/Chevron (owners of EI 338) and Pennzoil, and partners, Exxon, Mobil, POGO, and Cockrell (owners of EI 330), are drilling a joint horizontal well into a property line (EI 330/338) seismic amplitude target that was identified by our time-dependent, 4-D seismic techniques. This well was originally discussed between the companies at a meeting we assembled to search for the optimum "pathfinder" targets, and represents one of the first times Pennzoil, Chevron and Texaco have collaborated since all the law suits among them. The target is a low-drainage anomaly in a fault block that our technology isolated as fault-separated from a pressure depleted reservoir. Pressures from RFT's in this well were found to be higher than expected (approximately 2500 psi), as we predicted, and the companies are now proceeding with the horizontal completion. We are requesting the companies to allow us to report on the well as part of our 4-D

seismic poster in the Pathfinder session at the AAPG in Denver in June. Initial results from the lease line well appear to be successful.

e. Conoco has invited us to their Lafayette office on April 15th to discuss the possibility of extending wells in Conoco's Jolliet field (Green Canyon Block 184) to map fluid flow pathways. This invitation was a direct result of our discussion of future targets at the GBRN meeting held Feb. 1, 1994.

f. Attached in Task 1 - Attachment B is an article printed in The American Oil & Gas Reporter in Feb. 1994 that concludes with our strategies for making fault zone wells productive in the area.

g. Also attached in Task 1 - Attachment C, is a similar article about the Pathfinder well and GBRN/DOE project is being published in the May edition of the AAPG Explorer, as advertisement for the largest poster session at the convention on our well results. Anderson and Cathles are also presenting invited papers as part of the secondary migration symposium at the convention. This published article will be included in the next quarterly technical report.

h. Technology transfer also includes the following publications and abstracts for the first quarter of 1994 in Task 1 - Attachment D. Publications are also attached at the end of each task, if applicable. Additional publications are in press that are not listed here and will be included as publications occur.

Task 1 - Attachment A

Minutes of the Global Basins Research Network
Advisory Council Meeting
February 1, 1994
Houston Marriott Westside

The GBRN Advisory Council convened on February 1, 1994 at 8:05 am. The meeting was attended by:

David McCormick, Robert Brown, Richard Eisenberg, *Chevron*

Jay Shearer, Peter D'Onfro, Eric Michael, *Conoco*

Olivier Brévart, Jean Lacaze, *Elf Aquitaine*

Chris Shaw, *Exxon*

David Lawrence, *Shell*

Brad Moody, *Pennzoil*

Jim Lacey, Kent Rinehart, *Texaco*

Jean Whelan, *Woods Hole*

Peter Flemings, *Penn State*

Jeff Nunn, *Louisiana State*

Roger Anderson, *Lamont-Doherty*

Larry Cathles, *Cornell*

Paul Manhardt, *Computational Mechanics*

The first item of discussion was **future drilling plans of the GBRN**. Roger Anderson opened the discussion by noting that the DOE will evaluate all existing Class 1 Projects for possible extension. Since the GBRN/DOE Project is one of these, it is possible DOE funds could be obtained for follow-up drilling if an attractive target could be identified. Roger requested that the Advisory Council send a letter to him regarding future drilling that he could present to DOE to support of extension funds for the current GBRN/DOE project. The Chairman of the Advisory Council, Brad Moody, agreed to provide such a letter based on the discussion of the company representatives reported below.

Jim Lacey of Texaco stated that Texaco would continue to cooperate with the GBRN to put a scientific tail on other wells that companies might drill. Decisions for financial involvement would be based on how Texaco would benefit from the drilling, what could be learned from it, and what questions are outstanding. As background he said that he regarded the principal outstanding scientific question to be how hydrocarbons migrate. We assume they migrate up faults but he expressed pessimism that fault migration could be addressed by drilling because of the low probability of intersecting the right parts of the fault. Even if the right parts are hit and the faults are conduits, the economic issue is likely to remain how best to drill into productive reservoirs.

Robert Brown of Chevron stated that Chevron would be favorable to moving toward a well and that leverage on the research would be the key for them. He said it was not clear to him at this point how much scientific preparation would be needed. He advised against rushing into a new well, saying that the Pathfinder well was a bit hasty. Later Brown added that implicit but unsaid in much of the discussion was that the plumbing system of a basin needed to be understood and determined from seismic data.

David Lawrence from Shell said that Shell also would need to see the drilling program and the design of the research program before making a decision. He noted that the new 3D Shell/Exxon seismic data over half of the South Eugene Island area was due in March and it might help define targets. Reservoirs in low resistivity pay might explain the Pennzoil overproduction. Demonstrating this might be a target. Another fault system might be better than the South Eugene Island one drilled by the Pathfinder well. An important problem was the scaling capacities and transmissivity of a fault. Predictions of pressures near and across faults are important, especially from a drilling perspective. The core did not intersect a fracture zone and he subsequently seconded Texaco's interest in drilling a sand reservoir isolated in a fault and testing it to determine its dimensions and connections to other permeable zones. Determining the source of oil would be particularly critical. He recommended continued testing of the real time migration hypothesis and emphasized the importance of chemical fingerprinting of the oil.

Chris Shaw of Exxon stated it was premature to decide on a well. He would need to know where, when, and what questions would be addressed. Exxon would like to be more involved in the planning phase, especially in deciding what hypotheses would be tested. The well had been one of the highlights of the GBRN and had increased understanding of migration and contributed to research and production needs. Critical future needs are: understanding fluid properties; the sealing and transmissivity of faults; coring of listric faults (because they seldom outcrop); and understanding how reservoirs are charged. He suggested drilling where there was a significant change in the geometry of a fault to understand how fault geometry influences migration.

Jay Shearer of Conoco stated that we should think about drilling carefully before we go on. He **recommended continuing the GBRN membership agreements for three rather than one year.** THE ADVISORY COUNCIL VOTED TO REQUIRE THIS. MEMBERS THAT HAVE NOT YET SIGNED THE MEMBERSHIP AGREEMENTS SHOULD WRITE IN THE CHANGE FROM ONE TO 3 YEAR EXTENSION AND INITIAL THE CHANGES.

Shearer stated that fluid migration, the fault/seal mechanisms, and the nature of the pressure transition zone were particularly important and suggested the Joliett field might be a good place to test hypotheses. Conoco would like to be involved in formulating the hypotheses to be tested. He recommended drilling away from economic targets. The economics of a scientific hole compared to a scientific add-on to a commercial hole should be investigated. He also emphasized the importance of drilling the hanging wall of a fault since this area should be more brecciated and

perhaps therefore contain most of the migration pathways. To locate the fault it might be best to drill through and then sidetrack to core the fault.

Olivier Brévart of Elf Aquitaine stated that support from Elf would rest on technical merit and their reactions to future plans. The project, so far, was a success. The high points were the coring and the incorporation of fault models into general basin modeling. Weak points were the location of the well, weak post-stack migration, and lack of VSP. He was not confident of the core location and not sure of the need for corroborative studies. Acquisitions of 300 ft. of core in hard overpressure was unique. He suggested coring a source zone to investigate oil migration and whether total source thickness is important in oil migration.

Brad Moody of Pennzoil said he concurred in most of the previous comments but would **emphasize the need for a scientific hole.** He said he felt that decisions on the Pathfinder had been too much influenced by commercial pressures and the compromises had left everyone unsatisfied. The next well should be purely scientific even if this meant larger contributions from industry were needed.

There followed discussion of the costs of a purely scientific well and the cost levels that DOE might accept. Roger stated that the drilling had cost DOE about $2.2 million for the pathfinder and that the DOE could likely go to $5 million but not to $10 million.

The next topic of discussion was the **list of top and bottom ten performance categories** of the GBRN.

Robert Brown of Chevron started out. For top 10 he cited (1) energy and enthusiasm, (2) young organization with youth providing energy, (3) lack of compartmentalization and lack of competition in research, and (4) the close cooperation with industry, ability to tap expertise in companies, with both sides benefiting. On the last item he cited particularly the efforts of Exxon's Mike Wooten. THE COUNCIL VOTED THAT A LETTER THANKING MIKE SHOULD BE SENT TO HIM WITH A COPY TO KATE HADLEY FOR INCLUSION IN HIS FILE.

For bottom 10, Brown cited the need to get ideas out into the published scientific literature to obtain the critiques of others and new perspectives and ideas. The next 12 months might be a time to pull back and see what comes in.

Chris Shaw of Exxon spoke next. He provided written input which is attached to the minutes. Highlights of his top 10 items was the coring and core analysis and the planning that went into this activity. For worst 10 he cited: (1) lack of data in the Hypermedia data base, (2) faux pas that had GBRN should develop what it can while taking advantage of input from bothered Exxon's management, (3) the slowness of the modeling program and the fact that it did not provide any new technical capabilities, (4) some instances of poor communication where the principal Exxon representative did not know of events until after another in Exxon, (5) poor coordination of some activities, (6) the fact permission had been sought to obtain some log data and core samples but that these requests had not yet been followed up, and (7) the low credibility

of technical work (idea selling rather than careful documentation). He suggested a greater emphasis on the field and less numerical modeling. While Exxon is fully aware of the benefits of using computer models to aid in understanding geologic processes and basin evolution, and supports the use use of models for this purpose, they are less supportive of using GBRN funds to pay for code development.

Brown of Chevron commented that the role of models was to analyze data. He felt the project was in balance and voted to give the project its own head. The Exxon and others. For top 10 he listed (1) the cooperative sharing of data, (2) the non-threatening environment provided by the project for industry and research, (3) the coring and logging, (4) structural analysis and mapping, (5) the communication since spudding the well, and (6) the progress in analyzing data. He suggested there might be more effort put toward investigating the diagenetic history of the reservoir, the chemistry of the oils, and petrographic information. Chevron had laid off all their people associated with basin analysis. Chevron has reservoir modeling tools for reservoir scale modeling. He'd like to see P. Weimer and M. Rowan's data integrated into the models. He expressed the hope that HyperMedia data might be a available in the future. He was interested in obtaining the digital logs. THE DIGITAL LOGS WILL BE AVAILABLE BY ANONYMOUS FTP FROM PETER FLEMINGS AT PENN STATE UNIVERSITY. Brown stated again that he was impressed with the enthusiasm. The notoriety and fanfare had been beneficial and had kept several research areas going. He recommended keeping the program sharply in focus and the focus in front of the oil companies.

Jay Shearer of Conoco stated top 10: (1) the organization of the meeting ("all to point and all talks on time throughout day"), and (2) the geochemistry, especially the ideas of Jean Whelan and Larry Cathles and the PVT studies of oil, the pressure in seals and the relative permeability and plugging effects. Putting these ideas into the code was good. For the future a core hole into hard overpressure and a detailed look at geochemistry or a hole to investigate plugging of fine grained shales would be especially attractive. Reservoirs Inc. had done studies on a wide variety of cores contributed by industry and this data might be available to the GBRN and provide a starting point for these kinds of investigation.

Olivier Brévart stated he particularly wanted to comment on the modeling. Modeling helps to integrate understanding. The models developed have been doing this. The architecture of Akcess.Basin is particularly important because it allows introduction of new physical and chemical ideas and the testing of these ideas. It is the only code which allows this flexibility. The developer level of the code is thus very interesting. The code development has been slow, but not so slow if you look at all the work that has been done. The Akcess.Basin code has the greatest potential for evolution of any commercial code. He was not in favor of decreasing expenditures in this area. There is a great need to get 3 phase flow into the code. Inclusion of gas and oil as well as water is really necessary. He would also like to see more structural geology in the program.

Jim Lacey spoke for Texaco. Texaco's top 10 list included: (1) the DOE project and how it was run, (2) the technical successes in drilling, (3) the focus on hydrocarbon migration ("the biggest thing going for you"), and (4) the cooperation between academia and industry ("phenomenal"). On the less successful list he included: (1) the need to deliver 3D modeling "the single best thing to distinguish your work from that of others"), (2) delivery of 2D. On the latter he distinguished Texaco's position from Exxon's. Modeling was important and efforts in this areas should continue. However Texaco's modeling plate was full and it was unlikely they would acquire new models because of manpower limitations. They would likely look at our modeling over our shoulders and benefit in that way. They would like to see the chemical fractionation of hydrocarbons in various P-T regimes studied. This is likely to lead to something. The posters on sealing were potentially valuable. He would like to see this continue. From the operating company end, Texaco was grateful to the GBRN for bringing industry representatives together. There was great benefit from this. The GBRN/DOE project had revived interest in shelf exploration. This was good for the Gulf of Mexico. He recommended careful attention to alternative hypotheses for overproduction. The next drill hole will take more support than the Pathfinder. We will need to be able to argue why alternative hypotheses are not adequate.

THE NEXT ADVISORY COUNCIL MEETING WAS SET FOR THURSDAY JUNE 16TH IN DENVER. It will be a one day meeting with technical meeting in the morning and an Advisory Council meeting in the afternoon. Linda Uzmann will investigate possibile meeting locations.

There was a **discussion of efforts to recruit new company sponsors** for the GBRN. THE COUNCIL ENDORSED THE IDEA OF A RECRUITING MEETING IN MARCH AT WHICH PROSPECTIVE COMPANIES WOULD BE GIVEN A BROAD OVERVIEW OF THE GBRN/DOE ACTIVITIES. The current Affiliates will be invited to send representatives to that meeting.

The **issue of dues for new Affiliates was discussed.** IT WAS AGREED THAT THE POLICY ESTABLISHED AT THE LAST MEETING WOULD BE ADHERED TO. In particular new or re-joining Affiliates will: (1) pay $40,000 per year for 6 years or until their shortfall relative to other members is erased, (2) the new hires must pay in the year in which they join, and (3) the new or re-joins must commit to three years of membership.

Finally Larry Cathles **reviewed the 1993 budget** and expenditures with the Council, and **presented the 1994 budget** voted by the Management Council. the Council approved the budget as presented after some discussion.

The meeting was adjourned about noon.

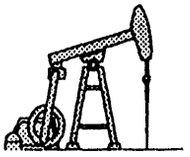

MEMO

Secondary Migration Section

To : GBRN January 28, 1994

Fm : Secondary Migration Section, Exxon Production Research Co.

Re : "Best/Worst" of GBRN participation, recommendations for future

The following comments are in response to your request in the fax dated January 26, 1994 for a list of:

1. the "top 10" things the GBRN has done for you and a list of the "bottom 10" things
2. recommendations for future GBRN projects or activities

BEST:

1. Concept of dynamic migration and trapping has lead us to critically review our previous ideas about hydrocarbon migration and entrapment.
2. Technical interactions between Haggerty and Flemings concerning effective stress
3. Technical interactions and exchange of data between Powell-McKenna and Flemings concerning temperature and pressure data in the Eugene Island area.
4. Collection of rock samples and log and fluid data from the Pathfinder well.
5. Participation on rig.
6. Communication of Pathfinder events and status with Corporate Affiliates.
7. Geologic investigations of RVE.
8. Coordination of rig logistics by Dave Roach.
9. Development of coring and core analysis plan (see #5 below).

WORST:

1. Hypermedia database of RVE.
2. Political faux pas.
   (e.g., Nelson's planetarium dialogue, Anderson's Oil & Gas Journal article)
3. Modeling program has been slow to develop and does not provide significant advance in technical capabilities over programs currently in use.
4. Lack of communication regarding GBRN progress and on-going activities
5. Poor coordination of some activities.
   (e.g., core analysis plan called for CAT scanning prior to any sampling, yet numerous samples were taken from core before CAT scanning could be accomplished)
6. Lack of follow-through on some proposed projects.
   (e.g., inorganic geochemical and porosity analyses of cores - we spent a fair amount of time and effort to secure permission from our Affiliates for Woods to sample Exxon cores and for Bohrer/Eiche to collect log data from cored wells. We have, however, not heard any follow-up about this project.)

7. Not coring either of the major faults in the Pathfinder well. *(We recognize problems in identifying coring points and the specific problems related to this particular well. Nevertheless, because coring the faults was a primary objective of the sampling program we felt that missing the faults was a low point.)*
8. Question about credibility of technical work (i.e., limit amount of "idea selling" and include discussions of data uncertainty).
   (e.g., extrapolation of temperature and pressure data to "verify" migration along fault)

RECOMMENDATIONS FOR FUTURE PROJECTS/ACTIVITIES:

In general, we would like to see a greater emphasis on detailed work and data collection/analysis at the field-scale as it relates to GBRN hypotheses of dynamic systems. A corresponding reduction in efforts on developing numerical models would be appropriate.

Chris Shaw
GBRN Corporate Affiliate representative,
Exxon Production Research Co.
(713) 965-4743

Aftab Alam
Landmark Graphics
713-560-1242

John Austin
Pennzoil
713-546-8422

Robert Beham
Conoco
518-269-3341

Jim Boles
Arco
214-754-3085 (temporary)
normally at:, University of California Santa Barbara

Mike Boyles
Shell
713-245-7641

Olivier Brévart
Elf Aquitaine
33 59 83 4335

Bob Brown
Chevron
318-989-3325

Denise Butler
Pennzoil
713-546-6357

David Chandler
Landmark Graphics
713-560-1200

Bill Clopine
Conoco, Inc. P.O. Box 2197
Houston, TX 77252-2197
713-293-3189, 713-293-3833 FAX
fedex:, Permian, 3048, 600 North Dairy Ashford
Houston, TX 77079-6651

Collee, Pierre
Baker Hughes Inteq
713-695-4548

Dick Conroy
Conroy & Associates, 3523 Crow Valley Dr.
Missouri City, TX 77459
713-437-0149, 713-499-0374 FAX
exploration consultants

Reinold Cornelius
512-918-2672, 521-918-9059 FAX

James DeGraff
Exxon Production Research
713-966-6446

Peter D'Onfro
Conoco
405-767-4022

Louise Durham
Durham & Associates, 2221 S. Voss Rd., Suite 207
Houston, TX 77057
713-784-5441, 713-781-1717 FAX
also: , 5261 Highland Rd., Suite 123
Baton Rouge, LA 70808
petroleum geologist & writer

Richard Eisenberg
Chevron petroleum Technology
310-694-9288

Dick Ellis
Pennzoil
713-546-4975

Brett Fossum
Conoco
713-293-2242, 713-293-4787 FAX

Brian Frost
Conoco
713-293-2859

Oliver Gross
Exxon
713-591-5152

Hadley, Kate
Exxon Production Research
713-965-4781, 713-966-6360 FAX

Susan Haggerty
Exxon Production Research
713-965-4307

Jim Handschy
Shell Development
713-245-7676

Stan Harrison
Exxon
713-591-5350

Bruce Hart
814-863-9663

Susan Herron
Schlumberger-Doll Research
203-431-5234

Russ Hertzog
Schlumberger
713-928-4817

Michael Honor
Schlumberger
713-368- 8135

Jie Huang
Exxon Production Research
713-965-4329

B Katz
Texaco
713-954-6093, 713-954-6113

Sidney Kaufman
713-952-7205
Cornell emeritus

William S. Killingsworth
Shell Offshore
504-588-6787

Alf Klaveness
713-468-5123, FAX 713-468-0900

Jean Lacaze
Elf Aquitaine
59 83 4511

Jim Lacey
713-954-6066
Texaco Advisory Council rep.

Roy Leadholm
Conoco, Inc.
713-293-2838

Steve Matsumoto
Landmark Graphics
713-560-1082

Martin Matthews
713-432-2387

Robert McCallister
Exxon Exploration
713-775-7353

David McCormick
Chevron Petroleum Technology
310-694-7360

Dennis McMullin
Landmark Graphics
713-560-1069

Eric Michael
Conoco
405-767-3177

Charles Morris
Schlumberger
713-368-8144, 713-368-8182 FAX

Wayne Orlowski
Conoco
713-293-1844, 713-193-3833 FAX

Bob Pottorf
Exxon Production Research
713-965-4135

Bill Powell
Exxon Production Research
713-965-4122

Janine Rafalska
Conoco
405-767-6046

Terry Ralston
Exxon Production Research
713-965-4532

Charles Rego
HyperMedia Corp.
713-293-0325

Kent Rinehart
Texaco
504-595-1173

Dave Roach
Lamont-Doherty
914-365-8330

Sheila Roberts
LSU
504-388-3988

Michael Robinson
Exxon
713-775-7169

Mark Rowan
University of Colorado
303-492-5014, 303-492-2606 FAX

Roger Sassen
University of Texas (?)

Deet Schumacher
Pennzoil
713-546-4028

Chris Shaw
Exxon Production Research
713-965-4743

Jay Shearer
Conoco
318-269-3381, 318-269-2381 FAX

David M. Sibley
Chevron
318-989-3338

Sid Siddiqui
Pennzoil
713-546-4777

Lori Summa
Exxon Production Research
713-965-7102

Keith Thompson
Petroleum & Geochemical Data
214-369-9225
consultant

Peter Vrolijk
Exxon Production Research
713-965-4151

Lloyd Wenger
Exxon Production Research
713-965-7293

Jean Whelan
Woods Hole Oceanographic Inst.
508-457-2000 ext. 2819, 508-457-2164 FAX

Paul G. Wilen
King Ranch Oil & Gas
713-873-2255, 713-873-4411 FAX

Ken Williams
Texaco E & P
713-432-6808, 713-661-7463 FAX

Jim R. Wood
Michigan Technological Univ.
906-487-2894

Richard Woodhams
Pennzoil
713-546-4036

Michael Wooten
Exxon Production Research
713-965-4500

Mark Zastrow
318-989-3326
Chevron

Wu-Ling Zhao
Exxon Production Research
713-965-4741

Task 1 - Attachment B

THE AMERICAN OIL & GAS REPORTER®

April 5, 1994

Dave Roach
GBRN Logistics
Lamont-Doherty Earth Obs.
Route 9W
Palisades, NY 10964

Dear Dave:

Please consider this letter permission on behalf of *The American Oil & Gas Reporter* for GBRN to republish in its DOE quarterly report the article titled "Field Demo Confirms Deep Potential," and written by Roger Anderson for the February 1994 issue of *The American Reporter.*

Our only request is that somewhere within the article you acknowledge original publication in *The American Oil & Gas Reporter.*

If there is anything else you require, please do not hesitate to contact us.

Sincerely,

Bill Campbell

Reprint removed

Bill Campbell
Managing Editor

Task 1 - Attachment C

May [illegible]

FOR: AAPG Explorer
Louise S. Durham
May 1994

Futuristic Concept May Spark New Play In Gulf

Just when you thought you had heard it all, now there's talk that the practice of drilling into reservoirs in order to produce oil and gas may become passé.

Before you scoff, take a look at a cutting edge project down Gulf of Mexico way at Eugene Island Block 330, which was featured in the recent CNN series on new sources of hydrocarbons. Some erudite folks are checking out a theory here that it may be possible to tap into and produce hydrocarbon "streams" as they migrate upward from deep source rocks toward shallower reservoirs.

This play concept has the potential to revolutionize the way operators select well locations. And, if successful, it could increase the undiscovered hydrocarbon reserve base in the Gulf by as much as a few billion barrels.

The research effort is being spearheaded by the Global Basins Research Network (GBRN), which was organized in 1989 as an Internet research consortium of geographically distant and separate academic institutions. The group's lofty goal is two-fold: to image and tap into active, or dynamic, hydrocarbon pathways and to identify the mechanisms that cause hydrocarbons to burst out of geopressured confines and begin upward migration. It has attracted the interest of a dozen oil and gas companies, mostly majors, and several communications and service companies, which have joined forces with the organization.

Basic to the GBRN methodology is the analysis of dynamic, time dependent phenomena, which transcends the usual subsurface observations that focus on stratigraphy and structure, and hones in on the visualization of physical and chemical influences of fluids as they move through the rock. Quantification of the changes in pressure, temperature, geochemistry and seismic amplitudes over time in a given area provides the clues to detect the presence of active hydrocarbon migration routes.

The research group looked at basins worldwide in search of a study area with a strong migration signal, and the Gulf basin, with its active sea floor seeps and vast available data base, was determined early on to be the primo locale for a migration phenomena study.

Eugene Island Block 330 field was selected for the initial field test site. This Pleistocene producing behemoth, which has coughed up more than one billion barrels of oil equivalent since production began in 1972, occurs as an anticlinal structure on the downthrown and low pressure side of an arcuate NW-SE-trending, pressure sealing growth fault. Dubbed the "A" fault or "Red" fault, this feature serves as the plumbing system for fluid movement in the field.

Peculiar things are happening here. The oil/water level is static, and the pressure has been increasing since 1987, according to Jeff Nunn, Louisiana State University

geophysicist and GBRN co-director. The field is depleting at an unusually slow rate, and Nunn points out, "So far, it's produced 103% of the estimated reserves."

One plausible explanation for this production anomaly is that initial reserve estimates may have been conservative, perhaps in part because they failed to take into account the reserves that were present in some of the silts or shaley sands that, owing to their inherently high irreducible water saturation, show a low resistivity reading on the logs. An inadequate understanding of these intervals could have eliminated significant reserves, and the GBRN scientists are investigating the extent of this potential contribution to overproduction.

Substantial clues for dynamic hydrocarbon replenishment have been identified here, however. Organic fingerprinting of the oil produced at Eugene Island shows geochemical variances over time from the same perforation depths in the same wells that suggest evidence for refilling of reservoirs.

Adding intrigue to the scenario are isotherm overlays on structure that show the 400,000 year old producing reservoirs to be four times hotter than expected. These hot spots, in tandem with pronounced pressure gradient bulges are centered over the major oil fields in the area.

Modeling of the fluid flow needed to produce these coupled anomalies requires a transient fluid burst up the

Red fault zone to have occurred within roughly the last 10,000 years.

The argument for active migration is enhanced by data acquired from 3-D seismic surveys, which indicate "trails" of seismic amplitude anomalies in several Eugene Island blocks. These "trails" connect to the Red fault zone either directly or, in some instances, indirectly by means of an antithetic fault that intersects the Red fault at depth.

Scientists with the GBRN believe that at least seven separate observed amplitude anomaly trails indicate the presence of migration pathways that extend downward into the deep, hard geopressure. This complex network of amplitude anomalies is thought to originate from three main source areas of presumably turbiditic sands, which are ponded among vast, vertical salt columns at depth. These turbidites may contain huge reservoirs that filled with hydrocarbons when the sands were initially capped with a shallow salt sheet in an earlier analog to the deepwater flexure trend. The now evacuated salt sill was fed by the vertical salt bodies.

Using multiple vintages of overlapping 3-D seismic surveys, referred to as 4-D seismic technology, the GBRN team imaged a hypothesized hydrocarbon migration pathway at Eugene Island 330 by fitting isosurfaces to high amplitude seismic strength reflection regions of the 4-D dataset, which consisted of 3-D surveys that were shot in 1985 and 1988 over a four-square mile area of the field. Changes in

the form of the amplitude isosurfaces were identified by superposing the surveys.

Because the seismic amplitude isosurface technique images acoustic impedance contrasts rather than active fluid flow, the observed differences in the amplitude isosurfaces might represent pressure changes caused by fluid movement out of the deep source beds, up along the Red fault zone, under and around a prominent salt overhang, and upward to the shallower, producing reservoirs.

Pennzoil Exploration and Production Co., which has been a participant in the GBRN effort essentially since its inception, agreed to let its EI #A-20 ST well be the guinea pig to test the dynamic hydrocarbon replenishment concept, and results are looking good.

With $10 million in the GBRN pockets, courtesy of the U.S. Department of Energy's (DOE) advanced oil recovery program, which industry participants will match dollar for dollar with goods and services, the research group kicked in on its part of the "Pathfinder" well at 7,300 ft. T.D., and took the drillbit down an additional 700 feet.

"We drilled into a low seismic amplitude target within the fault zone, seeking a spot where the fault was tightest," says Roger Anderson, senior research scientist at Columbia University's Lamont-Doherty Earth Observatory and GBRN co-director. He explains that the intent was to explore what it would take for deep oil to get through the tight

spot in the fault zone, rather than to find the optimal place to produce.

Numerous oil and gas bearing cores were recovered from the Red fault, and the test zone was a shale on shale contact, which nixes the probability that the hydrocarbons were sourced from nearby sands. High resolution resistivity imaging logs showed the high-angle fault zone dipping as expected and cut by natural vertical hydraulic fractures, confirming that the fault zone had, indeed, been isolated, according to Anderson.

The target area was perforated over a 40 foot interval and frac-packed, which involved opening the formation and pushing what is basically a gravel pack back into the fracture. Besides encouraging higher rate production by providing a larger cross sectional area for fluid flow, this relatively new completion technique maintains longer term well productivity because the fines, which tend to plug gravel packs in the small cross sectional area of the wellbore, take longer to plug the large surface area of the fracture pack.

Flow rate from the highly permeable propped zone in the Pathfinder maxed out at roughly 200 bbl/day, but the flow couldn't sustain itself, and the fracture system closed. Pennzoil senior petroleum engineering advisor, Dick Ellis, likens the effect to "sucking through a straw in a super thick milkshake." Without sufficient pressure control

at the surface to drawdown easily, the pull on the formation became increasingly more pronounced, while fluid production declined. Over time, the proppant sands apparently became embedded in the fracture walls, impeding the permeability of the zone until, ultimately, only the low intrinsic permeability of the shale matrix remained.

While the project team members found that they could reopen the fracture network by pumping into the fault zone at a rate of a few hundred psi, the fractures would tighten as soon as the pressure dropped.

Anderson speculates that one method to make such faults producible might be to perforate over greater intervals in order to create larger hydraulic fractures than the 70- by 30-foot fracture made at the Pathfinder well.

Other strategies he contemplates to activate production from fault zones include the use of deep injector wells to sweep oil up toward producing wells, wellbore orientation parallel to the fault plane to expose a greater surface area, and going after high seismic amplitude targets.

As to what's triggering the hydrocarbon movement upward from the deep geopressured turbidites, Anderson says it's likely that the formation pressures increase until the fracture closing stresses in the fault zone are periodically overcome, and large volumes of fluid are released out of the geopressured chambers to migrate into the fault plane prior

to the ensuing pressure drop which causes the fault to tighten once again. LSU's Nunn emphasizes that these transient fluid bursts are episodes that may continue for years, perhaps decades.

Analyses of the 340 feet of core retrieved from the Red fault, along with the array of physical and chemical data obtained in situ during the Pathfinder's logging program, will be rolling in during the next couple of years, and optimism is high over the possibility of drilling additional test wells in other locales.

While the findings gleaned from the Pathfinder data likely may pose more questions than answers, success can be defined in many ways. Anderson notes that a unique feature of DOE's underwriting of the project is that for the first time an academia-based project was able to test its modeling and data visualization results directly with the drillbit.

And the federal agency is happy. "We already consider the project to be a success from the standpoint of the scientific data acquired and DOE's reason for going in, which was to test the concept and collect data to confirm the validity of the geochemical evidence and the seismic amplitude anomalies," says Edith Allison, DOE project manager at the Bartlesville office. She adds that the agency hopes this ultimately will be a catalyst for industry to increase Gulf production.

While there may have been a tad of trepidation on the

part of the participants about entering into a field test that would be jointly run by industry and academia, all's well that end's well. Mike Osborne, Pennzoil's senior vice-president for North America, notes enthusiastically, "We were pleased with how smoothly everything went. It was like clockwork. The scheduling went well and the coring, logging and other evaluations went extremely well."

Columbia's Anderson would like to see this kind of academia-industry linkup become a trend in the oil patch. He points out that when a company is in a production mode, there's no time to think about what is discovered, and he suggests that the universities are a natural as the R&D labs of the future. Thirty-five scientists will have worked on the Pathfinder over a three-year period.

And they're eager to spread the word about their dynamic hydrocarbon migration research. Pennsylvania State University, in conjunction with the University of Colorado, organized a special poster session on the GBRN effort for the June 1994 AAPG Annual Meeting in Denver. Eighteen posters have been accepted for what the Penn State team says will be the largest single poster session at the meeting.

Check out this scene early on. It has all of the makings of an attention getter.

-End-

Task 1 - Attachment D

Reprint removed

TASK TWO

DATABASE

MANAGEMENT

Roger N.Anderson
LDEO

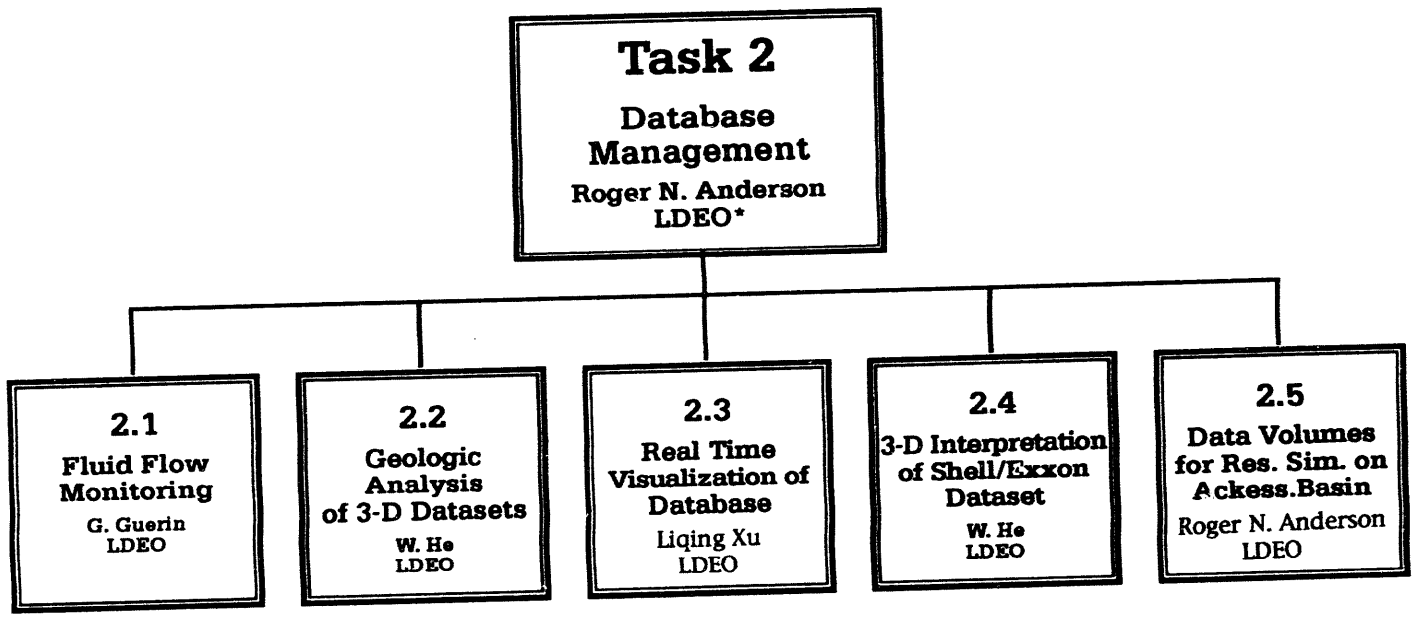
Task 2
Database Management
Roger N. Anderson
LDEO*
2.1
Fluid Flow Monitoring
G. Guerin
LDEO
2.2
Geologic Analysis of 3-D Datasets
W. He
LDEO
2.3
Real Time Visualization of Database
Liqing Xu
LDEO
2.4
3-D Interpretation of Shell/Exxon Dataset
W. He
LDEO
2.5
Data Volumes for Res. Sim. on Ackess.Basin
Roger N. Anderson
LDEO

Task Two - Database Management
Roger N. Anderson - Task Manager

OBJECTIVES: The objectives of this task are to accumulate, archive, and disseminate the geological information available within the area of research of this project; networked database creation, generation of new seismic interpretation with high-tech software, and real-time visualization of the on-line database.

SUMMARY OF TECHNICAL PROGRESS:

2.1 Fluid-Flow Monitoring of Industry Multiple 3-D Seismic Data Sets: We are currently working with two 3-D seismic surveys, the Texaco/Chevron data set and the Pennzoil et al data set. Liqing Xu completed coding 12 AVS modules to orient and cross-compare the data sets. The 4-D seismic interpretation process is continuing. A workshop is planned for the second week in April at L-DEO to review current progress and plan the tracking of flow pathways within individual 3-D surveys and combining 3-D surveys to examine similarities and contrasts over time.

2.2 Geological Analyses of Industry 3-D Seismic Surveys: Landmark has completed its task of comparing the traditional interpretation of the horizons and faults and the reinterpreted reflector horizons and faults as discussed in the previous quarterly report. The reinterpreted geologic data has been converted and exported to other databases as per previous reports. Integration of several data sets aided in the reassessment of the drilling location and the field demonstration experiment.

Lincoln Pratson's research during this quarter was divided between work on the computer algorithm for correlating well logs from Eugene Island, and submission of a manuscript to the

American Association of Petroleum Geologists Bulletin on the morphology and shallow stratigraphy of intraslope basins on the Louisiana continental slope seaward of Eugene Island. The deep structure within geopressures in the Eugene Island Field is directly correlatable to these deeper water surficial processes.

For the well log correlation, a subroutine of the correlation algorithm was developed for accounting for all possible correlations between any two related time series (different types of well logs, well logs and isotope records, etc.). Testing of this subroutine will be conducted in the upcoming quarter and will represent the completion of the second phase of algorithm development. Phase three begins with the implementation of statistical methodology for ranking all possible correlations.

The manuscript submitted to the AAPG Bulletin (anticipated publication date is 2nd or 3rd quarter 1994) is a detailed morphologic and near-surface stratigraphic analysis of intraslope basins on the eastern Louisiana continental slope. These basins are modern analogs of other large, oil and gas charged basins now buried beneath the Louisiana-Texas continental shelf, as well as Eugene Island. A principle goal of the analysis is to provide us with a reference to the possible dimensions and shapes of these shelf basins prior to their burial. Computer algorithms, traditionally employed for automatically mapping river networks in gridded land topography, are used to extract morphologic measurements of the intraslope basins from high-resolution, gridded multi-beam bathymetry. These are likely to directly convert to permeability fairways upon further burial, and thus may be the equivalents to the deep seismic connectivity we are mapping to the Fault Zone.

The basins average ~15 km in length, ~10 km in width, ~200 m in depth, and an areal extent of ~50 km^2. They exhibit distinctive correlations of basin area versus relief (i.e., hypsometric curves) and near-surface (< 2 seconds two-way travel time) stratal geometry's, which appear to reflect a continuum between two intraslope basin end-member morphologies. Analysis of the hypsometric curves points to the

transformation between basin end members being due to differences in amounts of basin subsidence relative to basin infilling.

2.3 Real-Time Visualization of Database: Our real-time database is on-line. Currently, L-DEO, LSU, PSU, and Cornell have the capability of sharing data and results. Each database is updated daily to insure the latest version of the database is accessible. We are in the process of loading the system with currently held data. All of the field demonstration experiment data has been loaded into the database. HyperMedia's activities for the first quarter of 1994 are described in section 5.6.1 of Task 5 of this report.

2.4 3-D Interpretation of the Shell 3-D Seismic Data: We expect the Shell 3-D seismic survey to be received by mid-April 1994. The transmittal letter from Shell has been written and forwarded to Exxon for their signature. Upon receipt, we will immediately difference that data set with the Pennzoil and Texaco/Chevron 3-D surveys.

2.5 Reformat Data Volumes for Simulation: Task 2.5 will be accomplished in Phase II of this project.

TASK THREE

FIELD

DEMONSTRATION

EXPERIMENT

Roger N. Anderson
LDEO

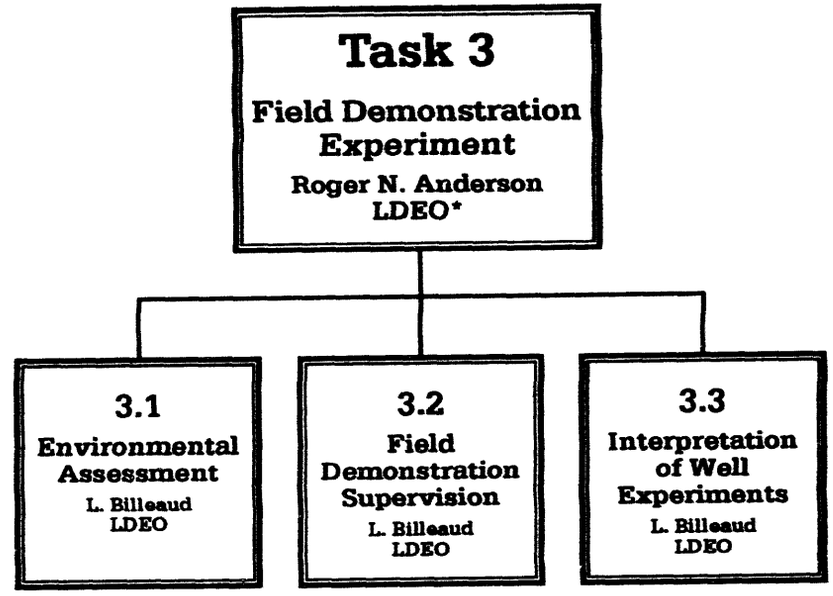
Task 3
Field Demonstration Experiment
Roger N. Anderson
LDEO*
3.1
Environmental Assessment
L. Billeaud
LDEO
3.2
Field Demonstration Supervision
L. Billeaud
LDEO
3.3
Interpretation of Well Experiments
L. Billeaud
LDEO

Task Three - Field Demonstration Experiment
Roger N. Anderson - Task Manager

OBJECTIVE: The objective of task three was to drill one well extension to test the Dynamic Enhanced Recovery Technologies objectives of this project. In November and December, 1993, we drilled into the fault zone in Eugene Island Block 330 (A20-ST) and performed the following experiments: whole coring, wireline logging, sidewall coring, formation pressure tests, stress tests, completion with frac-pack, flow test, and pressure transient test.

SUMMARY OF TECHNICAL PROGRESS:

3.1 Environmental Assessment: Sub-task 3.1 is completed and was discussed in 10/15/93 technical quarterly report.

3.2 Field Demonstration Well: Sub-task 3.2 is completed and was discussed in 1/15/94 technical quarterly report. Technology transfer of the field demonstration experiment data and results are discussed in Task 1.3 of this report.

3.3 Interpretation of Results of Well Experiments: The planning and arrangement of contractual relationships with third parties is complete, as well as, the acquisition of the borehole data and fluid samples. The interpretation of the results of the experiments will be reported as they occur in future DOE reports.

We are in the process of publishing a Pathfinder well data volume with all raw data, processed data, and some interpreted data from the well to be available in the form of a CD-ROM (modeled after the Initial Reports of the Deep Sea and Ocean Drilling Programs). Our goal is to submit a CD-ROM to the DOE with the Final Technical Report of Phase I of this project, and to circulate the CD-ROMs widely to increase the scientific output of our project and to spread the technologies. The preliminary Table of Contents is attached in Task 3 - Attachment A.

Task 3 - Attachment A
Field Demonstration Experiment - Pathfinder Well
Data Volume CD-ROM

Table of Contents

TASK FOUR

RESERVOIR

CHARACTERIZATION

Peter Flemings - Penn State

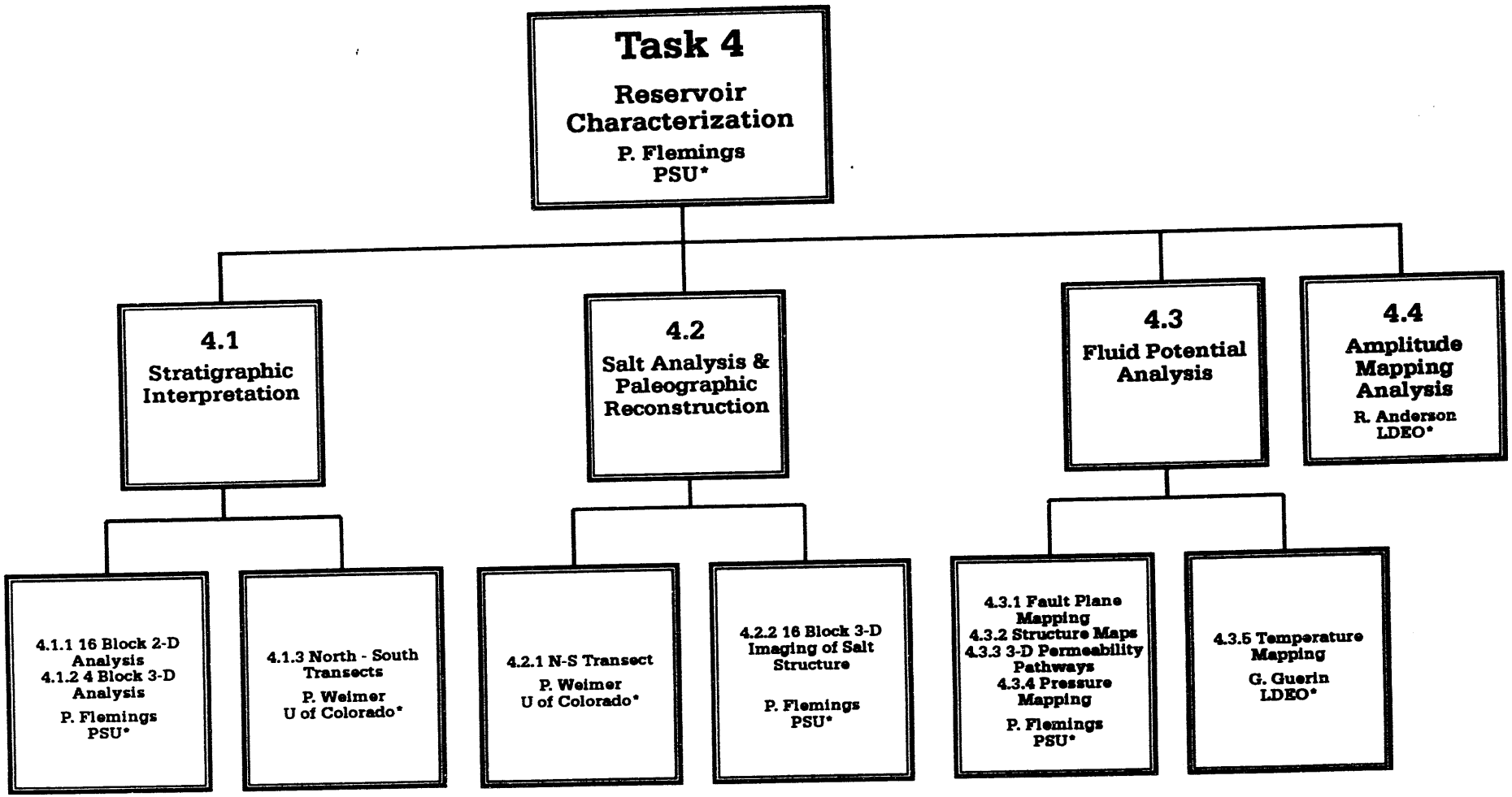
Task 4
Reservoir Characterization
P. Flemings
PSU*
4.1
Stratigraphic Interpretation
4.2
Salt Analysis & Paleographic Reconstruction
4.3
Fluid Potential Analysis
4.4
Amplitude Mapping Analysis
R. Anderson
LDEO*
4.1.1 16 Block 2-D Analysis
4.1.2 4 Block 3-D Analysis
P. Flemings
PSU*
4.1.3 North - South Transects
P. Weimer
U of Colorado*
4.2.1 N-S Transect
P. Weimer
U of Colorado*
4.2.2 16 Block 3-D Imaging of Salt Structure
P. Flemings
PSU*
4.3.1 Fault Plane Mapping
4.3.2 Structure Maps
4.3.3 3-D Permeability Pathways
4.3.4 Pressure Mapping
P. Flemings
PSU*
4.3.5 Temperature Mapping
G. Guerin
LDEO*

Penn State Quarterly Report

1.0 Overview

An outline of the individual tasks are provided below. Primary responsibility for tasks are shown in parentheses: PSU= Penn State University, CU= University of Colorado- Boulder, LDEO = Lamont-Doherty Earth Observatory. A detailed outline of Phase 1 completion dates as well as projected completion dates for Phase 2 will be found in Section 3.0. In the following sections we describe in further detail some of the individual research projects being pursued by the Penn State group. A calender of events is provided in Section 7.0.

Task 4: Reservoir Characterization

- 4.1: Stratigraphic Interpretation
  - 4.1.1: 16 Block 2-D Analysis (PSU)
  - 4.1.2: 4 Block 3-D Analysis (PSU)
  - 4.1.3: North-South Transects (CU)
- 4.2: Salt Analysis and Paleogeographic Reconstruction
  - 4.2.1: North-South Transects (CU & PSU)
  - 4.2.2: 16 Block 3-D Restoration (CU)
- 4.3: Fluid Potential Analysis (PSU)
  - 4.3.1: Fault Plane Mapping (PSU)
  - 4.3.2: Structure Maps (PSU)
  - 4.3.3: 3-D Permeability Pathways
  - 4.3.4: Pressure Mapping (PSU)
  - 4.3.5: Temperature Mapping (G. Guerin, LDEO)
- 4.4: Amplitude Mapping Analysis (R. Anderson, LDEO)

2.0 Database Update

At this point, we have all of the significant well data that we are going to obtain for the Eugene Island Area. These specific data are detailed in GBRN Technical Report 1.1. We have 3 seismic surveys and well data for over 460 wells. Blocks 314, 330, 331, 337, 338, and 339 contain extensive directional and wireline data as well as some sidewall core data and well event picks. Many of the wells outside of this 9-block area contain velocity, mud logger and directional data.

All of the new data acquired during the drilling of the Pathfinder well has been loaded into our Geolog database. This includes AIT, array sonic, DITE, DSI, LDS, MDT, geochemical, pressure and stress data. Both raw data and Schlumberger-processed data are included in these sets. A list of logs run on the Pathfinder well as well as full descriptions of these logs can be found in GBRN/DOE Pathfinder Data Volume.

3.0 Completion of Phase 1 Tasks & Projected Phase 2 Completion Dates

4.1: Stratigraphic Interpretation
Original: 10/92-11/94 Current: 10/92-11/94

4.1.1: 16 Block 2-D analysis (PSU)
Original Projection: 10/93
Current Projection: 4/94
This subtask will be completed by April 1. Details of this work will be published in Alexander and Flemings, "Stratigraphic Architecture and Evolution of a Plio-Pleistocene Salt Withdrawal Mini-Basin: Eugene Island, South Addition, Block 330, Offshore Louisiana", submitted to AAPG.

4.1.2: 4 Block 3-D analysis (PSU)
Original Projection: 11/94
Current Projection: 11/94
Work on this subtask is proceeding on schedule. Details of this work will be published in Hart et al., "Facies Architecture of a Shelf Margin Lowstand Complex, Eugene Island Block 330 Field, Louisiana Offshore", to be submitted to AAPG.

4.1.3: North-South Transects (CU)
Original Projection: 10/93
Current Projection: 5/94
This subtask will be completed by May 1.

4.2: Salt Analysis and Paleogeographic Reconstruction
Original: 10/92-11/94 Current: 10/92-8/95

4.2.1: North-South Transects (CU & PSU)
Original Projection: 10/94
Current Projection: 3/94
This subtask is complete. Details of this work, and the results from Subtask 4.1.3, will be published in Weimer and Rowan, "Regional Stratigraphic Interpretation across the Eugene Island 330 Field", submitted to AAPG.

4.2.2: 16 Block 3-D Restoration (CU)
Original Projection: 11/94
Current Projection: 8/95
This subtask is slightly behind schedule, because the CU group had been focussing on the timely completion of subtask 4.2.1.

4.3: Fluid Potential Analysis (PSU)
Original: 10/92-10/95 Current: 10/92-10/95

Task 4.3.5 - Temperature Mapping

From a set of temperature data from the EI 330 area, including the following Eugene Island Blocks 314, 315, 316, 331, 330, 329, 337, 338, 339, a 3D-map of the present-time temperature field was established by Gilles Guerin. Unfortunately, most of the temperatures available are Bottom Hole Temperatures (BHT) measured a short time after completion of drilling and mud circulation. Some have been corrected following different analytic methods, using the parameters available (shut-in time, circulation time, one or more measurements at a same depth). Most of these temperatures could not be corrected because of the absence of such parameters, and a general correction law has been applied to them, based on the data that was corrected. The next step, in progress, is to model what the temperature distribution in the same area would be in the case of a purely conductive regime. With a finite difference model using lithology properties, and particularly thermal conductivity, such a temperature map should point out areas where the thermal regime is, or has been, dominated by advective heat flow, and by the fracture opening/closing cycles within the fault system.

Task 4.4 - Amplitude Mapping Analysis

Progress continues toward the submission of a patent application for seismic amplitude mapping of the connectivity between shallow reservoirs and deep source regions. Distributary networks of high, but variable amplitudes are mapped within a 3-D seismic dataset with this technology. Intercomparisons between amplitude trails among 2 or more 3-D seismic surveys (termed 4-D seismic analysis) are possible utilizing this technology as well. The patent is for 3-D and 4-D Seismic Interpretation and Imaging Utilizing Amorphous Diffuse Intra- and Inter-Period (ADIP) Projectors".

The technology has been tested using the Pennzoil and Texaco/Chevron 3-D surveys shot in 1985 and 1988 respectively. We are anxiously awaiting the Shell/Exxon dataset shot in 1992 to further test the technology. Landmark Graphic has expressed an interest in evaluating the technique, and we are developing the strategy for an Alpha test in the Chevron Lafayette, Louisiana offices in 1994.

As discussed in Task 1, a horizontal well along the property line between Eugene Island blocks 330 and 338 is currently being drilled. The amplitude differencing scheme in the patent was instrumental in predicting that pressure depletion had not happened in the target reservoir, though significant oil and gas had been produced in the surrounding area.

We will be shifting further resources into the further development of these promising new technologies for tracing migration pathways in 3-D and 4-D seismic datasets. Albert Boulanger has accepted a science position in our project to further develop the "reduction to practice" of the patent. He was a senior scientist at Bolt, Beranek, and Newman in Boston, and is an expert in visualization and processing of very large datasets. This patent promises to be one of the most useful of the technologies developed by this project for transfer to industry.

2. Correlate shale fraction with core derived permeabilities and assess data quality.
3. Choose different 2D cross sections in Block 330 and generate statistical realizations of shale fraction constrained by stratigraphic interpretation. The appropriateness of using kriging (smooth interpolation) and fractal methods on the available data set is investigated.

Gamma ray and sonic logs are used to provide information regarding shale content and porosity within the GA interval. The low frequency, high resolution nature of wireline data makes it difficult to quantify lateral facies variations and hence the need to attempt fractal and/or geostatistical analysis of the data. Presently, ordinary kriging of shale fraction data from some wells in block 330 is being studied and the fractal nature of the wireline data (porosity and shale fraction) is to be established. Fractal analysis would seem to be an appropriate tool to utilize for this data set given the low frequency of measurements in the lateral direction in contrast to the much higher frequency in the vertical direction.

A qualitative estimate of sand distribution and continuity in the area is provided by seismic mapping and well log correlations. A correlation between high amplitude seismic anomalies (indicating presence of hydrocarbons) and shale fraction distribution is being attempted in order to define discontinuities in permeable zones within the GA sand. The sand does not seem to be laterally continuous over long distances and the presence of low permeability shale foresets separating sand foresets in the progradational delta front facies is a distinct possibility.

Future work will consist of further mapping and relating of shale fraction distribution to the stratigraphic framework of the area. A primary objective will be to integrate stratigraphic and statistical analyses to produce a geologically realistic distribution of sand/shale facies.

5.0 Facies Architecture in Eugene Island 330 Field

Work in this quarter has again centered on the GA Sand and adjacent stratigraphic units. Mapping of this sand in the 3-D seismic data sets is now complete, and fault control polygons have been generated in Landmark. Much work has been done on quality control and adding to the horizon picks which were entered into Geolog. Simultaneously, a Loglan (Geolog's Log Analysis Language) program has been developed which uses the gamma ray curve to extract lithology (using the relationship for Tertiary clastics) and, for any given stratigraphic interval, writes the thickness of sand (less than 33% shale), shaley sand/sandy shale (33-66% shale), and shale (greater than 66% shale) to the data set containing the horizon data. Electrofacies characterization of the GA Sand is shedding light on the structural development of the EI 330 Field. In particular, the distribution of sharp-based (erosive) contacts at the base of the sand, and the GA-1 sandbody (a distinct, separate unit overlying the main portion of the GA Sand) strongly suggest that the anticlinal "dome" centered in Block 330 was present during deposition of those sands. All of these data (wireline and seismic) are being exported to Z-Map III, and preliminary structure, isopach and electrofacies distribution maps have been prepared. Portions of

this work were presented as a poster at the GBRN Annual Meeting in Houston.

Following the GBRN Annual Meeting in Houston, Bruce Hart spent 3 days at Chevron in Lafayette, LA, working with David Sibley on the GA Sand and stratigraphically equivalent sands in Blocks 338 and 339 (Chevron's "4500' Sand"). Of particular significance is the integration of dipmeter and 3D seismic data. Previous work by Sibley had shown that paper dipmeter logs from this area could be digitized and the regional structural dip could be digitally "removed" (using Digirule, a program created by a Canadian software company) to display original depositional dips. Hart added to the digital database, and worked with Sibley on the interpretation of the data. Two principal dipmeter "facies", each associated with characteristic vertical successions of dips/azimuths and lithologies (gamma ray log), can be recognized and associated with seismic facies (where seismic frequency content permits). The first consists of continuous, sandier-upward delta slope clinoforms, with dip azimuths being continuous throughout the thickness of the unit (in the direction of progradation), but showing increasing slopes up-section (a reflection of the clinoform geometry). The second consists of sandy packages found at various stratigraphic levels with dips which point at high angles to the progradation direction (at times 180^{o} difference). These are interpreted as portions of the delta slope which were affected by mass-wasting. Current work focuses on understanding how reservoir heterogeneity related to these depositional characteristics has been affecting production. It is anticipated that this work will form the basis of a paper to be submitted to the American Association of Petroleum Geologists' Bulletin. While in Lafayette, Hart presented an hour long talk (to about 35 Chevron employees) on his previous work on the modern Fraser Delta and showed how that delta can be used as a modern analog to interpret deltaic deposits such as the GA Sand.

6.0 Pressure Mapping

Pressure data from the Pathfinder Well are being analyzed by Hart, Flemings and Deshpande. Discrete pressure measurements (including Repeat Formation Tester/Modular Dynamics Tester, production tests, and pressure tests conducted prior to stress tests) are being integrated with pressures derived from porosity data (see contribution by Deshpande/Flemings in last Quarterly Report for a summary of methodology). The results show that soft geopressures are found beneath the GA and HB Sands (fluid pressure gradient less than 0.65 psi/ft), and continue down to where the well crosses the B Fault splay at 6742'. Overpressures increase through the B, D and A Fault splays, with moderate geopressures (pressure gradient over 0.85 psi/ft) below about 6900'. Pressures calculated from the porosity measures correspond well with the direct pressure measurements. Since the method we use to derive pressure measurements from the wireline data examines only the role of compaction in the generation of overpressures, our success leads us to conclude that compaction is the primary force generating abnormal fluid pressures in the EI 330 Field area. Our work has been written up for inclusion in the volume summarizing the results of the Pathfinder drilling program (Hart, Deshpande and Flemings). Hart was responsible for organizing the sub-sampling and physical properties testing on core plugs at Core Laboratories' Houston and Carrollton facilities. It is

anticipated that the results of the physical properties tests will be combined with the pressure and porosity results described above for publication.

7.0 Penn State Calendar of Activities Related to Reservoir Characterization

1-5-94	Sent Charles Morris (Schlumberger) paper and digital stress test and flow test data.
1-31-94	B. Bishop attended week-long Z-MAP Plus training.
2-2-94	B. Hart visited Chevron to work with D. Sibley integrating dipmeter and seismic data.
2-7-94	Provided bottom hole temperature data for Gilles Guerin (LDEO).
2-14-94	Sent 8mm test tape of digital log data for blocks 330/337 to David Sibley (Chevron).
2-15-94	Sent 8mm tape of Pathfinder digital data to David McCormick (Chevron).
2-24-94	Sent Louise Durham figures to be used in her AAPG Explorer article.
2-25-94	Loaded raw data (received from Schlumberger) for Pathfinder Well.
2-28-94	Submitted article (with figures) describing the use of Landmark software on the drilling rig to Landmark's UserNet magazine.
3-15-94	Sent mud logger data for Pathfinder Well to Martin Schoell (Chevron).
3-29-94	Downloaded LDS data for Brooke Eiche (Cornell).

8.0 Summary

The Reservoir Characterization group has not significantly deviated from its projected schedule of completion dates. All of the subtasks which were to be completed within Phase I will be complete by June 1. The GANTT chart (Attachment 1) visually represents our progress and completions through the end of Phase I.

Questions regarding this report should be addressed to:
Beth Bishop (bethb@geosc.psu.edu)
(814)-863-9723

FORMATION PRESSURES IN THE PATHFINDER WELL

B.S. Hart, A. Deshpande, P.B. Flemings

Department of Geosciences, Pennsylvania State University
University Park PA 16802

Abstract

In this paper we present results of pressure measurements in the Pathfinder Well. Our data consist of: a) direct pressure measurements from production tests of the fault zone, wireline pressure measurements (Schlumberger's RFT/MDT tool) from just below the A Fault, and stress tests from above and below the A Fault; b) indirect pressure measurements obtained from drilling mud weights; and c) pressure values derived from the sonic log using a physically based model that relates shale compaction to effective stress. Soft geopressures are found below the GA and HB Sands down to just above the B Fault splay at 6742' MD (near 6520' TVD), and overpressures increase through the B, D and A Fault splays with moderate geopressures present below about 6900' MD (6700' TVD). The pressures we derive from the sonic log compare quite favorably with measured pressures. Since the model we employ to calculate overpressures assumes that compaction is the only force generating overpressures, the good agreement between calculated and measured values strongly suggests that compaction is the dominant force generating overpressures in the Eugene Island Block 330 Field area.

Introduction

The Pathfinder Well drilled from near-hydrostatic pore pressures to moderate geopressures, crossing in its path several fault splays which act as pressure seals. To understand the relationship between pressure and stress (Flemings et al., *this volume*), the in-situ conditions that guide fracture completion (Anderson et al., *this volume*) and the nature of fracture driven fluid flow, it is vital that the formation pressure field in the vicinity of the well be established. In this paper we attempt to integrate a variety of pressure indicators, including porosity, direct pressure measurements such as RFT (currently called Modular Dynamics Tester (MDT)) and production test data, drilling mud weights and formation pressures measured from a nearby well. Our objective is to characterize the pressure field in the vicinity of the Pathfinder Well. Since our direct formation pressure measurements cover a limited portion of the section, we employ a compaction relationship (where porosity in shales is an exponential function of effective stress) to predict pressures over longer intervals, and show that these calculated pressures compare well with the measured values.

The results presented here show that "soft" geopressures (fluid pressure gradient less than 0.65 psi/ft) begin beneath the IC Sand in the well (below about 6000' true vertical depth - TVD). Discrete pressure jumps are associated with the growth faults in the vicinity of the Pathfinder Well, suggesting that these features act as barriers to lateral flow. "Moderate" geopressures (fluid pressure gradient between 0.65 and 0.85 psi/ft[1]) are found in the lower portions of the well. Because the method we use in this paper to derive pressures from wireline data is based on the assumption that sediment compaction is the sole

[1] For ease of use in the petroleum industry, we use imperial measures in this paper. Appendix 1 provides a conversion chart that permits calculation of SI units.

force behind the generation of overpressures (see next section), the success we report here strongly supports the contention that compaction is the primary mechanism for the generation of overpressures in the Eugene Island Block 330 Field area.

Results

Direct Pressure Measurements

Three types of direct pressure measurement were collected from the Pathfinder well. These included: a) MDT, b) pressure measurements associated with the stress testing (see Flemings, *this volume*, for a discussion of stress test results) and c) production tests from the fault zone itself (see Anderson et al. *this volume*). The location in the Pathfinder well of the test locations described below is shown in Figure 1.

Modular Dynamics Tests

The initial experimental program included a suite of MDT measurements across the fault zone. However, the tool became stuck following the first measurement just below the fault zone at 7652' (TVD = 7308.8'), a second measurement was taken at the same location and no further MDT data were acquired. The Horner plots for the two tests are shown in Figure 2. For the first test (Fig. 2a), a value of $p^* = 6062.85$ psi (p^* is a pressure value extracted from the Horner plot which under some circumstances can be considered equivalent to the *in situ* formation pressure; see Dake (1978) for details) can be calculated. In the second test (Fig. 2b), the pressure rose more rapidly than expected after approximately 550 seconds, apparently the result of leakage around the testing device. The extrapolated pressure (p^*) for this test was 6125.23 psi. The *in situ* pressure values measured in these two tests can be converted to mud weights of 15.95 and 16.12 lb/gal (first and second MDT test respectively) using converted to equivalent mud weights using the formula:

$$mw = 0.052zp \quad (1)$$

where z is depth (TVD in feet) and p is pressure (psi).

Pressures During Stress Measurements

Formation pressure measurements were taken prior to each of the two stress tests. The measured depths of these tests were 7726' (test 1) and 7572' (test 2) (Fig. 3). Unfortunately, wellbore storage effects (afterflow) can be recognized in the pressure transient analyses from these tests (Charles Morris, personal communication, 1994), and so the extrapolated values of P^* will be greater than the true *in situ* formation pressure (Dake, 1978). Additionally, the pressure history during the two experiments was such that it was only possible to calculate a P^* for the second of the two tests (65' above the fault zone). Prior to stress test 2, the pressure test yielded a value of $P^* \approx 6000$ psi (Fig. 3) which is equivalent to a mud weight of approximately 15.95 lb/gal at the test depth. We emphasize that the p* value from stress test 2 is being employed here only to place an upper boundary on formation pressure.

Production Tests

The production testing (Anderson et al., *this volume*) provided several opportunities to calculate P^* using pressure transient analyses of shut- in tests. The interval shut in extended from 7610' to 7650' measured depth. The pressure history for the three shut in tests is shown in Figure 4. In each of the second and third shut in periods, the value of P^* is reduced with respect to the previous measurement. We interpret this to be the result of the low permeability of the formation. Thus, the first value of P^* (6088 psi, equivalent to 16.04 lb/gal at a mean TVD of 7630') provides the best estimate of original *in situ* reservoir pressure. A separate measurement, obtained during the frac-pack completion, yielded a P^* of 6133 psi, equivalent to at this depth 16.21 lb/gal.

Indirect Pressure Determination - Sonic Derived Pressures

Porosity and Pressure - Theoretical Basis

Athy (1930), and many other workers since, have suggested the existence of an exponential relationship between porosity and depth in young sedimentary basins of the general form:

$$\phi = \phi_0 e^{-\lambda z} \quad (2)$$

where ϕ_0 is original porosity at the sea floor, λ is a constant, and z is depth. It has often been suggested that in young sedimentary basins the porosity field deviates from this expected trend where fluid pressures are greater than hydrostatic (e.g. Fig. 5).

There continues to be much debate about the origin of overpressures, but there is a growing consensus that in the Gulf of Mexico, much of the development of overpressures can be understood in terms of compactional disequilibrium (e.g. Harrison and Summa 1991). When shale compacts freely, water is expelled and the porewater maintains a hydrostatic pressure gradient. When the permeability of the sediment is low enough that pore fluids do not freely escape, abnormal pressures (overpressures) result as the fluid assumes part of the load of the overlying sediment.

Compaction also influences sediment physical properties such as electrical conductivity, bulk density and seismic velocity, and many workers have used these properties to indirectly measure subsurface pressures (e.g. Eaton, 1975; Ham, 1966; Hottman and Johnson, 1965). These studies have been based on the recognition that changes in these properties follow linear trends in the zone of hydrostatic pore pressures (sediments freely dewater as they compact), and that departures from the linear trends can be used to calculated subsurface pressures.

In this paper, we express the porosity/depth relationship as one of porosity versus effective stress, modifying the Athy relationship:

$$\phi = \phi_0 e^{-\lambda\sigma} \quad (3)$$

where σ, the effective stress is expressed by the formula:

$$\sigma = \rho_r g z - p \quad (4)$$

and ρ_r is rock density, g is the gravitational constant and p is formation pressure. Inspection of equations 3 and 4 shows that porosity is an exponential function of depth in the hydrostatic zone since the relation between depth and effective stress is linear in that zone. However, when fluid pressures rise above hydrostatic values, porosities at that depth will exceed the values predicted by the normal compaction trend (Fig. 5).

We derive shale porosity from the sonic log using the empirical equation presented by Schlumberger (1989):

$$\phi = 0.67^{\frac{(\Delta t - t_{ma})}{\Delta t}} \quad (5)$$

where 0.67 is an empirically-derived constant, Δt is travel time (μsec/ft) from the sonic log, and t_{ma} is matrix velocity, here (in the absence of measured matrix velocities) taken to be 55.5. These porosity values can be used to derive formation pressure gradient (fpg) by inverting equation 2:

$$fpg = 1 - \frac{\log \frac{\phi_0}{\phi}}{0.434 \lambda z} \quad (6)$$

where 1 is the overburden pressure gradient (in psi/ft). Multiplication of the fluid pressure gradient by the depth (TVD, ft) yields the pressure. Work on sonic-derived porosities for several wells in the Block 330 Field area has shown that the constant λ is equal to 14.6×10^{-5} (Fig. 5) in the Eugene Island Block 330 Field area, and pressures calculated using equation 6 show good agreement with drilling mud weight (*cf.* Deshpande and Flemings 1994). Details of the derivation and use of equation 6 are presented in Appendix 2. In practice, we use the gamma ray log to separate sands and shales, then employ sonic log

values in equation 5 which have been "smoothed" using 50' moving intervals (100 measurements at .5' digital wireline data increments) to eliminate noise due to borehole effects or minor lithologic changes.

Sonic-Derived Pressures: Results

We used the smoothed sonic log to derive shale porosities in the Pathfinder well using equation 5. In Figure 6, we compare the sonic-derived shale porosities with those given by Schlumberger's density porosity tool, and show pressure gradient, overpressure and equivalent mud weight as calculated from our porosity measurements using the approach outlined above. Our calculated porosity values are approximately 25% greater than the density porosity values. We think this is principally because the values of the constants employed in equation 5 have not been calibrated to local conditions. We emphasize however that the pressures that we derive from the sonic-derived porosities depend not on the absolute value of the porosity, but rather on the deviation of the measured values from the empirically derived "normal" compaction trend.

Note that the sonic and density derived porosities track each other well (down to the lowest density porosity measurement at about 6900' MD), indicating that the relative porosity differences calculated using the sonic log are probably of the correct magnitude and sense. In general, the porosity decreases gently from the top of the well at about 4200' (MD) to about 6000', after which the porosity levels out. Below the "B" Fault (6742') porosity begins to increase before leveling out below 7300'. A slight increase (about 2%) in porosity is found across the "A" Fault.

The porosity values calculated with the sonic log were converted to pressure data using the approach outlined above (equation 6), and then converted to equivalent mud weights for comparison with drilling data (Fig. 6).

The pressure gradient calculated from the sonic-derived porosities is variable but generally about .5 psi/ft or less from the top of the well down to just above the "B" Fault at 6742' MD. Calculated overpressures are low or absent in this interval (generally less than 500 psi). The pressure gradient and overpressure both increase across the fault splays, with a nearly constant pressure gradient just over .8 psi/ft and overpressures of 2500-2600 psi calculated for the 700' below the A Fault. Mud weights derived from the pressure data will be discussed below. Because acoustic velocities (the tool we are using to derive porosities and, ultimately, pressures) are sensitive to both porosity and lithology (e.g. mixtures of sand and shale; *cf.* Marion et al., 1992), and the initial results presented here incorporate only a crude distinction between sands and shales, some of the "chatter" in the pressure data of Figure 6 may be due to variations in lithology.

In Figure 7 we compare the results of our sonic-derived pressure measurements (converted to equivalent mud weights) with mud weights taken from drilling data, and measured pressure data (also converted to equivalent mud weights). A gamma ray curve is provided for stratigraphic and lithologic reference. In general, both drilling and sonic-derived mud weights remain relatively constant down to the "B" Fault, although drillers increased the mud weight below 6500' MD in preparation for crossing that first fault splay. Calculated mud weight above the "B" Fault is approximately 11.5 lb/gal, whereas drilling data indicates values 2 lb/gal higher. Between the "B" and "D" faults, the data are too few to detect a clear trend (shales are not abundant in this interval, which is dominated by the MG Sand - see gamma ray curve). By the time the "D" Fault is reached, both measured and calculated mud weights show the effects of pressure increases - both mud weight measures are approximately 15 lb/gal at the top of this splay. Calculated values show a

deflection to lower mud weights associated with the OI-4 sand at approximately 7200-7300' MD. Drillers again increased mud weight (to 16.3 lb/gal) in preparation for crossing the next fault ("A" Fault) and maintained this value for the remainder of the drilling. Calculated mud weights suggest an increase in pressure equivalent to a mud weight increase of nearly 1 lb/gal across the "A" Fault. This value indicates a smaller change in pressure across this fault than that associated with the "B" and "D" faults which together account for an increase in calculated mud weight of 3.5 lb/gal.

In nearly all cases, the calculated mud weights are slightly lower (approximately 5 - 10%) than the measured mud weights. From experience, drilling mud weights are known to exceed those calculated from actual formation pressures by 10% (slightly overpressured drilling is common). The observed correspondence between calculated and measured mud weight values in the Pathfinder well therefore suggests that the calculated values must be close to the actual formation pressures. Anomalies are associated with the MG sands immediately below the "B" Fault and the OI-4 sands from 7200-7300'. The apparent lower pressures could represent pressure depletion in shales adjacent to the producing sands, or the effects of changing lithologies.

Also shown on the right side of Figure 7 are the mud weights calculated from the formation pressures measured during the MDT and shut-in/production tests which cluster together below 7600' MD (see Fig. 7b for a close up of the interval of the pressure tests). Maximum discrepancy between measured and calculated pressures is about 200 psi. The MDT results are within $^1/_2$ lb/gal of the values of the sonic-derived mud weights. The shut-in interval spans the fault zone (the 16.08 lb/gal value represents an average through this zone), while the sonic-derived mud weights indicate a $^1/_2$ lb/gal increase in pressure across the fault (from 15 to 15.5 lb/gal).

The mud weight derived from stress test 2 (known to overestimate the *in situ* pressure field, as described above) exceeds the value of the sonic-derived mud weight by 1 lb/gal. Also shown (7346' MD) is a point representing the initial formation pressure in the OI-4 sand as determined in the A-23 well a few hundred feet to the west of where that sand was penetrated by the Pathfinder well (data courtesy of Pennzoil). Assuming that pressures in the OI-4 and surrounding shales were in equilibrium in this fault bounded block prior to production, and compensating for the pressure effects of the hydrocarbon column in the sands, we have calculated a formation pressure equivalent to 14.8 lb/gal at this depth. This value matches almost exactly the value derived from the sonic log.

Discussion

The results presented herein indicate a generally good agreement between the mud weights calculated from the sonic log, and those measured during drilling operations. This suggests that the pressures we calculate are a good approximation of *in situ* formation pressures. Since the model we employ accounts only for the role of compaction in the generation of overpressures, the good results presented here suggest that compaction is the dominant force generating abnormal pressures in shallow portions (Plio-Pleistocene) of the Eugene Island Block 330 Field area.

The pressure data we have derived for the interval between 6000' and the "B" Fault suggest that "soft" overpressures are present beneath the HB/IC sands (Fig. 2). Abrupt jumps in pressure are associated with each of the fault splays, with most of the pressure increase associated with the "B" and "D" faults in the area of the Pathfinder well. The "A" Fault is associated with only a modest pressure jump (equivalent to approximately 1/2 lb/gal) at this location. Moderate geopressures are first found in the block between the B and D Faults,

and continue down to the base of the well. Our data and calculations indicate that hard geopressures (pressure gradient in excess of 0.85 psi/ft) are not found in the stratigraphic intervals we drilled.

We are currently investigating the origin of the apparent pressure excursions (such as those associated with the OI-4 and MG sands) which add a "sawtooth" character to the derived mud weight curve. Our hope is that by obtaining accurate measures of porosity, compressional wave velocities and grain sizes from core sub-samples, we will be able to quantify the sensitivity of our analytical technique to changes in these parameters.

Appendix 1. Conversion Table

1 ft	=	0.3048 m
1 psi	=	145.038 MPa
1 psi/ft	=	0.433 g/cm^3
1 lb/gal	=	8.3439 g/cm^3

Appendix 2. Derivation of Pressure Equations

We use the modified version of the Athy equation to determine "original" seafloor porosity ϕ_0 and λ from the zone of normal compaction (hydrostatic pressures):

$$\phi = \phi_0 e^{-\lambda\sigma}$$

This can be converted to:

$$\ln\phi = \ln\phi_0 - \lambda\sigma$$

which, upon conversion to base 10 logarithm becomes:

$$\log\phi = \log\phi_0 - 0.4343\lambda\sigma$$

in the hydrostatic zone, the effective stress (σ) is equal to the lithostatic gradient (here assumed to be 1 psi/ft) minus the fluid pressure gradient (here considered to be 0.465 psi/ft) times depth (ft), or:

$$\sigma = .535z$$

therefore:

$$\log\phi = \log\phi_0 - 0.232\lambda z$$

When shale porosity in the hydrostatic zone is plotted as a function of depth on semi-log paper, the slope of the line is equal to 0.232λ (allowing derivation of λ), and the intercept of the line is ϕ_0.

We are interested in calculating fluid pressure at depth in zones of abnormal fluid pressures, therefore we introduce the unknown variable x, which is the fluid pressure gradient we seek for a particular depth. We can introduce this unknown into the modified Athy equation, remembering that the effective stress is equal to the lithostatic gradient (here, 1 psi/ft) minus the fluid pressure gradient (x) times depth:

$$\phi = \phi_0 e^{-\lambda(1-x)z}$$

This can be rearranged as:

$$\log\phi = \log\phi_0 - 0.4343\lambda(1-x)z$$

which can be solved for the unknown fluid pressure gradient:

$$x = 1 - \frac{\log\frac{\phi_0}{\phi}}{0.4343\lambda z}$$

Multiplication of x by the depth (xz) yields the fluid pressure.

References

Athy, L.F., 1930. Density, porosity, and compaction of sedimentary rocks. Am.Assoc.Petrol.Geol.Bull., 14, 1-22.

Dake, L.P., 1978. Fundamentals of Petroleum Engineering. Elsevier, 443 p.

Deshpande, A. and Flemings, P.B., 1994. Effective stress, porosity, and abnormal pressures in the Eugene Island Block 330 Field. Abstracts, Am.Assoc.Petrol.Geol.Ann.Mtg., Denver, June 1994, *in press.*

Eaton, B.A., 1975. The equation for geopressure prediction from well logs. *Preprint*, 50th Annual Fall Meeting, Society of Petroleum Engineers/AIME, Dallas, Sept. 28-Oct.1, 1975, 11p.

Ham, H.H., 1966. A method of estimating formation pressures from Gulf Coast well logs. Transactions - Gulf Coast Association of Geological Societies, Volume XVI, 185-197.

Harrison, W.J. and Summa, L.L., 1991. Paleohydrology of the Gulf of Mexico Basin. American Journal of Science, 291, 109-176.

Holland, D.S., Leedy, J.B. and Lammelin, D.R. 1990. Eugene Island Block 330 Field - U.S.A., Offshore Louisiana. In: Structural Traps III, Tectonic Fold and Fault Traps. Treatise of Petroleum Geology Atlas of Oil and Gas Fields (compiled by E.A. Beaumont and N.H. Foster). Am.Assoc.Petrol.Geol., Tulsa, 103-143.

Hottman, C.E. and Johnson, R.K., 1965. Estimation of formation pressures from log-derived shale properties. Journal of Petroleum Technology, 717-722.

Marion, D., Nur, A., Yin, H. and Han, D., 1992. Compressional velocity and porosity in sand-clay mixtures. Geophysics, 57, 554-563.

Schlumberger, 1989. Log interpretation principles/applications. Schlumberger Educational Services, Houston, not consecutively paginated.

Figure Captions

1. Gamma ray and resistivity logs from lower portion of the Pathfinder well showing location of pressure measurements.
2. Horner plots from Modular Dynamics Tester measurements at 7652' (MD). a) Test 1, b) Test 2, note rapid build up of pressure due to leakage around seal of testing device. See text for further description.
3. Horner plot from pressure measurements preceding stress test #1. Wellbore storage effects were recognized in the pressure transient analyses, indicating that the value of P^* derived here is an overestimate of true formation pressures.
4. Pressure history of drillstem test and values of P^* calculated from pressure transient analyses for three shut-in intervals: 3-4, 5-6, 8-9. Formation pressures did not recover between shut-in intervals. See Anderson et al. (*this volume*) for a detailed discussion of production testing results.
5. Shale porosity vs depth plot for a well in the Eugene Island Block 330 Field. In the upper part of the sediment column, porewaters are in hydraulic communication with the surface and porosity is an exponential function of effective stress (σ).
6. Porosity logs and pressure measurements derived using equations described in text for Pathfinder well. Left: density (solid) and sonic (dashed) derived porosities. Sonic-derived porosity values exceed density-derived values, but the two curves track each other well, suggesting that *relative* porosity changes are being determined. Calculated pressure measurements discussed in text.

7. Comparison of measured (during drilling) and calculated mud weights. Also shown is mud weight value derived for OI-4 sand based on initial pressure (prior to production) of reservoir in A-23 well. a) entire well path, b) close up of lower portion of well. See text for further description.

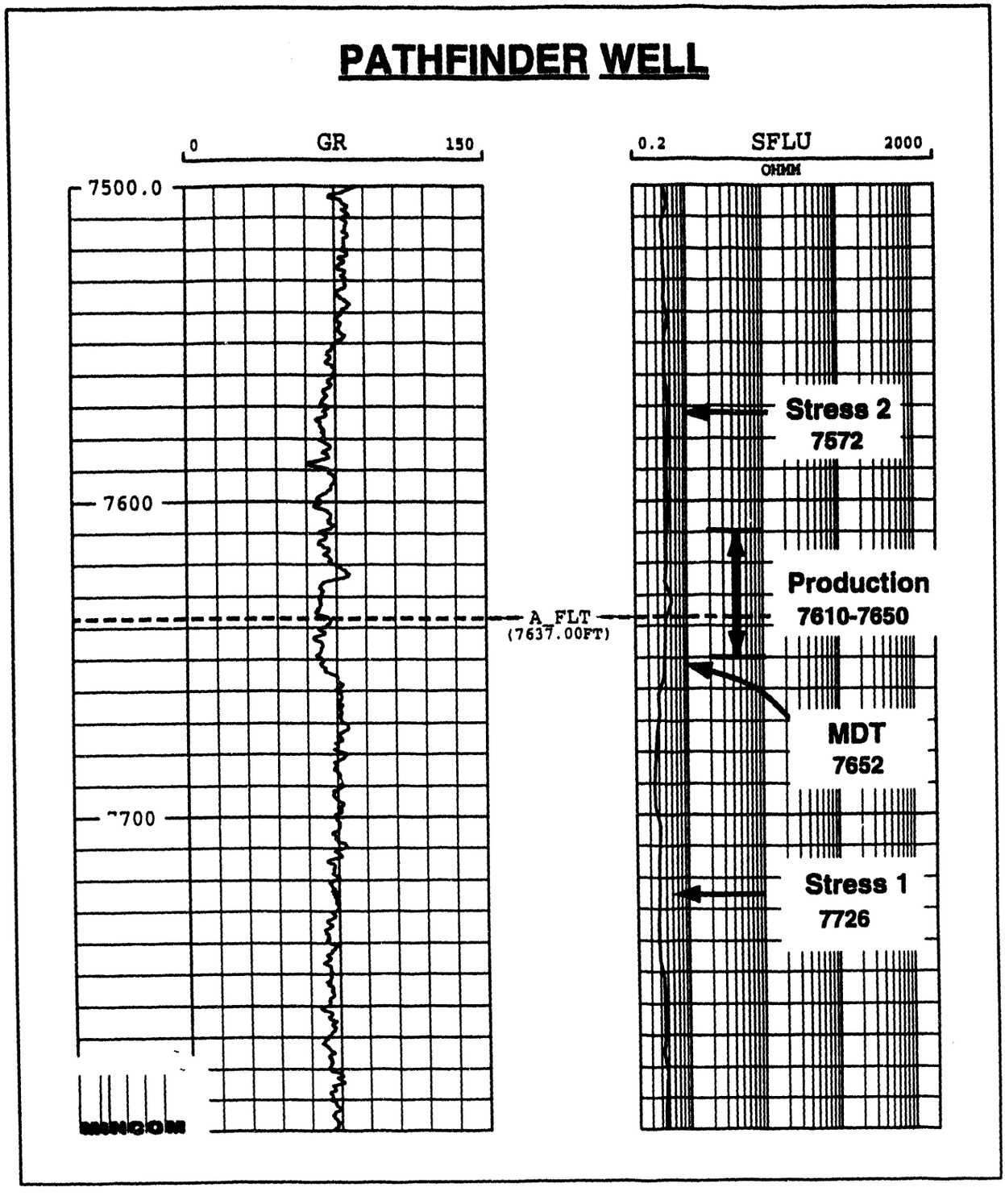

Hart, Deshpande and Flemings, Figure 1

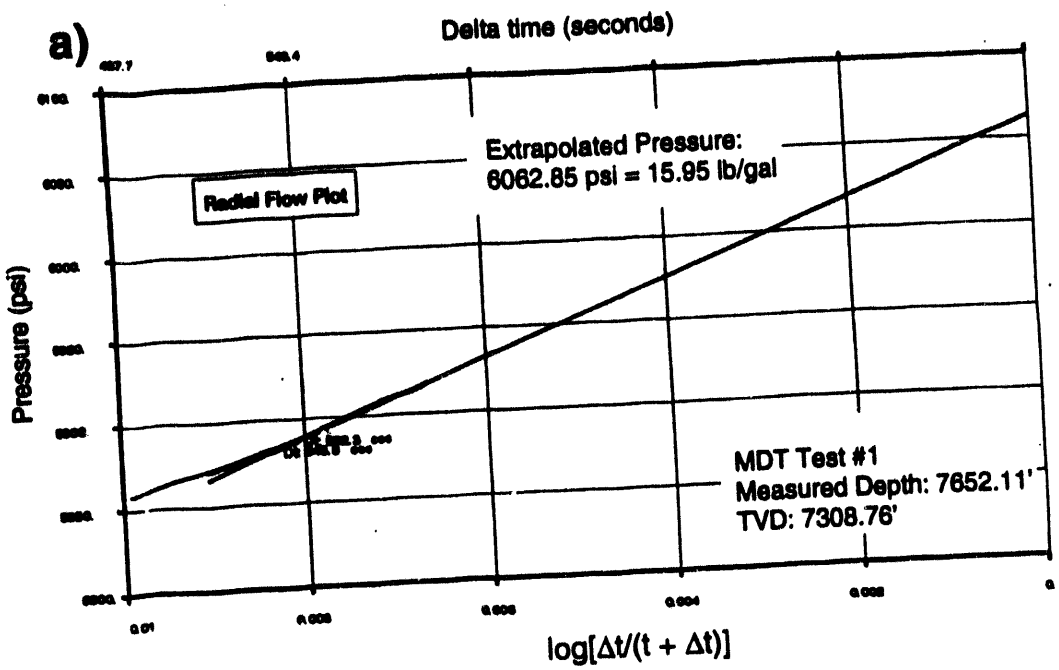

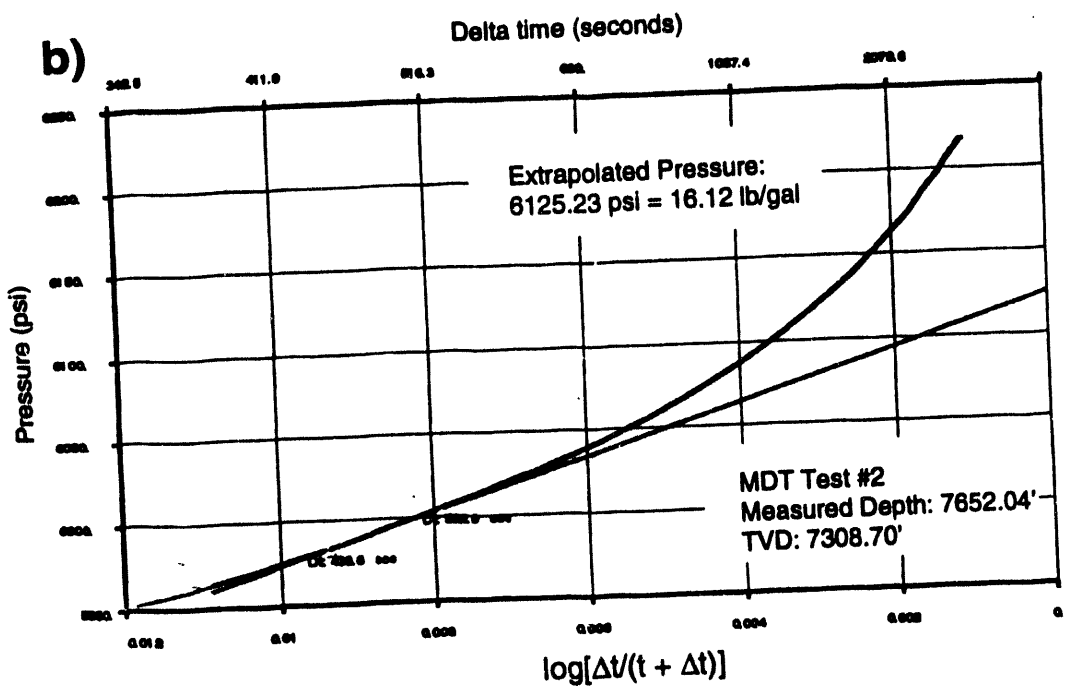

Hart, Deshpande and Flemings, Figure 2

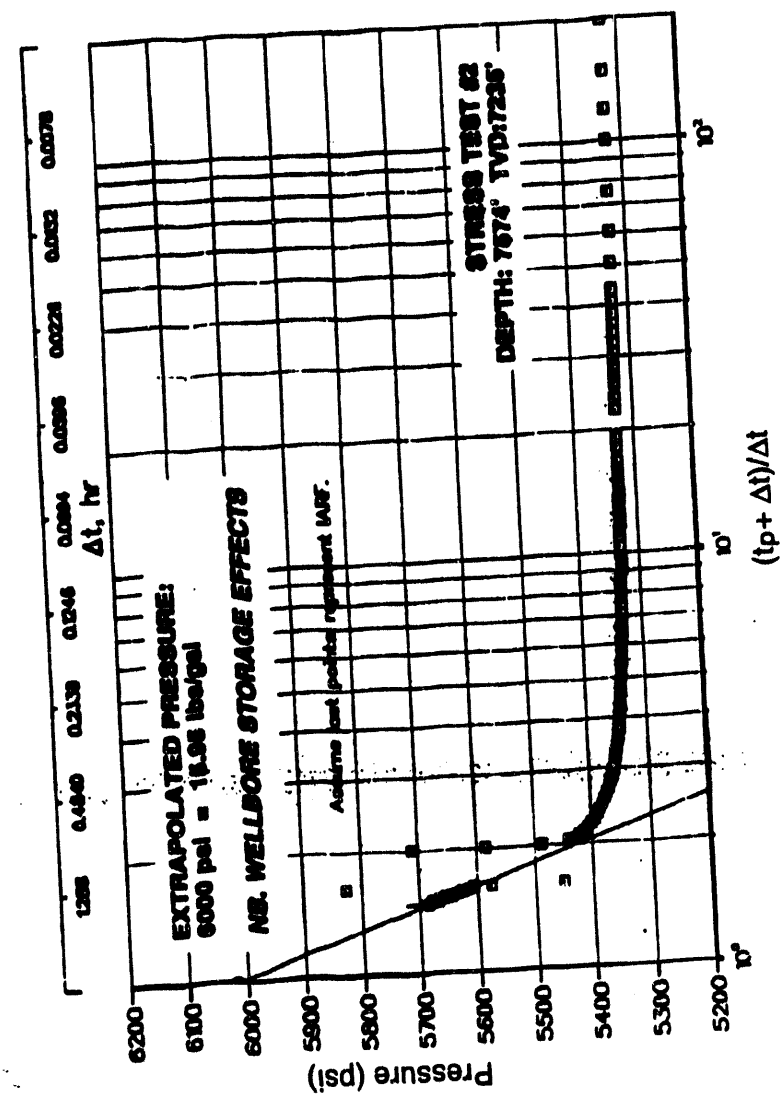

Hart, Deshpande and Flemings, Figure 3

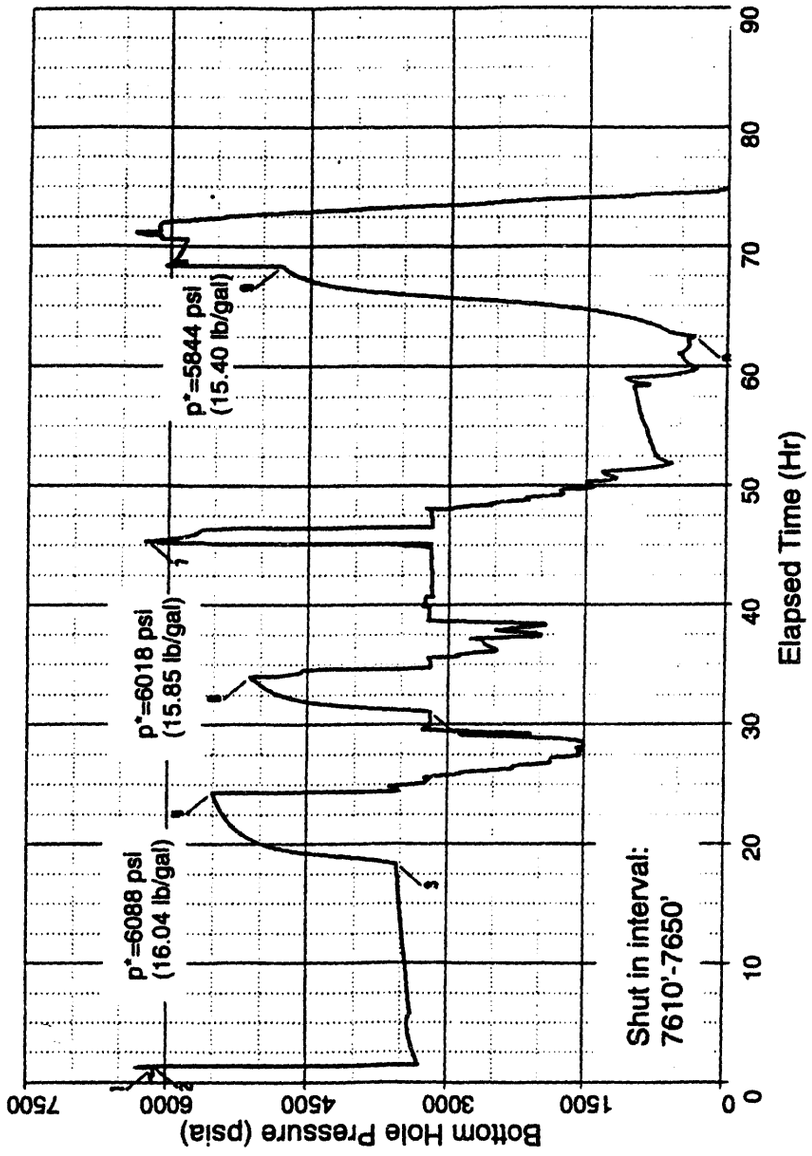

Hart, Deshpande and Flemings, Figure 4

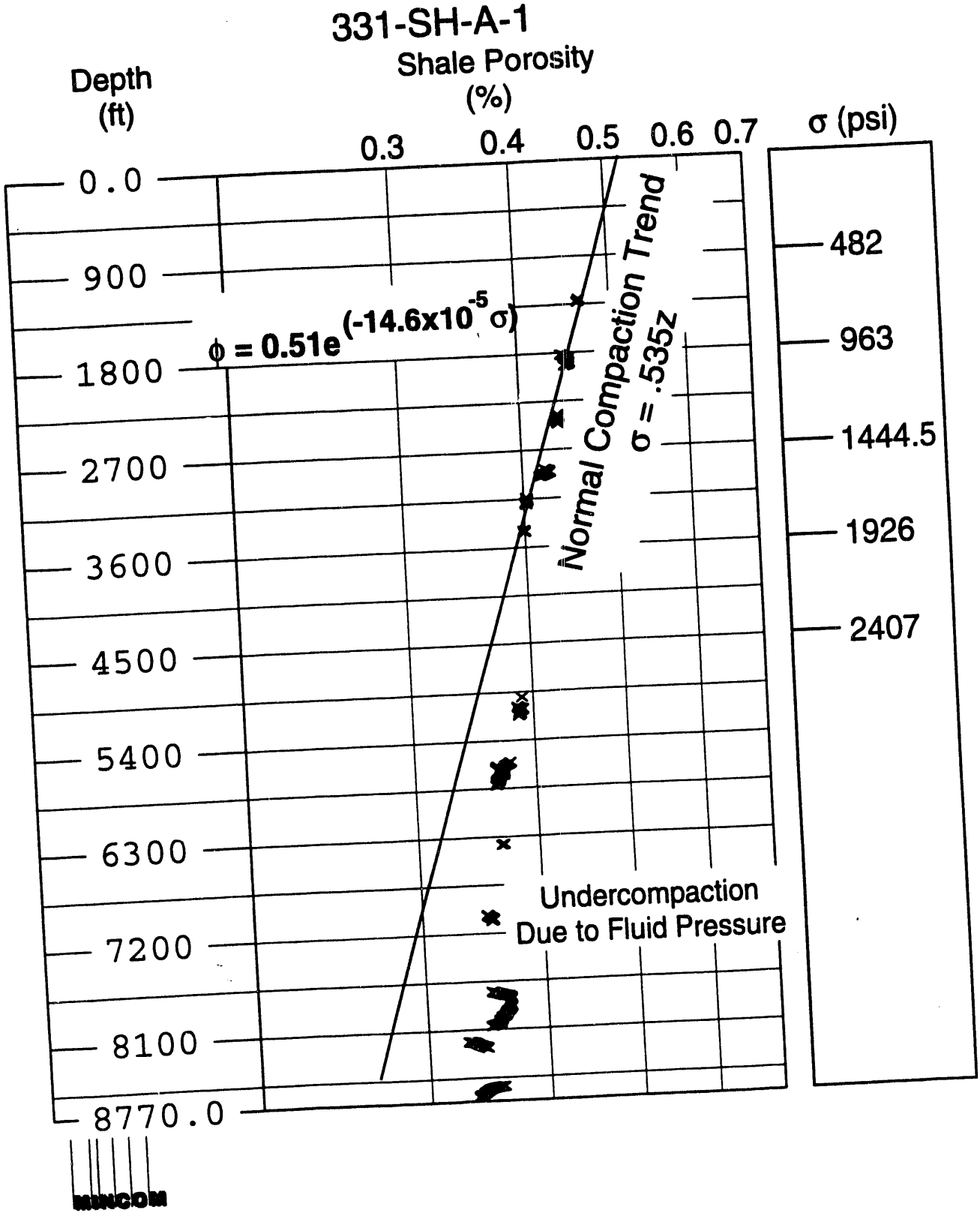

Hart, Deshpande and Flemings. Figure 5

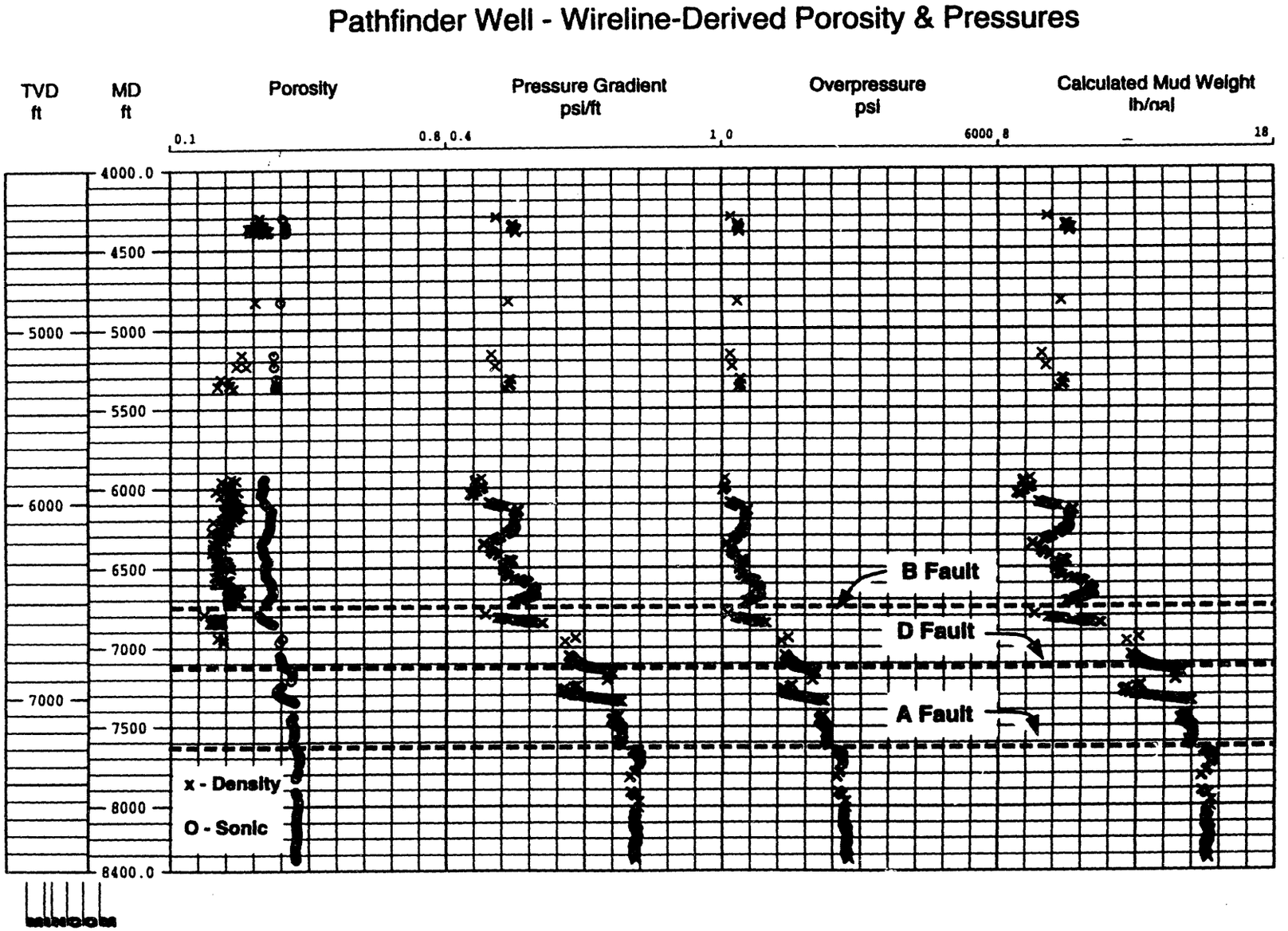

Hart, Deshpande and Flemings, Figure 6

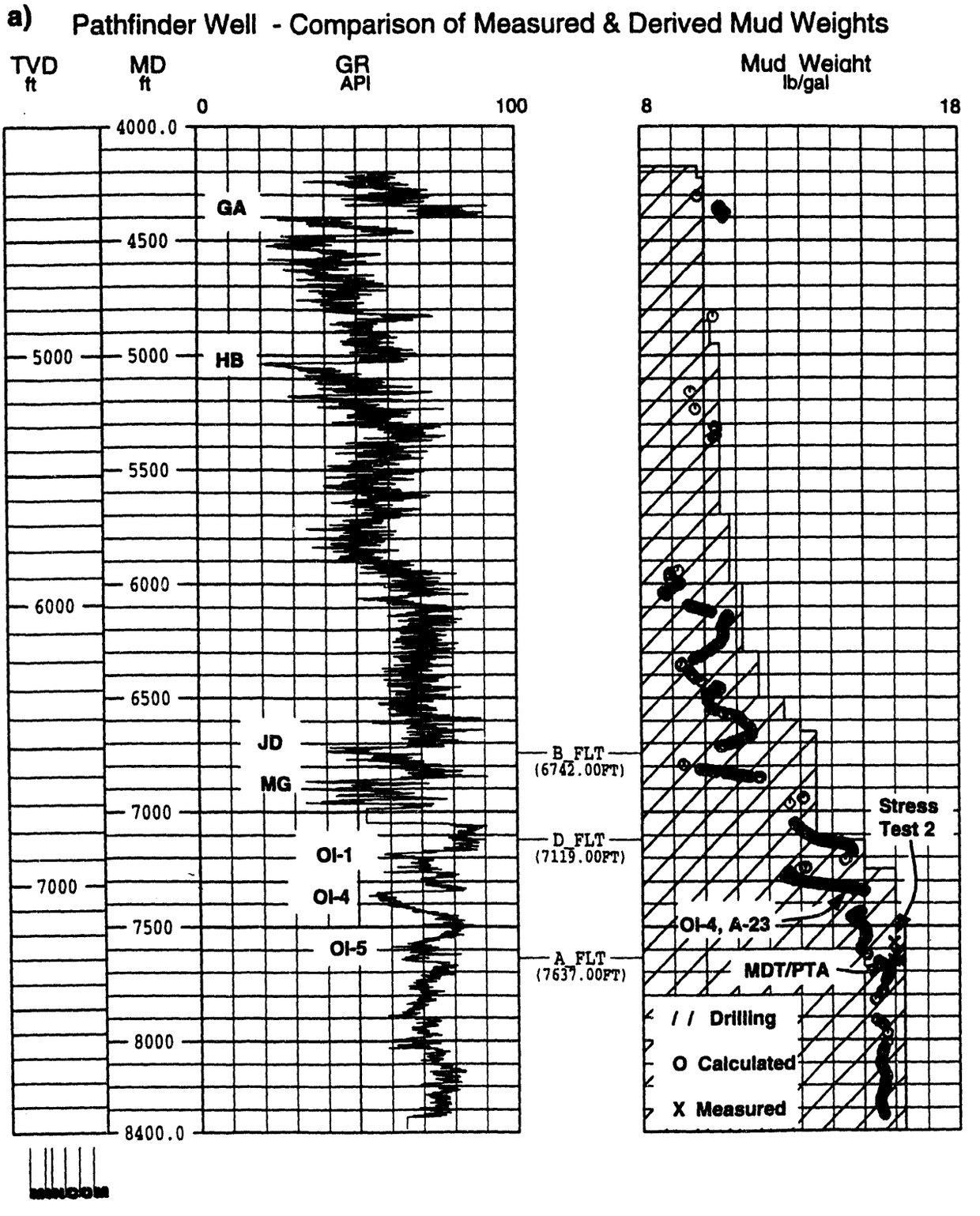

Hart, Deshpande and Flemings, Figure 7

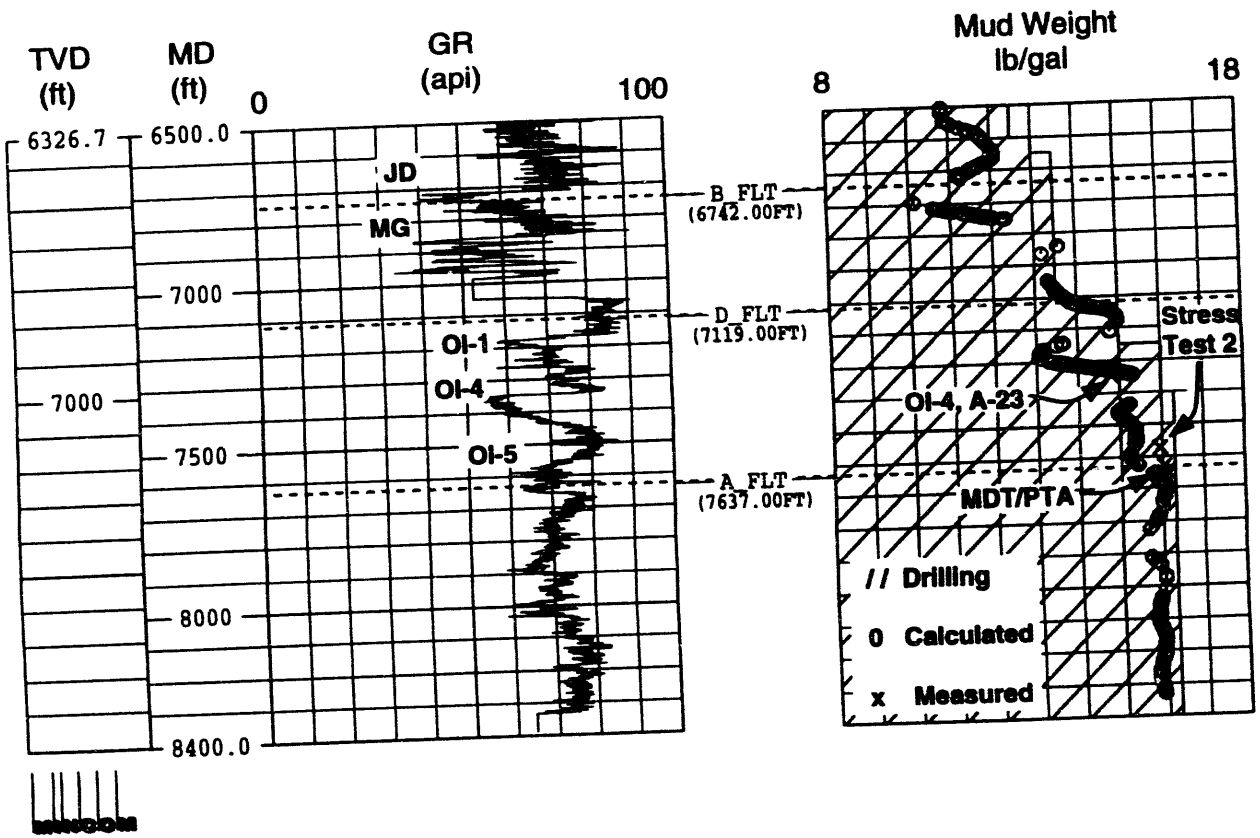

Hart, Deshpande and Flemings, Figure 7

TASK FIVE

MODELING

Larry Calthes - Cornell
Jeff Nunn - LSU

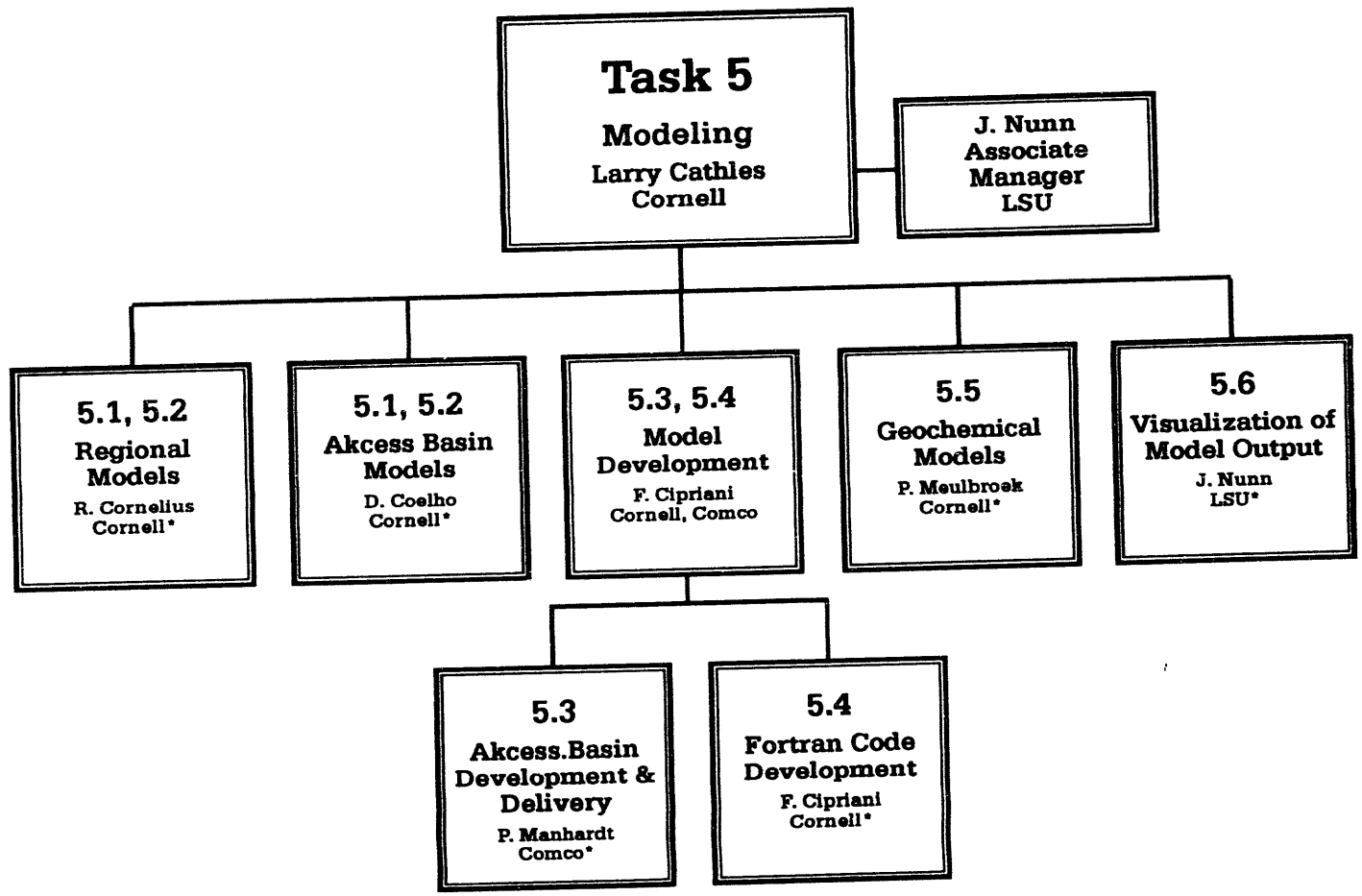
Task 5
Modeling
Larry Cathles
Cornell
J. Nunn
Associate
Manager
LSU
5.1, 5.2
Regional
Models
R. Cornelius
Cornell*
5.1, 5.2
Akcess Basin
Models
D. Coelho
Cornell*
5.3, 5.4
Model
Development
F. Cipriani
Cornell, Comco
5.5
Geochemical
Models
P. Meulbroek
Cornell*
5.6
Visualization of
Model Output
J. Nunn
LSU*
5.3
Akcess.Basin
Development &
Delivery
P. Manhardt
Comco*
5.4
Fortran Code
Development
F. Cipriani
Cornell*

5. Modeling

The major objectives for this quarter remained the same as last: (1) the integration of pre-processing and finite element modeling into a single user-friendly Akcess.Basin modeling system, (2) delivery of this system to our Corporate Affiliates, (3) completion of the conversion of templates from 2D to 3D, and (4) demonstration of realistic 3D modeling in the South Eugene Island Minibasin.

Although we thought we had substantially achieved the first objective last quarter, a strong flow of new ideas as we began to see what the modeling system could really do once integrated has led to many improvements this quarter. We have completed and augmented an improved Ageohist pre-processor and written a manual (attached at the end) that describes and illustrates in detail the processing of all the sections compiled to date. The output of this pre-processor is (1) movies of the basin evolution, and (2) all the unix files necessary to run Akcess.Basin.

The communications between the Ageohist pre-processor and Akcess.Basin have been augmented to include all the necessary input variables of Akcess.Basin. Running a case including pre-processing is literally as easy as typing "run". The pre-processor is included under and fully integrated with, the Akcess shell.

The interactive modeling tool, MODMAX has been extended so grid refinement, boundary conditions, initial conditions and material tables are all fully supported. The function of MODMAX is to provide for x-window (motif) graphics display of data which can then be modified using pull-down menu options and click and drag functions. This enables case studies to be carried out easily.

A final meeting of the modeling group to iron out all details of the 2D processing will occur May 24th to 29th at LSU. We are committed to an April 15th delivery to our Corporate Affiliates of the 2D Akcess.Basin modeling system

Progress has also been made toward 3D modeling. Pre-processors have been written to convert a series of parallel 2D models into the (macrofile) input for a 3D model. Sections for a local (SEI Minibasin) and a Regional 3D model have been assembled and processed in 2D. Critical missing parts of the 3D fortran have been completed. The main objective for next

quarter are testing 3D diapirism algorithms and then executing realistic 3D test cases.

The most important overall objective to be completed next quarter is a demonstration of realistic 3D modeling. It is the final critical part of phase 1.

5.1 Geologic Input

5.1.1 2-D flat files, SEI Minibasin Scale (100% completed)

Conversion was completed of the realistic (18 well 37 horizon) South Eugene island sections created last quarter from the geologic interpretation of Alexander and Flemings so that all wells are vertical and the horizons have common-age assignments. This resulted in the addition of several new utilities in the pre-processor. The set of four north-south "SEI Dimas" sections provides the input for generation of a 3D flat file, SEI Minibasin Scale (Task 5.2.2).

In addition a number of heuristic sections have been constructed to illustrate erosion, salt diapirism, and faulting. Three sections have been constructed in the Tampan Spur area of the North Sea. All of these sections, including the 3D sets of transects in the Gulf Coast have been assembled in an electronic Macintosh folder and can be processed by the Ageohist pre-processor. They thus serve as illustrations of the methods available for the input of geologic data to Akcess.Basin. A manual describing these examples and their processing has been written and is included at the end of this report. Although more sections will be processed in the future they will be done as part of student studies. The development and testing of input methodologies and the training of students that was the subject of this task is completed with the publishing of the Ageohist manual.

5.1.2 3-D flat files , SEI Minibasin Scale (100% completed)

Revised 3D flat files constructed at Cornell were visually inspected at ISU using GBRN-viewer and AVS. It was verified that the 4 profiles contain no errors that could be detected visually.

A C program has been completed that combines the sections in 5.2.1 to produce a 3D macrofile suitable for input to Akcess.Basin. The program is analogous to the 2D macrofile generator developed earlier. This completes the software developments needed to input three dimensional geologic data for 3D Akcess.Basin modeling. The 3-D macrofile generator can be applied to the four SEI Minibasin lines in 5.1.1, and also to the three, 300 km long N-S sections based on interpreted seismic lines contributed by Arco. The processing of the Arco lines to infer the history of salt diapirism was reported last quarter (Task 5.1.5). We thus are able to produce two 3D models addressing phenomena in the SEI area: one local and one regional. These two 3D geologic models complete this task. Future work will be reported under 5.2.4.

5.1.3 Realistic 3-D SEI description (30% completed)

The disk space required to process the Pennzoil 3D seismic survey was acquired and installed last quarter. Landmark techniques allow segments of well log traces to be plotted on a seismic section across a 3D survey wherever the wells pass within specified distance of a the section. A large number of well logs, previously converted from depth to time are being used to aid interpretation. A technique has been developed to output the x,y,z coordinates of the intersection of a chosen cross section and any picked surface. These coordinates can then be used to define the flat files needed by the Ageohist pre-processor. This methodology establishes the potential for a direct link between Landmark geologic interpretations and finite element Akcess.Basin geologic and fluid flow modeling, and will be a vital aid in the student modeling to be carried out under Task 5.2.4.

The Landmark was used this past quarter mainly to map the salt distribution in the SEI area. This is reported under task 5.1.7 (History of Salt Movement).

Major objectives for next quarter are: (1) the full development of an "automatic Ageohist section generator", (2) interpretation and Ageohist modeling of the development of the Red fault salt ridge, and (3) careful mapping of the faults and principal transgressive surfaces in the area of the Red fault that is the likely conduit of the hydrocarbons that filled the Pennzoil Block 330 reservoirs.

5.1.4 Present Porosity distribution (70% completed)

Major objectives for this quarter were to transfer the digital logs of the Pathfinder well to Cornell and to process them to predict porosity using the procedures developed in the previous quarter. The transfer has been accomplished and very interesting preliminary interpretations made. Parts of the fault zone have a Poisson's ratio very close to 0.5, suggesting that the fault zone is overpressured and acting like a fluid. This could explain the biogenic isotopic signatures of the hydrocarbons in the fault zone. A "fluid" clay would be impermeable to the movement of water, oil, or gas and could therefore trap and isolate bacterial gases produced when the zone was shallow. Porosities calculated from resistivity data show a large increase in porosity across the fault zone (from 12 to 35%). This increase could reflect the early development of overpressure (which would be compatible with the trapping of biogenic gas). The high porosities could alternatively have been created by block rotations caused by the fault movement. Although bloc rotations are observed in the core, an increase in porosity by this mechanism seems unlikely given the plastic (fluid) nature of the core.

The AVS techniques to process, cross plot and interpret, and ultimately to visualize in 3D that were initiated last quarter have been further developed. A major advance has been conversion of the data to field format. This allows AVS modules to be written to perform mathematical computations on the log data and makes possible a very flexible and powerful processing of log data. Calculations, manipulations, and comparisons of the logs can be strung together by dragging modules into a wiring diagram. Many variations in processing can be easily explored using this technique. An abstract reporting the early stages of this work has been submitted to AVS 94 to be held in Boston May 2-4, 1994. This abstract is attached at the end of this report.

Learning to construct the computational modules, writing specific modules to process our log data, and using these modules to process log data in the SEI

Minibasin are important objective for next quarter. Another high priority is to create the AVS networks needed to visualize the interpreted log data in 3-D. Once these tasks are completed, we should be rapidly able to define the porosity distribution in the SEI Minibasin in 3D using the digital logs from 43 wells provided by the Corporate Affiliates of the GBRN that we have loaded into AVS and also we should be able to process any of the 143 additional logs (largely form Pennzoil and Shell) that Penn State has loaded into the Landmark data base. The next step is modeling the porosity evolution of the SEI minibasin as one of the sub-projects in 5.2.4

5.1.5 Representative Volume Element (RVE) 2-D Seismic Lines (80% Completed)

Three, 300 km long interpreted seismic lines were processed last quarter to infer the salt movement and sedimentation history that could have affected the SEI Minibasin. The Colorado group has interpreted several higher resolution regional seismic lines that pass through the SEI area.

This quarter published salt literature has been studied to interpolate between the Arco lines and obtain sufficient resolution for an initial 3D regional salt redistribution model. The new sections of the interpolated regional model will be input to Akcess.Basin and combined wit the existing Arco lines using the Ageohist pre-processor. Akcess.Basin will then be used to assess he regional flux of water and hydrocarbons through the SEI Minibasin. We have previously run Akcess.Basin models to calculate overpressure development under heuristic salt sills. The second step will be to build more realistic model from the interpolated Arco lines. The final step will be to tie in the Colorado lines and produce as realistic a 3-D regional salt movement interpretation as possible. We hope to complete the second step next quarter. This last step is part of task 5.2.4, Specific Modeling Investigations.

5.1.6 Near Fault Details (10% Completed)

Work this quarter focussed on finishing the 25 block SEI interpretation based on the 2-D seismic profiles and well logs. This led to an understanding of when the salt migrated from center of the basin and the identification of a small down dropped graben within the center of the mini-basin. The seven mapped transgressive surfaces have been tied to 'regional' rises in sea level which have been noted in the literature. This allows us to calculate the accumulation rates within the mini-basin and upthrown areas. These rates range from 0.8 mm/yr in the shallowest section of the upthrown area to 3.6 mm/yr in the mini-basin during a time of progradation of the delta and provide a check for the calculations in the model. The 2D seismic and well log interpretation provides an excellent framework for modeling sedimentation and expulsion of fluids from the whole Minibasin.

What is now needed is a detailed mapping of the portion of the Red Fault system adjacent to the Pennzoil Block 330 fields through which hydrocarbons migrated into the Pennzoil reservoirs and which was drilled by the DOE Pathfinder well. A preliminary fault plain map has been constructed form the Pennzoil structure maps. It reveals juxtaposed sands in the shallow section, but not in the deeper section which contains several of the main reservoirs. We plan to map the principal transgressive surfaces and faults in the local recharge area. The transgressive

surfaces will be the same as in the 2D seismic interpretation and will be constrained by well logs as well as the 3D seismic data. Structure maps of the the of these surfaces will be output as paper sections. These paper sections will then be transformed to tops and bottoms of sands and hand processed to produce Allen Plane maps on the fault surface. The Allen Plane maps will show sand connections across the fault system and allow sand migration pathways up the fault to be mapped. They will form the basis of a fault trap analysis of Block 330.

At the same time sections across the transgressive surfaces will be output to the Ageohist pre-processor using the techniques described in Task 5.1.3. Fault macroelements will be flagged, and permeabilities assigned to the intra-fault zone elements in accord with the Allen Plane criteria. In this fashion Alan Plane flow can be calculated in Akcess.Basin. The calculated flow will apply not only to the present time, but also to all past times as the sand connections across the fault change over time in the developing Minibasin. This Access.Basin simulation of Allen plane flow will form the basis of part of one of the specific student thesis in Task 5.2.4.

5.1.7 History of Salt Movement (50% Completed)

The geometry of the salt at present is critical to the proper interpretation of temperature anomalies near the Pathfinder well. The evolution of the salt could be important to the proper interpretation of thermal maturity anomalies along the fault zone that was penetrated by the Pathfinder well.

Investigation of the present salt geometry was initiated this quarter using the Pennzoil 3-D survey and Landmark software. The analysis so far suggests that there have been several episodes of doming and silling on the salt ridge north of the Red fault. The first doming produced a salt sill. Differential loading of the sill by Plio-Pleistocene sediments then produced a later generation of domes. Withdrawal from the sill into these second-generation domes produced salt welds (windows of total salt evacuation) through which hydrocarbons would have been free to migrate. The salt movement on the ridge thus seems to be a small-scale version of the regional salt movements. Knowledge of when the salt migrated from the area is important, since the hydrocarbons that today fill the Block 330 reservoirs may have been generated at greater depths and trapped below the salt. Movement of the salt allowed the hydrocarbons to migrate into the overlying reservoirs of the EI 330 field.

The objectives for next quarter are to complete a careful mapping of the salt geometry near the Pennzoil oil reservoirs and the Pathfinder well and to use this geometric information as the basis for modeling thermal anomalies in the area in 3D, and, modeling the history of salt movement in 2D and, if code capabilities permit, in 3D.

5.1.8 Continuing modification of geologic input (Scheduled for initiation 7/1/94)

5.1.9 Geologic and Geochemical observations (~10% Completed; Scheduled for initiation 4/1/95)

The Landmark methods to display well information when the well passes within a specified distance of a selected seismic section that were described in Task 5.1.4 will be useful for the display and interpretation of chemical data. Sand, salt, and

fault distributions can be overlaid. The advantages of Landmark display of geochemical data will be investigated next quarter.

5.2 Model Simulations

5.2.1 2-D cross sections (100% Completed)

All the geologic sections discussed in Task 5.1 are now in Macintosh folders and all can be easily processed or re-processed with the Ageohist pre-processor as described in the Ageohist Manual attached at the end of this section. Example cases were developed and tested at LSU to insure compatibility with Akcess.Basin.

There was continued testing of Akcess.Basin at LSU. This testing included:

a) 1 km by 1 km box with salt wall on left side of domain:

i) Salinity only: Results show that saline water descended along the salt wall with high velocities and then spread laterally to the other side of the box.

ii) Coupled temperature and salinity: Flow pattern is similar to salinity only case, but results show the effect of downward flow on temperature isotherms near salt wall.

b) 1 km by 1 km box with salt column within domain: Coupled temperature and salinity results show that thermal buoyancy is not sufficient to reverse downward movement of saline waters next to the salt column unless background salinity is high. When background salinity is high, fluids move up along the salt column as the result of thermal buoyancy. These results are consistent with studies by Evans and Nunn, Jour. Geophys. Res., 1989.

Major additions to Akcess.Basin have also been made. These include the incorporation of a hydrocarbon maturation models programmed at Cornell, and fault venting models developed at LSU. A major effort was made over the last two months to incorporate all current developments into a common version of Akcess.Basin, and to structure this version with enough free variables so that the many student modeling projects that will form the basis of Phase 2 can be accommodated. Appropriate variables have been added to the code, and a seamless and easy flow from the preparation of geologic data through the processing of this data with Ageohist to the final Akcess.Basin finite element modeling has been largely achieved. This has proved much more difficult than originally envisioned. A major meeting of the group to iron out final processing and software communications problems is scheduled for March 24-28 at LSU. The aim is by shortly after this meeting to be able to run Akcess.Basin simulations of all the geologic histories in the Ageohist Manual (and more). These executed examples will serve both as starting points for the PhD projects of Phase 2 and also as a basic set of illustrations to be included in the delivery of the Akcess.Basin modeling system to our Corporate Affiliates promised for April 15, 1994. A full set of updated manuals will accompany this delivery.

5.2.2 3-D demonstrations (33% Completed)

The calculation of three dimensional venting on a parallel computer was demonstrated last quarter with the inclusion of a paper by Ruth ann Manning (et.

a.). Geologic data has been assembled into 3D macrofiles, and all the code required to run a 3D simulation has been developed, with the exception of fairly minor parts of the diapirism parts of the fortran hook (Tasks 5.4.1). Effort this quarter has been diverted to producing final 2D modeling system. This was the first priority because most of the issues faced in the 2D modeling must also be addressed in the 3D modeling, and because we have committed to delivery of the 2D Akcess.Basin system by April 15th.

The following heuristic 3D demonstrations are needed on the way to a realistic 3D demonstration (Task 5.2.3):

1. 3D venting with input overpressure
2. above plus 3D sedimentation
3. above plus 3D diapirism

The first demonstration has been achieved with simple lithology variations. The 3D temperature parts of this calculation need to be used to model the temperature field in a realistic SEI Minibasin to determine how salt and hydrocarbon structures influence the temperature field. This is planned, together with steps toward modeling realistic venting up the Red Fault sand units in the next quarter (see 5.1.7). Following this, and still next quarter, we plan demonstrations of steps 2 and 3. Their completion will complete this task.

5.2.3 3-D realistic SEI simulation (20% Completed)

The four SEI Dimas lines discussed in Task 5.1.2 have been processed with a new 3D macrofile generator to a 3D macrofile suitable for input to Akcess.Basin. The realistic SEI 3D model can be run as soon as Tasks 5.4.1 and 5.5.2 are completed. The partial completion reflects construction of the 3D macrofiles.

5.2.4 Specific Modeling Investigations (Scheduled for initiation 1/1/94)

A regional study was published this quarter that addresses general reasons for the location of the top of overpressure in the Gulf of Mexico Basin (abstract attached at end of this section). Finite difference models addressing the effects of salt movement on maturation, and the general effects of different compaction schemes on the evolution of sedimentary basins have also been constructed. These very large regional models by Ulisses Mello at Lamont will form an important framework for modeling that more specifically addresses the SEI Minibasin.

Work was initiated on venting on realistic 2D SEIDimas line 1. The grid was refined to minimize computational errors. The Red Fault was correctly placed in this modified grid. The consequences of venting were investigated. Results will be presented at the 1994 AAPG annual meeting in Denver.

5.2.5 Model Synthesis (scheduled for initiation 6/1/95)

5.2.6 Final Modeling Assessment (scheduled for initiation 6/1/95)

5.3 Akcess.basin preparation

5.3.1 3-D Template Preparation (80% Completed)

The TEMPLATE residuals for the basin modeling equations were extended from 2D to 3D. The AKCESS.BASIN Finite Element Matrix Library was extended to include gauss quadrature point variations of 1 to 4 in each coordinate direction or from 1 to 64 (4x4x4) for each finite element. The new capability was validation tested for quasi-linear conduction and convection, and is ready for incorporation into the overall 3D Basin model. With these accomplishments the 3D templates we need have been developed. They require testing. The main impediment to this is the availability of 3D graphic capability at CMC Paris where our main 3D developer is located. We are working on this problem; a partial and perhaps adequate solution is that he will be able to work on this problem for about a week at LSU at the end of March and early April.

5.3.2 Adaptation of Akcess.basin for parallel execution (80% Completed)

The current Akcess.Basin system is parallelized on the Kendall Square KSR1 (see last report) and this is adequate for the completion of Phase I tasks and for much of Phase II.

However, CMC has a number of ongoing projects aimed at providing a fast general PDE solver having unlimited algorithm variability using a TEMPLATE methodology (brochure attached) which will greatly benefit the DOE project. CMC is investigating, on a continuing basis the following means of increasing solution speed:

1.) Improve Non-linear stability (this reduces mesh requirements
2.) Improve convergence (reduces iterations and permits larger time steps
3.) Improve solver efficiency
4.) Improve code execution efficiency
5.) Parallel/Vector Processing.

In addition CMC is continuously seeking improvements in a factored solver, experimenting with Parallel Virtual Machine (PVM) implementation for efficient distributed processing, and adapting p-elements (imbedded grid refinement) to allow for automatic selective dynamic grid refinement. The results of this work will be incorporated into Akcess.Basin as soon as it is available. We will seek seamless incorporation of parallel techniques into Akcess.Basin. This ongoing effort is the reason for assigning an 80% rather than 100% completion of this task.

5.3.3 Two-phase templates (10% Completed)

A post doctoral researcher with experience in two phase flow modeling will be joining the Cornell group in April. His main job will be to develop 2 phase templates and assist in their implementation in 2 and 3D.

5.3.4 Consultation on and continued tuning of Akcess.basin (Scheduled for initiation 2/28/94)

This is late in starting. Consultation will begin after the March LSU meeting. We are still in the active program development stage.

5.4 Fortran Algorithms

5.4.1 Diapirism and compaction (70% completed)

Everything is now completed in 2D.

In 3D considerable work remains to be done. A great many changes have been made in the last quarter to the 2D code and we seek complete compatibility between 2D and 3D. This will require modifications to me 3D code. In principal 3D diapirism is a direct extension of 2D. We need, however, to be able to read multiple tabgro.txt files, need to be able to deflate salt structures to their starting configuration, need to be sure refinement works in 3D, etc. These are all straight-forward tasks but indexing is complicated in 3D and so we anticipate some effort will be required. The third heuristic test case described in Task 5.2.2 will be a simple test of the required 3D techniques. We expect to have tested 3D diapirism and compaction models by mid-May. This, next finishing everything regarding 2D, is our top modeling priority.

5.4.2 Fault Movement (50% Completed)

A method for computing extensional faulting while conserving sediment volume and allowing diapirism was reported last quarter. The method does not allow compaction, however, and based on this quarter's experience with the time required to produce a pull-down menu version of Ageohist, producing a version of this code user-friendly enough to be generally useable by the research group will be a time consuming effort. Also, our current experience suggests that most if not all of the faulting needed for studying the SEI minibasin and its regional context can be done with the sedimentation-driven fault models already put in user-friendly form. This task is considered to be of lower priority to the DOE project than the development of 3D models and inclusion of two phase flow in the calculations.

For this reason we have elected to significantly delay the deadline for this task, shifting intended completion from 6/31/94 to 12/31/94. By lowering the priority of this task and concentrating our resources on other areas we can produce a better product for the DOE project. Extensional faulting is an important long term goal. It is mainly a pre-processor development; the changes to Akcess.Basin will be minor. Our Corporate Affiliates have expressed a specific interest in faulting. We therefore, at this point, still wish to complete it, but at a lower priority.

5.4.3 Physical Property Algorithms (80% Completed)

The fabric theory algorithm has been completed and evaluated against other methodologies (cf., the MTU report by LUO et al reported last quarter). We know there will be a continuing need to implement alternative physical property algorithms, especially permeability. Consequently, this quarter we have included flags in the Ageohist pre-processor and Akcess.Basin that allow a user to select the physical property algorithms that he or she wishes to use in the Akcess.Basin calculations. This will, for example, allow a user to use a Karman-Kozeny relation for permeability rather than the fabric theory relation that is the default. Flags are included for permeability, compaction, thermal conductivity, porosity, and density models.

In addition we have generalized the material property flags to allow specific properties to be assigned to any element if its material property flag is negative. Material property flags are assigned to macroelements in the pre-processor and can be modified interactively using the Akcess system MODMAX. The properties are looked up from a table keyed to the value of the negative flag if the flag is negative. This provides a very flexible way to assign material properties in cases where the specific properties are known. This zone assignment scheme has been implimented and is currently being tested on a simple case. The one concept will will substantially increase the flexibility of Akcess.basin, especially for near surface environmental geology problems where direct measurements of hydrological properties are common.

5.4.4 Inorganic Alteration Algorithms (Scheduled for Initiation 3/31/94)

The objectives of this task are to incorporate chemical models from Tasks 5.5.3 and 5.5.4 into Akcess.Basin. This last quarter we incorporated organic maturation models. Models of the smectite-illite are almost ready for incorporation. Their incorporation is our principal goal for next quarter.

5.5 Chemical Models

5.5.1 Gas solubility and gas generation kinetics (90% Completed)

Incorporation of the Burnham maturation model into Akcess.Basin was reported last quarter. This quarter's objectives were to develop a 1D finite difference model of sedimentation and maturation. This has been accomplished and is being combined with fluid movements and phase separation effects. Discussion is given under 5.5.2 below.

5.5.2 Inorganic 1D alteration models with gas phase present (40% Completed)

Oil and gas transport are a fundamental part of inorganic alteration. Hydrocarbon maturation produces a gas phase into which volatiles partition. The loss of volatiles from the aqueous phase can produce significant inorganic alteration. Matching funds from the Gas Research Institute enabled the development last quarter of a finite element model that simulates the generation of oil and gas in a subsiding column onto which sediments are continuously being added. The finite element model calculates, from Burnham's kinetics, the rate and amounts of oil and gas that have been generated everywhere the column.

The syntax required to run C routines under fortran was extended to allow the running of C++ code. C++ allows treatment of compositions as a single variable and simplifies, both conceptually and in programming, the task of modeling the chemical changes in hydrocarbons as they separate into distinct oil and gas phases from a parent supercritical mixture.

The Mathmatica solutions reported last quarter that calculate the compositions of oil and gas after their separation from a deep supercritical mixture were converted this quarter to C++, and the C++ composition code is now being combined with the finite element calculations of oil and gas generation. The intent is to produce a model of the compositional changes in oils and gases as they are produced and migrate vertically from a basin. The ultimate objective is to be able to interpret the organic chemical variations we observe in the SEI Minibasin. Next quarter will

continue to focus on the organic aspects of this task. Calculations of inorganic alteration will begin in the following quarter.

5.5.3 Equilibrium inorganic chemical alteration (40% completed)

A series of CHILLER runs have been made this quarter to assess the nature and intensity of inorganic alteration that results from the reaction of sediments with their initial pore water. No fluid movement is involved in these calculations; the alteration is entirely driven by chemical exchanges between the sediment minerals and the original (immobile) pore water. The calculations have been carried out at 100°C on sediments with a mineralogy typical of those in the SEI Minibasin. They show that the alteration depends strongly on whether CO2 is supplied by organic reactions. If no CO2 is supplied, Ca Plagioclase converts to laumontite. If CO2 is supplied by organic reactions, the Ca plagioclase converts to calcite. The reactions are significant and it is vital that we fully assess this (no flow) kind of alteration before trying to interpret any additional alteration related to fluid flow. The objectives for next quarter are to run CHILLER simulations at temperatures other than 100°C, and to assess the impact on the alteration reactions of initial calcite in the sediments.

Modeling of the illite smectite reaction also progressed last quarter. Task 6 of the DOE project will generate a great deal of illite/smectite ratio data from the Pathfinder and surrounding wells, and it is important to have models to interpret this data. At present a model developed by Exxon that is significantly controlled by the activity of potassium is being used. We consider, however that the K/Na ration may be a more appropriate controlling variable and this is being investigated. In either case it should be possible to produce a model that takes into account sediment mineralogy but depends only on time and temperature for its calculated illite/smectite ratios. (1) Developing such a model, (2) calibrating it against illite/smectite ratios measured in the DOE samples, (3) incorporating the model into Akcess.Basin, and (4) using it as a predictive and investigative tool are the future goals of this part of this task. In the next quarter we hope to accomplish the first two or three of these goals.

5.5.4 Isotopic Alteration (10% completed)

This quarter the CHILLER code was modified to include the isotopic exchange between pore waters and sediments. The calculations need to be tested against Gulf Coast and other field data. Like the chemical calculations of Task 5.5.3 they can be carried out as a post-processing step on the output form Akcess.Basin. Thus the chemical and isotopic models will be relatively simple to combine with Akcess.Basin.

5.6 Visualization of Model Output

5.6.1 Common Computing Environment (100% Completed)

Liken software on Sparc10 at LSU, CMC, and Cornell. This application will be used to run APL preprocessor. Hyperedge software was ported to Solaris Operating System on Sparc10 at LSU. Coordinated with John Ameson and Charley Kego of Hypermedia on installation of and/or training on Hyperedge at Cornell, Michigan Tech., Penn State, and Woods Hole. Developed user interface components (Startup and Browser) to automatically enter information and results from Akcess.basin simulations into Hyperjournals. Hyperjournals will be used to

share model results between GBRN sites, train new users of Akcess.basin and transfer technology to industry.

Two modeling workshops were held at LSU: One in February and one in late March. We now have over 10 researchers with substantial familiarity with the Akcess.Basin modeling system. A simple set of notes was developed to train new users on Akcess.Basin 3.1.

AKCESS.Basin executes under control of the AKCESS.* STRM file. This file allows for recursive execution of modules for pre-processing, model execution and post-processing graphics. Some of the modules such as the AGEOHIST preprocessor, MODMAX model changer and VIEW2 graphics/movie viewer allow the user to specify and adjust input and view save and retrieve graphics. This module interaction using compatible data structures provides a seamless modeling environment that leaves the analyst free to experiment and analyze the results of complex basin parameter variations without concern over complex file handling and machine operation.

5.6.2 Standardized Input Data File and Macrofile Generation (50% Completed)

The AGEOHIST pre-processor was substantially impoved this quarter and is fully described in the attached geohist manual. All of the cases run to date are preserved in a set of folders and can be processed and run easily. They constitute an effective set of traaining examples.

Macrogen 2D was extensively altered to accommodate changes in Akcess.basin 3.1. Changes include different handling of fault/seal flag, individual interpolation flags for each Akcess.basin variable, nodal numbering scheme that is consistent with ModMax software to visually inspect and alter macrofiles, addition of physical property zones to override lithologically determined hydrologic properties (e.g., permeability) and automatic refinement of macroelements according to some maximum width and height of a refined element.

Macrogen 3D software was developed and subsequently modified to include new features described above for Macrogen 2D. 3D realistic macrofile, tabgro and seal files generated from 3D flatfiles for SEI as described in section 5.1.2. Files have been visually inspected for errors. We are waiting for implementation of 3D realistic version of Akcess.basin to continue development of Macrogen 3D.

5.6.3 Visualization and Image Transmission (30% Completed)

Testing of the Motif graphical user interface version of GBRN-Viewer was completed. Fixed bugs to scalar field interpolation and rubber band box zoom. Added user selectable x,y,z ranges and multiple scalar fields associated with one x,y grid. Beta version of software will be released to other GBRN sites next quarter.

In the next quarter, the animation section of GBRN-viewer will be incorporated into a separate GBRN-Player which will allow us to distribute images or animations of our results to industry over the network.

Next quarter, we will add isosurfaces and begin looking at ways to view vector fields to 3D AVS visualization network. 3D visualization work has slowed until we have 3D model results to visualize.

Table 1. Gantt Chart for Task 5, Modeling. Entries revised from last quarter of 93 are indicated by an asterisk (*). Fully completed tasks are indicated by a pound sign (#).

Task #	Name	Start (including the dates)	Finish	
5.1	**Geologic Input**	10/1/92	10/31/95	
5.1.1	2-D flat files	10/1/92	6/30/93	#
5.1.2	3-D flat files	3/1/93	4/30/94	#
5.1.3	Realistic 3-D SEI description	6/1/93	6/30/94	*
5.1.4	Present Porosity distribution	10/1/92	7/31/94	
5.1.5	Representative Volume Element (RVE) 2-D Seismic Lines	10/1/92	7/31/94	
5.1.6	Near Fault Details	10/1/93	10/30/95	
5.1.7	History of Salt Movement	1/1/93	6/30/95	
5.1.8	Continuing modification of Geologic input	7/1/94	6/30/95	
5.1.9	Geologic and Geochemical observations	4/1/95	10/30/95	
5.2	**Model Simulations**	10/1/92	10/30/95	
5.2.1	2-D cross sections	10/1/92	6/30/93	#
5.2.2	3-D demonstrations	2/1/93	6/30/94	*
5.2.3	3-D realistic SEI simulation	8/1/93	6/30/94	*
5.2.4	Specific Modeling Investigations	1/1/94	6/30/95	
5.2.5	Model Synthesis	6/1/95	10/30/95	
5.2.6	Final Modeling Investigations	6/1/95	10/30/95	
5.3	**Akcess.basin preparations**	10/1/92	6/30/95	
5.3.1	3-D template	10/1/92	4/30/94	*
5.3.2	Adaptation of Akcess.basin for parallel execution	3/1/93	4/30/94	*
5.3.3	Two-phase templates	7/1/93	12/31/94	*
5.3.4	Consultation and continued tuning of Akcess.Basin	2/28/94	6/30/95	

5.4 Fortran Algorithms		10/1/92	3/31/95
5.4.1	Diapirism and Compaction	10/1/92	6/30/94
5.4.2	Fault Movement	2/1/93	12/31/94 *
5.4.3	Physical Property Algorithms	10/1/93	3/31/95
5.4.4	Inorganic Alteration Algorithms	4/1/94	1/31/95
5.5 Chemical Models		10/1/92	2/28/95
5.5.1	Gas solubility and generation kinetics	10/1/92	6/30/94
5.5.2	Inorganic 1D alteration models with gas phase present	6/30/93	12/31/94 *
5.5.3	Equilibrium inorganic chem. alteration	10/1/92	12/31/94 *
5.5.4	Isotopic Alteration	7/1/94	2/28/95
5.6 Visualization of Model Output		1/1/93	10/30/95
5.6.1	Common Computing Environment	1/1/93	9/30/93
5.6.2	Standardized Input Data File and Macrofile Generation	1/1/93	10/31/95
5.6.3	Visualization and Image Transmission	1/1/93	10/31/95

Reports and Abstracts

Two **abstracts** were submitted and accepted this quarter and one **paper** was published: The abstracts were submitted to the Margins Session of the American Geophysical Union and to AVS 94 to be held in Boson May 2-9. Both are attached below. The paper was published in the Journal of Geophysical Research; its abstract is attached below.

$TITLE$
Sedimentation, Salt Diapirism, Fluid Flow and Hydrocarbon Migration# in an Area of Very Active Sedimentation Offshore Louisiana, Gulf of# Mexico

[*L M Cathles*] (Cornell University, Ithaca, NY 14853; 607-# 272-1773; e-mail: cathles@geology.cornell.edu); R N Anderson# (Lamont-Doherty Earth Observatory, Route 9W Palisades,# NY 10964; 914-365-8335; email: anderson@lamont.ldgo.columbia.edu);# J Nunn (Lousiana State University, Baton Rouge, LA 70803; 504-388-# 6657; email: jeff@squirt.geol.lsu.edu), and The Global Basins# Research Network

The Eugene Island Block 330 field lies ~140 km southwest ot New Orleans in the Gulf of Mexico. It contains over a billion barrels of oil and gas equivalent hydrocarbons in Pleistocene sediments. This, and hydrocarbon seeps in the general area, attest to recent and continuing hydrocarbon migration in an area of very rapid (>2 km/ma) sedimentation. The Global Basins Research Network is investigating how hydrocarbons are moving up a growth fault system on the southern margin of a salt ridge just north of the Eugene Island Block 330 to fill the Block 330 reservoirs. The investigation is based on large amounts of contributed industry data and includes the analysis of multiple 3D seismic surveys, digital well logs, modeling of regional and local sedimentation, compaction, salt diapirism and fluid flow. With matching funds from DOE an 8000' scientific well was drilled into the fault zone this last winter to obtain core, logs, and fluid samples from the proposed migration pathway within the fault zone. Modeling and analysis of the data are ongoing at the present time. The talk will describe the current status of data analysis and interpretation.

AVS Techniques for Well Log Analysis of the Eugene Island Field
Track: Oil and Gas Exploration and Production

B.S. Eiche, M.L. Hauck, L.M. Cathles, and E.P. Bagdonis

Abstract

Standard well log analysis can evaluate characteristics of subsurface formations. The rock properties are defined by responses recorded by various tools. The properties such as porosity, lithology, density and resistivity define different rock formations. Other measured properties such as well diameter help to screen out poor data. Typically, well logs are evaluated by "eyeballing" the paper copy. AVS provides a visual means of evaluating different well logs. This study demonstrates how various subsurface rock geometries can be defined using well log analysis techniques within AVS.

Well log analysis is an important tool in understanding the subsurface rock formations. It can reveal information concerning rock structure and rock composition or lithology. The data available from well logging exists in a form where multiple parameters are typically measured over a certain depth interval.

In the Eugene Island Field, Block 330, Louisiana, a well was drilled by the Global Basin Research Network in November 1993. Over sixty well log traces were recorded over the same depth interval. This data provides an ideal testbed for developing AVS-based log interpretation methods.

The well log data obtained is in ASCII format in columns and rows. The portion of the data set in this paper consists of15 columns (traces or data types) and 2886 rows(depth). The data types include the diameter of the well, sonic travel time, gamma ray, compressional and shear velocities, and X and Y coordinates.

The analysis of this data begins with a first order observation of the data in AVS. In **Graph Viewer** the data is entered by selecting **Read Data**, and then **Read ASCII file**. **Plot as XY Data** is chosen and then the significant columns to be viewed are selected. In Figure 1 the data columns selected represent the caliper and true vertical depth. The file containing the data is chosen and the plot containing the data appears on the screen. The y-axis should be selected to represent the depth component of data and the **Axis Display** should be changed to plot depth increasing downward on the plot. The axis can be further customized by editing the **Number of Tics** and **Decimal Precision**. **Titles, Labels and Legends** are added to provide clear explanation of the graph. To save and print this on a printer, the **Write Data** and **Write Postscript** are selected. A new file name is entered and a system command outside of AVS must be given to submit the print job.

Multiple plots can be made for the various parameters available in the data set. Each parameter may be plotted against depth. The resulting curves are similar to the well log traces available in paper copy from the well log company which made the measurements. At this point the advantage AVS provides is the ability to customize the log. AVS allows the manipulation of the axis range to expand or reduce for the detail of observation required.

A more significant advantage of AVS occurs when crossplots are produced. Crossplots remove the depth component from the data and plot well

characterization parameters against each other. This kind of plot reveals significant groupings or trends within the data and quickly shows data points which do not match the data or do not belong in the trend. The crossplots are an excellent way to verify data and observe data trends. Crossplotting parameters can be useful for rock typing, locating anomalies, evaluating water saturation and defining porosity.

The method for producing crossplots is similar to the method used to produce the X-Y plot described above except other data parameters are substituted for the depth. An example of the crossplot data is in Figure 2 which shows the resistivity log versus the gamma ray log. The gamma ray log indicates the lithology of the rock while the resistivity indicates the type of fluid present. Two distinctive groupings are apparent, one is sand and the other shale. Establishing a typical range for that rock type helps identify poor or anomalous data.

To this point the direct use of an ASCII file has been discussed. AVS is more powerful when the modules are used to manipulate the log data. The modules can only handle AVS field files. They will not read ASCII files except for the **File Descriptor** module. The ASCII log data is converted to an AVS Field File using the **File Descriptor** module. This module is brought into the work space using the **Network Editor**. The raw log data is in one dimensional format. It only becomes two dimensional after the X and Y components are used for a plot.

The following parameters were used for the file description:

Dimension of compute space	1
Dimension of physical space	Not Applicable
Vector length	15
Data type	float
Uniform	uniform
Labels	enter all 15 labels
Dimension	ASCII, float, line-word
Data	File based, ASCII, float, line-word
Points	Not Applicable
Variables	Not Applicable

The data file has 15 columns and 2886 rows. The vector length is 15 and the 15 labels are entered to help keep track of the data. The data file itself must be edited and the number 2886 should be on the top line by the left margin to identify the file length to AVS. The description of the Data requires that each data column is defined using a line# and word# entry.

This describes the location and format of the data. How to determine the correct line and word number identification in the above description is explained in the AVS documentation.

Additional modules should be brought down to help save and view the description. Connecting the **Print Field** and **Write Field** modules below the **Field Descriptor** helps save and view the description.

At this point the data should be saved as an AVS Field File and can be used in the **Read File** module. The **Extract Scalar** module allows the use of unique data elements. These data elements can then be applied to industry equations developed using the **Field Math** modules.

The applications from this point are as vast as the entire well logging industry. Various programs exist in the industry to help with log analysis. A unique advantage in using AVS for this analysis is the capacity to view the well log data in three dimensions. Traditional views have been within two axes. Adding the third axis and interpreting its significance will be helpful in understanding the correlation of well log properties.

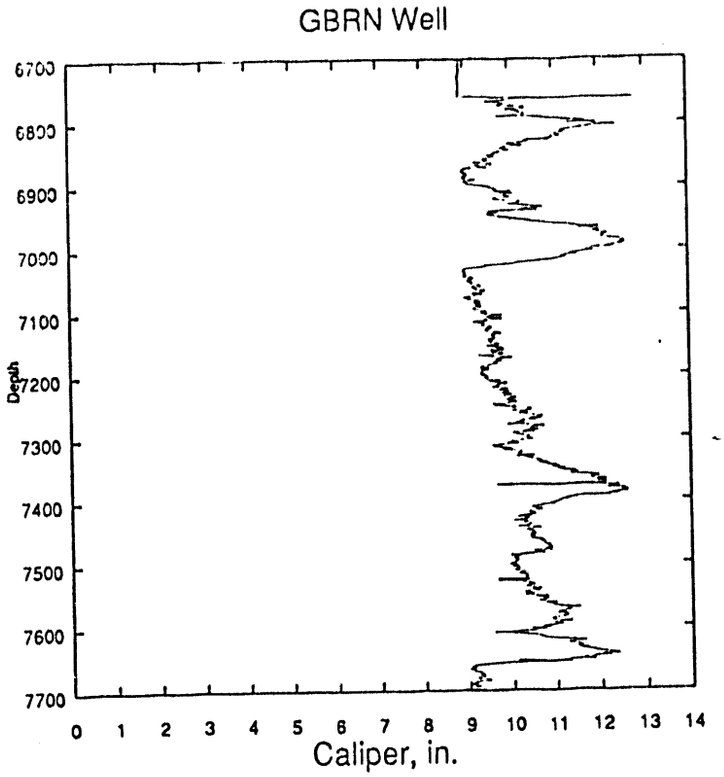

Figure 1

Traditional crossplot

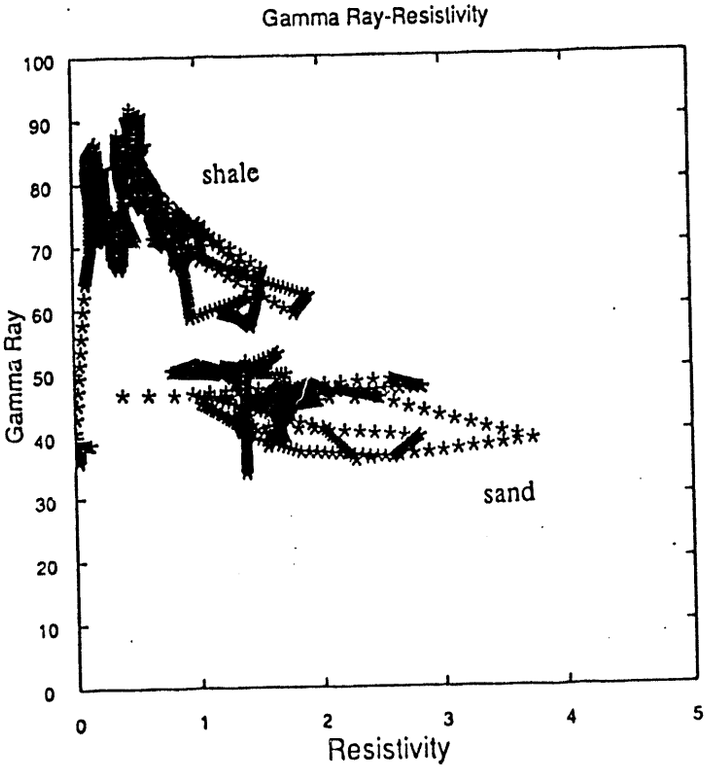

Figure 2

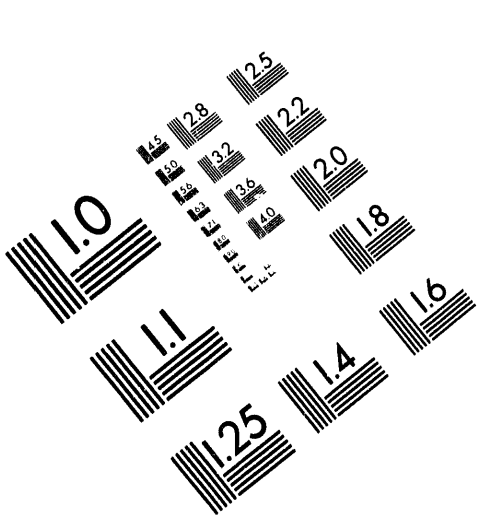

AIIM

Association for Information and Image Management
1100 Wayne Avenue, Suite 1100
Silver Spring, Maryland 20910
301/587-8202

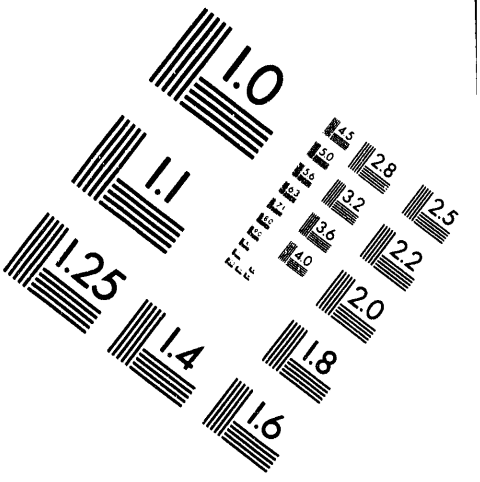

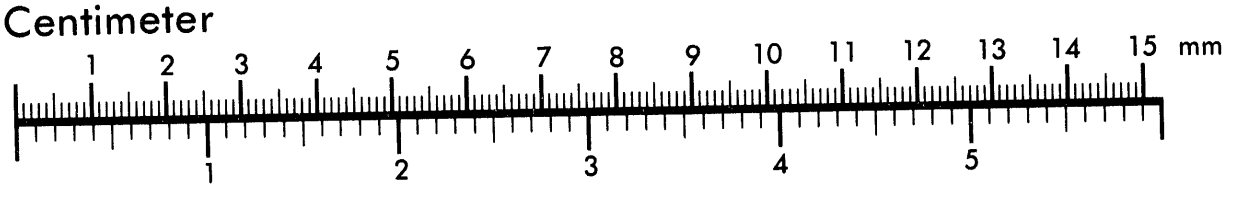

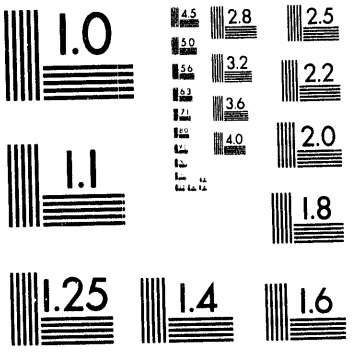

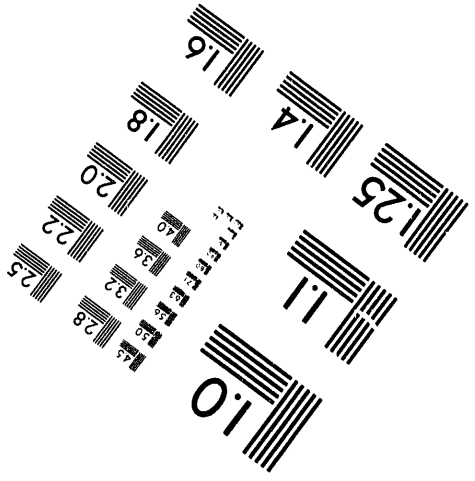

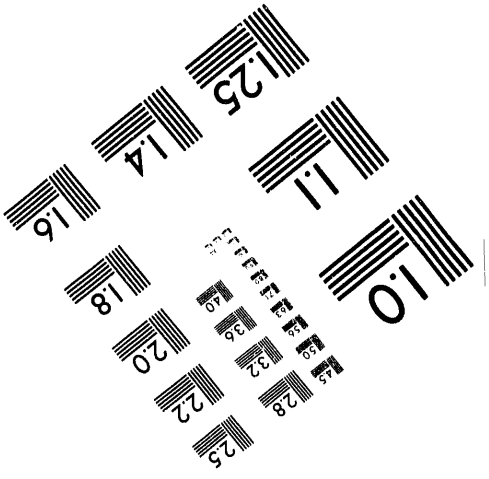

2 of 3

Enclosures:

1. AGEOHIST Manual

2. CMC Template Brochure

*AKCESS.**

A SOFTWARE PLATFORM FOR *RAPID* IMPLEMENTATION OF FINITE ELEMENT MODELS

A Product of

Computational Mechanics Corporation

Knoxville, Tennessee 37919-3382 U.S.A.

*AKCESS.** -- *THE SOFTWARE PLATFORM*

AKCESS.* is a *totally new* software platform from CMC for truly general applications of computer based modeling. Historically, computational fluid dynamics (CFD) algorithms have been directly coded for specific applications. The programs were designed for very specific theories and problem classes. ***AKCESS.****, *the first of its kind*, was specifically developed to shorten the problem definition/solution cycle.

AKCESS.* is a modern, UNIX® based software platform that is X-Windows (MOTIF) compatible. Finite element weak statement algorithm TEMPLATES are available for diverse applications in **fluid mechanics, heat transfer** and **mass transport** simulations. With the executable version, the user can solve interdisciplinary real-world problems having unlimited boundary condition specifications and arbitrary geometries. Input data are developed interactively using simple point-and-click operations.

The developer version of ***AKCESS.**** allows for changes to the computational algorithm. The scientist/engineer need not be a coding expert to modify an algorithm. It is simply a matter of altering a few lines of TEMPLATE instructions using any text editor or word processor. TEMPLATES are in English and are easily read and understood. They can be concatenated to form complex interdisciplinary algorithm classes. The TEMPLATES also give the algorithm developer the opportunity to communicate directly with the end-user by using familiar vocabulary and terminology. We've made it easy. **You** write the template and **you** decide what to run...all in a fraction of the time required to write a custom application.

The compute engine underlying ***AKCESS.**** has been optimized for maximum execution efficiency. It was designed to run on parallel hardware platforms and will continue to be supported as new state of the art systems emerge. It represents an entirely new level of software reliability. Its wide applicability means only this one system is needed for many diverse applications in fluid/thermal system simulation. As UNIX®-based platforms advance, ***AKCESS.**** will become even more valuable to perform the computations necessary for accurate modeling of real world interdisciplinary problems.

All you need is one platform...*AKCESS.**

>>>>> AVAILABLE TEMPLATES <<<<<

*AKCESS.*4-CFD
Flow Models

***AKCESS.*4-CFD** is a collection of TEMPLATES for Reynolds-averaged Navier-Stokes PDEs, viscous/inviscid turbulence modeling, buoyancy, and mixed-convection.

*AKCESS.*BASIN
Geologic Sedimentary Basin Model

***AKCESS.*BASIN** includes moving mesh, sedimentation, compaction, sediment heating, thermal conductivity, hydrocarbon (oil and gas) generation, salt diapirism, faulting, permeability variations, phase phenomena, chemistry, and fluid flow.

*AKCESS.*INJECT
Flow Injection Models

***AKCESS.*INJECT** is a Reynolds-averaged Navier-Stokes injector application which includes viscous/inviscid turbulence modeling with heat transfer, options for multiple species equilibrium chemistry, and a wide range of Mach numbers.

*AKCESS.*CKV
Commercial Kitchen Ventilation Model

***AKCESS.*CKV** includes buoyant mixed-convection flow simulations (powered/make-up/short-circuit hoods, cook tops, fryers, and ovens) connected to room HVAC system with obstructions, sources, and sinks in commercial kitchen environments.

*AKCESS.*1-2-3 *The Tutorial*

AKCESS.*1-2-3** is a collection of example TEMPLATES for 1, 2 and 3 dimensional steady and unsteady scalar PDEs. It provides *rapid* familiarization with topical finite element algorithm methods and hands-on experience with ***AKCESS.* features. The tutorial focuses on accuracy, convergence, and discretization error mechanism assessments while addressing progressively more detailed problems. ***AKCESS.*1-2-3** is included in all platform installations.

*AKCESS.** FEATURES

NEW CONCEPT FOR F. E. MODELING

Software platform separates modeling tasks of algorithm development and code development

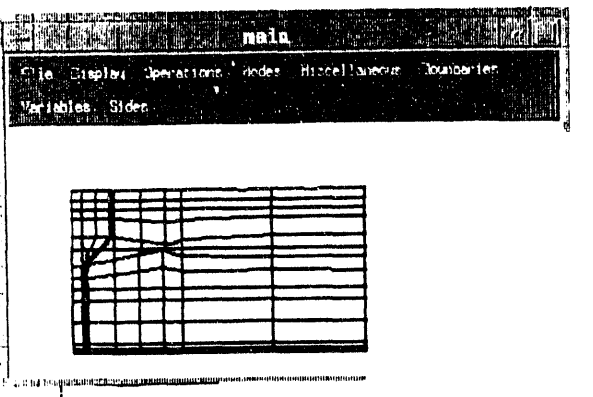

INTERDISCIPLINARY, 'REAL' MODELS

2D and 3D Multiple Coupled Systems
Unlimited Boundary and Initial Conditions Specifications
Flexible Grid Attraction
TEMPLATE Names can use Familiar Terminology
☞Unlimited Equation Closure Options
Parallel/Distributed Computing for Comprehensive 3D Modeling

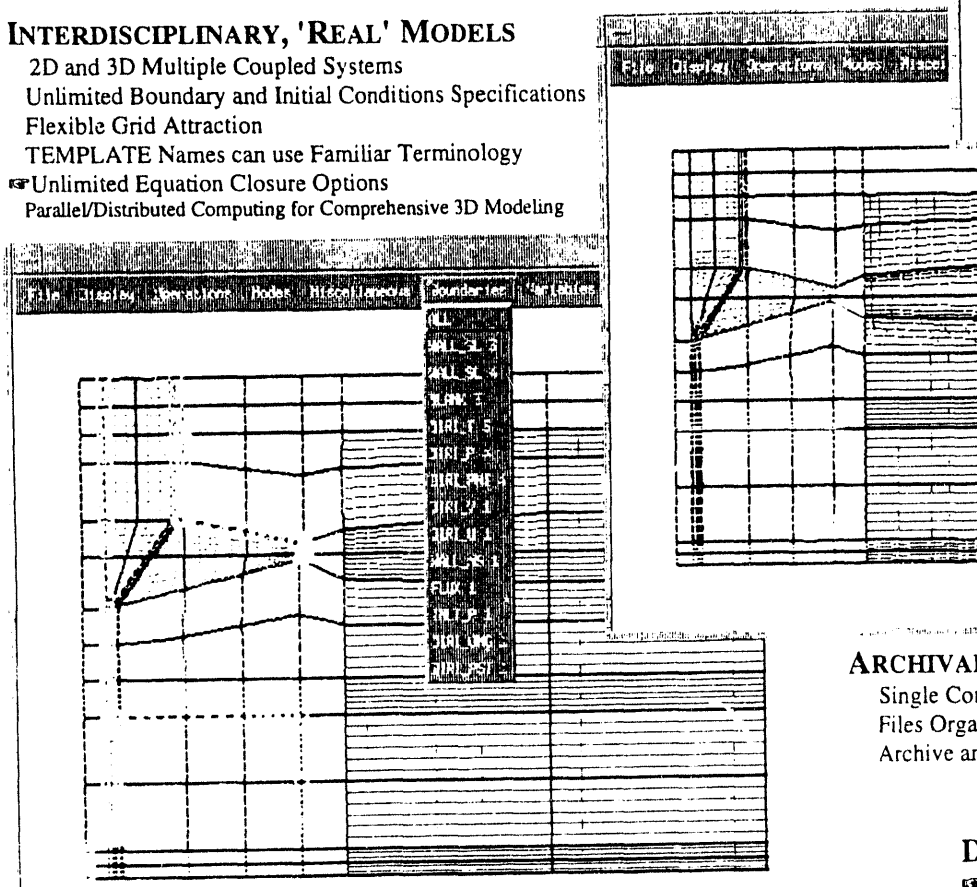

ACCURACY CONTROL

Transient Convergence Criteria
Automatic Step Sizing
Grid Accuracy Measures
Detailed Debug Print

ARCHIVAL MODELS (FILE MANAGEMENT)

Single Command, Multiple File Transfer
Files Organized by JOB and CASE
Archive and Retrieve Commands

DESIGNER FRIENDLY

☞Templates can be Customized for Application
☞Full Vocabulary Control
Pre- and Post-Processing Tools (interactive Graphics)
Array Manipulation Tools
Single Command Operation

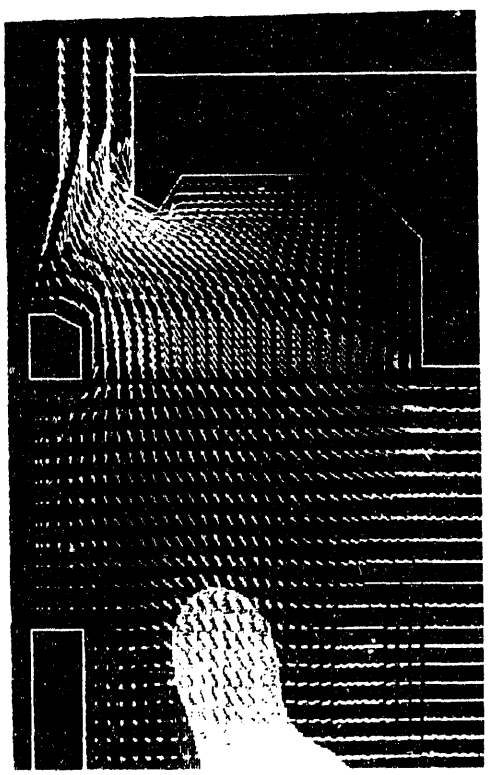

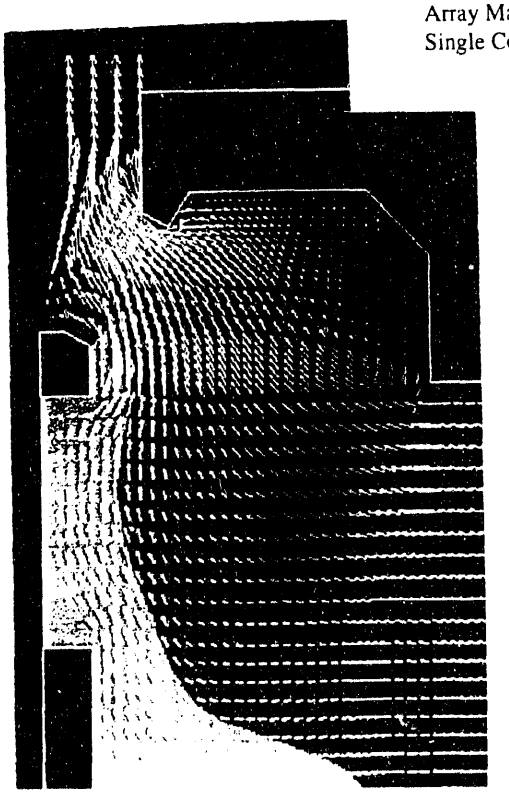

ECONOMIC MODELING

Off-the Shelf Modeling Platform
☞Methodology for Specialization
☞Evolutionary New Models
Self-Communicating Usage

TRANSPORTABLE

UNIX®/X-Window (Motif) Compatible
Fortran and "C: Coded
No Data Obsolescence

☞(Developer Version Only)

AVAILABILITY & PRICING

STANDARD LICENSE OPTIONS:

- **ANNUAL** Annually renewable - includes maintenance, enhancements, and one set of manuals

	Executable	Developer
Single User	$10,000	$20,000
Network	$20,000	$40,000

- **PERPETUAL** One-time purchase includes maintenance for one year and one set of Manuals

Single User	$20,000	$40,000
Network	$40,000	$80,000

STANDARD LICENSE[1]	*AKCESS.** is licensed for use on a single processor workstation[2].
SINGLE USER	Allows operation from a workstation console only.
NETWORK	Allows remote operation for unlimited users over a network.
DEVELOPER	Includes all TEMPLATE facilities for algorithm construction.
EXECUTABLE	Excludes all TEMPLATE facilities for algorithm construction.
MAINTENANCE	Provides periodic Notices and bug fixes.
ENHANCEMENTS	Provides periodic program Improvements and Upgrades.

SERVICE OPTIONS:

- **ENHANCEMENTS**

Single User	$ 7,500	$15,000
Network	$15,000	$30,000

- **TRAINING & TUTORIALS** (Organized Periodically or On-Site) - Contractual - Quoted Separately
- **HOT-LINE (Phone)**

Single User	$ 1,000	$ 2,000
Network	$ 2,000	$ 4,000

- **MANUALS & BOOKS** (Volume Discounts Available)

*AKCESS.**	Reference Guide	$ 100
*AKCESS.***1-2-3**	Tutorial	$ 150

[1]Includes 1-2-3 TEMPLATES and Example Cases
[2]Site License and Multi-Processor System Installations

Educational and Early Release Discounts Quoted Separately

Prices subject to changes without notice

Pub. No. BRAKS1193

COMPUTATIONAL MECHANICS CORPORATION

601 Concord Street, Suite 116
Knoxville, TN 37919-3382 U.S.A.

For More Information Contact: Sandy D. Carciofi, Marketing Administrator

EMail sandy@comco3.akcess.com

☎ (615) 546-3664

FAX: (615) 546-7463

AGEOHIST

A Basin Modeling Pre-Processor

for

AKCESS.BASIN

The AGEOHIST processor was written by L. Cathles, Cornell University. The software was developed using APL.68000, a proprietary product of MicroAPL Ltd, which has given permission for a runtime version of APL.68000 to be included with the software. Copywright and intellectual property rights of APL68000 remain vested in MicroAPL Ltd. APL.68000 is a trademark of MicroAPL Ltd.

AGEOHIST is distributed as part of the AKCESS.BASIN Basin Modeling System developed by The Global Basins Research Network and Computational Mechanics Corporation, Knoxville, Tennessee. For further information please call Computational Mechanics at 615-546-3664.

I. introduction

The AGEOHIST pre-processor provides a simple way to describe the present state of a sedimentary basin and the way it evolved over geologic time to reach that state. The output of AGEOHIST is a movie of the evolution of the basin and all the files required to simulate fluid flow and hydrocarbon migration over geologic time using AKCESS.BASIN.

AGEOHIST assumes that the geologic evolution of an area is determined mainly by the pattern of sedimentation. Spatial changes in sedimentation are accommodated either by the diapiric movement of underlying strata or faulting. The strata compact as they are loaded, and compaction is arrested by sealing. No horizontal extension is allowed and although non-vertical pseudo-wells can be used, non-uniform sedimentation with non-vertical wells produces artificial changes in sediment volume that can be significant. Vertical wells produce no volume errors and are thus preferred. A second pre-processor called AGEOHIST2 permits horizontal extension along non-vertical wells and adjusts stratal thicknesses so that volume is strictly conserved but does not consider compaction.

2. Data Input Requirements

The minimum information which must be supplied to AGEOHIST is conveyed in four short ASCII files. Two other input files and a description file are optional. The input files as well as internal communication files and output files (which will be described later) are listed in Table 1.

Table 1: The AGEOHIST Files

Required Input	Output
aafacts	AKFLAT
columntrans	tabgro.txt
sflat	tabseal.txt
timedepth	matrlprop.txt
Optional Input	**Internal**
agedim	***flat***
agedata	***tabgro***
DESCRIBECASE	***seal***
	agelist

The required input files provide the following information: The present geometry and lithology of the basin is contained in ***'sflat'*** (for short flat) file. The ***'facts'*** file provides facts about ***sflat*** and the simulation to be run. The ***'columntrans'*** file specifies how the columns in ***sflat*** correspond to those in the full ***'flat'*** file that will be filled in by the pre-processor. Finally the ***'timedepth'*** file gives the coefficients of a third order polynomial that converts time in seconds to depth in feet.

The ***facts*** file conveys the size of ***sflat***, the number of pseudowells and age horizons in ***flat***, a code for whether compaction is linear of exponential with effective stress, and two conversion factors that are applied to the horizontal and vertical scales (before time-to-depth conversion). The ***facts*** file entries are defined in Table 2. The conversion constants allow the user to input depth and horizontal distance in convenient units (for example centimeters measured from the top of a seismic section). The pre-processor converts centimeters to distance in kilometers, or, in the case of depth, to seconds. The ***timedepth*** file provides the constants needed to convert seconds of two way travel time to depth in feet, and then the pre-processor converts feet to kilometers. The entries in the ***timedepth*** file are defined in Table 3.

Table 2: The Facts File

# lines in ***sflat***	# columns in ***sflat***
# wells in ***flat***	exponential (=1) or linear (=0) compaction
# wells in ***flat***	# Horizons in ***flat***
x conversion factor	y conversion factor

Table 3: The Time-Depth File

A1 A2 A3 A4

where:

$$Z[ft] = A1 + A2\ t + A3\ t^2 + A4\ t^3$$

Note that if the flat file inputs depth directly in kilometers, the ***time-depth*** file has the following form:

0 -3280.839895 0 0.

The ***columntrans*** file lists the flat file column numbers of all the columns in the ***sflat*** file. The **Geology Flat File** or ***flat*** file for short is a 28 column file as defined in Table 4. The ***sflat*** file generally contains at least 8 columns: (1) the well number, (2) the horizon number, (3) the x and (4) z (depth) location of each horizon, the fraction (5) sand, (6) shale, and (7) salt of each pseudowell-age horizon intersection (node), and the (8) heat flow at each node. It may also include the sea depth at the time each horizon was deposited, the depth to the present top of geopressure, and other present descriptors such as organic matter content and type.

Table 4 The Geology Flat File

w#,H#,x1-3,f1-5,F,Int,A,d,jo,S,Igro,Iflt,So,Sg,Ioilg,p1,f,T,C,C/D,KER,Ike
w#,H#,x1-3,f1-5,F,Int,A,d,jo,S,Igro,Iflt,So,Sg,Ioilg,p1,f,T,C,C/D,KER,Ike
|--location-|--lithol--|-cond-|-geology-|--fluids--|-pres cond--|-orgncs-|

1. Well number
2. Horizon number
3-5. The x1,x2, x3 location of the age horizon-well intersection (node), x2 = vertical, positive up
6-10. Lithology at each node, fsd,fsh,fcarbsd,fcarbmud, fsalt
11 Fault /seal code (1=seal, >1=fault) = F
12. Interp. code = Int
    =0 lith. const over element
    =1 vertical interpolation
    =2 horizontal interpolation,
    =3 both horiz. and vert. interp.)
13. Age of the time surface, =A.
14. Depth of water (always positive) at A, =d.
15. Basal heatflow at the well location at A in HFU=jo
16. Average sedimentation (erosion) rate over the next interval upsection (m/yr), =S.
17. A sediment inflation code that ties the node to the

Diapirism Flat File (*tabgro*), =lgro.

18. Fault block code, =lflt.
19-20. Present oil and gas saturation of node, = So, Sg.
21. Oil and gas interpolation code (see 12), =loilg.
22. Present excess pressure at node, =p1.
23. Present porosity of the rock at nodes, =f.
24. Present temperature at node (0 if not known), =T.
25. Present salinity of pore fluids (0 if not known), =C.
26. Calcite/dolomite ratio of overlying interval, =C/D.
27. Kerogen grade at node (g kerogen / g sediment), =KER.
28. Kerogen type, =lker.

3. How Does AGEOHIST Work?

Briefly the AGEOHIST pre-processor works as follows: First the present state of the basin is analyzed to infer the present porosity profile in each pseudowell. The present porosity and the present thickness of the strata are used to make a first guess at the uncompacted sedimentation rate. Second modifications are made to these inferences from the present state of the basin to account for erosion and diapirism. The processing thus takes place in two phases, the first based strictly on what is presently observed and the second based on geologic inferences of past geologic events.

In the first phase of processing, lithology-dependent linear or exponential compaction is computed as a function of depth until a seal is encountered. Below the seal there is no further compaction if the seal is a migrating seal that moves to maintain a constant depth. If the seal is fixed to a particular strata the porosity below the seal is a slightly compacted version of the porosity profile that starts at the surface. It is slightly compacted because fluid pressure is assumed not to exceed ~80% of lithostatic, and thus ~20% of the lithostatic load above the seal still produces compaction. The fraction of lithostatic load that pore pressure can attain can be input by the user.

A fixed seal always coincides with a particular time-stratigraphic horizon. A migrating seal, however, may coincide with an age-horizon defined in ***sflat***, or may lie between and cross-cut age horizons. In this latter case the seal horizon is given a horizon number of zero in the ***sflat*** file. The depth information is used to compute compaction and porosity in the flat file, and retained in the *seal* file, but the transgressing seal horizon is not included the ***flat*** file. The porosity profiles and strata thicknesses in each well are used to compute the uncompacted sedimentation rates that are required to deposit the material presently lying between age horizons. Corrections for diapiric thinning and thickening are made later where appropriate.

The second phase of processing takes into account erosion and diapirism. If there has been erosion, the sedimentation rate of the ***flat*** file is edited to include appropriate negative sedimentation rates. If there has been diapirism it is described in a ***'tabgro'*** file. The tabgro file conveys the starting time for the model simulation and lists the (compacted) thicknesses of diapirically-affected strata at all horizon ages spanned by the model simulation. The nodes below the diapirically-affected parts of a strata are flagged in column 17 of the ***flat*** file to a correspondingly-numbered entry in the *tabgro* file. The compacted thickness of the strata overlying this node are filled in later either manually or automatically, based on the assumption that space accommodation is provided by salt movement.

The final step in processing is to run a forward simulation of the geologic history defined by the ***flat***, ***tabgro*** and ***seal*** files. The simulation is a cinema of the geologic history and also produces all the files needed to run Akcess.Basin. If there has been erosion the cinema is automatically played twice. In this way the compaction that occurs before erosion is properly included in the ***flat*** file.

Processing of the ***sflat*** file, creation of the ***flat*** file, editing of the sedimentation rate, construction of the diapirism (***tabgro***) file, and the playing of the final cinema are all achieved by executing functions from pull down menus. Comments that appear on the screen guide the user through the processing. At all stages of processing the basin may be viewed as horizon or patterned lithology plots (slower). Again the pull down menus are used to view the basin. The graphics that are produced during processing may be avoided (for increased computation speed). If requested, a geohistory movie is constructed that can be rapidly replayed and saved for later retrieval. Hard copy plots of the movie and a log of the processing session may be requested from Macintosh machines. UNIX files created at the end of the pre-processing session are, upon request, automatically transmitted to the case folder. The files are all that is required to run AKCESS.BASIN.

The commands and menus of the AGEOHIST pre-processor are described below: A typical processing session and several examples of basin simulations are provided. Each basin modeling case is kept in a separate **case folder** that contains all the input, output and UNIX files needed to run models of that basin.

4. Getting Started

To start simply insert the GBRN/AGEOHIST diskette and copy the AGEOHIST Program, the AGEOHIST Case File, and the APL68000 Runtime II program to your Macintosh by dragging the Icons to the desired disks or folders on your system.

Begin AGEOHIST by double clicking on the AGEOHIST icon. The program will then bring up a **dialog box** and ask you to select (by double clicking) the ***aafacts*** file in the **case folder** of interest. AGEOHIST learns the path to the case folder in this fashion. The case folder path can be listed at any time by selecting **Write folder name** from the Help menu.

A. The Edit Menu

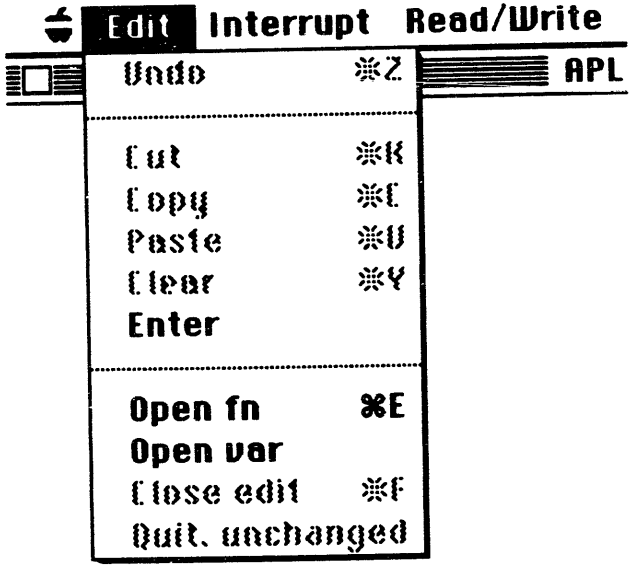

5. Using the Menus

The main processing menu is the Execution Menu. Other menus control editing, plot type, movie construction and replay, etc. The Menus are described below in the order of their appearance on the screen.

This menu is taken from the APL68000 processor. It is used in this application to edit variable arrays. The **cut**, **copy**, **paste**, and **clear** commands can all be used in editing data in standard Macintosh fashion. When editing of a variable is complete, the **Close edit** (*f) command can be used to close the editing session and save the results, or the session can equivalently be ended by clicking the box in the upper left hand corner of the editing frame.

Use the **Quit, unchanged** menu bar to close the editor without incorporating changes.

B. The Interrupt Menu

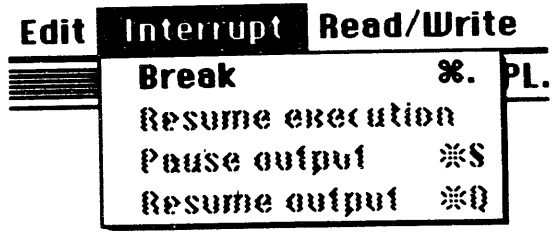

The interrupt menu allows the user to suspend the operation of a function. This can be useful to provide more time to view a plot, for example. Plotting can be suspended by depressing the mouse button while the cursor is on the Interrupt menu. Longer pauses are best achieved by highlighting and releasing the **Pause** output bar. Output is resumed by selecting the **Resume output** bar. With the Runtime APL Processor, executing **Break** will cause the application to terminate in the same fashion as selecting **Quit** in the Execution menu.

C. The Read/Write Menu

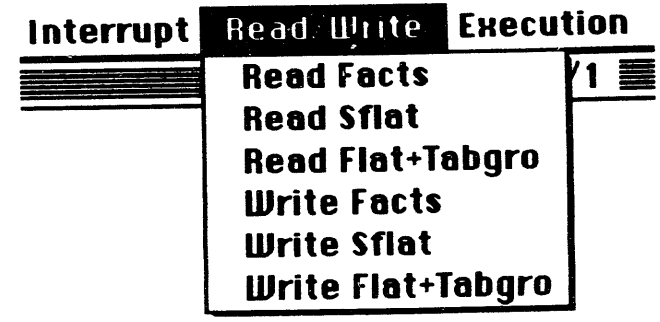

The Read/Write menu is used to read or write information from the selected Macintosh folder. For example the ***aafacts*** file may be read from the folder selected at the start of the session by selecting **Read Facts**. The ***aafacts*** file can then be edited using the Editing menu, and the modified facts file written to the Case Folder for permanent archival by selecting **Write Facts**.

The same is the case for the ***sflat***, and ***flat***, *tabgro* and *seal* files. Note that although the **Read Flat+Tabgro** and **Write Flat+Tabgro** menu bars suggest only the ***flat*** and ***tabgro*** files are read or written, the ***seal*** file (if it exists) is also read or written.

D. The Execution Menu

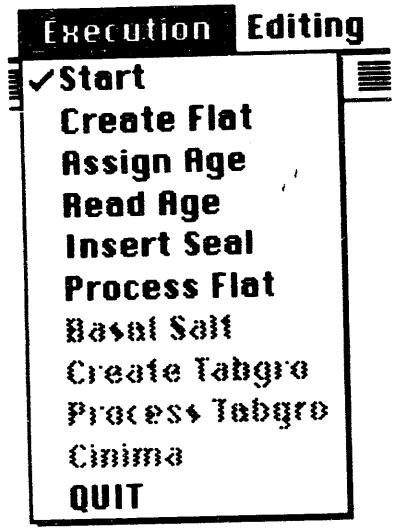

The Execution Menu is the heart of the AGEOHIST pre-processor. Entries in this menu are checked (√) after they are selected to remind the user of the processing steps that have been completed. The first phase of processing (direct observational evidence) must be completed before the second phase (geological inferences) can begin. Thus the second phase is disabled (light outline) until **Process Flat** has been executed or until valid flat, tabgro, and seal files have been read in using the **Read Flat+Tabgro** command in the **Read/Write** menu.

For example, the **Start** menu bar is already checked because the ***aafacts*** and ***sflat*** files were read from the case folder when the ***aafacts*** file was selected by the user at the beginning of the session. The **start** menu bar can non-the-less be selected again and a new case selected by selecting the ***aafacts*** file in another case folder. The **Start** menu bar will remain checked if this is done.

The ***sflat*** file can be checked for errors by using the Plot Sflat command in the Plotting menu.

The next step in processing is usually the creation of a full flat file from ***sflat*** and ***columntrans***. This is accomplished by selecting the **Create Flat** menu bar.

Assign Age is used to assign ages to strata by linear interpolation (according to depth) from know ages at particular strata. The user must have previously placed two files in the case folder. The first, labeled *agedim*, (note the name of the file in the folder is not italicized) gives the number of strata whose ages are specified in the second file. The second file is the *agedata* file. It contains two lines. The first lists the strata numbers whose ages are known (counted from

the present top surface of the basin), separated by tabs of spaces. The second line lists the ages of those strata in millions of years, again separated by spaces or tabs. **Assign Age** takes the *agedim* and *agedata* files and uses them to assign ages to all the other strata in the ***flat*** file in the folder file in the case folder. It does this by averaging the thickness of the strata between specified horizons over all the wells in the ***flat*** file, and interpolating the ages in proportion to these average thicknesses. This kind of age averaging is useful when there are many thin strata in a basin whose ages are inaccurately known.

Assign Age records the ages assigned in the case folder and preserves them also in an internal variable. If another profile with the same number of wells and horizons is processed next, this same age sequence can be assigned to the new profile by selecting the **Read Age** command. If the ***agelist*** has been copied into the new case folder, **Read Age** will read it from the folder. In this way a series of complex seismic lines can be processed with the same age assignments as is required for a 3D model.

The ***sflat*** file may of may not have defined a seal. If a seal has not been defined in ***sflat***, one may be inserted along any time-stratigraphic age horizon using **Insert Seal**. If **Insert Seal** is selected the user will be asked to identify the seal horizon in terms of the number of horizons down from the top (=1) of the basin. This command inserts the seal code in plane 11 of the ***flat*** file. The user will also be able to select a fixed or migrating seal. If the seal is fixed, a seal thickness is requested. This thickness must be smaller than the minimum thickness of the overlying strata.

Once the stratal ages have been defined and any seal inserted, the flat file may be processed to determine the present porosity profile and the uncompacted sedimentation rates needed to deposit the strata as they presently appear in the basin. This is done using **Process Flat.** The ***flat*** file is processed assuming linear or exponential compaction as specified in the ***aafacts*** file, and assuming that there is no further compaction under the seal. Processing determines the material properties from the lithologies specified in the flat file and then determines the present porosity at all nodes. The porosity and present strata thickness is then used to compute the sedimentation rate between horizons, assuming there has been no diapiric movement of material and no erosion.

If these processes have occurred, corrections are made to the sedimentation rate in subsequent processing steps.

Basal Salt provides one way to easily input diapirism. It inserts diapirism ties in plane 17 of the flat file and assures that these are the only tied nodes. The base layer should be entirely salt. If this is not the case, the flat file should be edited using **Part Flat** in the editing menu. The **Basal Salt** function provides the proper input for automatic construction of the ***tabgro*** file.

Create Tabgro creates a ***tabgro*** file. The user is asked to define the time at which the model should start from a list provided. If the flat file contains diapirism ties, the tabgro file is set up to include one row for each of these nodes. The diapiric nodes have the correct final thicknesses; the user must fill in appropriate thicknesses at intermediate times.

Process Tabgro provides a graphically interactive or automated way to fill in the ***tabgro*** file. Under option 1, **Process Tabgro** assumes that basal salt withdraws from areas of extra sedimentation and automatically fills in the thickness changes of these strata. Unless the **No Plots** option in the Printing menu is selected, plots of the sedimentation rate are interspersed with plots of the evolving basin, as processing occurs.

Under Option 2 of **Process Tabgro** diapirism is plotted for each modification the user makes in the ***tabgro***, and the user is given the option to make corrections before proceeding. In this case, as in Option 1, the user may select the silent option at any time and have the processor proceed automatically without user modification. A good procedure is to execute Process Tabgro twice: Once automatically to obtain salt movement from the pattern of sedimentation, and then in edit mode to refine the automatic interpretation.

The final step in the processing is running **Cinima.** Cinima presents a movie of basin evolution from the sedimentation rates in ***flat*** and the diapirism specified in ***tabgro.*** The movie is recorded so that it can be played back at high speed if the **Make Movie** option is checked in the Movies menu. Recording is automatic if the **Line Plots** option of the Printing menu is selected. Otherwise the **Make Movie** option of the Movies menu must be specifically selected. Plots of the basin evolution are presented in time sequence. At the end of the cinema the user may request

that the files required to run AKCESS.BASIN be output to the case folder. If this is done the **AKFLAT, *tabgro.txt*, *tabseal.txt*,** and ***matrlprop.txt*** files will be written out in UNIX format. They are read automatically from the case folder by AKCESS.BASIN. A hard copy of all **Cinima** plots can be printed if **Laser Plots in Cinima** is selected in the Printing menu. Note if this is done the user will see no plots on the screen during **Cinima** execution. They all go to the printer. Particular frames of a movie can be viewed, copied and printed using the **Select Frame** option of the Movies menu.

QUIT terminates AGEOHIST.

E. The Editing Menu

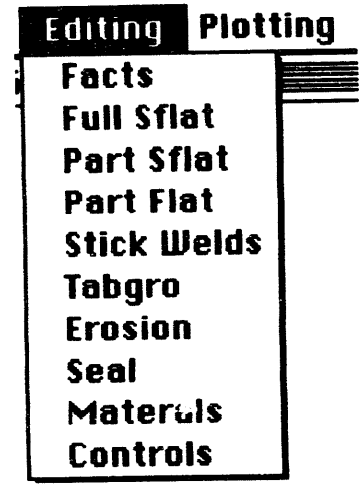

The Editing menu is used to edit files. Editing is done, Macintosh fashion, by cutting and pasting. This is briefly described in the Edit menu and should be familiar to Macintosh users. Information can be transferred from other applications using the clipboard.

Selection of the proper menu bars leads to the full screen editor appearing and offering the opportunity to edit the full ***aafacts***, ***sflat***, and ***tabgro*** files. Editing of one data plane from the ***sflat*** or ***flat*** files may also be requested. If these menu bars are selected, the user is asked for the data plane he or she wishes to edit. For example the

well numbers in the ***sflat*** file may be edited by selecting **Part Sflat** and electing the appropriate data plane (usually the second). The horizon depths in the ***flat*** file can be edited by selecting **Part Flat** and electing the fourth data plane, etc.

Stick Welds is used to edit the tabgro file so that areas where salt has withdrawn are not re-inflated. It can be used interactively, in which case plots of the strata thickness over time are presented for all nodes that go to zero thickness anytime during basin evolution. The user asked if he or she wishes to keep the stata stuck (at zero thickness) at all later (or earlier) times. If the silent (no questions) mode is selected, the processing assumes all welds after they are formed, no questions are asked, and no plots are presented.

Finally the **Erosion** menu bar can be used to input erosion. If **Erosion** is selected the user is presented with a table of the uncompacted stratal thicknesses deposited in the time interval between each pair of time horizons. Erosion is input by editing the thicknesses presented to increase the stratal thicknesses at earlier times and offset these increases with negative deposition (erosion) at later times. If the increased deposition and erosion cancel, the final basin will have the observed present form.

The seal file may be edited by selecting **Seal**.

The user can change the constants that control the fabric theory material properties algorithm by selecting **Materials** under the Editing menu. The array will appear and the edited version will be communicated to AKCESS.BASIN through the UNIX file ***matrlprop.txt*** file.

Finally important control parameters can be changed in **Controls**. These parameters include the code that controls whether compaction is exponential or linear, the maximum pore pressure as a fraction of lithostatic, and the fraction of cross-cutting fabric elements.

F. The Plotting Menu

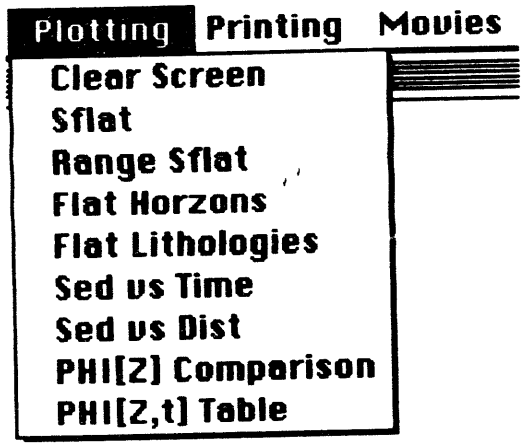

The Plotting menu allows the user to obtain plots of the sflat and flat files, as well as plots of sedimentation rate versus time and distance.

Clear Screen clears the screen.

Sflat plots the short flat file. ***sflat***. If there is a cross-cutting seal, it is plotted as a thicker line. Otherwise horizons and pseudo-wells are plotted as lines to present a cross section of the basin. The plot is also placed in the clipboard where it can be pasted into documents and reports.

A subsection of ***sflat*** or ***flat*** may be plotted using **Range Sflat**. If this menu bar is selected the user is asked for the starting well and number of wells, and the starting strata (numbered from the top down) and number of strata, and just these wells and strata are plotted. If a large range is selected the wells to the edge of the basin or strata to the bottom of the basin are plotted. The user need not worry that too many wells or strata have been selected.

The flat file may be plotted in two modes: If **Flat Horizons** is selected, the horizons and pseudo-wells are plotted as lines as with the Sflat command. If **Flat Lithologies** is selected the lithology is shown as standard patterns between are horizons and pseudowells. The lithology of the lower left hand node controls the pattern. The pattern is not interpolated between wells and horizons. Lithology plots are slower to plot than Horizon plots, but are sometimes necessary to visualize and edit the lithology of a basin. It is for this reason that a choice is given. Both plots are copied into the clipboard automatically.

Sed vs Time plots the uncompacted sedimentation rate as a function of time for each pseudo-well. It plots 5 wells at a time.

Sed vs Distance does the same for the sedimentation rates along each age horizon, presenting 5 horizons at a time.

Finally **PHI[z] Comparison** plots, with a thin line, the initial (first processing phase) estimate to the porosity as a function of depth for a selected well and compares it to the final porosity as a function of depth calculated in **Cinima** and plotted with a thicker line. If the analysis is valid, the two porosity profiles should be closely similar. If they are not, because for example the initial (phase 1) estimates have not taken into account the effects of erosion, they may be made similar by re-processing phase 1. This is done by executing the **Re-Process** option in the execution menu. The **Cinima** porosities are placed in the ***flat*** file and used to obtain more accurate uncompacted sedimentation rates. A few re-process iterations will lead to consistent initial and final porosity profiles, as illustrated in the Heuristic South Eugene Island example at the end of this manual.

The evolution of porosity in any well can be viewed by selecting **PHI[z,t] Table.**

G. The Printing Menu

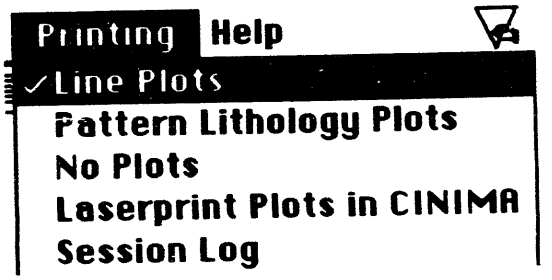

The printing menu allows the user to control the kinds of plots that will appear when the various functions in the Execution menu are executed. The entries are checked when they are selected. **Line Plots** is the default and it is checked in the illustration above. If **Line Plots** is selected, the basin plots in Process Tabgro and Cinima will be simple line plots of the horizons and pseudo-wells similar to the plots produced by **Flat Horizons** in the Plotting menu. If **Pattern Lithology Plots** is selected, the plots will include lithologic patterns between horizons and wells, and resemble the **Flat Lithology** plots of the Plotting menu.

The **No Plots** option may be selected to avoid plotting. This significantly speeds processing.

A record of the geohistory developed by the pre-processor may be obtained on Macintosh machines by routing the graphical output of Cinima to a laser printer (or Imagewriter). This is done by selecting **Laser Plots in Cinima**. If this option is selected no plots appear on the screen. The plots are printed. Plotting is slow for Pattern Lithology Plots of cases with many wells and strata. This option is not available when AGEOHIST is run under Liken on SUN and other UNIX machines.

A log of the session may be obtained by selecting the **Session Log** menu bar. If this is done the No Plots option is automatically selected and a complete record of the session with start time and finish time is output to the laser printer. Session logging is also available only on Macintosh machines and is not at present available under Liken on UNIX machines.

H. The Movies Menu

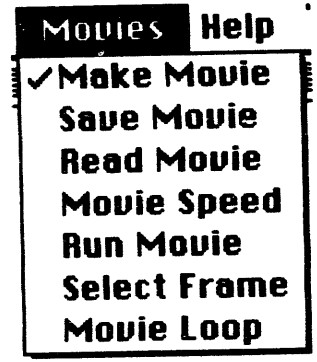

The movies menu allows the user to make and save a movie of the geohistory calculated by **Cinima**, and to play it back at movie speeds. Clicking on **Make Movie** causes a movie to be recorded when **Cinima** is executed. The plots are of the type selected in the printing menu. Executing **Save Movie** saves the movie in the **Case Folder. Read Movie** reads the movie from the case folder. Reading and then running a movie provides a quick way to review a basin model.

The speed of the movie can be adjusted with **Movie Speed**. Normally a speed of 1 is appropriate. The time delay between frames is proportional to the geologic interval between strata and one frame is output for every age horizon in the model.

Select Frame allows the user to select one frame from the movie for close investigation. The frame selected is put into the clipboard as well as output to the screen. This allows a frame from the movie to be pasted into a report. In the process, it can be re-sized. This was the procedure used to produce the figures in this report.

Finally **Movie Loop** causes the movie to loop back to the beginning, after a brief pause. This allows the movie to be viewed multiple times and more easily studied.

I. The Help Menu

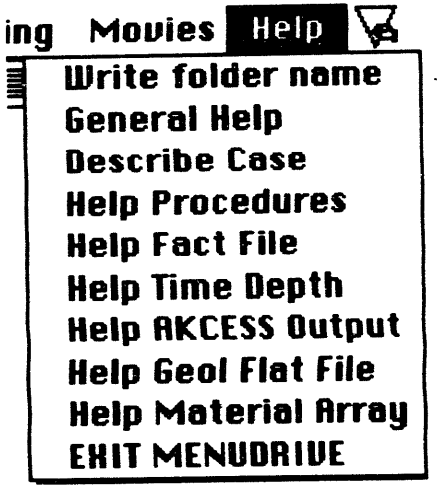

Finally help in a number of topics is available from the Help menu. **General Help** briefly describes how to use the AGEOHIST pre-processor. Typical processing steps are described in **Help Procedures**. Descriptions of some of the input and output files are given in **Help Fact File, Help Time Depth,** and **Help AKCESS Output.** The flat file entries are defined in **Help Geol Flat File**. The material property parameters are defined in **Help Material Array**.

A description of the current case can be obtained by selecting **Describe Case.** When Describe Case is selected a 71 column wide by 50 line long text file called *DESCRIBECASE* that describes the case is read from the case folder. Such files have been prepared for all the examples provided in AGEOHIST. The user may produce his own and place it in his case folder using any editor. The file must be 71 columns wide (with the last column a carriage return character), and 50 lines long. The "show invisible" capability of many editors makes construction of such files easy in the Macintosh environment.

The final menu bar, **EXIT MENUDRIVE**, is for developer versions of the code only. Selecting this entry with Runtime Versions of the code will cause the application to quit.

Under the developer version, **EXIT MENUDRIVE** can be used to exit menu-driven execution and enter the APL mode. This allows examining parts of variables, performing simple calculations, and executing functions not in the menus. Return to menu drive is achieved by typing **MENUDRIVE** followed by a carriage return. Users that do not know APL should not use this option; it is not an option for Runtime use of AGEOHIST.

6. A Typical Processing Session

In the following the menu is indicated first followed by a colon and the menu bar executed under that menu. a brief comment indicates the process invoked.

Execution: Start
Choose the desired case folder by selecting the appropriate ***aafacts*** file.

Plotting: Sflat
Plotting: Part Sflat
Editing: Full Sflat
Inspect the ***sflat*** file and correct any errors.

Execution: Create Flat
Create a ***flat*** file; menu will be checked after execution.

Execution: Assign Age
Execution: Read Age
Assign or read ages for minor strata.

Execution: Insert Seal
Insert a seal at a specified horizon number (horizons counted from top down).

Execution: Process Flat
Process the ***flat*** file to guess the present porosity distribution and infer from this the past sedimentation rates, assuming linear or exponential compaction as indicated in the ***aafacts*** file, and the seal location and sediment lithologies specified in the ***flat*** file.

Execution: Basal Salt
Insert tabgro ties in the bottom layer of the basin which is assumed to be salt.

Execution: Create Tabgro
Create a ***tabgro*** file; select the starting time for modeling from a list provided.

Execution: Process Tabgro (option 1)

Fill in the entries of the ***tabgro*** file assuming that above average sediment deposition is accommodated by salt movement to areas of below average sedimentation..

Movies: Movie

Click on the movie capability.

Execution: Cinima

Review the evolution of the basin and write the files needed to run AKCESS.BASIN in the case folder.

Movies: Run Movie

Play the movie back. The speed can be changed using the Change Speed menu bar.

7. Examples

A large number of examples are provided to serve as examples to a new user. The examples are of two kinds: Heuristic cases that illustrate simple procedures, and realistic basin simulations. Each example is described by a DESCRIBECASE file in its case folder. Parts of these summaries and figures from the processing are reproduced below.

A. Sand Box

The case of uniform sand sedimentation can be described by a very simple ***sflat*** file. The first two wells of this file are shown below.

1	1	0	0	1	0
1	2	0	–0.5	1	5
1	3	0	–1	1	10
1	4	0	–1.5	1	15
1	5	0	–2	1	20
1	6	0	–2.5	1	25
1	7	0	–3	1	30
1	8	0	–3.5	1	35
1	9	0 –	4	1	40
2	1	10	0	1	0
2	2	10	–0.5	1	5
2	3	10	–1	1	10
2	4	10	–1.5	1	15
2	5	10	–2	1	20
2	6	10	–2.5	1	25
2	7	10	–3	1	30
2	8	10	–3.5	1	35
2	9	10	–4	1	40

The other wells are similar, each offset from the previous by 10 km. The ***sflat*** file can be viewed:

Plotting: Sflat

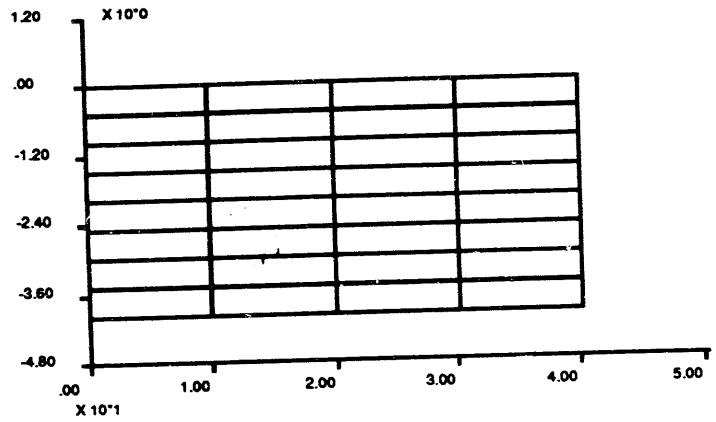

Alternatively a lithology plot of the ***flat*** file can be obtained:

Execution:	Create Flat
Plotting:	Flat Lithology

The lithology plot shows that the sediment is all sand.

The geohistory can be calculated:

Execution:	Process Flat (phase 1 processing to guess porosity from present state of basin and obtain the uncompacted sedimentation rates)
Execution:	Create Tabgro (input model start at 35 ma)
Execution:	Cinima (calculate the basin evolution)
Movie:	Run Movie (runs movie of the basin evolution just calculated)
Plotting:	PHI[z] Comparison (compares the phase 1 Process Flat estimate of porosity with the porosity determined by Cinima [light line])

The geologic history shows simply a single uniform macro layer being added at each time interval and is not very interesting. The first and last frames of the cinema are reproduced below using:

Movies:	Select Frame

and the pasting the image, which is also placed in the clipboard, into this document.

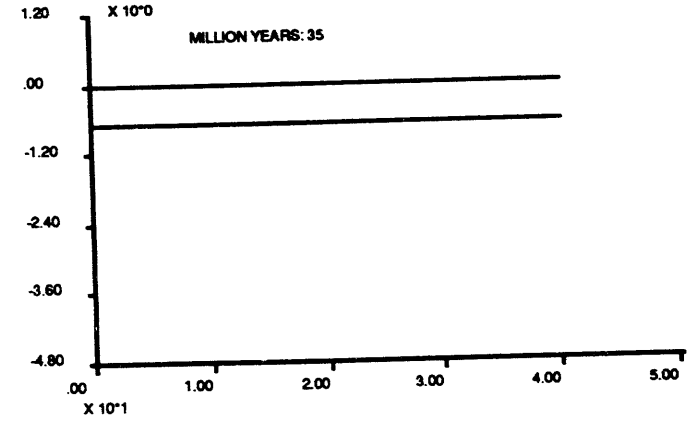

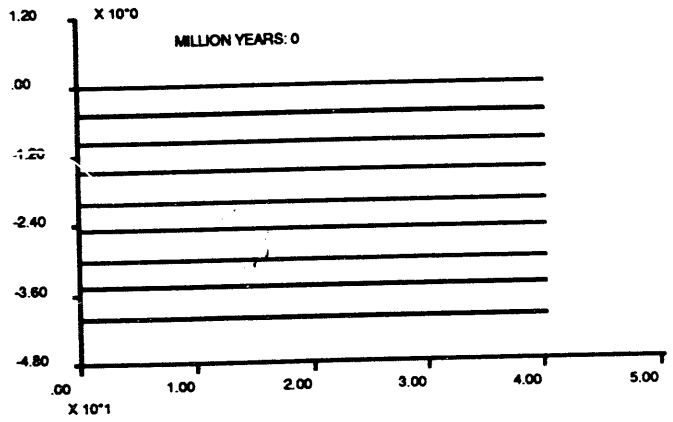

The compaction that takes place as sedimentation occurs is clearly evident. The basin today has uniformly spaced strata of equal thickness, but the lower layers were initially much thicker. With burial they have been compacted.

The PHI[z] Comparison plot shows that the method is valid and summarizes the steps taken in pre-processing in its caption. It is reproduced below for this simple no-seal case. It shows a simple linear decrease in porosity with depth because the linear compaction rule is specified in the ***facts*** file.

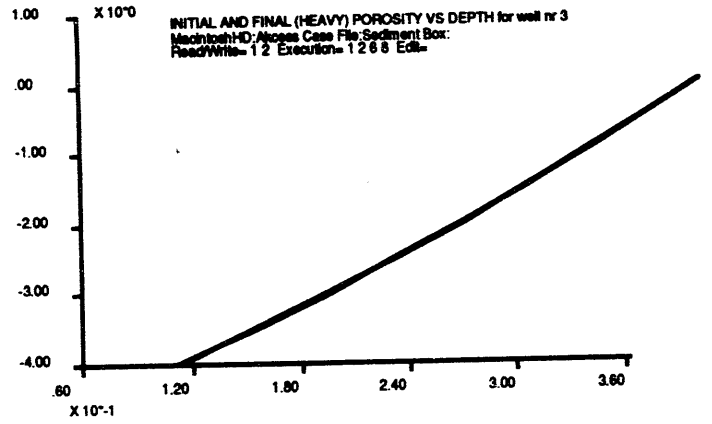

The same plots assuming exponential compaction can be obtained by editing the exponential control parameter to specify exponential compaction:

Editing: Controls (toggle on exponential compaction)

This is entirely equivalent, but easier, than editing the ***facts*** file using Editing: Facts and changing it:

from		to	
45	6	45	6
5	0	5	1
5	9	5	9
1	1	1	1

This can be verified by looking at the ***facts*** file using Editing: Facts before and after changing the exponential compaction toggle.

Execution of the steps above from Execution: Process Flat on yields very similar geologic history plots and the

following exponential compaction porosity versus depth curve:

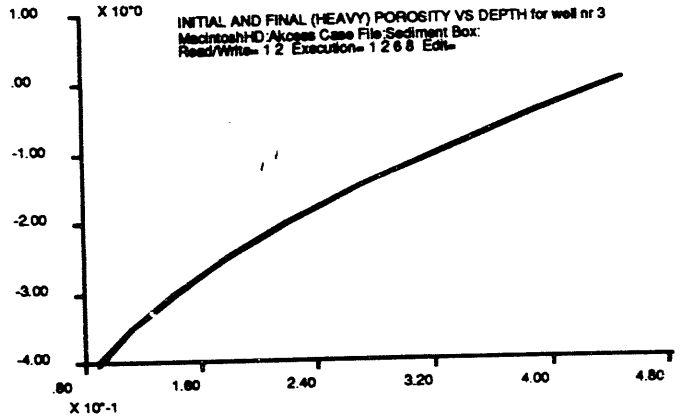

A seal fixed to one of the stratigraphic horizons may be inserted. The fixed seal arrests compaction when the seal is buried. The degree to which compaction is arrested depends on how closely pore pressure can approach lithostatic. If pore pressure can reach lithostatic pressures there is no further compaction with burial. If pore pressure can only reach some fraction of lithostatic before the over-pressured fluids vent, one minus that fraction of the lithostatic load is supported and compresses the sediments. The fraction of lithostatic pressure that the pore pressure can achieve is specified through a dialog in Editing: Controls. The porosity depth plots for linear compaction and maximum pore pressure to lithostatic fractions of 0.8 (the default) and 1.0 are shown below along with the procedures to obtain them.

Execution: Start (choose Sand Box case)
Execution: Create Flat
Execution: Insert Seal (fixed seal with thickness 0.1 km at hrzn 4)
Plotting: Flat Horizons
Execution: Process Flat
Execution: Cinima
Plotting: PHI[z] Comparison

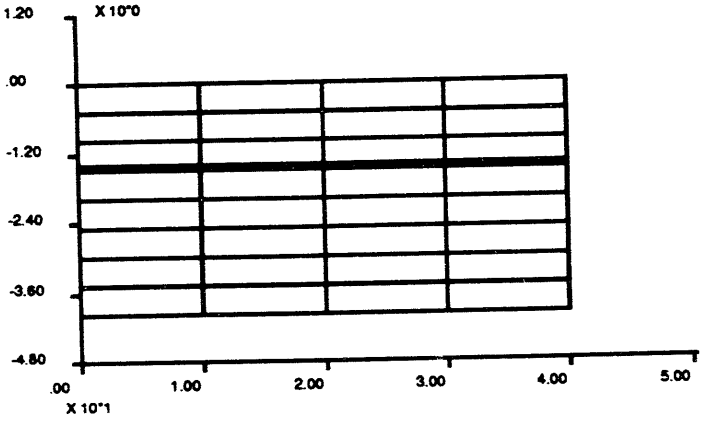

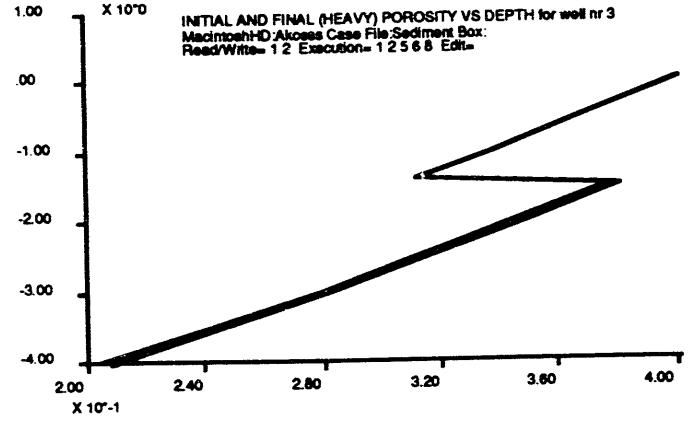

The 0.1 km seal can be seen just above the 4th horizon in the first plot, and with the maximum pore pressure 0.8 lithostatic it can be seen from the second plot that there

has been some compaction to ~38% porosity of the 4th sand layer from its initial porosity of 40%.

If the fraction of lithostatic pressure that pore pressure can attain is changed to 1.0, there is no compaction of the 4th layer:

Editing: Controls(change Pmax/Lith fraction from 0.8 to 1.0)
Execution: Process Flat
Execution: Cinima
Plotting: PHI[z] Comparison

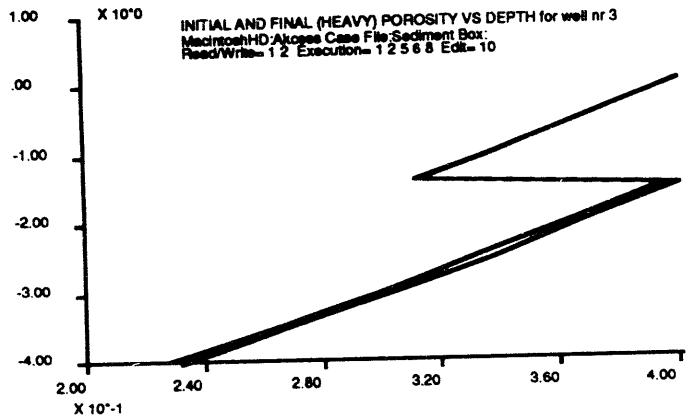

Finally a migrating seal may be inserted by appropriately flagging a horizon in the flat file. This could be done on any strata. Here the base of the seal just inserted is chosen:

Editing: Controls (change Pmax back to 0.8)
Execution: Insert Seal (migrating a hrzn 5)
Execution: Process Flat
Execution: Cinima

Plotting: PHI[z] Comparison

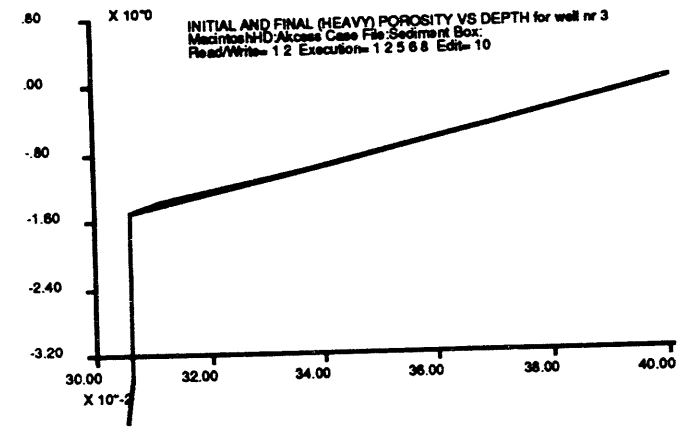

Notice that the porosity is constant under the seal because the seal migrates upward to maintain a constant depth and the strata cross the seal and have their compaction arrested at the same depth and porosity.

B. SEI No Seal

A simplified geological model of the South Eugene Island area with no seal provides a basic example. The ***aafacts***, ***aafacts***, ***columntrans***, and ***timedepth*** files needed to run this case are contained in SEI No Seal folder. The case can be run from start to finish:

Execution: Start (pick ***aafacts*** from case folder)
Plotting: Sflat (provides a view of ***sflat***)
Execution: Process Flat (phase 1 processing to guess porosities and uncompacted sedimentation rates from flat)
Execution: Basal Salt (put tabgro ties in ***flat*** in preparation for automatic

processing of ***tabgro***)

Execution: Create Tabgro (create a tabgro shell)

Execution: Process Tabgro (pick salt diapirism derived from sedimentation pattern option)

Execution: Cinima (produces Akcess files)

Plotting: PHI[z] Comparison (compares initial, Process Flat, and final, Cinima, estimates of porosity for a selected well

The results are similar to the seal cases of SEI Heuristic discussed below. Because of its importance in illustrating Akcess.Basin, the geohistory and summary PHI[z] Comparison plots are reproduced below in full. Her and elsewhere the geohistory is obtained from:

Movies: Select Frame

and simply pasted into this manuscript. The last illustration is pasted from Plotting: PHI[z] Comparison.

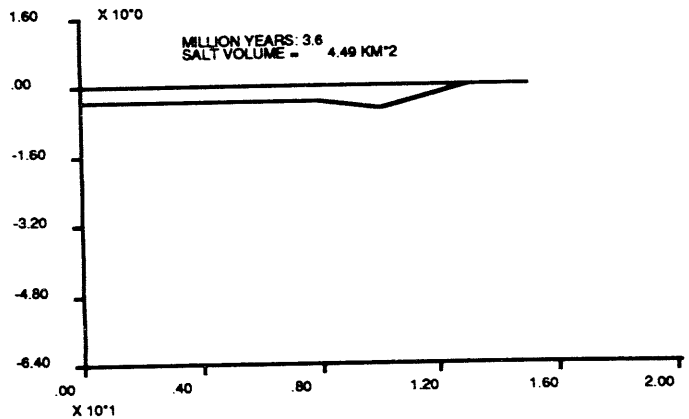

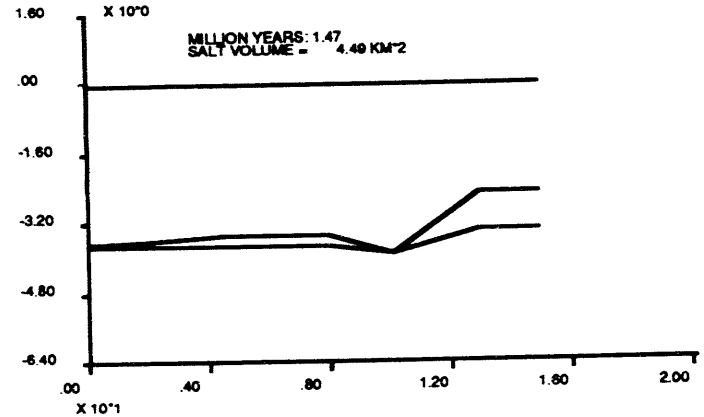

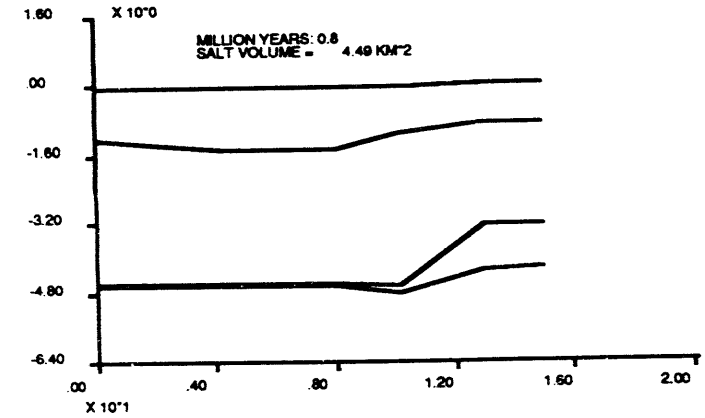

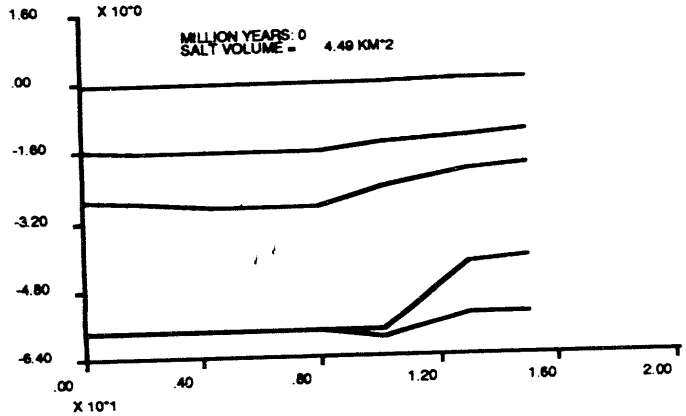

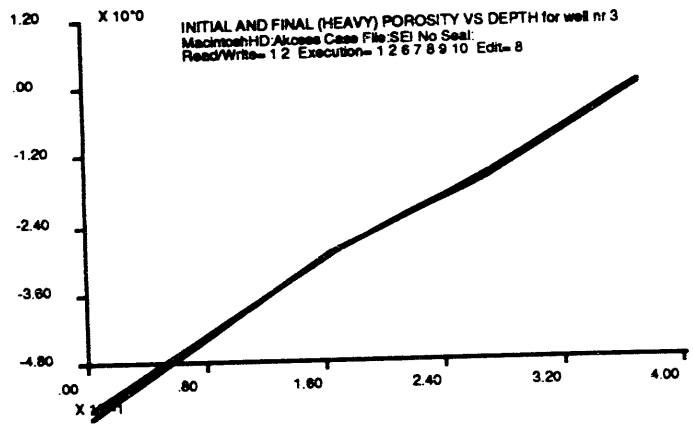

C. SEI Heuristic

This heuristic South Eugene Island example illustrates a number of procedures when a seal is present in a case with few enough wells and horizons that execution times are very fast and the arrays can be easily viewed and altered.

1. Transgressing Seal, Input Salt Diapirism:

The ***sflat*** file contains a seal which transgresses lithology. This can be seen:

Execution: Start
Plotting: Sflat

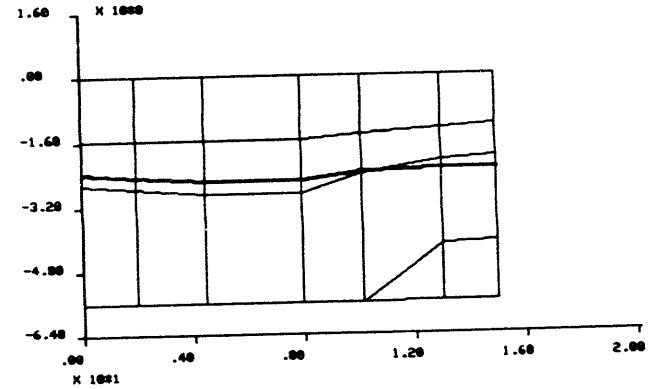

The ***sflat*** file is first processed to create a full flat file, and processed to obtain an initial estimate of porosity as a function of depth and the uncompacted sedimentation rates in each well by issuing the commands listed immediately below. The transgressing seal in the ***sflat*** file shown above is used to estimate porosity.

Execution: Create Flat
Execution: Process Flat

Now phase 1 processing is complete, so the diapirism commands have been enabled in the Execution menu.

Diapirism is added by introducing tabgro ties in plane 17 in ***flat*** , creating a ***tabgro*** file and filling in its entries:

Editing: Part Flat (flat column 17)

select plane 17 and fill in entries in the bottom two age horizons:

0	0	0	0	8	0	0
1	2	3	4	5	6	7

Execution: Create Tabgro

select a starting time of 3.6 ma.

Editing: Tabgro

fill in the *tabgro* entries to produce the following table:

–7	3.6	1.47	0.8	0
1	0.5	0.3	0.1	0.003
2	0.5	0.3	0.1	0.003
3	0.5	0.3	0.1	0.003
4	0.5	0.3	0.1	0.003
5	0.5	0.8	1.1	1.405
7	0.5	0.8	1.1	1.466
8	3.201	2.5	3	3.201

Note that node 8 starts with a thickness of 2.5 km (because its base is the 1.47 ma horizon) and then increases thickness to 3.201 km as material is pushed aside from the growing salt dome. The thickness at 3.6 ma must be the same as at the present time. the thickness at this time is in a sense irrelevant since the strata has not been deposited at this time, but the processor requires the convention that the final thickness be input at these pre-deposition times.

The geologic history of sedimentation and diapirism iewed by

Execution: Cinima

produces the following geohistory:

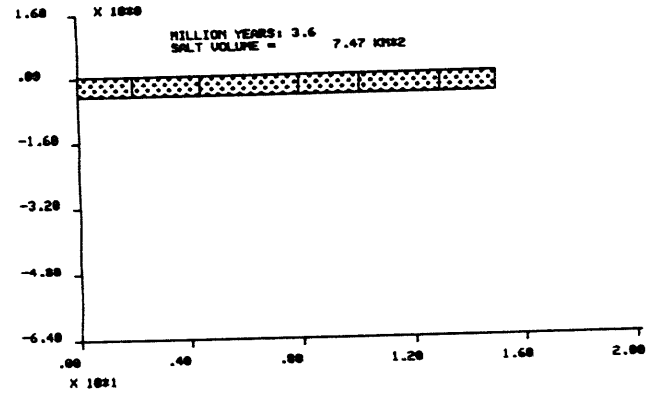

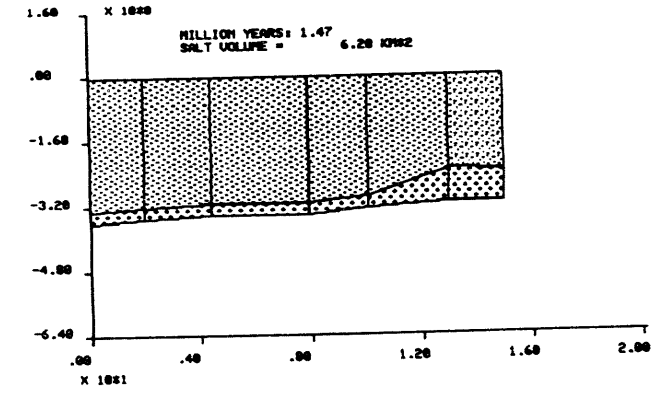

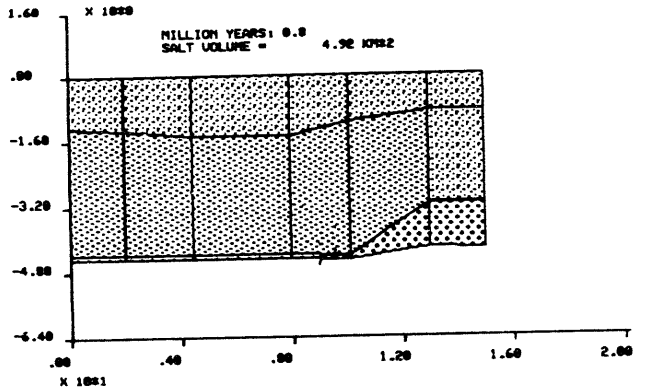

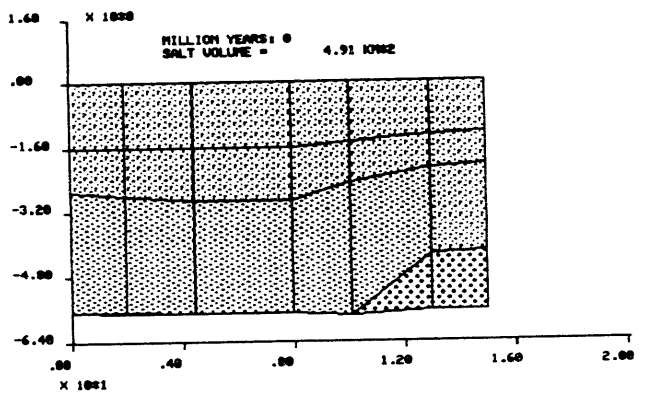

The porosity profile inferred by phase 1 processing and determined by Cinima (heavier line) are compared:

Plotting: PHI[z] Comparison.

Execution of this command produces the following plots for wells 1 and 7:

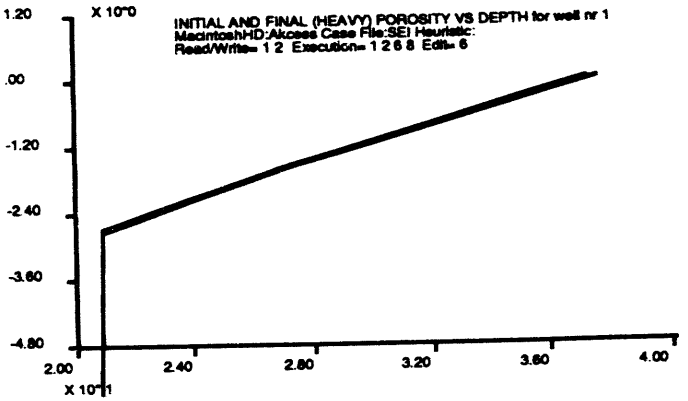

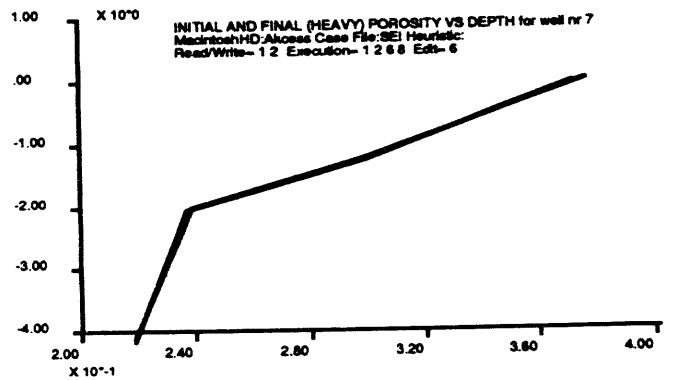

Notice that a record is presented of the processing history. Note also that porosity is a constant 21% below the seal when the seal lies above the second to bottom node (well 1) but that in well 7 where the seal lies below the second to bottom node there porosity appears to decrease from about 24% to 22% under the seal. This is an artifact of the coarse macronode resolution.

The flat, tabgro, and seal files can be saved for later use:

Read/Write: Write Flat+Tabgro

These files will be used in example 5 below.

2. Transgressing Seal, Automatic Salt Diapirism

Alternatively, the SEI Heuristic case can be processed so that a diapirism file that conserves salt is created:

Execution:	Start (select SEI Heuristic)
Execution:	Create Flat
Execution:	Process Flat
Execution:	Basal Salt
Execution:	Create Tabgro
Execution:	Process Tabgro (From Sediment Pattern)
Execution:	Cinima
Movies:	Run Movie

Note the movie can be run because line plots is the default option and movies are automatically recorded with this option. The above sequence of commands produces the following geohistory:

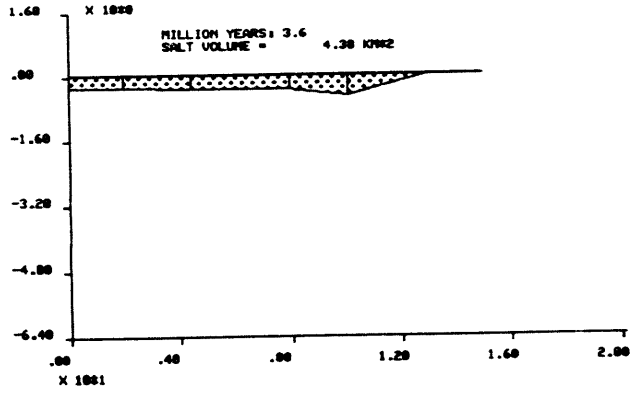

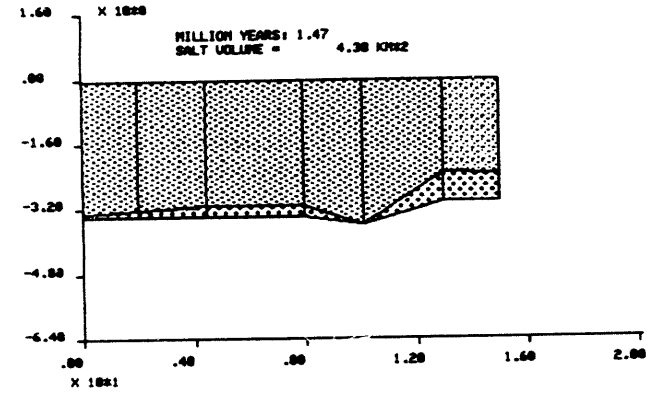

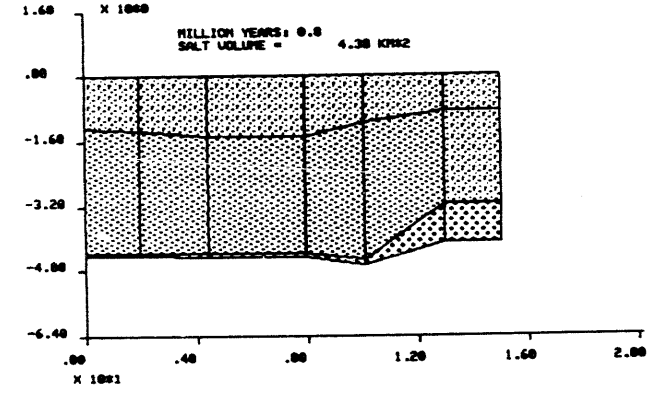

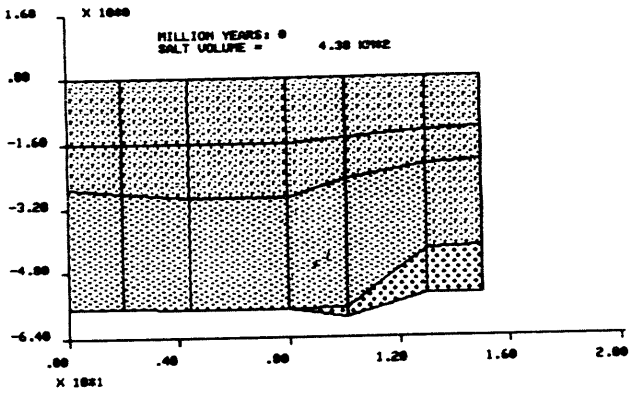

The porosity profile maintains constant porosity under the seal as in the case above (since only the salt movement has changed). This is illustrated for the first well by the section pasted from Plotting: Porosity[z]:

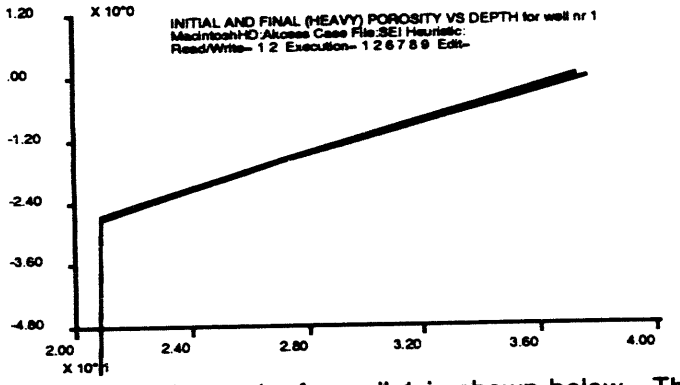

The evolution of porosity for well 1 is shown below. The uncompacted porosity of the top (surface node) changes slightly as the lithology changes from shale to sandy shale. the porosity decreases linearly until the seal develops and is then arrested. The bottom layer is salt with a porosity of zero.

3.6 ma	1.47 ma	0.8 ma	0 ma
0	0	0	0.38
0	0	0.38	0.27
0	0.37	0.28	0.21
0.35	0.21	0.21	0.21
0	0	0	0

3. Transgressing Seal, Combined Automatic and Manual Salt Diapirism

The salt distribution in the above example can be changed easily with the editing mode of Execution: Process Tabgro. For example the initial thickness of the salt sheet could be made more uniform by editing so that it is 0.5 km thick under the future salt dome at 3.6 ma. 0.3 km (rather that 0 km) thick at the margin at 1.47 ma, and 0 km thick at the margin at 0 ma. The resulting geohistory then looks:

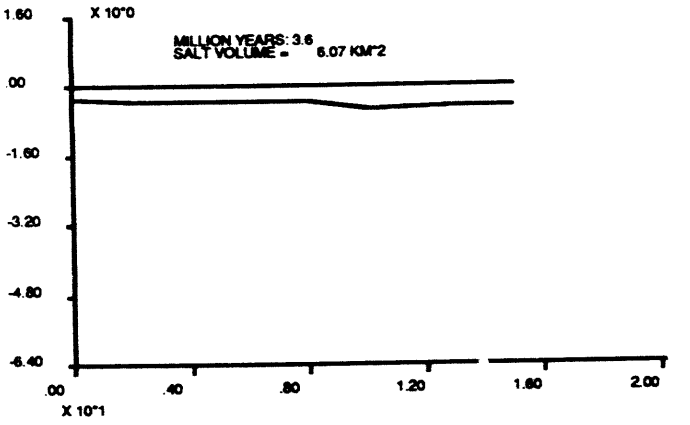

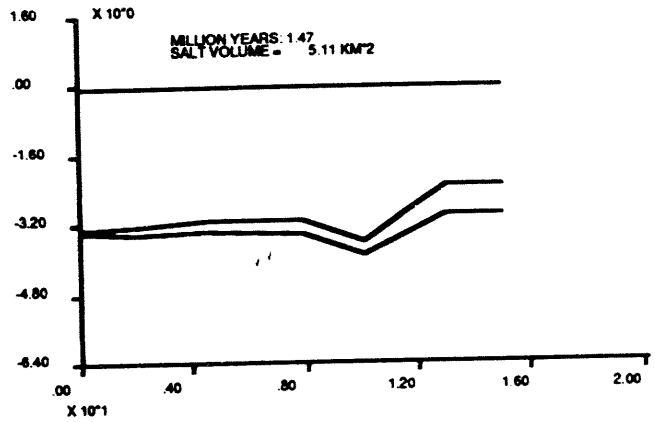

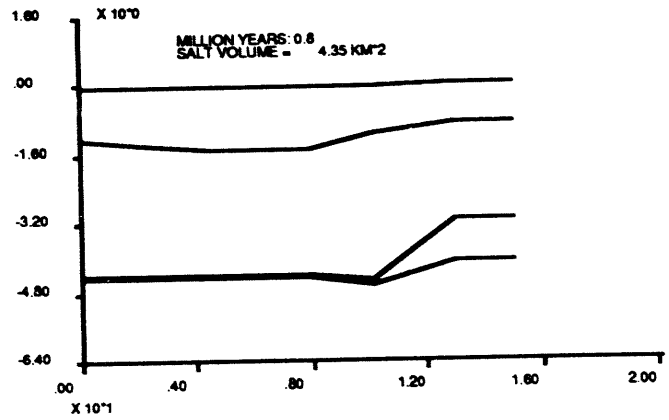

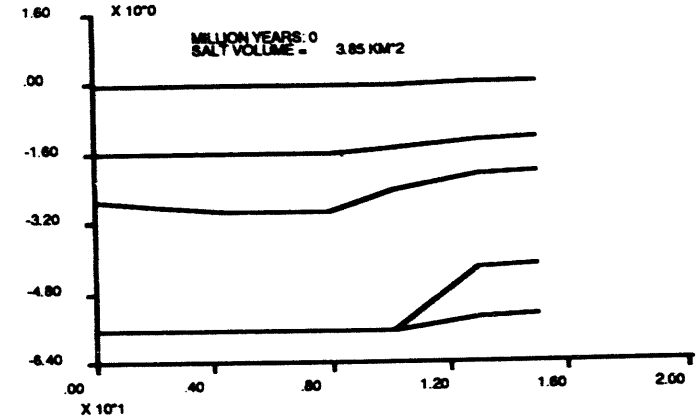

4. *Replacing the Transgressing, Migrating Seal with a Seal Fixed to a Particular Strata*

Finally a seal can be inserted and fixed to a strata. This needs, in this case, to be done after the initial flat file is processed since a pre-existing seal can be replaced but a cross-cutting seal cannot be replaced before it is processed. The commands are:

Execution: Start
Execution: Create Flat
Execution: Process Flat
Execution: Insert Seal (3d horizon, 0.2 km)
Execution: Process flat
Execution: Basal Salt
Execution: Create Tabgro
Execution: Process Tabgro (from sediment pattern)
Execution: Cinima

The inserted seal is shown in the diagram below. It is the narrow band enclosed by horizons 3 and 4.

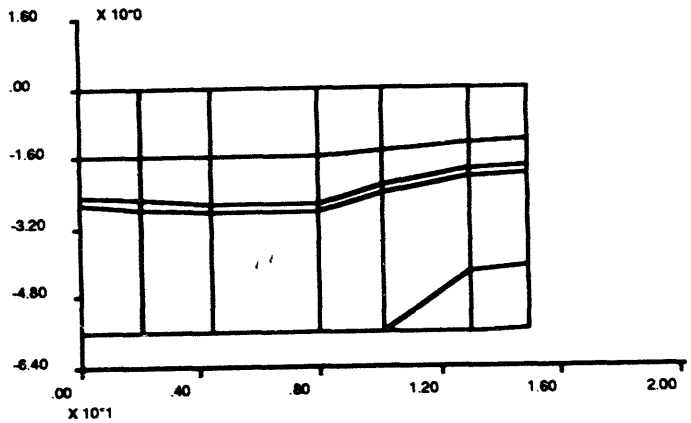

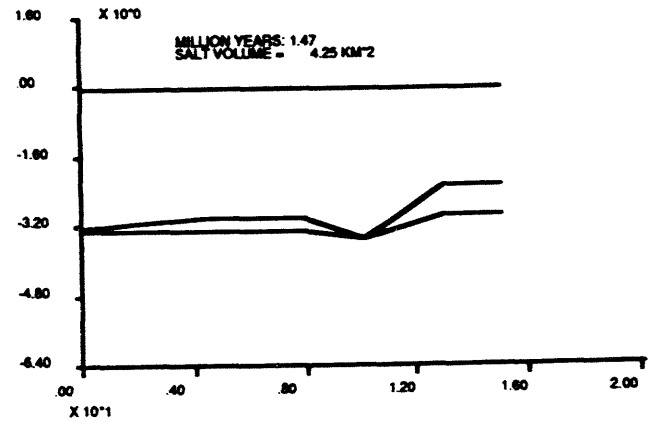

The geohistory in the fixed seal case is:

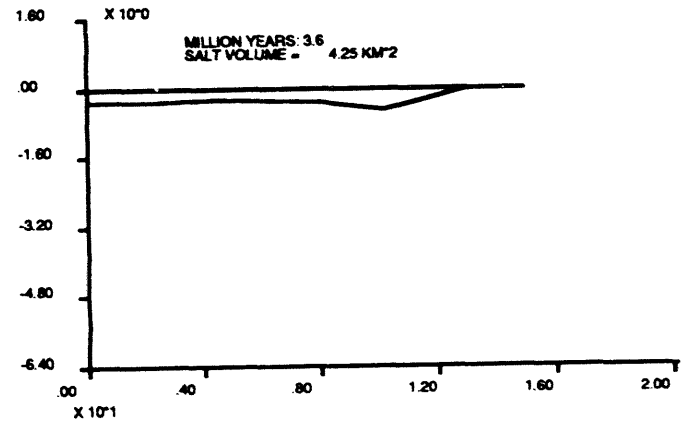

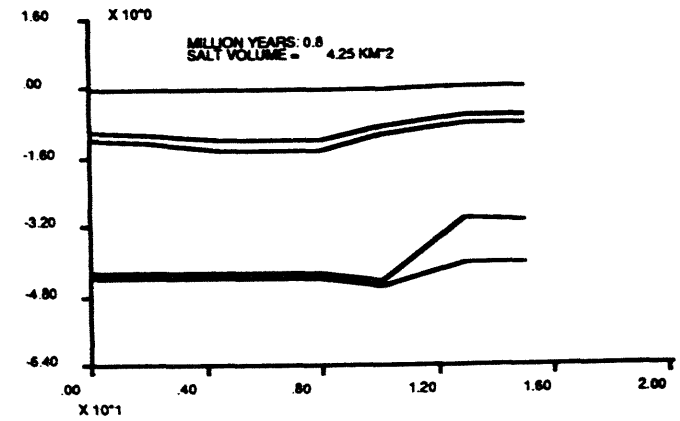

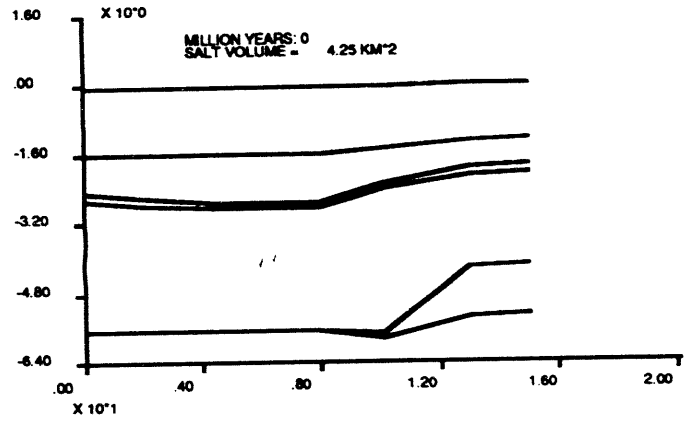

The base of the salt differs a little from the original flat file since it is constrained by salt conservation. The other strata are identical.

The porosity profile below the fixed seal is a normal compaction profile, arrested at the time the seal is buried and slightly compacted thereafter because the maximum fluid pressure is only 0.8 of lithostatic. The porosity profile can be viewed for the first well using:

Plotting: Porosity[z]:

The result is:

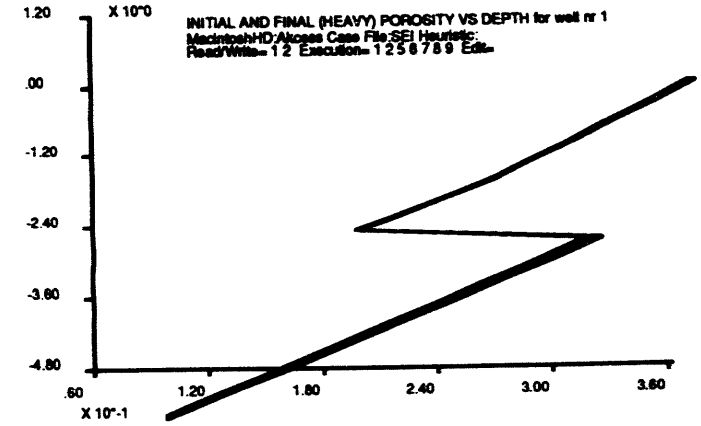

The porosity evolves with time:

3.6	1.47	1.34	0.80	0 ma
0	0	0	0	0.376
0	0	0	0.376	0.271
0	0	0.369	0.297	0.198
0	0.369	0.359	0.346	0.326
0.355	0.132	0.131	0.118	0.098
0	0	0	0	0

Again the porosity in the basal salt layer is zero (and is omitted from the plots). The sediments under the seal, which forms in this case at the surface, are compacted as they are buried by the ~20% of the lithostatic load that is not supported by increases in pore pressure.

5. No Seal Case

The simplest case is where there is no seal at all. One way to run this case is to delete the horizons with "0"

horizon numbers from the flat file, decrement the horizon number in the ***facts*** file by one, and re-run the case. Another way to run the case is by processing the flat file as in example 1 above and zeroing out the seal file. The commands for this latter procedure are listed below. Note to save time we can read in the tabgro file that we saved in example 1.

Execution:	Start
Execution:	Process Flat
Edit:	Seal (replace all entries with 0)
Read/Write:	Write Flat+Tabgro (select tabgro only, not the flat or seal)
Edit:	Part Flat (fill in the bottom of data plane 17 as in example 1 to tie the tabgro nodes to ***flat***)
Execution:	Cinima
Plotting:	PHI[z] Comparison

The Geohistory plots are very similar to those in example 1 and are not reproduced. The porosity-depth plot is of course quite different because there is no seal. The linear (except for lithologic variations) compaction of well 3 is shown below:

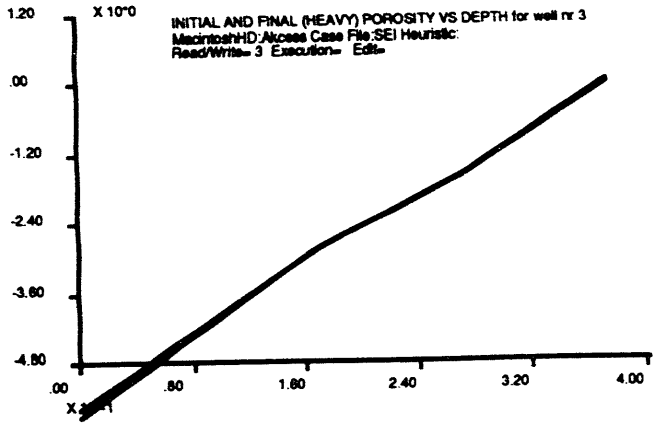

Very similar results but slightly incorrect results could be obtained:

Execution:	Start
Read/Write:	Read Flat+Tabgro (read ***flat*** and ***tabgro***)
Execution:	Cinima
Plotting:	PHI[z] Comparison

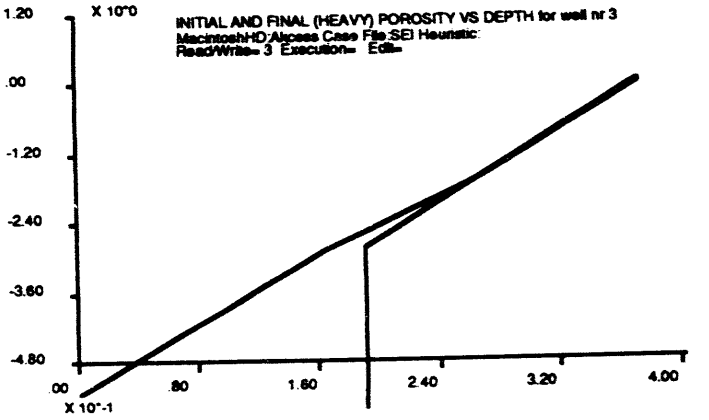

In this case the initial porosity profile assumes a seal (as indicated by the arrested compaction below ~2 km depth). The final (no seal) porosity-depth profile is very similar to that above, but the depths are slightly different because the initial (processing phase 1) porosities in the deeper parts of the section are higher than they should be if no seal is present.

B. Erosion Heuristic

This case illustrates how the sedimentation rate in FLAT may be edited to take into account erosion.

First examine the ***sflat*** file:

Execution: Start (select Erosion Heuristic)
Plotting: Sflat

Notice that the flat file has an obvious unconformity surface. The nature of this surface may be seen better by viewing the flat file in a plot style that shows lithology:

Execution: Create Flat
Plotting: Flat Lithologies

The flat file is now processed to obtain a first guess at sediment porosities and the uncompacted sedimentation rates:

Execution: Process Flat

The erosion is restored by editing the sedimentation rate. This could be done by editing the uncompacted sedimentation rate:

Editing: Erosion

This shows the kilometers of uncompacted sediment deposition over the time interval between each pair of strata (listed at the base of each interval). The array is changed:

.00	.00	.00	.00	
1.06	1.06	1.06	1.06	
1.15	1.15	1.15	1.15	Initial Sediment
.37	.00	.00	.00	Thickness Array
1.32	.37	.00	.37	
.981	.441	.271	.44	

.00	.00	.00	.00	
1.06	1.06	1.06	1.06	
1.15	1.15	1.15	1.15	Edited Sediment
.37	−.63	−1.2	−.63	Thickness
Array				
1.32	1	1.2	1	
.981	.441	.271	.44	

Then run the case:

Execution: Create Tabgro (select start 25 ma)
Execution: Cinima

You will notice that Cinima is executed twice. This is because the porosities of strata compacted before erosion are not properly guessed by the initial phase I processing. The porosities are properly computed by Cinima, however, and in the second pass these porosities are inserted into the flat file so that the flat file has good estimates of the porosities and Cinima computes better uncompacted sedimentation rates in the strata underlying the unconformity.

The result of Execution: Cinima is:

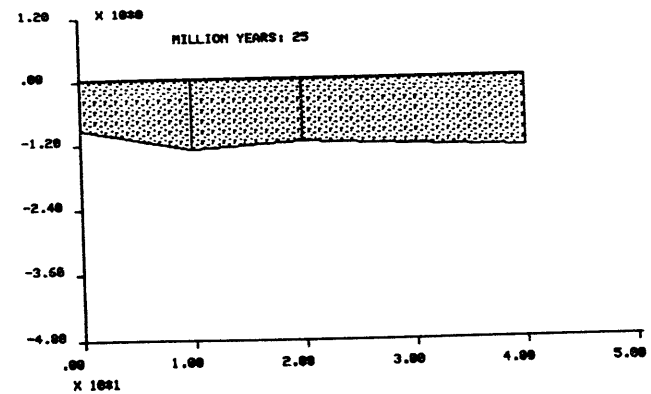

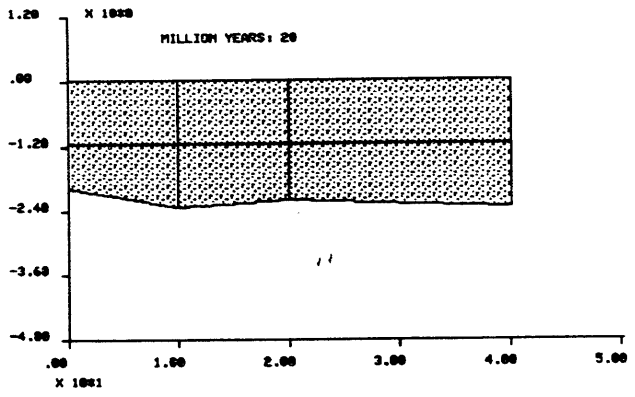

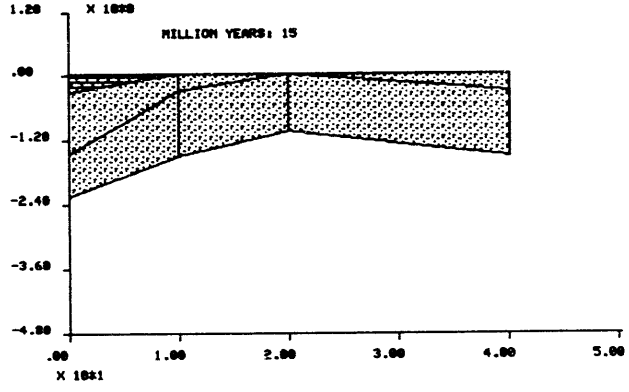

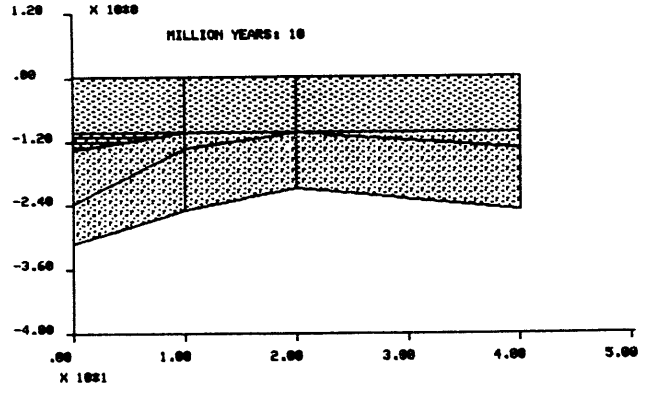

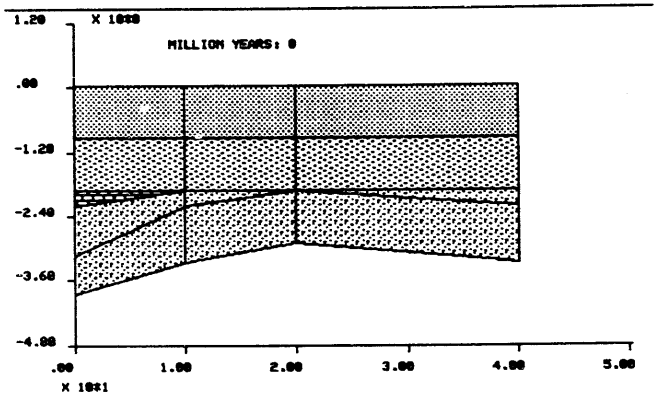

The porosity profile for this no-seal case is obtained from Plotting: PHI[z] Comparison and is:

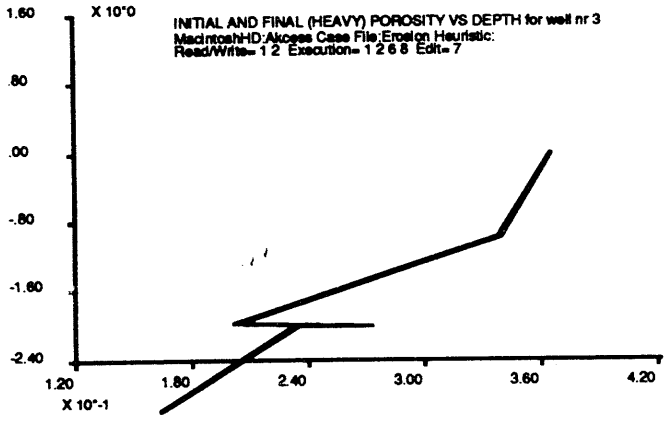

The compaction profile is basically a linear decreases with depth. The variations in porosity are due to variations in lithology. The initial and final porosity profiles overlap as one line.

A seal may be inserted at the base of the horizon overlying the unconformity (the third horizon):

Execution: Start (select Erosion Heuristic)
Execution: Create Flat
Execution: Insert Seal (fixed seal at hrzn 3)
Execution: Process Flat
Editing: Erosion (increases S and erode)
Execution: Create Tabgro (start at 25 ma)
Execution: Cinima
Plotting: PHI[z] Comparison

The result is similar to above to 15 ma when the seal is laid down. The final basin looks:

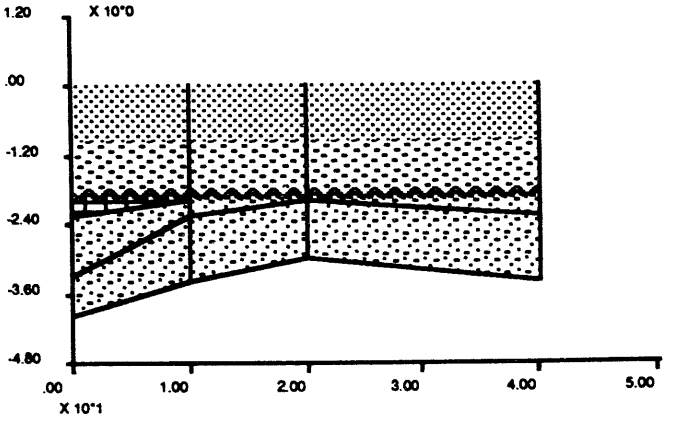

The summary porosity comparison plot for the third well is:

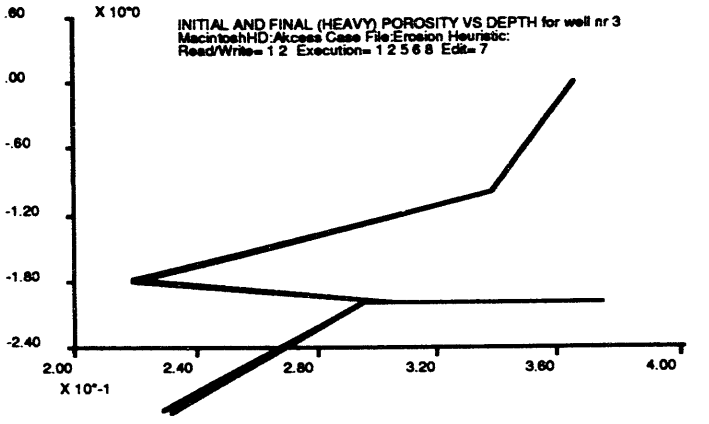

C. SEI Dimas

The SEIDIMAS series is based on maps prepared by Laurel Alexander and Peter Flemings. The maps show the depth in seconds to major flooding surface time horizons. Four sections each with 37 stratigraphic horizons were

prepared from these maps by Dimas Coehlo. The sections were originally tabulated in an ***sflat*** file that had 11 non-vertical wells. Time was manually converted to depth.

The ***sflat*** file was edited using:

Plotting:	Range Sflat
Editing:	Part Sflat.

The wells were straightened using: wellskeep NEWWELLS xlist. This is a function available to the advanced user who knows APL. It is not, at present, on one of the menus.

The ages of the major flooding surfaces were recorded in the *agedata* file. The horizon numbers and ages of these strata were:

1	2	6	12	18	28	32	36	37
0	0.44	0.575	0.95	1.37	1.47	2.2	5	7

The dimensions of *agedata* are given in *agedim*. The ***flat*** file was created and ages assigned to the strata between the 9 listed above:

Execution:	Create Flat
Execution:	Assign Age or
Execution:	Read Age

The later (Read Age) age assignment was used after SEIDIMAS4. This is to assure that the same ages are assigned to the horizons in all the SEI sections.

A migrating seal was inserted at horizon 18 using:

Execution:	Insert Seal

Finally the files were processed to completion and viewed in movie form:

Execution:	Process Flat
Execution:	Basal Salt
Execution:	Create Tabgro
Execution:	Process Tabgro
Edit: Stick	Welds (optional)
Read/Write:	Write Flat + Tabgro
Plotting:	Flat Horizons
Movies:	Make Movie
Execution:	Cinima
Movies:	Run Movie

Selected frames from the resulting geohistory movie are reproduced below.

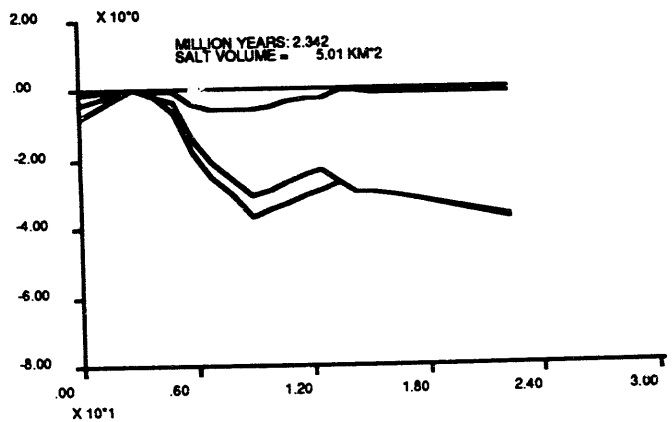

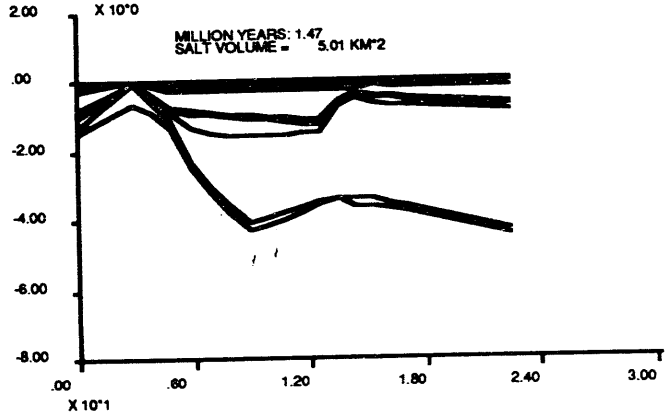

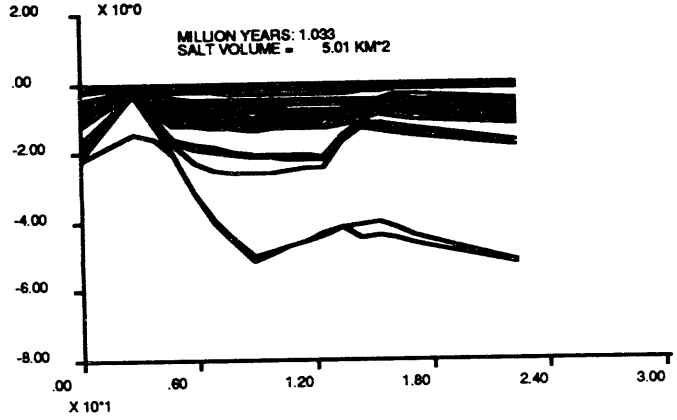

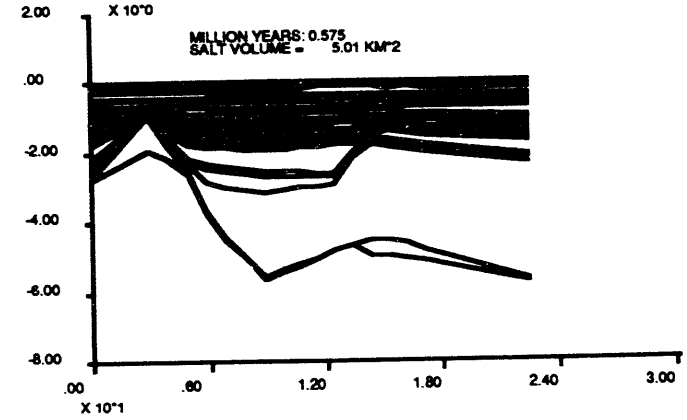

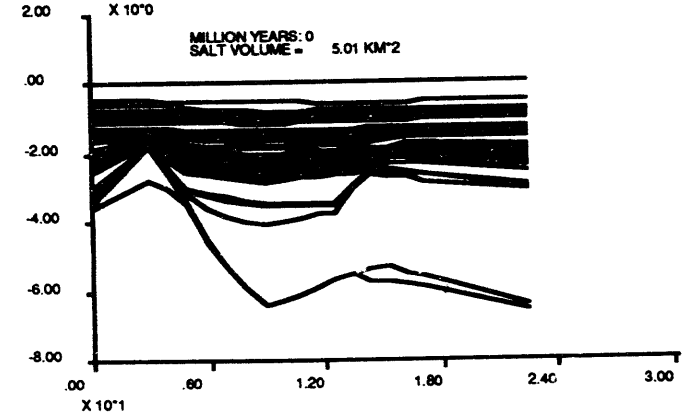

D. Regional Arco Lines

Four 300 km long regional lines were contributed by ARCO. ***sflat*** files for were prepared for all by Jackie Huntoon and Reinold Cornelius. This was done by measuring the interval from the sediment water interface to reflectors identified on the Arco lines in centimeters at 26 pseudowell locations. A conversion factor from cm to seconds was provided in FACTS. Finally a polynomial to convert time to depth was determined from the MMS shot

point data and input in file ***timedepth***. The result is that in processing into the ***flat*** file, the ***sflat*** is inverted and depth is in kilometers rather than a centimeter measure of two way seismic travel time.. When ***sflat*** is converted to a ***flat*** file using the time-to depth polynomial, the section inverts and depth is in kilometers.

The SFLAT files were processed:

Execution:	Create Flat
Execution:	Process Flat
Execution:	Basal Salt
	Creates tabgro ties at salt base.
Execution:	Create Tabgro
	Time 17.4 = start of modeling.
Execution:	Process Tabgro
	Option 1 to infer *tabgro* from S
Editing:	Stick Welds
	Zero all profiles to left (1).
Movies:	Make Movie
Execution:	Cinima
Read/Write:	Write Flat + Tabgro
	Write out flat, tabgro and seal
Movies:	Run Movie
Execution:	Quit

Selected frames from the geohistory movie are reproduced below.

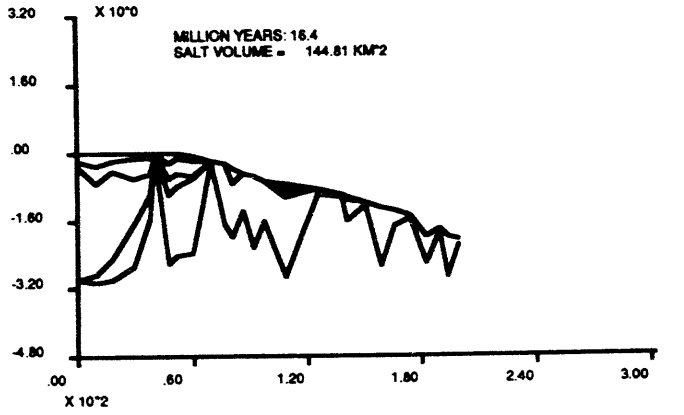

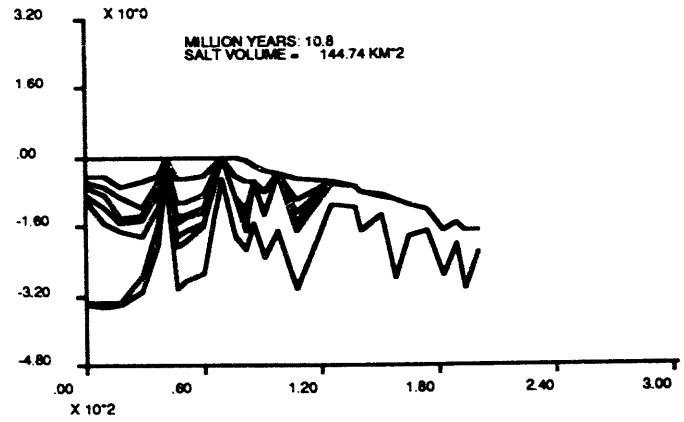

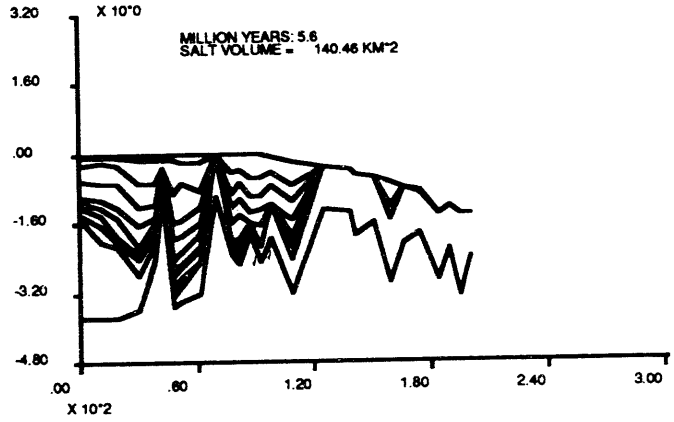

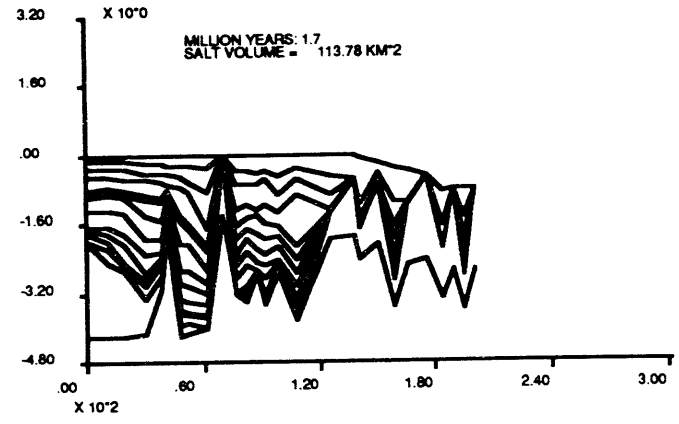

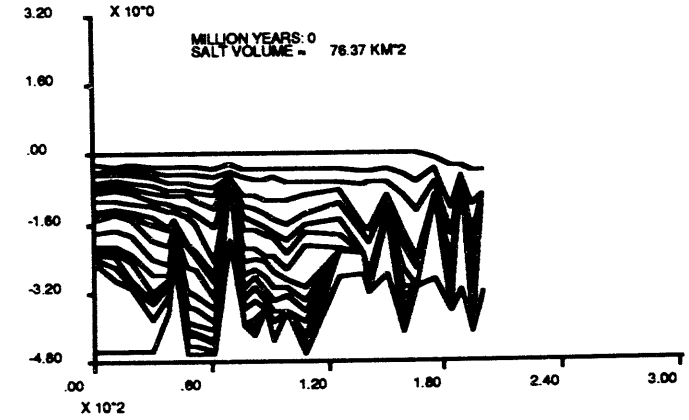

E. The North Sea

The geology Tampan Spur area of the North Sea was compiled as a project by the Cornell Case Histories in Ground Water Hydrology class, GS 502. The section runs NW-SE across the Tampan Spur and Viking Graben. This case illustrates how unequal sedimentation and slanted wells can simulate faulting. The small errors in sediment volume caused by scissoring between non-vertical wells is ignored in this case.

The initial ***sflat*** file looks:

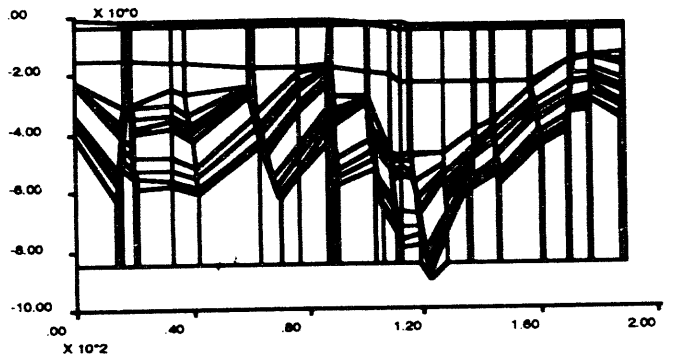

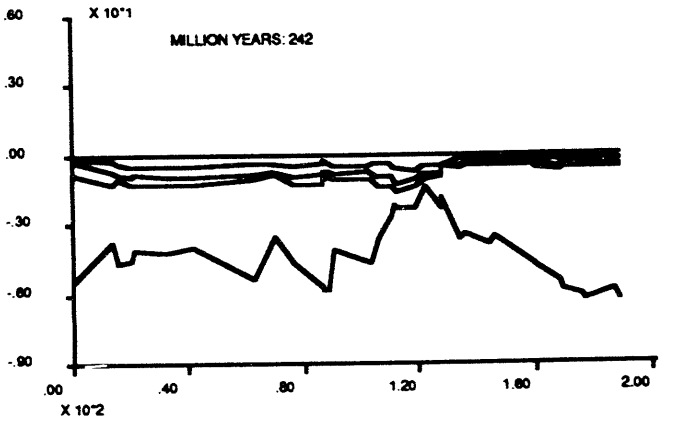

It was processed:

Execution: Start
Execution: Create Flat
Execution: Insert Seal (fixed to horizon 5)
Execution: Process Flat
Edit: Erosion (make deposition at intervals prior to 144 ma relatively uniform)
Execution: Create Tabgro (start at 268 ma)
Execution: Cinima
Movies: Run Movie

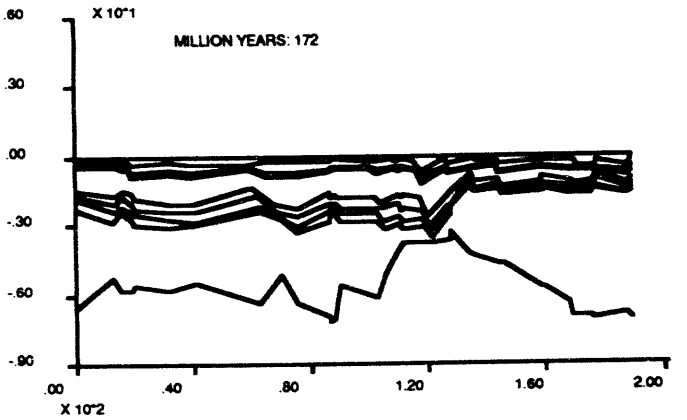

The resulting geohistory is:

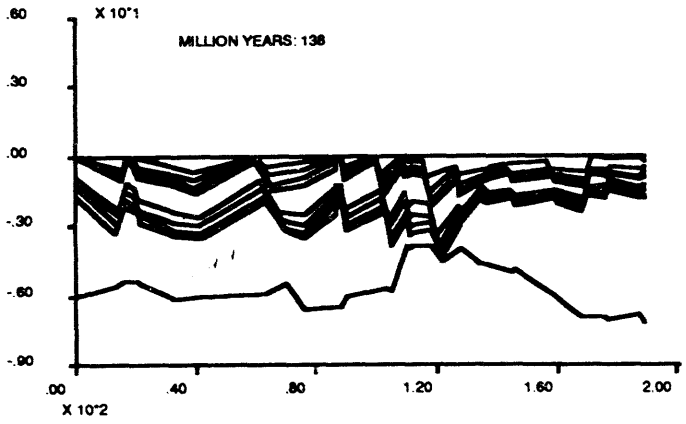

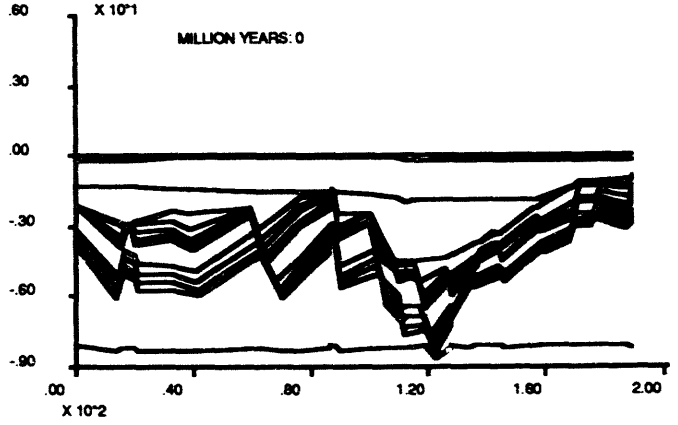

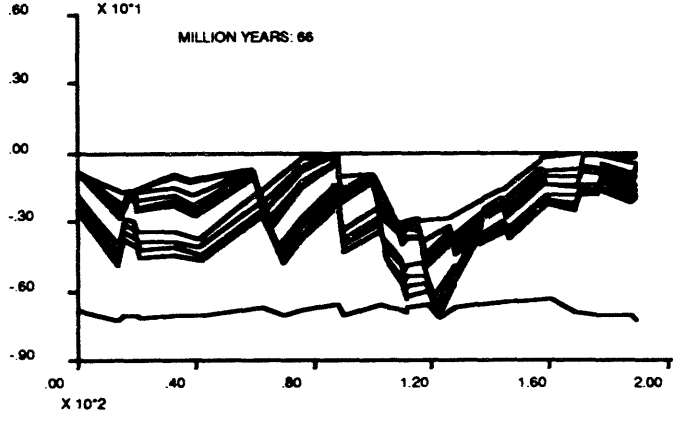

The porosity profile along the 8th well was obtained from Plotting: PHI[z] Comparison. The profile shows normal compaction above the seal, and arrested normal compaction below the seal. Variations from a smooth trend are due to lithilogy variations.

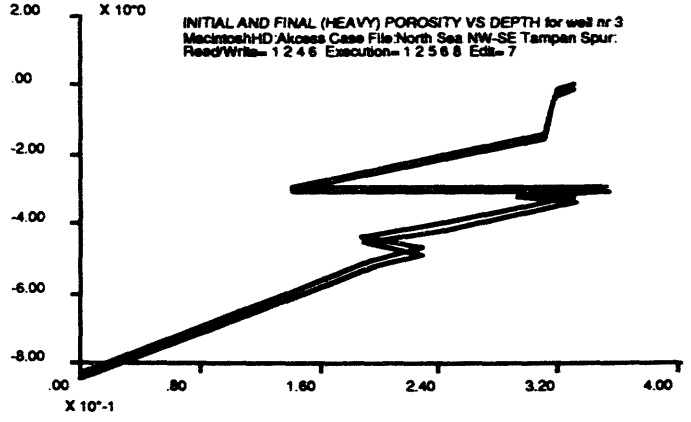

TASK SIX

GEOCHEMISTRY

Steven Losh - Cornell

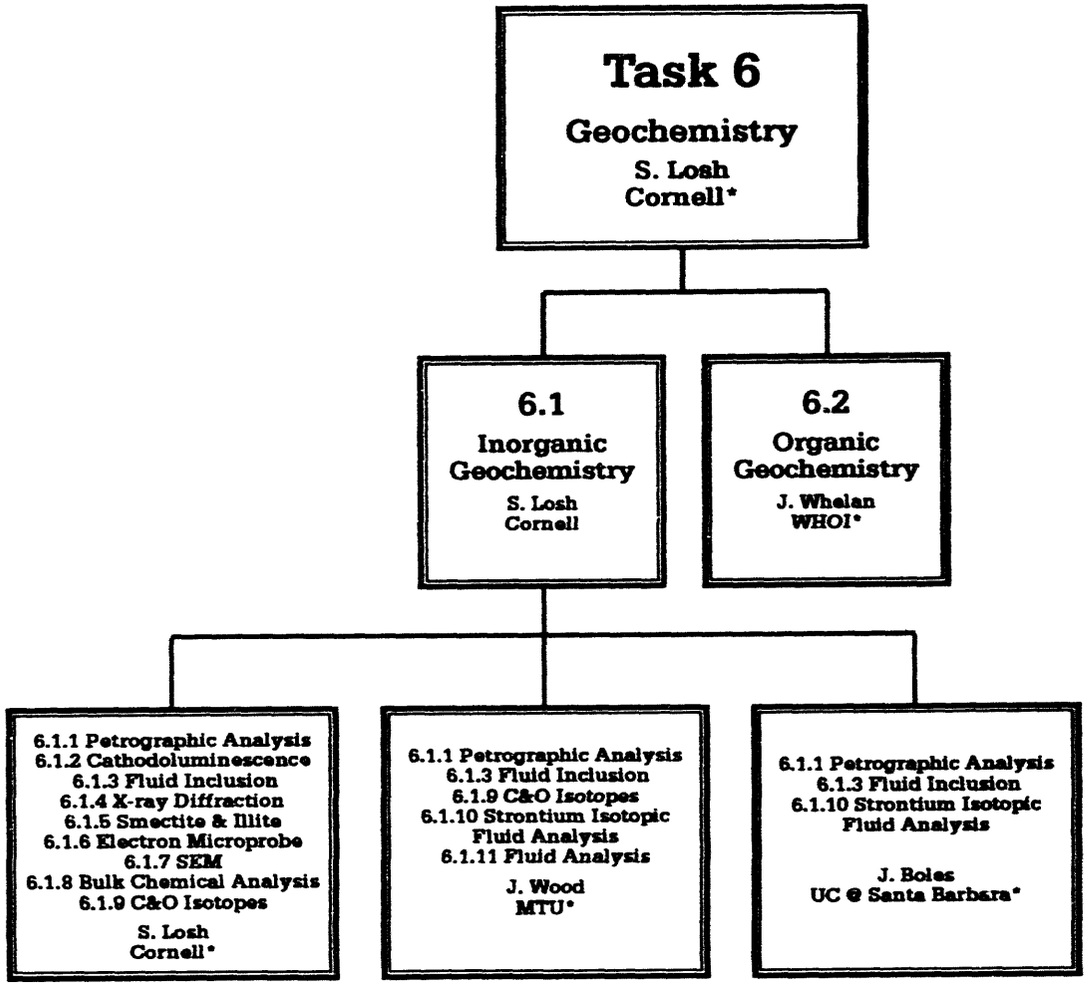
Task 6
Geochemistry
S. Losh
Cornell*
6.1
Inorganic Geochemistry
S. Losh
Cornell
6.2
Organic Geochemistry
J. Whelan
WHOI*
6.1.1 Petrographic Analysis
6.1.2 Cathodoluminescence
6.1.3 Fluid Inclusion
6.1.4 X-ray Diffraction
6.1.5 Smectite & Illite
6.1.6 Electron Microprobe
6.1.7 SEM
6.1.8 Bulk Chemical Analysis
6.1.9 C&O Isotopes
S. Losh
Cornell*
6.1.1 Petrographic Analysis
6.1.3 Fluid Inclusion
6.1.9 C&O Isotopes
6.1.10 Strontium Isotopic Fluid Analysis
6.1.11 Fluid Analysis
J. Wood
MTU*
6.1.1 Petrographic Analysis
6.1.3 Fluid Inclusion
6.1.10 Strontium Isotopic Fluid Analysis
J. Boles
UC @ Santa Barbara*

TASK 6. GEOCHEMISTRY

Task 6.1 Inorganic Geochemistry

Subtask 6.1.1 Petrography. Thin sections have been prepared from eight sidewall core samples from the main fault zone at 7611 - 7636.1. These rocks are shaly silts to silty shales; with one exception at 7625, they show no discernible evidence of shear. At this time, more sections are being made.

Also reported under this subtask are sidewall core data (Table 6-1-1); approximately 240 sidewall cores were taken from the well. Subsamples of selected sidewall cores were sent to Woods Hole Oceanographic Institute for vitrinite reflectance and organic geochemical analysis, and to Exxon Production Research for capillary entry pressure tests and analysis of smectite-illite transformation in fault zone rocks. Furthermore, nearly 400 samples have been taken from the whole core (Table 6-1-2) by both academic and industry researchers.

Laser particle size analysis has been performed on twelve samples from the whole core (Figure 6-1-1); these samples were collected from sandy intervals as noted on the core log.

CAT scanning of core has been performed by Exxon Production Research and Shell Oil Company Bellaire Lab (Table 6-1-3). This work was carried out in order to evaluate optimum locations for sampling of core, and to investigate density variations related to faulted shales.

A large amount of rock property data has been and is being collected, primarily relating to porosity and permeability at overburden stress, capillary entry pressure, v_p/v_s measurements, bulk density, particle size analysis, and Coulomb failure criteria. In addition, permeability data at atmospheric pressure has been collected (Table 6-1-4)

Work has continued on orienting the core in space. We have measured the angular relationship between slab cuts and the orientation markings put on the core as it was being pulled out of the core shuttle prior to being cut into sections. A number of locations have been identified where the core bedding dip matches the apparent dip recorded by the FMI; these sections of core are used as reference points for rotating the remaining sections from that particular core into alignment. The structural orientations recorded on the core log are then rotated using a stereonet program. When necessary, structures are rotated additionally if the slab face was not cut parallel with their maximum dip direction; the amount of additional rotation is based on the angular difference between the maximum dip amount recorded by x-ray fluoroscopy and the apparent dip recorded on the core log.

Subtask 6.1.2 Cathodoluminescence. Eight thin sections from sidewall cores from 7611

to 7636.1 feet (logger's depth) were examined under the cathode ray apparatus. Two main types of luminescent carbonate were seen: brightly-luminescent detrital calcite, and dull orange-red luminescent, probably diagenetic, carbonate. Neither type is present in amounts exceeding 3%. No micro-veins were seen.

Subtask 6.1.5. Smectite-illite transition. Work has continued on cuttings from Block 338, and has begun on cuttings and core samples from the Pathfinder well.

Subtask 6.1.8. Bulk chemical analysis. Eighteen core plugs have been analyzed (table 6-1-5) for major element oxides, sulfur, and several minor elements through Schlumberger (analyses were carried out at X-Ray Assay Labs, Don Mills, Ontario). These samples are from undeformed shale, and will serve as a basis for comparison with samples from fault zones.

Subtask 6.1.9. C and O isotopes. Work has continued on the carbon dioxide extraction line at Cornell. The line is nearing completion and is anticipated to be operational within a month.

Subtask 6.1.11. Fluid analysis. Major element analytical work has been completed on 22 brine samples collected from Blocks 330 and 316 in January of this year (table 6-1-6). Notably, there are significant salinity differences between the shallow GA sands (mostly over 90,000 ppm Cl), slightly deeper HB sands (between 50,000 and 60,000 ppm Cl), and still deeper OI sands (33,000 to 90,000 ppm Cl). The L-1 sands in the footwall have about the same salinity as the most saline OI brine, between 90,000 and 100,000 ppm Cl.

Iodine-129 dating will be performed at University of Rochester in April on all 22 brine samples. An analytical priority list has been established. In addition, organic acid determinations are underway at WHOI (subtask 6.2.b.8, next section)

TABLES.

Table 6-1-1. Sidewall core report for Pathfinder well, showing locations of samples taken by WHOI (W in left margin of report, except on page 10, where sample recipient is listed on right hand side of the report) and by Exxon Production Research (EPR; where only a chip was taken for capillary entry pressure analysis, the sample is marked EPR-CEP)

Table 6-1-2. Sample list for whole core. Depths are those given on core inner tube and are uncorrected for core gamma or adjustment to rectify driller and logger depths. The types of work being done by each researcher is as follows (not all analyses listed are being done on all samples taken by the investigator): Losh (Cornell) - petrography, x ray diffraction, SEM, probe, cathodoluminescence, stable isotopes, as appropriate. Boles (UCSB) - petrography and stable isotopes on siderite concretions. Penn State, Bruce Hart - physical and mechanical properties, primarily overburden porosity and liquid permeability, capillary entry pressure, shear and compressional velocity, laser particle size analysis, and Coulomb failure testing (on selected samples). Wood (MTU) - smectite - illite transformation. Butler (Pennzoil) - paleontology. Woods Hole - vitrinite reflectance, sorbed gases, organic geochemistry. Exxon (EPR) - bulk density, petrography, X-ray diffraction, smectite-illite analysis, capillary entry pressure determinations. Shell (Bellaire Lab) - capillary entry pressure, petrography, SEM.

Table 6-1-3. CAT scan intervals requested on whole core at Exxon Production Research. Shell Bellaire Labs also CAT scanned cores 5/2, 5/13, 5/16, and 6/3

Table 6-1-4 Profile permeameter data for core 4, section 15, containing 7-inch thick fluorescent sand. Measurements were carried out at atmospheric pressure.

Table 6-1-5. Bulk chemical composition of eighteen samples from the whole core. Depths are given as part of the sample numbers. Analyses carried out by X-Ray Assay Labs.

Table 6-1-6. Brine chemical analyses, carried out at University of Michigan in the lab of Dr. Lynn Walter. Samples are from Blocks 330 and 316 (marked). Temperatures are not ambient formation values.

FIGURE

Figure 6-1-1. Laser particle size analyses for twelve whole core samples, primarily from sands. Sampling and analyses were carried out by Core Labs

CORE LABORATORIES - NEW ORLEANS

ompany : Pennzoil Expl. & Prod. Company
/ell : OCS-G-2115 No. A-20 S/T
eld : Eugene Island Blk. 330
ɔcation : Offshore, Louisana

SIDEWALL CORE ANALYSIS REPORT

CL File No : 57161-11410
Date : 1-Dec-93
Analyst : RH
Drilling Fluid : Novasol

Sample Recovery Inches	Sample Depth feet	Kair (Empirical) md	Porosity Fluid %	Probable Production	Saturations by Volume				Crit Water %	Gas Det	Descriptions
					Oil PV %	Water PV %	Oil BV %	Gas BV %			
0.8	5382.0	2.3	19.2	Low Perm	0.8	87.9	0.1	2.2	72	3	Slt shy calc spts yel-wh fluor
W 1.0	5385.0	6.1	20.7	LP-Oil	5.9	77.5	1.2	3.4	71	25	Slt vshy lam C scalc stks yel-wh fluor 15% Slt wtol.
1.2	5387.0	20.0	24.4	Oil	10.4	74.6	2.5	3.7	66	20	Slt shy lam F stks bt yel-wh fluor 60% Slt
1.2	5391.0	2.0	18.0	Low Perm	0.9	83.6	0.2	2.8		3	Shale sslty vcalc spts yel-wh fluor
1.5	5393.0	3.1	20.3	Low Perm	3.8	80.2	0.8	3.3		5	Shale w/Slt lam scalc stks bt yel-wh fluor
0.6	5395.0	3.7	22.2	Low Perm	0.0	82.0	0.0	4.0	75	0	Slt vshy ssdy calc no fluor
1.2	5397.0	90.0	29.8	Oil	7.0	77.6	2.1	4.6	57	25	Sd vfgr sshy lam G vslty stks yel-wh fluor 50% Sd (29 API)
1.0	5400.0	4.8	21.5	Low Perm	0.0	81.4	0.0	4.0	73	0	Sd vfgr vshy slty scalc no fluor
1.0	5402.0	4.1	20.7	Low Perm	0.0	85.5	0.0	3.0	73	0	Sd vfgr vshy slty calc no fluor
1.0	5406.0	6.9	21.6	LP-Oil	6.2	75.4	1.3	4.0	72	30	Sd vfgr vshy lam C stks yel-wh fluor 15% Sd
1.2	5413.0									0	Shale w\Slt lam scalc no fluor
1.5	5415.0									0	Shale sslty calc no fluor
1.5	5419.0									0	Shale sslty calc no fluor
1.2	5423.0									0	Shale sslty scalc no fluor
1.5	5425.0	3.9	18.0	Low Perm	0.0	86.1	0.0	2.5	70	0	Sd vfgr vshy slty calc no fluor
1.5	5427.0	5.6	20.5	Low Perm	0.0	84.2	0.0	3.2	71	0	Sd vfgr vshy scalc no fluor
1.2	5430.0	3.2	19.8	Low Perm	0.0	86.1	0.0	2.7	73	0	Slt vshy lam C ssdy calc no fluor 15% Slt
Bad 1.5	5436.0	2.7	18.2	Low Perm	0.0	83.7	0.0	3.0	71	0	Slt vshy lam C calc no fluor 15% Slt
1.5	5440.0	2.9	19.1	Low Perm	0.0	84.7	0.0	2.9	72	0	Slt vshy lam G calc no fluor 40% Slt
1.5	5444.0	1.8	18.8	Low Perm	0.0	86.8	0.0	2.5	72	0	Slt vshy lam C vcalc no fluor 10% Slt
0.8	5457.0	3.5	18.7	Low Perm	0.0	84.4	0.0	2.9	71	0	Slt vshy ssdy calc no fluor
1.0	5458.0									0	Shale slty calc no fluor
1.0	5459.0									0	Shale calc no fluor
1.0	5461.0	1.2	20.5	Low Perm	1.0	90.2	0.2	1.8		0	Shale w/Slt lam scalc stks bt yel-wh fluor
1.5	5464.0	1.5	16.8	Low Perm	0.0	88.0	0.0	2.0	69	0	Slt vshy lam BC dense scalc no fluor 25% Slt
0.1	5468.0									0	Mudcake

Table 6-1-1. Sidewall core report

CORE LABORATORIES - NEW ORLEANS

ompany : Pennzoil Expl. & Prod. Company
Vell : OCS-G-2115 No. A-20 S/T
ield : Eugene Island Blk. 330
ocation : Offshore, Louisana

SIDEWALL CORE ANALYSIS REPORT

CL File No : 57161-11410
Date : 1-Dec-93
Analyst : RH
Drilling Fluid : Novasol

Sample Recovery Inches	Sample Depth feet	Kair (Empirical) md	Porosity Fluid %	Probable Production	Saturations by Volume				Crit Water %	Gas Det	Descriptions
					Oil PV %	Water PV %	Oil BV %	Gas BV %			
1.2	5475.0									0	Shale sslty calc no fluor
1.5	5477.0									0	Shale slty calc no fluor
0.4	5479.0	160.0	30.9	Oil	7.7	74.7	2.4	5.4	51	12	Sd vfgr vsshy vslty scalc yel-wh fluor (29 API)
0.4	5481.0	240.0	33.0	Oil	7.6	76.1	2.5	5.4	48	0	Sd vfgr vsshy lam G vslty stks yel-wh fluor 90% Sd
W 0.6	5483.0	290.0	33.6	Oil	8.9	71.1	3.0	6.7	47	5	Sd vfgr vsshy vslty bt yel-wh fluor (30 API)
W 1.2	6200.0	19.0	23.7	Oil	10.9	72.0	2.6	4.0	66	30	Sd vfgr vshy vcalc mott yel-wh fluor (30 API)
1.2	6202.0	6.0	21.8	LP-Oil	6.4	76.9	1.4	3.6	72	5	Sd vfgr vshy vcalc mott yel-wh fluor
W 1.5	6359.0									0	Shale calc no fluor
1.2	6361.0									0	Shale calc no fluor
1.2	6367.0									0	Shale ssdy calc no fluor
1.5	6385.0	3.2	19.8	Low Perm	0.0	83.3	0.0	3.3	73	0	Sd vfgr vshy vslty calc no fluor
1.2	6387.0	3.5	20.4	Low Perm	0.0	86.2	0.0	2.8	74	0	Sd vfgr vshy vslty calc no fluor
1.2	6389.0	12.0	21.7	Oil	6.8	74.9	1.5	4.0	67	6	Sd vfgr vshy slty scalc mott yel-wh fluor (29 API)
W 1.2	6391.0	17.0	22.4	Oil	9.0	73.5	2.0	3.9	66	20	Sd vfgr vshy lam G scalc stks yel-wh fluor 40% Sd
1.0	6400.0	4.0	20.1	Low Perm	0.0	85.5	0.0	2.9	73	0	Sd vfgr vshy slty calc no fluor
1.2	6410.0									0	Shale slty scalc no fluor
1.0	6411.0									0	Shale slty scalc no fluor
1.5	6418.0	1.3	19.0	Low Perm	1.3	90.0	0.3	1.6		0	Shale slty calc stks yel-wh fluor
1.5	6419.0	1.8	19.7	Low Perm	1.6	87.9	0.3	2.1		5	Shale w/Slt lam calc stks yel-wh fluor
1.2	6420.0	32.0	28.1	Oil	21.7	57.8	6.1	5.8	66	80	Slt shy lam B scalc stks bt yel-wh fluor 50% Slt (29 API)
1.0	6424.0	21.0	24.8	Oil	15.0	62.0	3.7	5.7	66	85	Sd vf-fgr vshy lam G slty stks yel-wh fluor 60% Sd
1.5	6431.0	1.4	21.3	Low Perm	1.0	92.0	0.2	1.5		7	Shale spts yel-wh fluor
1.2	6441.0									0	Shale calc no fluor
1.5	6445.0	2.2	19.7	Low Perm	1.3	89.4	0.3	1.8		0	Shale ssdy calc mott yel-wh fluor

Table 6-1-1 (cont'd)

CORE LABORATORIES - NEW ORLEANS

ompany : Pennzoil Expl. & Prod. Company
/ell : OCS-G-2115 No. A-20 S/T
eld : Eugene Island Blk. 330
ocation : Offshore, Louisana

SIDEWALL CORE ANALYSIS REPORT

CL File No : 57161-11410
Date : 1-Dec-93
Analyst : RH
Drilling Fluid : Novasol

Sample Recovery Inches	Sample Depth feet	Kair (Empirical) md	Porosity Fluid %	Probable Production	Saturations by Volume				Crit Water %	Gas Det	Descriptions
					Oil PV %	Water PV %	Oil BV %	Gas BV %			
W 1.2	6449.0	6.0	20.5	LP-Oil	5.5	78.5	1.1	3.3	70	30	Sd vf-fgr vshy calc mott yel-wh fluor
1.2	6451.0									0	Shale calc no fluor
1.5	6454.0									0	Shale w/Slt calc no fluor
1.5	6458.0	3.4	20.2	Low Perm	0.0	87.3	0.0	2.6	73	0	Slt vshy sndy calc no fluor
	6462.0										Empty bottle
0.8	6466.0									0	Shale calc no fluor
1.5	6471.0									0	Shale calc no fluor
1.2	6473.0	2.1	19.5	Low Perm	3.1	88.8	0.6	1.6	73	0	Slt vshy lam C calc stks bt yel-wh fluor 10% Slt
1.5	6475.0	2.9	21.2	Low Perm	5.7	83.7	1.2	2.3	75	30	Slt vshy lam C scalc stks yel-wh fluor 20% Slt
1.2	6479.0	7.2	21.6	LP-Oil	8.7	78.5	1.9	2.8	71	30	Sd vfgr vshy lam G calc stks yel-wh fluor 40% Sd (29 API)
0.6	6481.0	1.7	20.1	LP-Oil	2.5	89.0	0.5	1.7		0	Sd vfgr vshy lam G calc stks yel-wh fluor 40% Sd (29 API)
	6485.0										Empty bottle
0.8	6492.0									0	Shale calc no fluor
W 1.2	6503.0									0	Shale calc no fluor
1.2	6505.0									0	Shale calc no fluor
1.5	6507.0	2.6	21.1	Low Perm	0.0	86.1	0.0	2.9	75	0	Slt vshy calc no fluor
1.2	6512.0	4.4	20.0	Low Perm	0.0	88.0	0.0	2.4	72	0	Sd vfgr vshy slty scalc no fluor
1.5	6528.0	5.1	20.8	Low Perm	0.0	85.6	0.0	3.0	72	0	Sd vfgr vshy slty scalc no fluor
1.0	6532.0									0	Shale slty calc no fluor
1.2	6540.0									0	Shale calc no fluor
1.5	6546.0									0	Shale sndy calc no fluor
W 0.8	6556.0	22.0	24.2	Oil	8.8	76.1	2.1	3.7	65	35	Sd vfgr vshy lam G scalc stks bt yel-wh fluor (32 API)
1.5	6564.0									0	Shale sslty scalc no fluor
1.5	6590.0	5.5	21.5	LP-Oil	5.3	81.2	1.1	2.9	72	0	Slt vshy lam C calc stks yel-wh fluor 40% Slt
1.5	6591.0									0	Shale slty vcalc no fluor

Table 6-1-1 (cont'd)

CORE LABORATORIES - NEW ORLEANS

ompany : Pennzoil Expl. & Prod. Company
ell : OCS-G-2115 No. A-20 S/T
eld : Eugene Island Blk. 330
ocation : Offshore, Louisana

SIDEWALL CORE ANALYSIS REPORT

CL File No : 57161-11410
Date : 1-Dec-93
Analyst : RH
Drilling Fluid : Novasol

Sample Recovery Inches	Sample Depth feet	Kair (Empirical) md	Porosity Fluid %	Probable Production	Saturations by Volume				Crit Water %	Gas Det	Descriptions
					Oil PV %	Water PV %	Oil BV %	Gas BV %			
1.2	6592.0									0	Shale calc no fluor
1.2	6599.0	2.0	18.3	Low Perm	2.4	84.9	0.4	2.3		0	Shale calc stks bt yel-wh fluor
1.5	6601.0	2.4	19.1	Low Perm	3.8	86.0	0.7	1.9		15	Shale calc stks bt yel-wh fluor
1.5	6603.0									0	Shale calc no fluor
1.2	6605.0	3.7	20.9	Low Perm	5.3	84.9	1.1	2.1	74	40	Slt vshy calc mott yel-wh fluor
1.2	6607.0	14.0	23.8	Oil	11.7	75.5	2.8	3.0	68	60	Sd vfgr vshy lam C slty scalc stks bt yel-wh fluor (30 API)
1.5	6609.0	8.3	22.2	LP-Oil	10.8	79.3	2.4	2.2	71	60	Slt shy calc mott yel-wh fluor
1.5	6611.0	155.0	31.8	Oil	8.3	66.7	2.6	7.9	52	90	Sd vfgr sshy lam G vslty scalc stks bt yel-wh fluor (30 API)
1.5	6613.0	2.7	18.8	Low Perm	3.3	88.7	0.6	1.5		10	Shale ssdy calc spts yel-wh fluor
1.2	6615.0									0	Shale calc no fluor
1.2	6617.0									0	Shale calc no fluor
1.5	6712.0									0	Shale vcalc no fluor
1.2	6713.0									0	Shale vcalc no fluor
1.0	6714.0									0	Shale vcalc no fluor
1.2	6715.0									0	Shale vcalc no fluor
1.2	6716.0	17.0	23.1	Oil	8.4	77.5	1.9	3.3	66	40	Sd vf-fgr vshy vfoss mott yel-wh fluor (30 API)
1.5	6741.0	4.0	18.4	Low Perm	0.0	86.4	0.0	2.5	71	0	Sd vf-fgr vshy foss no fluor
1.5	6741.1	3.8	19.0	Low Perm	0.0	84.5	0.0	2.9	71	0	Sd vf-fgr vshy foss no fluor
1.5	6742.0	3.1	17.6	Low Perm	0.0	85.8	0.0	2.5	69	0	Sd vf-fgr vshy foss spts ft min fluor
1.2	6742.1	5.8	20.1	Low Perm	0.0	87.1	0.0	2.6	70	0	Sd vf-fgr vshy foss no fluor
1.2	6743.0	4.2	19.4	Low Perm	0.0	82.1	0.0	3.5	71	0	Sd vf-fgr vshy foss no fluor
1.2	6744.0									0	Shale sfoss no fluor
0.4	6745.0									0	Mudcake w/tr Shale
1.5	6746.0	6.2	21.1	Low Perm	0.0	85.8	0.0	3.0	71	0	Sd vf-fgr vshy foss no fluor

Table 6-1-1 (cont'd)

CORE LABORATORIES - NEW ORLEANS

ompany : Pennzoil Expl. & Prod. Company
'ell : OCS-G-2115 No. A-20 S/T
eld : Eugene Island Blk. 330
ocation : Offshore, Louisana

SIDEWALL CORE ANALYSIS REPORT

CL File No : 57161-11410
Date : 1-Dec-93
Analyst : RH
Drilling Fluid : Novasol

Sample Recovery Inches	Sample Depth feet	Kair (Empirical) md	Porosity Fluid %	Probable Production	Saturations by Volume				Crit Water %	Gas Det	Descriptions
					Oil PV %	Water PV %	Oil BV %	Gas BV %			
1.2	6747.0	3.3	17.8	Low Perm	0.0	87.5	0.0	2.2	70	0	Sd vf-fgr vshy foss no fluor
0.5	6748.0									0	Mudcake
W 1.5	6749.0									0	Shale scalc no fluor
1.2	6840.0	4.7	19.2	Low Perm	0.0	87.0	0.0	2.5	70	0	Sd vf-fgr vshy foss no fluor
W 1.5	6840.1	5.5	20.6	Low Perm	0.0	85.5	0.0	3.0	71	0	Sd vf-fgr vshy foss no fluor
1.2	6860.0	7.4	21.5	LP-Oil	5.8	75.8	1.2	4.0	71	5	Sd fgr vshy (50% mudcake) foss mott yel-wh fluor
0.5	6863.0	5.2	21.9	Low Perm	0.0	84.8	0.0	3.3	73	0	Sd vf-fgr shy lmy ft min fluor
0.6	6865.0	4.4	20.8	Low Perm	0.0	80.4	0.0	4.1	73	0	Sd vf-fgr shy (50% mudcake) lmy ft min fluor
0.8	6869.0	6.8	21.2	LP-Oil	5.3	82.0	1.1	2.7	71	3	Sd vf-fgr vshy lmy mott yel-wh fluor
0.6	6882.0	100.0	31.7	Oil	7.6	68.5	2.4	7.6	57	10	Sd vfgr sshy vslty scalc bt yel-wh fluor (31 API)
0.4	6892.0									0	Mudcake
0.4	6902.0									0	Mudcake w/tr Sd yel-wh fluor
W 0.6	6906.0	65.0	30.0	Oil	10.5	73.7	3.2	4.7	60	5	Sd vfgr sshy vslty scalc bt yel-wh fluor
0.5	6926.0									0	Mudcake
0.4	6928.0									0	Mudcake w/tr Sd yel-wh fluor
0.8	6947.0	50.0	27.2	Oil	11.7	61.8	3.2	7.2	61	7	Sd vf-fgr shy slty bt yel-wh fluor (32 API)
0.3	6953.0									0	Mudcake
W 0.8	6956.0	37.0	26.6	Oil	15.9	65.7	4.2	4.9	63	7	Sd vfgr shy slty bt yel-wh fluor
0.6	6959.0	28.0	25.9	Oil	11.3	70.7	2.9	4.7	65	8	Sd vfgr shy lam F vslty stks bt yel-wh fluor (32 API)
1.0	6962.0									0	Mudcake

Table 6-1-1 (cont'd)

CORE LABORATORIES - NEW ORLEANS

ompany : Pennzoil Expl. & Prod. Company
ell : OCS-G-2115 No. A-20 S/T
eld : Eugene Island Blk. 330
cation : Offshore, Louisana

SIDEWALL CORE ANALYSIS REPORT

CL File No : 57161-11410
Date : 1-Dec-93
Analyst : RH
Drilling Fluid : Novasol

Sample Recovery inches	Sample Depth feet	Kair (Empirical) md	Porosity Fluid %	Probable Production	Saturations by Volume				Crit Water %	Gas Det	Descriptions
					Oil PV %	Water PV %	Oil BV %	Gas BV %			
W 1.2	7157.0	2.2	20.0	Low Perm	1.3	87.9	0.3	2.2	75	0	Slt vshy scalc no fluor
1.2	7158.0	4.1	21.6	Low Perm	1.0	84.6	0.2	3.1	75	0	Slt vshy scalc no fluor
	7169.0										Empty Bottle
	7172.0										Empty Bottle
	7174.0										Empty Bottle
0.6	7177.0	9.8	25.1	Low Perm	2.0	84.2	0.5	3.5	72	0	Sd vfgr shy vslty no fluor
0.6	7178.0	82.0	27.8	Gas *	6.3	63.3	1.8	8.5	57	20	Sd vfgr sshy vslty no fluor
1.2	7179.0	36.0	27.2	Gas *	1.7	75.6	0.5	6.2	64	0	Sd vfgr shy slty slig no fluor
0.7	7180.0	65.0	27.3	Gas *	1.9	50.9	0.5	12.9	57	0	Sd vfgr shy slty no fluor
0.7	7182.0	320.0	29.9	Gas *	1.5	52.2	0.4	13.8	43	10	Sd vf-fgr sshy slty no fluor
0.8	7184.0	8.5	22.6	Low Perm	4.2	75.0	0.9	4.7	73	20	Sd vfgr vshy lam G no fluor 25% Sd
0.8	7185.0	740.0	29.8	Gas *	2.6	65.8	0.8	9.4	37	15	Sd vf-fgr sshy slty ft fluor
1.0	7186.0	9.3	24.3	Low Perm	2.9	75.4	0.7	5.3	72	0	Sd vf-fgr vshy lam F slig no fluor 45% Sd
1.0	7187.0	6.8	22.5	Low Perm	2.3	76.7	0.5	4.7	73	0	Sd vfgr vshy slig no fluor
1.2	7188.0	8.8	23.2	Low Perm	0.9	80.2	0.2	4.4	72	20	Sd vfgr vshy slig no fluor
1.2	7189.0	17.0	25.3	Gas *	2.6	65.8	0.7	8.0	70	0	Sd vfgr shy vslty slig no fluor
1.2	7192.0	2.9	19.9	Low Perm	2.4	80.5	0.5	3.4	73	0	Sd vfgr vshy lam C no fluor 20% Sd
0.8	7196.0	4.7	20.9	Low Perm	1.7	82.8	0.4	3.2	72	0	Sd vfgr vshy lam D no fluor 15% Sd
tc 0.8	7198.0	8.3	22.0	Low Perm	1.6	79.4	0.3	4.2	71	0	Sd vfgr vshy no fluor
W 1.7	7202.0	7.1	22.4	Low Perm	1.8	81.3	0.4	3.8	72	0	Sd vfgr vshy mott no fluor
1.1	7206.0	9.4	23.5	Low Perm	1.1	85.2	0.3	3.2	72	7	Sd vfgr vshy mott no fluor
0.9	7208.0	6.8	21.8	Low Perm	2.4	79.2	0.5	4.0	72	0	Sd vfgr vshy lam C spts yel-wh fluor 15% Sd
1.0	7215.0	3.9	20.0	Low Perm	1.0	79.2	0.2	4.0	72	7	Sd vfgr vshy no fluor
0.6	7221.0	2.8	20.5	Low Perm	1.2	84.2	0.3	3.0	73	6	Slt vshy no fluor
0.8	7222.0									0	Shale no fluor
	7233.0										Empty Bottle

Table 6-1-1 (cont'd)

CORE LABORATORIES - NEW ORLEANS

ompany : Pennzoil Expl. & Prod. Company
'ell : OCS-G-2115 No. A-20 S/T
eld : Eugene Island Blk. 330
ıcation : Offshore, Louisana

SIDEWALL CORE ANALYSIS REPORT

CL File No : 57161-11410
Date : 1-Dec-93
Analyst : RH
Drilling Fluid : Novasol

Sample Recovery Inches	Sample Depth feet	Kair (Empirical) md	Porosity Fluid %	Probable Production	Saturations by Volume				Crit Water %	Gas Det	Descriptions
					Oil PV %	Water PV %	Oil BV %	Gas BV %			
	7234.0										Empty Bottle
0.7	7256.0	8.6	23.8	Low Perm	2.5	80.2	0.6	4.1	72	9	Sd vf-fgr vshy lam F stks yel-wh fluor 35% Sd
1.1	7258.0	6.3	21.5	Low Perm	1.3	80.4	0.3	3.9	71	0	Sd vfgr vshy no fluor
	7260.0										Empty Bottle
0.8	7347.0	75.0	27.2	Oil	8.9	55.3	2.4	9.7	57	40	Sd vf-fgr shy slty bt yel-wh fluor
1.2	7350.0	70.0	27.4	Oil	14.6	63.4	4.0	6.0	57	10	Sd vf-fgr shy slty calc bt yel-wh fluor (37 API
1.0	7352.0	22.0	23.1	Oil	8.9	66.7	2.0	5.6	64	4	Sd vf-fgr vshy slty calc bt yel-wh fluor
	7354.0										Empty bottle
1.0	7356.0	35.0	25.9	Oil	11.6	69.7	3.0	4.8	63	20	Sd vf-fgr shy vslty scalc bt yel-wh fluor
1.2	7360.0	32.0	25.4	Oil	10.8	72.0	2.7	4.4	64	18	Sd vf-fgr shy vslty calc mott bt yel-wh fluor
1.2	7362.0	40.0	26.5	Oil	9.6	62.9	2.5	7.3	63	12	Sd vf-fgr shy vslty calc mott bt yel-wh fluor (
	7364.0										Empty bottle
1.5	7366.0	26.0	24.2	Oil	12.2	70.7	3.0	4.1	64	16	Sd vf-fgr vshy slty calc mott bt yel-wh fluor
1.5	7368.0	17.0	23.0	Oil	10.9	71.3	2.5	4.1	66	12	Sd vf-fgr shy vslty scalc yel-wh fluor
	7377.0										Empty bottle
1.2	7379.0	6.4	22.2	LP-Oil	6.8	76.7	1.5	3.6	72	14	Sd vf-fgr vshy slty calc mott yel-wh fluor (37
	7386.0										Empty bottle
1.2	7389.0	5.2	23.4	LP-Oil	4.7	77.9	1.1	4.1	74	4	Sd vfgr shy vslty scalc mott dull yel-wh fluor
1.0	7406.0	190.0	33.1	Oil	7.4	64.1	2.4	9.4	51	30	Sd vfgr sshy lam B vslty stks bt yel-wh fluor 60% Sd (38 A
1.2	7435.0	1.7	20.6	Low Perm	1.9	84.0	0.4	2.9		4	Shale scalc spts bt yel-wh fluor
										0	Shale slty no fluor
1.2	7449.0										
0.6	7467.0	1.0	16.7	Low Perm	0.0	85.2	0.0	2.5	70	0	Slt sshy (50% mudcake) dense calc no fluor

Table 6-1-1 (cont'd)

CORE LABORATORIES - NEW ORLEANS

ompany : Pennzoil Expl. & Prod. Company
/ell : OCS-G-2115 No. A-20 S/T
eld : Eugene Island Blk. 330
ocation : Offshore, Louisana

SIDEWALL CORE ANALYSIS REPORT

CL File No : 57161-11410
Date : 1-Dec-93
Analyst : RH
Drilling Fluid : Novasol

Sample Recovery Inches	Sample Depth feet	Kair (Empirical) md	Porosity Fluid %	Probable Production	Saturations by Volume				Crit Water %	Gas Det	Descriptions
					Oil PV %	Water PV %	Oil BV %	Gas BV %			
1.5	7491.0									0	Shale scalc no fluor
1.5	7492.0									0	Shale scalc no fluor
1.2	7493.0									0	Shale scalc no fluor
	7494.0										Empty bottle
1.5	7495.0									0	Shale no fluor
	7500.0										Empty bottle
1.5	7501.0									0	Shale no fluor
	7502.0										Empty bottle
1.2	7503.0									0	Shale no fluor
1.2	7504.0									0	Mudcake
0.8	7518.0									0	Shale scalc no fluor
1.0	7521.0									0	Mudcake w/tr Sd
1.2	7525.0									0	Shale no fluor
	7527.0										Empty bottle
1.0	7529.0									0	Shale no fluor
1.2	7532.0									0	Shale no fluor
1.2	7534.0									0	Shale no fluor
1.0	7541.0	18.0	24.1	Oil	15.6	69.3	3.7	3.6	67	20	Sd vfgr vshy lam C stks bt yel-wh fluor 15% Sd
0.2	7542.0									0	Mudcake
1.0	7543.0									0	Shale no fluor
1.2	7544.0									0	Shale no fluor
1.2	7545.0									0	Shale no fluor
1.5	7549.0									0	Shale slty no fluor
1.2	7550.0									0	Shale slty no fluor
1.2	7551.0									0	Shale no fluor
1.2	7552.0	1.5	20.6	Low Perm	2.0	89.1	0.4	1.8		0	Shale slty spts yel-wh fluor

Table 6-1-1 (cont'd)

CORE LABORATORIES - NEW ORLEANS

ompany : Pennzoil Expl. & Prod. Company
ell : OCS-G-2115 No. A-20 S/T
eld : Eugene Island Blk. 330
ocation : Offshore, Louisiana

CL File No : 57161-11410
Date : 1-Dec-93
Analyst : RH
Drilling Fluid : Novasol

SIDEWALL CORE ANALYSIS REPORT

Table 6-1-1 (cont'd)

Sample Recovery Inches	Sample Depth feet	Kair (Empirical) md	Porosity Fluid %	Probable Production	Saturations by Volume Oil PV %	Water PV %	Oil BV %	Gas BV %	Crit Water %	Gas Det	Descriptions
1.6	7554.0									0	Shale slty scalc no fluor
0.8	7555.0									0	Shale calc no fluor
	7557.0										Empty bottle
1.6	7561.0	2.2	21.5	Low Perm	3.0	86.0	0.8	2.2		5	Shale w/Slt lam calc stks yel-wh fluor
1.6	7565.0									0	Shale slty calc no fluor
1.2	7567.0									0	Mudcake
1.2	7569.0									0	Shale slty calc no fluor
1.2	7571.0	3.3	19.9	Low Perm	2.4	87.4	0.5	2.0	73	0	Sd vfgr vshy lam C scalc stks yel-wh fluor 18%
0.4	7573.0									0	Mudcake
1.0	7575.0									0	Shale slty calc no fluor
1.2	7577.0	3.0	21.7	Low Perm	0.0	85.8	0.0	3.1	75	0	Slt vshy sdy calc no fluor
1.0	7579.0									0	Mudcake
1.2	7580.0									0	Shale calc no fluor
1.5	7581.0									0	Shale slty calc no fluor
1.0	7583.0									0	Mudcake
1.0	7585.0									0	Shale (50% mudcake) calc no fluor
1.2	7587.0	1960.0	34.3	Oil	16.7	55.6	5.7	9.6	38	40	Sd vf-fgr cln salty (50% mudcake) bt yel-wh flu
1.2	7589.0									0	Shale calc no fluor
	7591.0										Empty bottle
1.5	7593.0									0	Shale calc no fluor
1.2	7595.0									0	Shale calc no fluor
	7597.0										Empty bottle
W 1.2	7599.0									0	Shale slty sdy scalc no fluor
1.2	7601.0	2.7	17.0	Low Perm	0.0	87.7	0.0	2.1		0	Lime sdy (50% mudcake) spts min fluor
	7609.0										Empty bottle
W 1.2	7611.0									0	Shale slty calc no fluor

CORE LABORATORIES - NEW ORLEANS

Company : Pennzoil Expl. & Prod. Company
Well : OCS-G-2115 No. A-20 S/T
Field : Eugene Island Blk. 330
Location : Offshore, Louisana

SIDEWALL CORE ANALYSIS REPORT

CL File No : 57161-11410
Date : 1-Dec-93
Analyst : RH
Drilling Fluid : Novasol

Table 6-1-1 (cont'd)

Sample Recovery Inches	Sample Depth feet	Kair (Empirical) md	Porosity Fluid %	Probable Production	Saturations by Volume				Crit Water %	Gas Det	Descriptions
					Oil PV %	Water PV %	Oil BV %	Gas BV %			
1.5	7617.0									0	Shale silty ssdy calc no fluor EPR
	7621.0										Empty bottle
1.2	7625.0									0	Shale vcalc no fluor WHOI; EPR-CEP
1.0	7627.0									0	Mudcake
	7629.0										Empty bottle
1.2	7631.0	3.8	19.8	Low Perm	0.0	83.2	0.0	3.3	73	0	Sd vfgr vshy vcalc no fluor EPR
1.2	7633.0									0	Shale silty ssdy vcalc no fluor WHOI; EPR-CEP
1.2	7635.0									0	Shale silty ssdy vcalc no fluor EPR
1.2	7636.0									0	Shale silty ssdy vcalc no fluor WHOI; EPR-CEP
1.0	7636.1									0	Shale silty ssdy vcalc no fluor EPR
1.2	7637.0	2.6	20.6	Low Perm	2.0	84.6	0.4	2.8	74	6	Sd vfgr vshy lam C vsilty vcalc stks yel-wh fluo WHOI; EPR-CE
1.0	7639.0									0	Shale silty no fluor EPR
1.0	7641.0	5.1	20.9	LP-Oil	6.3	80.9	1.3	2.7	72	8	Slt vshy lam C scalc stks bt yel-wh fluor 15% S WHOI; EPR-C
1.2	7643.0									0	Mudcake w/tr Shale [illegible]
1.2	7651.0									0	Shale scalc no fluor EPR
1.5	7653.0	2.3	20.5	Low Perm	2.5	86.5	0.5	2.3	74	5	Slt vshy lam C stks bt yel-wh fluor 5% Slt WHOI; EPR CEP
1.2	7655.0									0	Mudcake w/tr Shale [illegible]
1.0	7657.0									0	Shale silty ssdy scalc no fluor EPR
1.0	7659.0									0	Mudcake
1.0	7661.0									0	Shale scalc no fluor EPR-CEP; WHOI

NOTES

In productive zones, the log calculated water saturation should be less than the Critical Water Saturation.
LP-Oil: Low permeability with possible oil production
* Oil saturations are believed to be due to contamination from the drilling fluid.

Table 6-1-2. Samples taken from whole core

Sample	Depth (driller)	Party
1	7650.60	Losh
2	7651.80	Losh
3	7657.00	Losh
4	7669.45	Losh
5	7711.70	Losh
6	7714.00	Losh
7	7716.60	Losh
8	7723.00	Losh
9	7723.70	Losh
10	7729.00	Losh
11	7732.50	Losh
12	7733.20	Losh
13	7734.90	Losh
14	7736.10	Losh
15	7736.35	Losh
16	7737.85	Losh
17	7741.40	Losh
18	7746.00	Losh
19	7873.10	Losh
20	7874.20	Losh
21	7874.70	Losh
22	7878.90	Losh
23	7890.25	Losh
24	7896.50	Losh
25	7906.20	Losh
26	7913.50	Losh
27	7919.30	Losh
28	7923.80	Losh
29	7925.05	Losh
30	7934.00	Losh
31	7952.10	Losh
32	7955.00	Losh
33	7963.90	Losh
34	7965.30	Losh
35	7969.50	Losh
36	7969.90	Losh
37	7971.40	Losh
38	7975.00	Losh
39	7985.00	Losh
40	7993.70	Losh
41	7993.90	Losh
42	7994.40	Losh
1	7744.50	Boles
2	7753.00	Boles
3	7755.40	Boles
4	7758.30	Boles
5	7766.70	Boles
6	7768.50	Boles

Table 6-1-2 (cont'd)

Sample	Depth (driller)	Party
1	7657.50	Penn State
2	7669.00	Penn State
3	7681.50	Penn State
4	7712.00	Penn State
5	7718.50	Penn State
6	7729.00	Penn State
7	7746.50	Penn State
8	7753.50	Penn State
9	7764.00	Penn State
10	7778.20	Penn State
11	7790.50	Penn State
12	7802.50	Penn State
13	7814.50	Penn State
14	7826.00	Penn State
15	7837.50	Penn State
16	7838.70	Penn State
17	7849.40	Penn State
18	7861.80	Penn State
19	7862.80	Penn State
20	7878.20	Penn State
21	7886.00	Penn State
22	7898.50	Penn State
23	7911.50	Penn State
24	7923.50	Penn State
25	7934.30	Penn State
26	7962.50	Penn State
27	7963.00	Penn State
28	7970.40	Penn State
29	7982.50	Penn State
30	8006.50	Penn State
1	7650.90	Bruce Hart
2	7650.90	Bruce Hart
3	7650.90	Bruce Hart
4	7651.15	Bruce Hart
5	7712.00	Bruce Hart
6	7712.00	Bruce Hart
7	7712.00	Bruce Hart
8	7712.00	Bruce Hart
9	7729.00	Bruce Hart
10	7729.00	Bruce Hart
11	7729.00	Bruce Hart
12	7729.00	Bruce Hart
13	7745.60	Bruce Hart
14	7745.60	Bruce Hart
15	7745.60	Bruce Hart
16	7745.60	Bruce Hart
1	7651.50	Wood
2	7654.50	Wood

Table 6-1-2 (cont'd)

Sample	Depth (driller)	Party
3	7657.55	Wood
4	7660.50	Wood
5	7663.55	Wood
6	7666.50	Wood
7	7669.55	Wood
8	7672.50	Wood
9	7675.55	Wood
10	7678.50	Wood
11	7681.55	Wood
12	7684.50	Wood
13	7687.50	Wood
14	7690.50	Wood
15	7693.55	Wood
16	7696.50	Wood
17	7699.30	Wood
18	7701.70	Wood
19	7711.50	Wood
20	7714.50	Wood
21	7717.55	Wood
22	7720.50	Wood
23	7723.55	Wood
24	7726.50	Wood
25	7729.55	Wood
26	7732.50	Wood
27	7735.55	Wood
28	7738.20	Wood
29	7740.70	Wood
30	7743.50	Wood
31	7746.55	Wood
32	7749.50	Wood
33	7752.55	Wood
34	7755.50	Wood
35	7758.55	Wood
36	7761.50	Wood
37	7764.55	Wood
38	7767.70	Wood
39	7770.60	Wood
40	7771.50	Wood
41	7774.50	Wood
42	7777.55	Wood
43	7780.50	Wood
44	7783.55	Wood
45	7786.50	Wood
46	7789.55	Wood
47	7792.50	Wood
48	7795.55	Wood
49	7798.50	Wood
50	7801.55	Wood

Table 6-1-2 (cont'd)

Sample	Depth (driller)	Party
51	7804.50	Wood
52	7807.55	Wood
53	7810.50	Wood
54	7813.55	Wood
55	7816.50	Wood
56	7819.55	Wood
57	7822.50	Wood
58	7825.55	Wood
59	7827.85	Wood
60	7829.60	Wood
61	7831.70	Wood
62	7834.50	Wood
63	7837.55	Wood
64	7840.50	Wood
65	7843.55	Wood
66	7846.50	Wood
67	7849.55	Wood
68	7852.00	Wood
69	7855.05	Wood
70	7858.50	Wood
71	7861.55	Wood
72	7864.50	Wood
73	7867.55	Wood
74	7870.50	Wood
75	7873.55	Wood
76	7876.50	Wood
77	7879.55	Wood
78	7882.50	Wood
79	7885.55	Wood
80	7888.50	Wood
81	7891.55	Wood
82	7894.50	Wood
83	7897.55	Wood
84	7900.50	Wood
85	7903.55	Wood
86	7906.90	Wood
87	7910.50	Wood
88	7913.50	Wood
89	7916.55	Wood
90	7919.50	Wood
91	7922.55	Wood
92	7925.50	Wood
93	7928.55	Wood
94	7931.50	Wood
95	7934.55	Wood
96	7937.35	Wood
97	7939.25	Wood
98	7951.50	Wood

Table 6-1-2 (cont'd)

Sample	Depth (driller)	Party
99	7954.50	Wood
100	7957.55	Wood
101	7960.50	Wood
102	7963.55	Wood
103	7966.50	Wood
104	7969.55	Wood
105	7972.50	Wood
106	7975.55	Wood
107	7978.35	Wood
108	7981.35	Wood
109	7984.50	Wood
110	7987.30	Wood
111	7990.05	Wood
112	7993.30	Wood
113	7996.50	Wood
114	7999.55	Wood
115	8002.50	Wood
116	8005.50	Wood
117	8008.50	Wood
118	8011.15	Wood
119	8013.05	Wood
1	7650.25	Butler
2	7658.80	Butler
3	7662.20	Butler
4	7674.30	Butler
5	7686.30	Butler
6	7698.30	Butler
7	7716.30	Butler
8	7724.40	Butler
9	7737.30	Butler
10	7740.30	Butler
11	7751.30	Butler
12	7759.80	Butler
13	7770.30	Butler
14	7782.30	Butler
15	7794.20	Butler
16	7806.30	Butler
17	7818.30	Butler
18	7830.35	Butler
19	7842.30	Butler
20	7854.30	Butler
21	7866.30	Butler
22	7872.40	Butler
23	7872.70	Butler
24	7890.70	Butler
25	7908.30	Butler
26	7917.70	Butler
27	7921.30	Butler

Table 6-1-2 (cont'd)

Sample	Depth (driller)	Party
28	7929.70	Butler
29	7950.20	Butler
30	7958.60	Butler
31	7964.60	Butler
32	7968.30	Butler
33	7976.50	Butler
34	7986.70	Butler
35	7995.20	Butler
36	8000.40	Butler
37	8004.20	Butler
38	8012.10	Butler
1V	7650.90	Hart
2V	7650.90	Hart
3V	7650.90	Hart
4V	7651.15	Hart
5V	7712.00	Hart
6V	7712.00	Hart
7V	7712.00	Hart
8V	7712.00	Hart
9V	7729.00	Hart
10V	7729.00	Hart
11V	7729.00	Hart
12V	7729.00	Hart
13V	7745.60	Hart
14V	7745.60	Hart
15V	7745.60	Hart
16V	7745.60	Hart
	7654.4 , 56.0	Woods Hole
		Woods Hole
	7659.7- 61.0	Woods Hole
		Woods Hole
	7666.4 , 66.8	Woods Hole
		Woods Hole
	7673.7 , 73.8	Woods Hole
		Woods Hole
	7678.7 , 78.9 , 79.0	Woods Hole
		Woods Hole
	7683.6	Woods Hole
		Woods Hole
	7690.5	Woods Hole
		Woods Hole
		Woods Hole
		Woods Hole
		Woods Hole
		Woods Hole
	7714	Woods Hole
		Woods Hole
		Woods Hole

Table 6-1-2 (cont'd)

Sample	Depth (driller)	Party
		Woods Hole
	7726.3 , 27.0	Woods Hole
		Woods Hole
	7133.8	Woods Hole
		Woods Hole
	7737.9 , 38.1 , 39.2	Woods Hole
		Woods Hole
		Woods Hole
		Woods Hole
	7748.9 , 49.1 , 51.0	Woods Hole
		Woods Hole
	7755.2-.3 , 57.0	Woods Hole
		Woods Hole
	7760.1	Woods Hole
		Woods Hole
	7769.1	Woods Hole
		Woods Hole
		Woods Hole
	7775 , 75.2	Woods Hole
		Woods Hole
	7782	Woods Hole
		Woods Hole
		Woods Hole
		Woods Hole
	7793.8	Woods Hole
		Woods Hole
	7797.8	Woods Hole
		Woods Hole
	7803.5 , 04.6	Woods Hole
		Woods Hole
		Woods Hole
		Woods Hole
	7816.4 , 16.7 , 16.8	Woods Hole
		Woods Hole
	7823 , 24.0	Woods Hole
		Woods Hole
		Woods Hole
		Woods Hole
		Woods Hole
	7834.1 , 34.3 , 34.4 , 36.0	Woods Hole
		Woods Hole
	7841	Woods Hole
	7842.5 , 43.0 , 44.6	Woods Hole
	7846.6 , 46.5 , 45.0 , 47.0	Woods Hole
	7849 , 49.5	Woods Hole
	7851.5 , 53.6 , 52.2 , 51.0 , 53.0	Woods Hole
	7855 , 57.0	Woods Hole
	7859	Woods Hole

Table 6-1-2 (cont'd)

Sample	Depth (driller)	Party
	7861	Woods Hole
	7863 , 65.0 , 65.2 , 64.8	Woods Hole
	7867	Woods Hole
	7869 , 71.0 , 72.0	Woods Hole
	7873.0 , 74.6	Woods Hole
	7875.3 , 75.0 , 77.0	Woods Hole
	7879.0 , 78.9 , 80.3	Woods Hole
	7881 , 83.0 , 82.6 , 81.8	Woods Hole
	7885	Woods Hole
	7887 , 89.0 , 87.8	Woods Hole
	7891	Woods Hole
	7893,95.0,94.0,94.8,95.1,93.2,93.8	Woods Hole
	7897	Woods Hole
	7899 , 7901	Woods Hole
	7903	Woods Hole
	7905 , 07.0	Woods Hole
	7909 , 11.0	Woods Hole
	7913 , 15.0	Woods Hole
	7917 , 19.0	Woods Hole
	7921	Woods Hole
	7923	Woods Hole
	7925 , 27.0	Woods Hole
	7929	Woods Hole
	7931 , 33.0 , 32.4	Woods Hole
	7935	Woods Hole
	7937 , 39.0 , 36.4	Woods Hole
		Woods Hole
		Woods Hole
		Woods Hole
		Woods Hole
	7961.8 , 62.2	Woods Hole
		Woods Hole
	7966.3	Woods Hole
		Woods Hole
	7971.8 , 74.0	Woods Hole
		Woods Hole
		Woods Hole
		Woods Hole
	7988 , 85.4	Woods Hole
		Woods Hole
		Woods Hole
		Woods Hole
	7995.5 , 97.7	Woods Hole
		Woods Hole
		Woods Hole
		Woods Hole
	8008	Woods Hole
		Woods Hole

Table 6-1-2 (cont'd)

Sample	Depth (driller)	Party
	8012.1	Woods Hole
	7717.70	Exxon
	7734.90	Exxon
	7736.00	Exxon
	7736.45	Exxon
	7741.05	Exxon
	7849.85	Exxon
	7879.65	Exxon
	7887.50	Exxon
	7890.00	Exxon
	7932.00	Exxon
	7932.40	Exxon
	7935.50	Exxon
	7952.00	Exxon
	7964.05	Exxon
	7972.00	Exxon
	8010.80	Exxon
	8012.00	Exxon
	7727.50	Shell
	7728.00	Shell
	7728.80	Shell
	7729.60	Shell
	7956.60	Shell
	7957.20	Shell
	7957.90	Shell
	7958.40	Shell

Table 6-1-3. Intervals requested by Exxon Production Research for CAT scanning

Core	Section	Top	Bottom
1	1	7651	7653
	2	7654	7656
	12	7684	7685.5
	16	7695.5	7697
2	3	7716.5	7718.5
	4	7719.5	7720.5
	9	7734	7737
	10	7737	7739
	11	7740.5	7741.5
	12	7743	7744.5
3	14	7809	7812
	18	7821.5	7822.5
4	7	7848.5	7850.5
	17	7878.5	7880
5	4	7900.5	7901.75
	7	7910	7912
→	13	7927	7930
	15	7934.5	7936
6	1	7953.5	7955.5
→	3	7959.5	7961.5
	4	7960	7962
	5	7962	7965
	21	8010	8011

Table 6-1-4. PROFILE PERMEABILITY

PENNZOIL EXPLORATION & PRODUCTION
Pathfinder Well
OCS-G-2115 No. A-20 S.T.
Eugene Island Block 330
Offshore, LA
Core Laboratories File No. 57151-17815

PROFILE PERMEABILITY DATA

Core No. 4 - Tube 15

Point Number	Depth ft	Kair md	Kl md
1	7872.133	0.51	0.33
2	7872.249	0.01	0.00
3	7872.334	0.00	0.00
4	7872.416	0.49	0.32
5	7872.500	0.13	0.06
6	7872.585	0.21	0.12
7	7872.670	0.09	0.04
8	7872.737	3.59	2.81
9	7872.835	4.60	3.65
10	7872.921	224.00	212.00
11	7873.003	734.00	708.00
12	7873.003	635.00	611.00
13	7873.092	162.00	152.00
14	7873.177	188.00	177.00
15	7873.260	133.00	124.00
16	7873.342	107.00	99.00
17	7873.420	230.00	218.00
18	7873.539	0.00	0.00
19	7873.600	0.00	0.00
20	7873.668	0.00	0.00
21	7873.750	0.00	0.00
22	7873.850	0.00	0.00
23	7873.915	0.28	0.16
24	7874.070	0.00	0.00
25	7874.014	0.10	0.05
26	7874.181	0.02	0.00
27	7874.234	62.40	57.00
28	7874.348	0.00	0.00
29	7874.424	4.03	3.17
30	7874.490	0.20	0.11
31	7874.598	0.33	0.20
32	7874.687	101.00	93.90
33	7874.771	1.95	1.46
34	7874.850	0.00	0.00
35	7874.940	0.00	0.00
36	7875.000	0.00	0.00

Table 6-1-5. Bulk chemical data

1. These are Pennzoil core elemental analyses.

2. Core depths are from 7857'-7921', however the depths may need to be reassigned, when comparing to logs.

3. Whole rock and trace elemental analysis was done by XRAL Laboratories 1885 Leslie St., Don Mills, Ont. Canada M3B 3J4 Telephone (416) 445 5755

4. Call me or Susan Herron (SDR), if you have any questions.

5. B, Ba, Gd, Th, U, Rb, Sr, Y, Zr are reported in ppm, all others in wt %.

18 24
W.O. 017053

B	NA	MG	AL	SI	P	S-LO	K	CA	TI
CR	MN	FE	RB	SR	Y	ZR	NB	BA	GD
TH	U	LOI	SUM						
17815-9-7857.0									
79.000	1.300	1.060	7.130	31.800	.050	.360	2.120	.560	.481
-999.000	.050	2.820	118.000	231.000	24.000	318.000	24.000	10600.000	9.700
9.300	2.800	5.310	99.946						
17815-11-7861.0									
88.500	1.470	1.170	7.460	30.700	.070	.140	2.250	.670	.446
-999.000	.050	3.920	120.000	157.000	28.000	299.000	34.000	559.000	5.500
10.100	2.900	6.250	100.308						
17815-13-7865.0									
67.000	1.450	.850	6.500	33.500	.050	.350	2.080	.590	.399
-999.000	.040	2.810	91.000	167.000	26.000	356.000	21.000	1790.000	5.200
8.900	2.600	4.550	100.327						
17815-15-7869.0									
84.000	1.380	1.060	7.240	31.800	.050	.210	2.160	.650	.444
-999.000	.050	3.230	117.000	171.000	38.000	341.000	24.000	3390.000	6.800
10.200	2.800	5.550	100.392						
17815-17-7873.0									
41.500	1.610	.450	5.070	36.300	.040	.150	1.870	.690	.251
-999.000	.030	1.200	75.000	273.000	17.000	379.000	18.000	1060.000	3.700
6.000	1.500	4.350	100.200						
17815-19-7877.0									
79.000	1.510	.980	6.990	32.500	.060	.220	2.160	.650	.432
-999.000	.060	2.980	103.000	153.000	28.000	391.000	25.000	618.000	4.800
9.700	2.700	5.100	100.361						
17815-21-7881.0									
73.500	1.510	.910	6.670	33.000	.060	.220	2.130	.660	.408
-999.000	.060	2.870	97.000	181.000	27.000	374.000	34.000	1510.000	4.600
8.100	2.300	4.750	100.242						
17815-23-7885.0									
89.500	1.440	1.210	8.230	30.000	.060	.290	2.390	.580	.457

Table 6-1-5 (cont'd)

-999.000	.050	3.820	149.000	160.000	28.000	255.000	29.000	813.000	4.700
8.700	2.800	6.300	100.262						
17815-25-7889.0									
88.500	1.370	1.170	8.200	30.200	.060	.210	2.400	.610	.467
-999.000	.050	3.770	131.000	152.000	27.000	288.000	41.000	546.000	5.100
9.800	2.700	6.200	100.345						
17815-27-7893.0									
99.500	1.480	1.320	9.000	28.000	.060	.710	2.520	.560	.457
.010	.050	4.620	162.000	179.000	17.000	208.000	32.000	3480.000	5.800
10.400	3.000	7.250	100.205						
17815-29-7897.0									
96.000	1.440	1.270	9.050	29.000	.060	.330	2.550	.450	.475
-999.000	.050	3.970	143.000	155.000	26.000	228.000	35.000	567.000	5.700
9.800	3.100	6.550	100.245						
17815-31-7901.0									
106.000	1.420	1.300	9.140	28.000	.070	.270	2.540	.650	.468
-999.000	.050	4.380	157.000	168.000	13.000	221.000	40.000	3250.000	7.600
11.600	3.200	7.400	100.314						
17815-33-7905.0									
119.000	1.490	1.340	9.350	27.700	.070	.130	2.610	.580	.479
.010	.050	4.630	161.000	142.000	27.000	204.000	43.000	588.000	6.500
11.700	3.200	7.350	100.257						
17815-35-7909.0									
90.000	1.280	1.300	8.260	25.100	.080	1.320	2.240	.720	.453
.010	.060	4.950	95.000	429.000	21.000	137.000	31.000	55800.000	6.300
7.600	2.500	9.230	100.545						
17815-37-7913.0									
100.000	1.430	1.330	9.530	27.700	.070	.270	2.600	.630	.469
.010	.050	4.480	151.000	185.000	21.000	182.000	23.000	2950.000	6.600
11.400	3.200	7.250	100.487						
17815-39-7917.0									
97.500	1.400	1.220	9.260	28.600	.060	.430	2.570	.500	.498
.010	.050	4.320	164.000	161.000	24.000	218.000	28.000	600.000	6.000
12.600	3.300	6.750	100.500						
17815-41-7921.0									
86.500	1.340	1.290	8.870	28.000	.060	.640	2.450	.570	.486
.010	.050	4.250	136.000	223.000	36.000	206.000	20.000	13900.000	9.800
11.500	3.200	7.160	100.246						
17815-43-7925.0									
91.500	1.390	1.380	8.970	27.200	.070	.330	2.530	.660	.474
.010	.060	4.720	139.000	219.000	24.000	188.000	37.000	10600.000	9.700
10.200	3.100	7.850	100.170						

This attached addition is the analyses for the liquid mud sample obtained just before logging.

1 24
W.O. #25062

B	NA	MG	AL	SI	P	S-LO	K	CA	TI
CR	MN	FE	RB	SR	Y	ZR	NB	BA	GD
TH	U	LOI	SUM						
LIQUID-MUD									
33.500	.410	-999.000	1.750	7.420	.030	9.700	.720	.600	.042
.020	.030	.910	-999.000	1260.000	-999.000	17.000	-999.000	414999.969	3.000
2.100	.900	6.080	75.514						

weight before drying: 1594.7 g
weight after drying: 1084.3 g

EUGENE ISLAND - WATER CHEMISTRY
MAJOR IONS (mg/L)

HORIZON	WELL	TEMP (C)	pH	Na	Ca	Mg	Sr	K	Cl	SO4
OI-5	A2	39.4	7.03	19900	1550	506	43.8	122	33100	1.8
HB-2	B17D	34.4	7.15	31200	2030	1360	73.1	186	54600	<3
HB-1	B2ST	33	7.12	32800	2020	1310	94.1	242	55800	<3
HB-1	C2	47	6.81	31200	2110	1330	85	251	56000	<3
HB-1	C3D		7.05	32200	2310	1490	108	276	60900	<3
JD	A11	38.2	6.93	33400	3920	1680	150	251	63400	<3
OI-4	A23		7.03	33200	3460	1050	142	251	64000	<3
MG-3	B9	25.6	6.47	38600	4000	1660	161	300	73700	1.4
GA-2	C2D	43.2	6.9	47100	2880	1420	159	273	79200	<3
MG	A9	38.5	6.77	48800	2260	863	147	471	80200	<3
KE	A6ST		6.91	43400	4130	1820	142	373	80800	<3
L-1	A10			48700	3380	1540	128	309	85400	<3
OI	A14A	35.1	6.97	51600	2940	813	227	240	90000	<3
L-1	A4	37.8	6.82	51900	3270	1530	174	344	90800	<3
GA-2	C7ST	28	6.91	51800	3050	1560	163	255	91200	<3
GA-2	B16D	34.4	7.07	52200	3170	1490	170	237	92500	<3
L-1	A8A		6.46	54100	2640	1280	153	303	94100	<3
GA-2	C20	24	6.91	54000	3150	1500	182	271	96600	<3
GA-2	B1D	33	6.79	56200	3260	1350	186	255	97100	<3
GA-2	B18D	30	7.05	57200	3550	1700	197	303	98600	<3
GA-2	C6D		6.9	56400	3320	1390	199	288	103000	<3
GA-2	C13D	40	7.04	58200	3330	1350	198	295	103100	<3

Table 6-1-6. Brine chemical analyses

04/04/94

EUGENE.WK4

Figure 6-1-1. Laser particle size analysis

Western Atlas International
A Litton Dresser Company

CORE LABORATORIES

Company	GBRN	Depth	7834.4	File Number	57161-11412A
Well	OCS-G 2115 No. A-20, S/T	Field	Eugene Island Block 330	Date	2-Dec-93
Parish	Offshore	State	Louisiana	Analysts	Ligon

Laser Particle Size Analysis

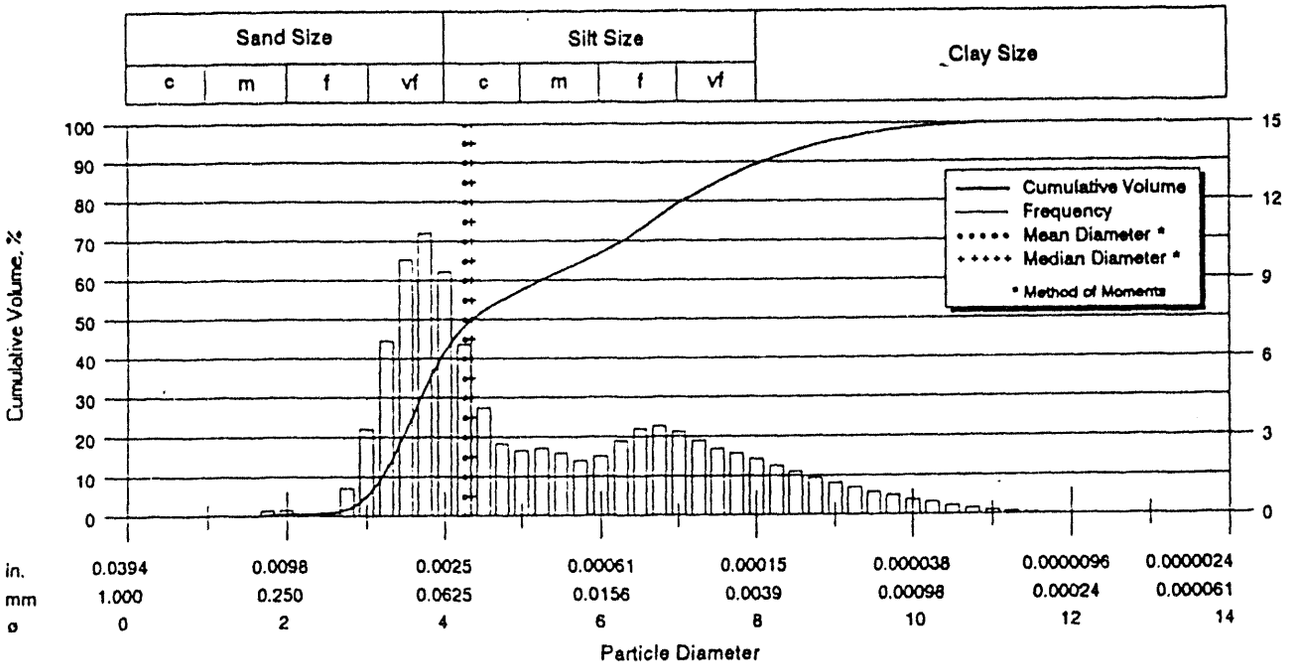

Particle Size Distribution

	[U.S. Sieve]	Diameter [in]	[mm]	[phi]	Volume, % [Inc.]	[Cum.]
Coarse Sand	20	0.0331	0.84	0.25	0.00	0.00
	25	0.0280	0.71	0.50	0.00	0.00
	30	0.0232	0.59	0.75	0.00	0.00
	35	0.0197	0.50	1.00	0.00	0.00
Medium Sand	40	0.0165	0.42	1.25	0.00	0.00
	45	0.0138	0.35	1.50	0.02	0.02
	50	0.0118	0.30	1.75	0.19	0.21
	60	0.0098	0.25	2.00	0.21	0.42
Fine Sand	70	0.0083	0.210	2.25	0.06	0.48
	80	0.0070	0.177	2.50	0.15	0.63
	100	0.0059	0.149	2.75	1.06	1.69
	120	0.0049	0.125	3.00	3.29	4.98
Very Fine Sand	140	0.0041	0.105	3.25	6.68	11.66
	170	0.0035	0.088	3.50	9.78	21.44
	200	0.0029	0.074	3.75	10.80	32.24
	230	0.0025	0.063	4.00	9.32	41.56
Silt	270	0.0021	0.053	4.25	6.56	48.12
	325	0.0017	0.044	4.50	4.09	52.21
	400	0.0015	0.037	4.75	2.76	54.97
	450	0.0012	0.031	5.00	2.49	57.46
	500	0.0010	0.025	5.32	3.26	60.72
	635	0.0008	0.020	5.64	2.87	63.59
		0.00061	0.0156	6.00	3.18	66.77
		0.00031	0.0078	7.00	12.70	79.47
		0.00015	0.0039	8.00	9.90	89.37
Clay		0.000079	0.0020	9.00	6.12	95.49
		0.000039	0.00098	10.0	3.17	98.66
		0.000019	0.00049	11.0	1.14	99.80
		0.0000094	0.00024	12.0	0.19	99.99
		0.0000047	0.00012	13.0	0.01	100.00
		0.0000039	0.00010	13.3	0.00	100.00

Sorting Statistics

Parameter	[Moment]	[Trask]	[Inman]	[Folk]
Mean, in	0.0020	0.0011	0.0009	0.0012
Mean, mm	0.0520	0.0288	0.0238	0.0303
Mean, phi	4.2656	5.1185	5.3904	5.0434
Median, in	0.0019	0.0019	0.0019	0.0019
Median, mm	0.0491	0.0491	0.0491	0.0491
Median, phi	4.3493	4.3495	4.3495	4.3495
Std Deviation, in	0.0017	0.0152	0.0096	0.0104
Std Deviation, mm	0.0448	0.3888	0.2462	0.2672
Std Deviation, phi	4.4813	1.3627	2.0220	1.9038
Skewness	1.1010	1.2603	0.7901	0.5285
Kurtosis	3.0150	0.3146	0.4571	0.7864
Mode, mm	0.0806			
95% Confidence	0.0432			
Limits, mm	0.0608			
Variance, mm2	0.0020			
Coef. of Variance, %	86.11			

Percentiles [volume, %]	Particle Diameter [in]	[mm]	[phi]
5	0.0049	0.1249	3.0009
10	0.0042	0.1088	3.2005
16	0.0038	0.0968	3.3684
25	0.0033	0.0834	3.5830
50	0.0019	0.0491	4.3495
75	0.0004	0.0099	6.6540
84	0.0002	0.0059	7.4124
90	0.0001	0.0037	8.0806
95	0.0001	0.0021	8.8933

Figure 6-1-1 (cont'd)

Western Atlas International
A Litton Dresser Company

CORE LABORATORIES

Company	GBRN	Depth	7842.5	File Number	57161-11412A
Well	OCS-G 2115 No. A-20, S/T	Field	Eugene Island Block 330	Date	2-Dec-93
Parish	Offshore	State	Louisiana	Analyst	Ligon

Laser Particle Size Analysis

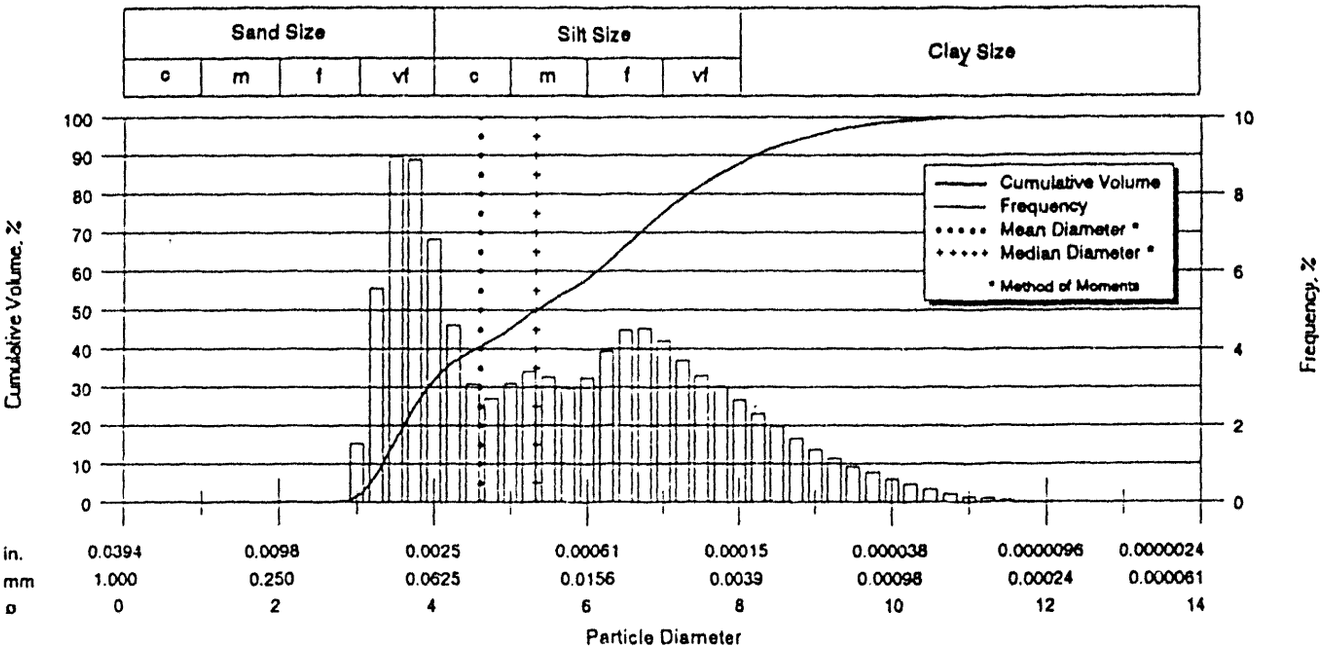

Particle Size Distribution

	[U.S. Sieve]	Diameter [in]	[mm]	[phi]	Volume, % [Inc.]	[Cum.]
Coarse Sand	20	0.0331	0.84	0.25	0.00	0.00
	25	0.0280	0.71	0.50	0.00	0.00
	30	0.0232	0.59	0.75	0.00	0.00
	35	0.0197	0.50	1.00	0.00	0.00
Medium Sand	40	0.0165	0.42	1.25	0.00	0.00
	45	0.0138	0.35	1.50	0.00	0.00
	50	0.0118	0.30	1.75	0.00	0.00
	60	0.0098	0.25	2.00	0.00	0.00
Fine Sand	70	0.0083	0.210	2.25	0.00	0.00
	80	0.0070	0.177	2.50	0.00	0.00
	100	0.0059	0.149	2.75	0.00	0.00
	120	0.0049	0.125	3.00	1.52	1.52
Very Fine Sand	140	0.0041	0.105	3.25	5.57	7.09
	170	0.0035	0.088	3.50	8.97	16.06
	200	0.0029	0.074	3.75	8.89	24.95
	230	0.0025	0.063	4.00	6.82	31.77
Silt	270	0.0021	0.053	4.25	4.62	36.39
	325	0.0017	0.044	4.50	3.08	39.47
	400	0.0015	0.037	4.75	2.70	42.17
	450	0.0012	0.031	5.00	3.10	45.27
	500	0.0010	0.025	5.32	4.36	49.63
	635	0.0008	0.020	5.64	3.98	53.61
		0.00061	0.0156	6.00	4.54	58.15
		0.00031	0.0078	7.00	17.17	75.32
		0.00015	0.0039	8.00	12.68	88.00
Clay		0.000079	0.0020	9.00	7.27	95.27
		0.000039	0.00098	10.0	3.41	98.68
		0.000019	0.00049	11.0	1.13	99.81
		0.0000094	0.00024	12.0	0.19	100.00
		0.0000047	0.00012	13.0	0.00	100.00
		0.0000039	0.00010	13.3	0.00	100.00

Sorting Statistics

Parameter	[Moment]	[Trask]	[Inman]	[Folk]
Mean, in	0.0016	0.0009	0.0008	0.0009
Mean, mm	0.0410	0.0242	0.0211	0.0222
Mean, phi	4.6093	5.3659	5.5678	5.4939
Median, in	0.0010	0.0010	0.0010	0.0010
Median, mm	0.0246	0.0246	0.0246	0.0246
Median, phi	5.3481	5.3477	5.3477	5.3477
Std Deviation, in	0.0015	0.0152	0.0093	0.0104
Std Deviation, mm	0.0380	0.3885	0.2384	0.2666
Std Deviation, phi	4.7190	1.3641	2.0685	1.9074
Skewness	0.6870	0.9157	0.3464	0.1773
Kurtosis	-0.8940	0.3309	0.3930	0.7315
Mode, mm	0.0883			
95% Confidence	0.0335			
Limits, mm	0.0484			
Variance, mm2	0.0014			
Coef. of Variance, %	92.68			

Percentiles [volume, %]	Particle Diameter [in]	[mm]	[phi]
5	0.0043	0.1101	3.1829
10	0.0039	0.0989	3.3380
16	0.0035	0.0885	3.4984
25	0.0029	0.0743	3.7515
50	0.0010	0.0246	5.3477
75	0.0003	0.0079	6.9803
84	0.0002	0.0050	7.6355
90	0.0001	0.0034	8.2165
95	0.0001	0.0020	8.9457

Figure 6-1-1 (cont'd)

Western Atlas International
A Litton Dresser Company

CORE LABORATORIES

Company	GBRN	Depth	7846.6	File Number	57161-11412A
Well	OCS-G 2115 No. A-20, S/T	Field	Eugene Island Block 330	Date	2-Dec-93
Parish	Offshore	State	Louisiana	Analysts	Ligon

Laser Particle Size Analysis

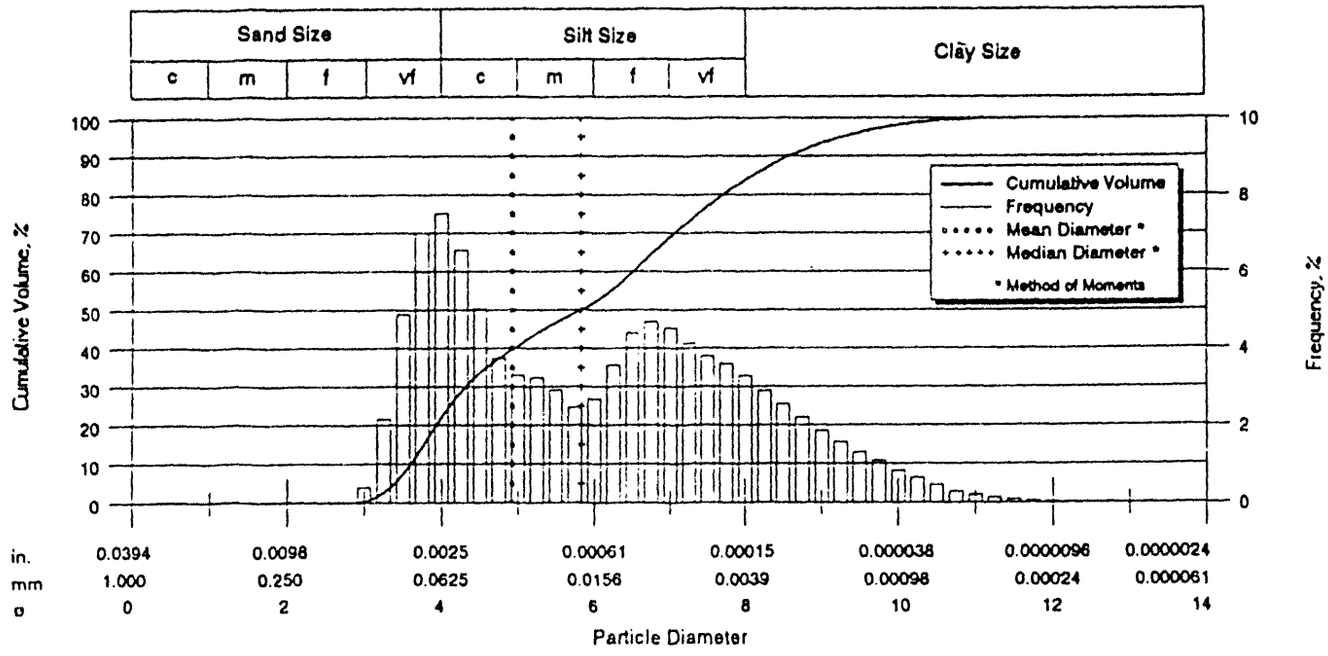

Particle Size Distribution

	[U.S. Sieve]	Diameter [in]	[mm]	[phi]	Volume, % [Inc.]	[Cum.]
Coarse Sand	20	0.0331	0.84	0.25	0.00	0.00
	25	0.0280	0.71	0.50	0.00	0.00
	30	0.0232	0.59	0.75	0.00	0.00
	35	0.0197	0.50	1.00	0.00	0.00
Medium Sand	40	0.0165	0.42	1.25	0.00	0.00
	45	0.0138	0.35	1.50	0.00	0.00
	50	0.0118	0.30	1.75	0.00	0.00
	60	0.0098	0.25	2.00	0.00	0.00
Fine Sand	70	0.0083	0.210	2.25	0.00	0.00
	80	0.0070	0.177	2.50	0.00	0.00
	100	0.0059	0.149	2.75	0.00	0.00
	120	0.0049	0.125	3.00	0.39	0.39
Very Fine Sand	140	0.0041	0.105	3.25	2.15	2.54
	170	0.0035	0.088	3.50	4.90	7.44
	200	0.0029	0.074	3.75	7.00	14.44
	230	0.0025	0.063	4.00	7.52	21.96
Silt	270	0.0021	0.053	4.25	6.56	28.52
	325	0.0017	0.044	4.50	5.01	33.53
	400	0.0015	0.037	4.75	3.75	37.28
	450	0.0012	0.031	5.00	3.30	40.58
	500	0.0010	0.025	5.32	4.10	44.68
	635	0.0008	0.020	5.64	3.44	48.12
		0.00061	0.0156	6.00	3.73	51.85
		0.00031	0.0078	7.00	17.18	69.03
		0.00015	0.0039	8.00	14.80	83.83
Clay		0.000079	0.0020	9.00	9.50	93.33
		0.000039	0.00098	10.0	4.74	98.07
		0.000019	0.00049	11.0	1.57	99.64
		0.0000094	0.00024	12.0	0.30	99.94
		0.0000047	0.00012	13.0	0.05	99.99
		0.0000039	0.00010	13.3	0.01	100.00

Sorting Statistics

Parameter	[Moment]	[Trask]	[Inman]	[Folk]
Mean, in	0.0013	0.0007	0.0006	0.0007
Mean, mm	0.0329	0.0187	0.0167	0.0169
Mean, phi	4.9245	5.7386	5.9078	5.8833
Median, in	0.0007	0.0007	0.0007	0.0007
Median, mm	0.0175	0.0175	0.0175	0.0175
Median, phi	5.8332	5.8343	5.8343	5.8343
Std Deviation, in	0.0013	0.0154	0.0091	0.0101
Std Deviation, mm	0.0322	0.3953	0.2322	0.2600
Std Deviation, phi	4.9572	1.3390	2.1064	1.9434
Skewness	0.8840	0.8895	0.2359	0.1020
Kurtosis	-0.3760	0.3272	0.3947	0.7390
Mode, mm	0.0736			
95% Confidence	0.0266			
Limits, mm	0.0392			
Variance, mm2	0.0010			
Coef. of Variance, %	97.75			

Percentiles [volume, %]	Particle Diameter [in]	[mm]	[phi]
5	0.0037	0.0952	3.3932
10	0.0032	0.0825	3.5987
16	0.0028	0.0717	3.8014
25	0.0023	0.0579	4.1092
50	0.0007	0.0175	5.8343
75	0.0002	0.0061	7.3679
84	0.0002	0.0039	8.0142
90	0.0001	0.0026	8.5784
95	0.0001	0.0016	9.2689

Figure 6-1-1 (cont'd)

Western Atlas International
A Litton Dresser Company

CORE LABORATORIES

Company	GBRN	Depth	7849.5	File Number	57161-11412A
Well	OCS-G 2115 No. A-20, S/T	Field	Eugene Island Block 330	Date	2-Dec-93
Parish	Offshore	State	Louisiana	Analysts	Ligon

Laser Particle Size Analysis

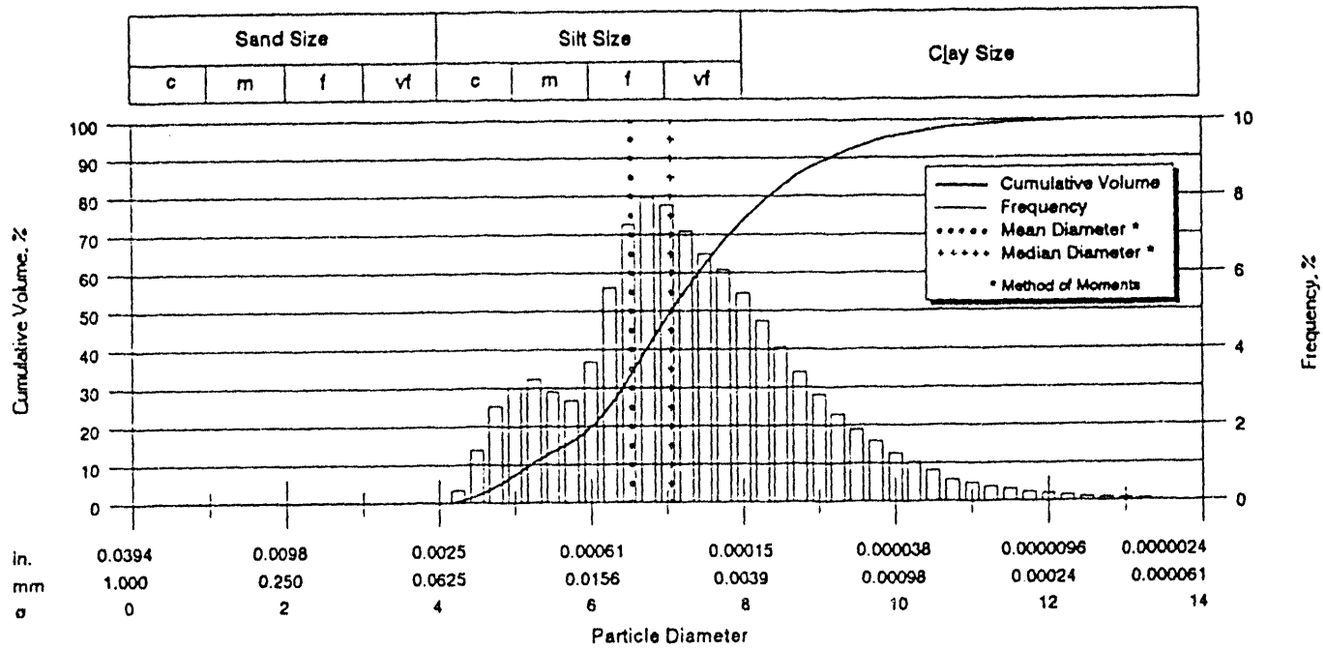

Particle Size Distribution

	[U.S. Sieve]	Diameter [in]	[mm]	[phi]	Volume, % [Inc.]	[Cum.]
Coarse Sand	20	0.0331	0.84	0.25	0.00	0.00
	25	0.0280	0.71	0.50	0.00	0.00
	30	0.0232	0.59	0.75	0.00	0.00
	35	0.0197	0.50	1.00	0.00	0.00
Medium Sand	40	0.0165	0.42	1.25	0.00	0.00
	45	0.0138	0.35	1.50	0.00	0.00
	50	0.0118	0.30	1.75	0.00	0.00
	60	0.0098	0.25	2.00	0.00	0.00
Fine Sand	70	0.0083	0.210	2.25	0.00	0.00
	80	0.0070	0.177	2.50	0.00	0.00
	100	0.0059	0.149	2.75	0.00	0.00
	120	0.0049	0.125	3.00	0.00	0.00
Very Fine Sand	140	0.0041	0.105	3.25	0.00	0.00
	170	0.0035	0.088	3.50	0.00	0.00
	200	0.0029	0.074	3.75	0.00	0.00
	230	0.0025	0.063	4.00	0.00	0.00
Silt	270	0.0021	0.053	4.25	0.33	0.33
	325	0.0017	0.044	4.50	1.42	1.75
	400	0.0015	0.037	4.75	2.48	4.23
	450	0.0012	0.031	5.00	3.02	7.25
	500	0.0010	0.025	5.32	4.09	11.34
	635	0.0008	0.020	5.64	3.49	14.83
		0.00061	0.0156	6.00	4.89	19.72
		0.00031	0.0078	7.00	28.63	48.35
		0.00015	0.0039	8.00	25.17	73.52
Clay		0.000079	0.0020	9.00	14.99	88.51
		0.000039	0.00098	10.0	7.05	95.56
		0.000019	0.00049	11.0	2.87	98.43
		0.0000094	0.00024	12.0	1.12	99.55
		0.0000047	0.00012	13.0	0.41	99.96
		0.0000039	0.00010	13.3	0.04	100.00

Sorting Statistics

Parameter	[Moment]	[Trask]	[Inman]	[Folk]
Mean, in	0.0004	0.0003	0.0003	0.0003
Mean, mm	0.0108	0.0070	0.0069	0.0071
Mean, phi	6.5288	7.1563	7.1821	7.1399
Median, in	0.0003	0.0003	0.0003	0.0003
Median, mm	0.0075	0.0075	0.0075	0.0075
Median, phi	7.0556	7.0554	7.0554	7.0554
Std Deviation, in	0.0004	0.0177	0.0144	0.0139
Std Deviation, mm	0.0106	0.4545	0.3696	0.3572
Std Deviation, phi	6.5652	1.1377	1.4361	1.4854
Skewness	1.7840	1.0119	0.2029	0.1016
Kurtosis	2.9520	0.2328	0.7633	1.1299
Mode, mm	0.0099			
95% Confidence	0.0088			
Limits, mm	0.0129			
Variance, mm2	0.0001			
Coef. of Variance, %	97.47			

Percentiles [volume, %]	Particle Diameter [in]	[mm]	[phi]
5	0.0014	0.0355	4.8147
10	0.0011	0.0270	5.2124
16	0.0007	0.0186	5.7460
25	0.0005	0.0133	6.2379
50	0.0003	0.0075	7.0554
75	0.0001	0.0037	8.0748
84	0.0001	0.0025	8.6181
90	0.0001	0.0018	9.1584
95	0.0000	0.0011	9.8790

Figure 6-1-1 (cont'd)

Western Atlas International
A Litton Dresser Company

CORE LABORATORIES

Company	GBRN	Depth	7851.5	File Number	57161-11412A
Well	OCS-G 2115 No. A-20, S/T	Field	Eugene Island Block 330	Date	2-Dec-93
Parish	Offshore	State	Louisiana	Analysts	Ligon

Laser Particle Size Analysis

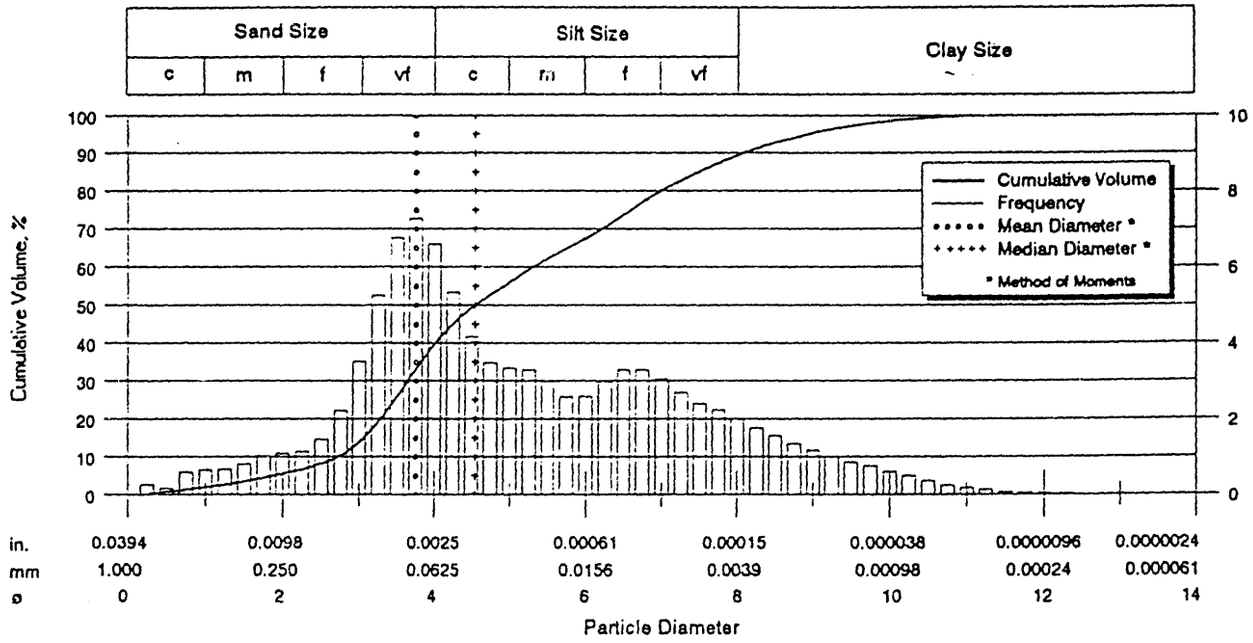

Particle Size Distribution

	[U.S. Sieve]	Diameter [in]	[mm]	[phi]	Volume, % [Inc.]	[Cum.]
Coarse	20	0.0331	0.84	0.25	0.50	0.50
Sand	25	0.0280	0.71	0.50	0.16	0.66
	30	0.0232	0.59	0.75	0.59	1.25
	35	0.0197	0.50	1.00	0.65	1.90
Medium	40	0.0165	0.42	1.25	0.68	2.58
Sand	45	0.0138	0.35	1.50	0.80	3.38
	50	0.0118	0.30	1.75	1.01	4.39
	60	0.0098	0.25	2.00	1.08	5.47
Fine	70	0.0083	0.210	2.25	1.13	6.60
Sand	80	0.0070	0.177	2.50	1.47	8.07
	100	0.0059	0.149	2.75	2.22	10.29
	120	0.0049	0.125	3.00	3.52	13.81
Very Fine	140	0.0041	0.105	3.25	5.24	19.05
Sand	170	0.0035	0.088	3.50	6.76	25.81
	200	0.0029	0.074	3.75	7.26	33.07
	230	0.0025	0.063	4.00	6.60	39.67
Silt	270	0.0021	0.053	4.25	5.33	45.00
	325	0.0017	0.044	4.5	4.16	49.16
	400	0.0015	0.037	4.75	3.48	52.64
	450	0.0012	0.031	5.00	3.35	55.99
	500	0.0010	0.025	5.32	4.19	60.18
	635	0.0008	0.020	5.64	3.58	63.76
		0.00061	0.0156	6.00	3.69	67.45
		0.00031	0.0078	7.00	12.63	80.08
		0.00015	0.0039	8.00	9.33	89.41
Clay		0.000079	0.0020	9.00	5.83	95.24
		0.000039	0.00098	10.0	3.21	98.45
		0.000019	0.00049	11.0	1.27	99.72
		0.0000094	0.00024	12.0	0.26	99.98
		0.0000047	0.00012	13.0	0.02	100.00
		0.0000039	0.00010	13.3	0.00	100.00

Sorting Statistics

Parameter	[Moment]	[Trask]	[Inman]	[Folk]
Mean, in	0.0029	0.0012	0.0010	0.0012
Mean, mm	0.0741	0.0305	0.0264	0.0309
Mean, phi	3.7540	5.0341	5.2444	5.0154
Median, in	0.0017	0.0017	0.0017	0.0017
Median, mm	0.0425	0.0425	0.0425	0.0425
Median, phi	4.5574	4.5576	4.5576	4.5576
Std Deviation, in	0.0044	0.0150	0.0089	0.0089
Std Deviation, mm	0.1120	0.3847	0.2285	0.2279
Std Deviation, phi	3.1584	1.3782	2.1295	2.1336
Skewness	3.7120	1.1026	0.4040	0.2832
Kurtosis	17.1200	0.2914	0.6563	0.9256
Mode, mm	0.0806			
95% Confidence	0.0522			
Limits, mm	0.0961			
Variance, mm2	0.0125			
Coef. of Variance, %	151.20			

Percentiles [volume, %]	Particle Diameter [in]	[mm]	[phi]
5	0.0105	0.2697	1.8908
10	0.0059	0.1516	2.7212
16	0.0045	0.1154	3.1148
25	0.0035	0.0901	3.4723
50	0.0017	0.0425	4.5576
75	0.0004	0.0103	6.5959
84	0.0002	0.0060	7.3739
90	0.0001	0.0037	8.0802
95	0.0001	0.0020	8.9450

Figure 6-1-1 (cont'd)

Western Atlas International
A Litton Dresser Company

CORE LABORATORIES

Company	GBRN	Depth	7844.6	File Number	57161-11412A
Well	OCS-G 2115 No. A-20, S/T	Field	Eugene Island Block 330	Date	2-Dec-93
Parish	Offshore	State	Louisiana	Analyst	Ligon

Laser Particle Size Analysis

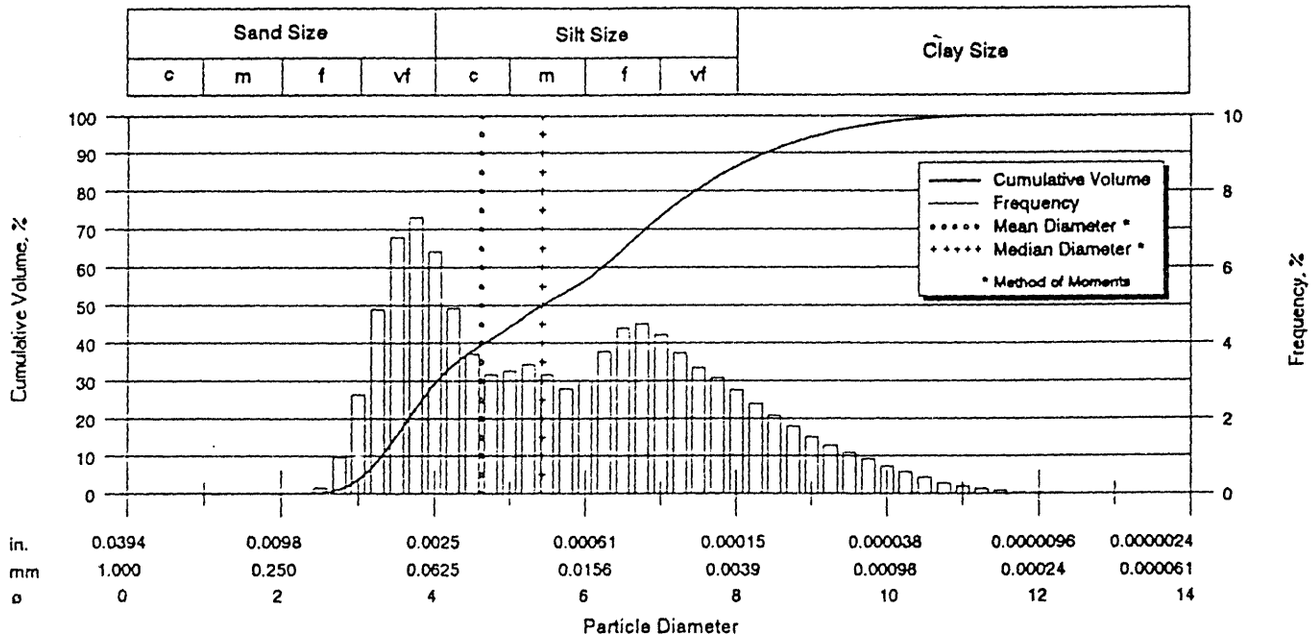

Particle Size Distribution						
	[U.S. Sieve]	Diameter [in]	[mm]	[phi]	Volume, % [Inc.]	[Cum.]
Coarse Sand	20	0.0331	0.84	0.25	0.00	0.00
	25	0.0280	0.71	0.50	0.00	0.00
	30	0.0232	0.59	0.75	0.00	0.00
	35	0.0197	0.50	1.00	0.00	0.00
Medium Sand	40	0.0165	0.42	1.25	0.00	0.00
	45	0.0138	0.35	1.50	0.00	0.00
	50	0.0118	0.30	1.75	0.00	0.00
	60	0.0098	0.25	2.00	0.00	0.00
Fine Sand	70	0.0083	0.210	2.25	0.00	0.00
	80	0.0070	0.177	2.50	0.15	0.15
	100	0.0059	0.149	2.75	0.97	1.12
	120	0.0049	0.125	3.00	2.65	3.77
Very Fine Sand	140	0.0041	0.105	3.25	4.89	8.66
	170	0.0035	0.088	3.50	6.79	15.45
	200	0.0029	0.074	3.75	7.32	22.77
	230	0.0025	0.063	4.00	6.41	29.18
Silt	270	0.0021	0.053	4.25	4.93	34.11
	325	0.0017	0.044	4.50	3.71	37.82
	400	0.0015	0.037	4.75	3.15	40.97
	450	0.0012	0.031	5.00	3.28	44.25
	500	0.0010	0.025	5.32	4.36	48.61
	635	0.0008	0.020	5.64	3.82	52.43
		0.00061	0.0156	6.00	4.23	56.66
		0.00031	0.0078	7.00	16.91	73.57
		0.00015	0.0039	8.00	12.93	86.50
Clay		0.000079	0.0020	9.00	7.77	94.27
		0.000039	0.00098	10.0	3.99	98.26
		0.000019	0.00049	11.0	1.46	99.72
		0.0000094	0.00024	12.0	0.27	99.99
		0.0000047	0.00012	13.0	0.01	100.00
		0.0000039	0.00010	13.3	0.00	100.00

Sorting Statistics				
Parameter	[Moment]	[Trask]	[Inman]	[Folk]
Mean, in	0.0016	0.0009	0.0008	0.0008
Mean, mm	0.0406	0.0227	0.0200	0.0210
Mean, phi	4.6231	5.4614	5.6458	5.5738
Median, in	0.0009	0.0009	0.0009	0.0009
Median, mm	0.0232	0.0232	0.0232	0.0232
Median, phi	5.4297	5.4297	5.4297	5.4297
Std Deviation, in	0.0016	0.0152	0.0089	0.0099
Std Deviation, mm	0.0402	0.3894	0.2289	0.2531
Std Deviation, phi	4.6385	1.3606	2.1271	1.9824
Skewness	0.9710	0.9216	0.3190	0.1627
Kurtosis	-0.0180	0.3215	0.4255	0.7622
Mode, mm	0.0806			
95% Confidence Limits, mm	0.0327 – 0.0485			
Variance, mm2	0.0016			
Coef. of Variance, %	98.94			

Percentiles [volume, %]	Particle Diameter [in]	[mm]	[phi]
5	0.0046	0.1186	3.0761
10	0.0039	0.1010	3.3074
16	0.0034	0.0872	3.5187
25	0.0027	0.0703	3.8310
50	0.0009	0.0232	5.4297
75	0.0003	0.0073	7.0918
84	0.0002	0.0046	7.7730
90	0.0001	0.0030	8.3789
95	0.0001	0.0018	9.1404

Figure 6-1-1 (cont'd)

Western Atlas International
A Unit of Dresser Company

CORE LABORATORIES

Company	GBRN	Depth	7865	File Number	57161-11412A
Well	OCS-G 2115 No. A-20, S/T	Field	Eugene Island Block 330	Date	2-Dec-93
Parish	Offshore	State	Louisiana	Analyst	Ligon

Laser Particle Size Analysis

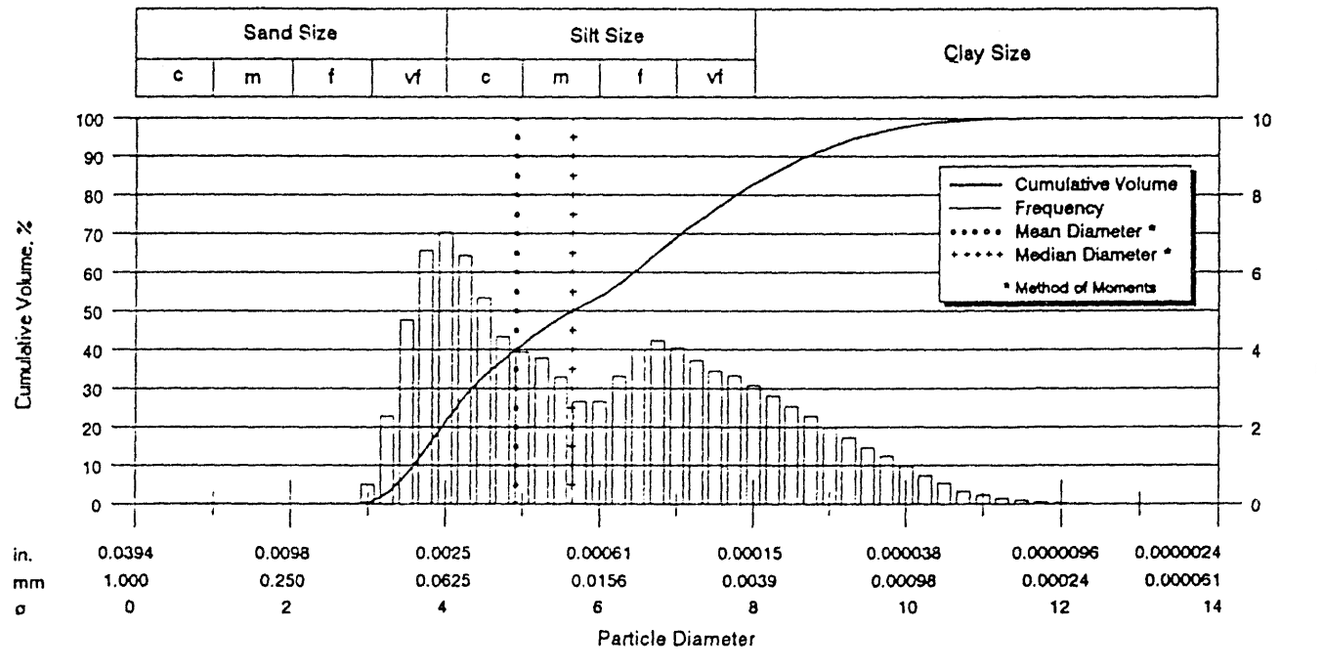

Particle Size Distribution

	[U.S. Sieve]	Diameter [in]	[mm]	[phi]	Volume, % [Inc.]	[Cum.]
Coarse Sand	20	0.0331	0.84	0.25	0.00	0.00
	25	0.0280	0.71	0.50	0.00	0.00
	30	0.0232	0.59	0.75	0.00	0.00
	35	0.0197	0.50	1.00	0.00	0.00
Medium Sand	40	0.0165	0.42	1.25	0.00	0.00
	45	0.0138	0.35	1.50	0.00	0.00
	50	0.0118	0.30	1.75	0.00	0.00
	60	0.0098	0.25	2.00	0.00	0.00
Fine Sand	70	0.0083	0.210	2.25	0.00	0.00
	80	0.0070	0.177	2.50	0.00	0.00
	100	0.0059	0.149	2.75	0.00	0.00
	120	0.0049	0.125	3.00	0.51	0.51
Very Fine Sand	140	0.0041	0.105	3.25	2.29	2.80
	170	0.0035	0.088	3.50	4.77	7.57
	200	0.0029	0.074	3.75	6.57	14.14
	230	0.0025	0.063	4.00	7.04	21.18
Silt	270	0.0021	0.053	4.25	6.44	27.62
	325	0.0017	0.044	4.50	5.32	32.94
	400	0.0015	0.037	4.75	4.33	37.27
	450	0.0012	0.031	5.00	3.95	41.22
	500	0.0010	0.025	5.32	4.78	46.00
	635	0.0008	0.020	5.64	3.86	49.86
		0.00061	0.0156	6.00	3.77	53.63
		0.00031	0.0078	7.00	15.62	69.25
		0.00015	0.0039	8.00	13.57	82.82
Clay		0.00007[6]	0.0020	9.00	9.61	92.43
		0.000039	0.00098	10.0	5.41	97.84
		0.000019	0.00049	11.0	1.83	99.67
		0.0000094	0.00024	12.0	0.30	99.97
		0.0000047	0.00012	13.0	0.03	100.00
		0.0000039	0.00010	13.3	0.00	100.00

Sorting Statistics

Parameter	[Moment]	[Trask]	[Inman]	[Folk]
Mean, in	0.0013	0.0007	0.0006	0.0007
Mean, mm	0.0331	0.0183	0.0161	0.0172
Mean, phi	4.9192	5.7692	5.9595	5.8576
Median, in	0.0008	0.0008	0.0008	0.0008
Median, mm	0.0199	0.0199	0.0199	0.0199
Median, phi	5.6540	5.6538	5.6538	5.6538
Std Deviation, in	0.0013	0.0155	0.0088	0.0099
Std Deviation, mm	0.0321	0.3962	0.2264	0.2533
Std Deviation, phi	4.9608	1.3359	2.1428	1.9810
Skewness	0.9130	0.9586	0.3402	0.1928
Kurtosis	-0.2320	0.3187	0.4009	0.7569
Mode, mm	0.0672			
95% Confidence	0.0268			
Limits, mm	0.0394			
Variance, mm2	0.0010			
Coef. of Variance, %	97.16			

Percentiles [volume, %]	Particle Diameter [in]	[mm]	[phi]
5	0.0037	0.0960	3.3809
10	0.0032	0.0825	3.5990
16	0.0028	0.0710	3.8167
25	0.0022	0.0566	4.1437
50	0.0008	0.0199	5.6538
75	0.0002	0.0059	7.3946
84	0.0001	0.0036	8.1022
90	0.0001	0.0024	8.6985
95	0.0001	0.0015	9.3847

Figure 6-1-1 (cont'd)

Western Atlas International
A Litton Dresser Company

CORE LABORATORIES

Company GBRN
Well OCS-G 2115 No. A-20, S/T
Parish Offshore

Depth 7873
Field Eugene Island Block 330
State Louisiana

File Number 57161-11412A
Date 2-Dec-93
Analysts Ligon

Laser Particle Size Analysis

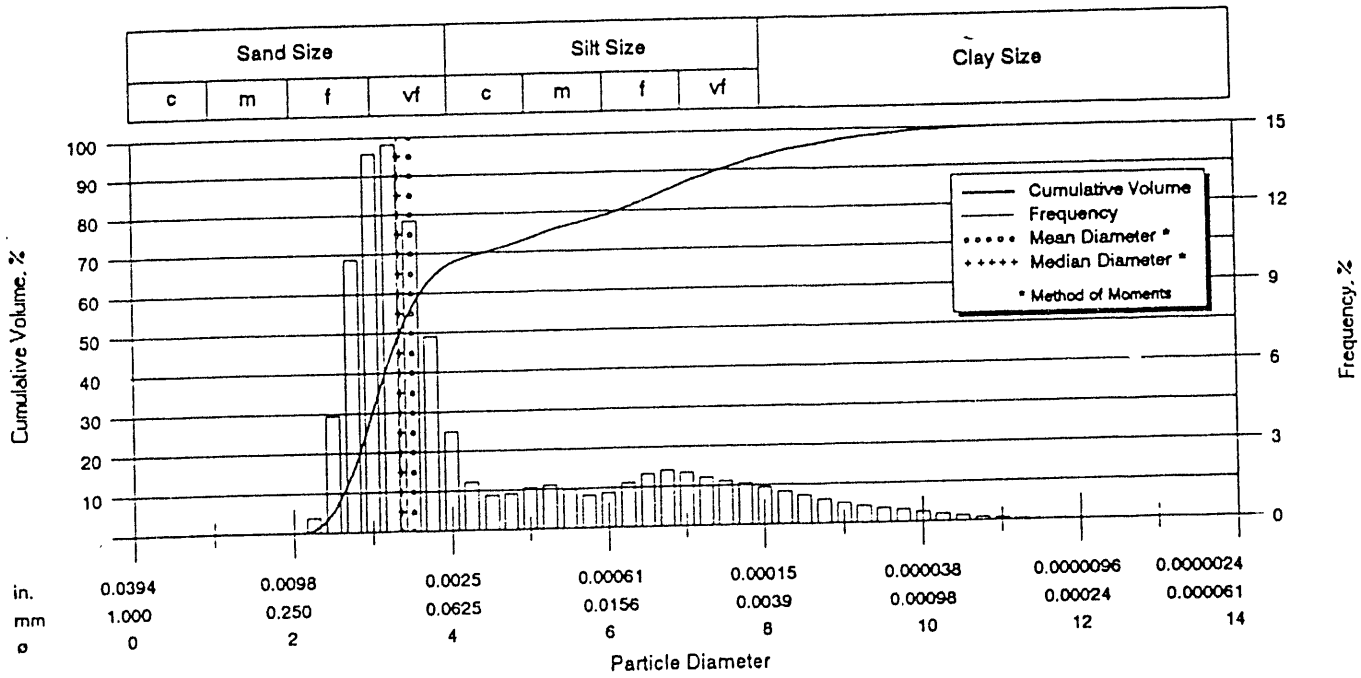

Particle Size Distribution

	[U.S. Sieve]	Diameter [in]	[mm]	[phi]	Volume, % [Inc.]	[Cum.]
Coarse Sand	20	0.0331	0.84	0.25	0.00	0.00
	25	0.0280	0.71	0.50	0.00	0.00
	30	0.0232	0.59	0.75	0.00	0.00
	35	0.0197	0.50	1.00	0.00	0.00
Medium Sand	40	0.0165	0.42	1.25	0.00	0.00
	45	0.0138	0.35	1.50	0.00	0.00
	50	0.0118	0.30	1.75	0.00	0.00
	60	0.0098	0.25	2.00	0.00	0.00
Fine Sand	70	0.0083	0.210	2.25	0.56	0.56
	80	0.0070	0.177	2.50	4.40	4.96
	100	0.0059	0.149	2.75	10.31	15.27
	120	0.0049	0.125	3.00	14.37	29.64
Very Fine Sand	140	0.0041	0.105	3.25	14.72	44.36
	170	0.0035	0.088	3.50	11.75	56.11
	200	0.0029	0.074	3.75	7.37	63.48
	230	0.0025	0.063	4.00	3.74	67.22
Silt	270	0.0021	0.053	4.25	1.83	69.05
	325	0.0017	0.044	4.50	1.31	70.36
	400	0.0015	0.037	4.75	1.35	71.71
	450	0.0012	0.031	5.00	1.57	73.28
	500	0.0010	0.025	5.32	2.09	75.37
	635	0.0008	0.020	5.64	1.74	77.11
		0.00061	0.0156	6.00	1.82	78.93
		0.00031	0.0078	7.00	7.79	86.72
		0.00015	0.0039	8.00	6.47	93.19
Clay		0.000079	0.0020	9.00	4.00	97.19
		0.000039	0.00098	10.0	2.01	99.20
		0.000019	0.00049	11.0	0.69	99.89
		0.0000094	0.00024	12.0	0.11	100.00
		0.0000047	0.00012	13.0	0.00	100.00
		0.0000039	0.00010	13.3	0.00	100.00

Sorting Statistics

Parameter	[Moment]	[Trask]	[Inman]	[Folk]
Mean, in	0.0034	0.0023	0.0015	0.0020
Mean, mm	0.0881	0.0586	0.0381	0.0521
Mean, phi	3.5049	4.0934	4.7158	4.2636
Median, in	0.0038	0.0038	0.0038	0.0038
Median, mm	0.0974	0.0974	0.0974	0.0974
Median, phi	3.3593	3.3593	3.3593	3.3593
Std Deviation, in	0.0023	0.0154	0.0101	0.0107
Std Deviation, mm	0.0578	0.3947	0.2588	0.2744
Std Deviation, phi	4.1130	1.3413	1.9503	1.8658
Skewness	-0.0790	1.3637	1.0674	0.7019
Kurtosis	-1.0860	0.2422	0.5070	1.0307
Mode, mm	0.1271			
95% Confidence	0.0768			
Limits, mm	0.0994			
Variance, mm2	0.0033			
Coef. of Variance, %	65.61			

Percentiles [volume, %]	Particle Diameter [in]	[mm]	[phi]
5	0.0069	0.1765	2.5019
10	0.0063	0.1603	2.6411
16	0.0057	0.1471	2.7654
25	0.0051	0.1317	2.9247
50	0.0038	0.0974	3.3593
75	0.0010	0.0261	5.2621
84	0.0004	0.0098	6.6661
90	0.0002	0.0057	7.4660
95	0.0001	0.0030	8.3803

Figure 6-1-1 (cont'd)

Western Atlas International
A Litton Dresser Company

CORE LABORATORIES

Company	GBRN	Depth	7874.6	File Number	57161-11412A
Well	OCS-G 2115 No. A-20, S/T	Field	Eugene Island Block 330	Date	2-Dec-93
Parish	Offshore	State	Louisiana	Analyst	Ligon

Laser Particle Size Analysis

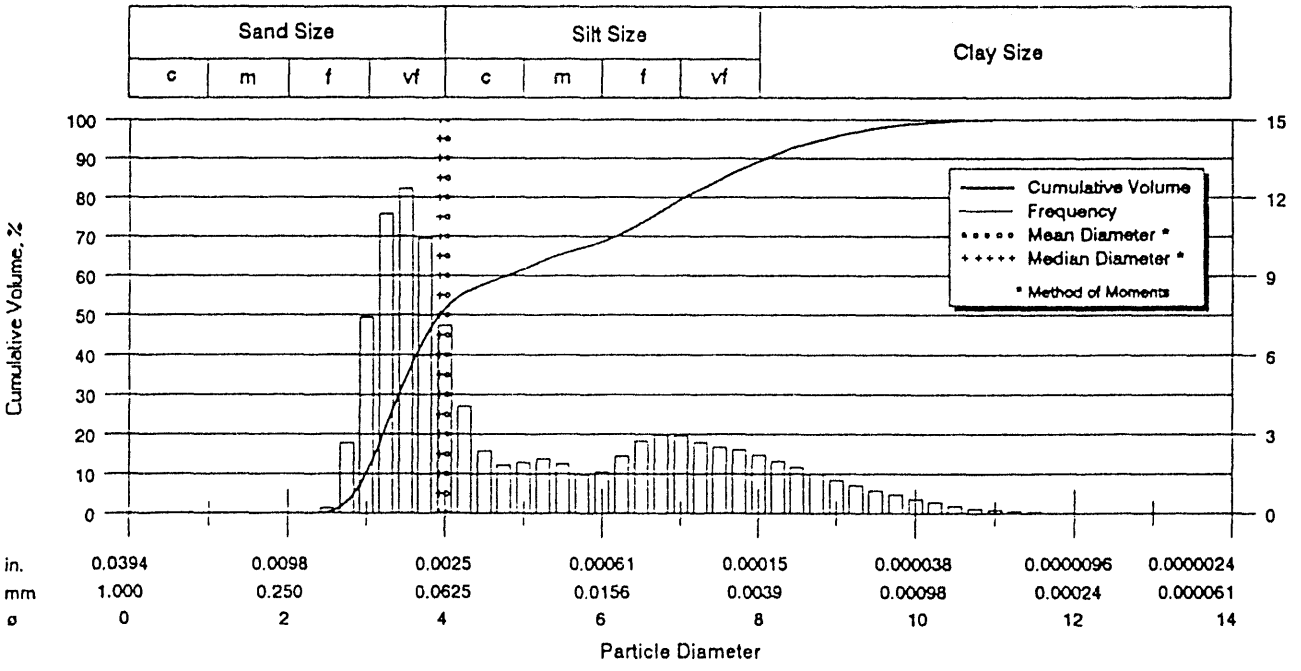

Particle Size Distribution						
	[U.S. Sieve]	Diameter [in]	[mm]	[phi]	Volume, % [Inc.]	[Cum.]
Coarse Sand	20	0.0331	0.84	0.25	0.00	0.00
	25	0.0280	0.71	0.50	0.00	0.00
	30	0.0232	0.59	0.75	0.00	0.00
	35	0.0197	0.50	1.00	0.00	0.00
Medium Sand	40	0.0165	0.42	1.25	0.00	0.00
	45	0.0138	0.35	1.50	0.00	0.00
	50	0.0118	0.30	1.75	0.00	0.00
	60	0.0098	0.25	2.00	0.00	0.00
Fine Sand	70	0.0083	0.210	2.25	0.00	0.00
	80	0.0070	0.177	2.50	0.19	0.19
	100	0.0059	0.149	2.75	2.66	2.85
	120	0.0049	0.125	3.00	7.40	10.25
Very Fine Sand	140	0.0041	0.105	3.25	11.38	21.63
	170	0.0035	0.088	3.50	12.33	33.96
	200	0.0029	0.074	3.75	10.44	44.40
	230	0.0025	0.063	4.00	7.11	51.51
Silt	270	0.0021	0.053	4.25	4.06	55.57
	325	0.0017	0.044	4.50	2.35	57.92
	400	0.0015	0.037	4.75	1.83	59.75
	450	0.0012	0.031	5.00	1.93	61.68
	500	0.0010	0.025	5.32	2.63	64.31
	635	0.0008	0.020	5.64	2.16	66.47
		0.00061	0.0156	6.00	2.19	68.66
		0.00031	0.0078	7.00	10.78	79.44
		0.00015	0.0039	8.00	9.81	89.25
Clay		0.000079	0.0020	9.00	6.47	95.72
		0.000039	0.00098	10.0	3.18	98.90
		0.000019	0.00049	11.0	0.98	99.88
		0.0000094	0.00024	12.0	0.12	100.00
		0.0000047	0.00012	13.0	0.00	100.00
		0.0000039	0.00010	13.3	0.00	100.00

Sorting Statistics				
Parameter	[Moment]	[Trask]	[Inman]	[Folk]
Mean, in	0.0024	0.0012	0.0010	0.0014
Mean, mm	0.0613	0.0319	0.0257	0.0351
Mean, phi	4.0275	4.9709	5.2837	4.8340
Median, in	0.0026	0.0026	0.0026	0.0026
Median, mm	0.0654	0.0654	0.0654	0.0654
Median, phi	3.9348	3.9346	3.9346	3.9346
Std Deviation, in	0.0019	0.0146	0.0088	0.0098
Std Deviation, mm	0.0479	0.3756	0.2253	0.2525
Std Deviation, phi	4.3847	1.4127	2.1500	1.9858
Skewness	0.2260	1.4198	0.8893	0.6318
Kurtosis	-1.2030	0.3241	0.3979	0.7455
Mode, mm	0.0967			
95% Confidence	0.0519			
Limits, mm	0.0707			
Variance, mm2	0.0023			
Coef. of Variance, %	78.06			

Percentiles [volume, %]	Particle Diameter [in]	[mm]	[phi]
5	0.0054	0.1396	2.8411
10	0.0049	0.1256	2.9933
16	0.0044	0.1139	3.1337
25	0.0039	0.1002	3.3185
50	0.0026	0.0654	3.9346
75	0.0004	0.0101	6.6232
84	0.0002	0.0058	7.4337
90	0.0001	0.0037	8.0920
95	0.0001	0.0022	8.8521

Figure 6-1-1 (cont'd)

Western Atlas International
A Litton Dresser Company

CORE LABORATORIES

Company	GBRN	Depth	7878.9	File Number	57161-11412A
Well	OCS-G 2115 No. A-20, S/T	Field	Eugene Island Block 330	Date	2-Dec-93
Parish	Offshore	State	Louisiana	Analyst	Ligon

Laser Particle Size Analysis

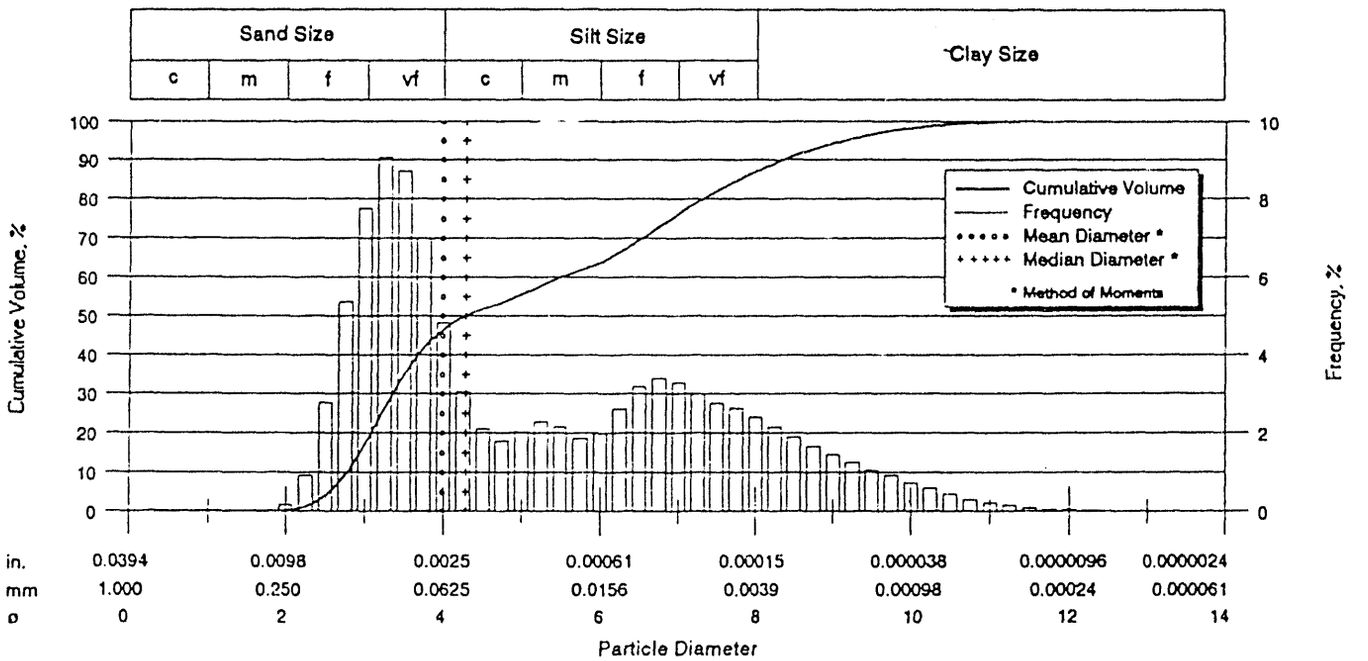

Particle Size Distribution

	[U.S. Sieve]	[in]	[mm]	[phi]	Volume, % [Inc.]	[Cum.]
Coarse	20	0.0331	0.84	0.25	0.00	0.00
Sand	25	0.0280	0.71	0.50	0.00	0.00
	30	0.0232	0.59	0.75	0.00	0.00
	35	0.0197	0.50	1.00	0.00	0.00
Medium	40	0.0165	0.42	1.25	0.00	0.00
Sand	45	0.0138	0.35	1.50	0.00	0.00
	50	0.0118	0.30	1.75	0.02	0.02
	60	0.0098	0.25	2.00	0.15	0.17
Fine	70	0.0083	0.210	2.25	0.92	1.09
Sand	80	0.0070	0.177	2.50	2.77	3.86
	100	0.0059	0.149	2.75	5.36	9.22
	120	0.0049	0.125	3.00	7.77	16.99
Very Fine	140	0.0041	0.105	3.25	9.05	26.04
Sand	170	0.0035	0.088	3.50	8.72	34.76
	200	0.0029	0.074	3.75	7.01	41.77
	230	0.0025	0.063	4.00	4.83	46.60
Silt	270	0.0021	0.053	4.25	3.06	49.66
	325	0.0017	0.044	4.50	2.09	51.75
	400	0.0015	0.037	4.75	1.78	53.53
	450	0.0012	0.031	5.00	2.01	55.54
	500	0.0010	0.025	5.32	2.92	58.46
	635	0.0008	0.020	5.64	2.58	61.04
		0.00061	0.0156	6.00	2.79	63.83
		0.00031	0.0078	7.00	12.47	76.30
		0.00015	0.0039	8.00	10.77	87.07
Clay		0.000079	0.0020	9.00	7.14	94.21
		0.000039	0.00098	10.0	3.95	98.16
		0.000019	0.00049	11.0	1.52	99.68
		0.0000094	0.00024	12.0	0.30	99.98
		0.0000047	0.00012	13.0	0.02	100.00
		0.0000039	0.00010	13.3	0.00	100.00

Sorting Statistics

Parameter	[Moment]	[Trask]	[Inman]	[Folk]
Mean, in	0.0025	0.0012	0.0010	0.0012
Mean, mm	0.0632	0.0300	0.0249	0.0317
Mean, phi	3.9846	5.0601	5.3270	4.9802
Median, in	0.0020	0.0020	0.0020	0.0020
Median, mm	0.0512	0.0512	0.0512	0.0512
Median, phi	4.2866	4.2866	4.2866	4.2866
Std Deviation, in	0.0023	0.0141	0.0076	0.0086
Std Deviation, mm	0.0584	0.3627	0.1953	0.2211
Std Deviation, phi	4.0976	1.4633	2.3561	2.1773
Skewness	0.6920	1.2095	0.6678	0.4593
Kurtosis	-0.4490	0.3301	0.3996	0.7351
Mode, mm	0.1059			
95% Confidence	0.0517			
Limits, mm	0.0746			
Variance, mm2	0.0034			
Coef. of Variance, %	92.46			

Percentiles [volume, %]	Particle Diameter [in]	[mm]	[phi]
5	0.0066	0.1693	2.5625
10	0.0057	0.1455	2.7813
16	0.0050	0.1276	2.9709
25	0.0042	0.1072	3.2217
50	0.0020	0.0512	4.2866
75	0.0003	0.0084	6.8985
84	0.0002	0.0049	7.6830
90	0.0001	0.0031	8.3499
95	0.0001	0.0018	9.1576

Figure 6-1-1 (cont'd)

Western Atlas International
A Litton/Dresser Company

CORE LABORATORIES

Company	GBRN	Depth	7880.3	File Number	57161-11412A
Well	OCS-G 2115 No. A-20, S/T	Field	Eugene Island Block 330	Date	2-Dec-93
Parish	Offshore	State	Louisiana	Analysts	Ligon

Laser Particle Size Analysis

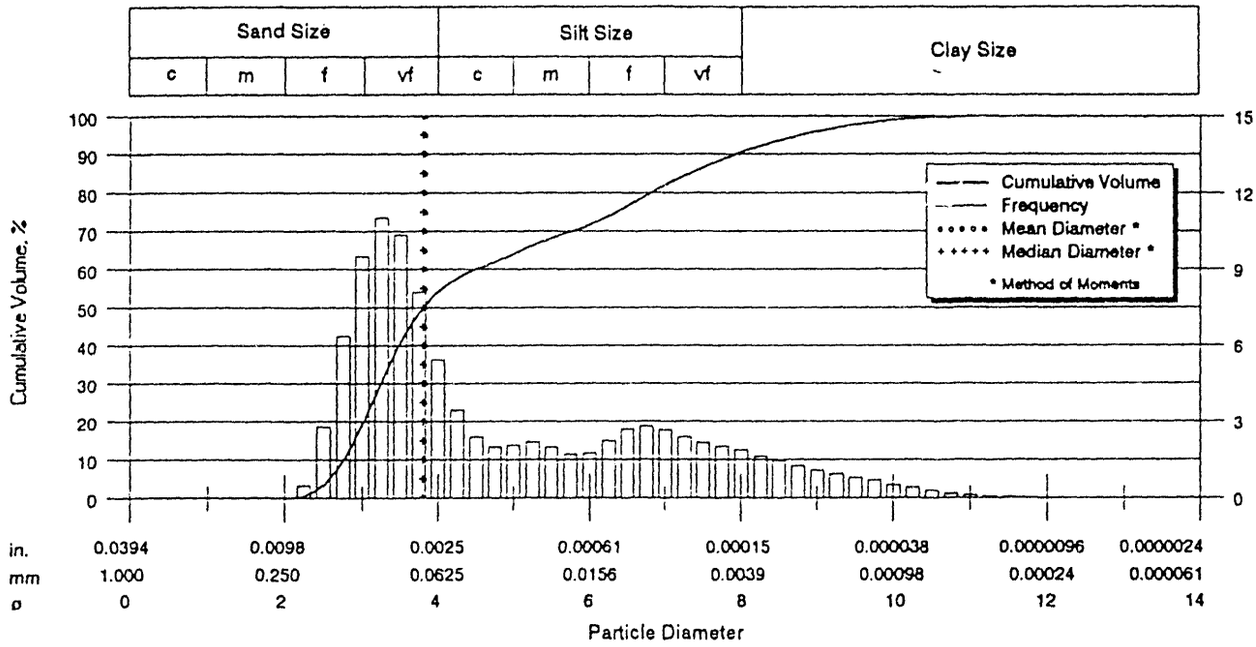

Particle Size Distribution

	[U.S. Sieve]	Diameter [in]	[mm]	[phi]	Volume, % [Inc.]	[Cum.]
Coarse	20	0.0331	0.84	0.25	0.00	0.00
Sand	25	0.0280	0.71	0.50	0.00	0.00
	30	0.0232	0.59	0.75	0.00	0.00
	35	0.0197	0.50	1.00	0.00	0.00
Medium	40	0.0165	0.42	1.25	0.00	0.00
Sand	45	0.0138	0.35	1.50	0.00	0.00
	50	0.0118	0.30	1.75	0.00	0.00
	60	0.0098	0.25	2.00	0.00	0.00
Fine	70	0.0083	0.210	2.25	0.50	0.50
Sand	80	0.0070	0.177	2.50	2.78	3.28
	100	0.0059	0.149	2.75	6.37	9.65
	120	0.0049	0.125	3.00	9.53	19.18
Very Fine	140	0.0041	0.105	3.25	11.02	30.20
Sand	170	0.0035	0.088	3.50	10.38	40.58
	200	0.0029	0.074	3.75	8.09	48.67
	230	0.0025	0.063	4.00	5.44	54.11
Silt	270	0.0021	0.053	4.25	3.44	57.55
	325	0.0017	0.044	4.50	2.39	59.94
	400	0.0015	0.037	4.75	2.00	61.94
	450	0.0012	0.031	5.00	2.07	64.01
	500	0.0010	0.025	5.32	2.78	66.79
	635	0.0008	0.020	5.64	2.38	69.17
		0.00061	0.0156	6.00	2.47	71.64
		0.00031	0.0078	7.00	10.37	82.01
		0.00015	0.0039	8.00	8.44	90.45
Clay		0.000079	0.0020	9.00	5.46	95.91
		0.000039	0.00098	10.0	2.94	98.85
		0.000019	0.00049	11.0	1.01	99.86
		0.0000094	0.00024	12.0	0.14	100.00
		0.0000047	0.00012	13.0	0.00	100.00
		0.0000039	0.00010	13.3	0.00	100.00

Sorting Statistics

Parameter	[Moment]	[Trask]	[Inman]	[Folk]
Mean, in	0.0028	0.0015	0.0012	0.0016
Mean, mm	0.0708	0.0373	0.0299	0.0400
Mean, phi	3.8197	4.7453	5.0657	4.6442
Median, in	0.0028	0.0028	0.0028	0.0028
Median, mm	0.0717	0.0717	0.0717	0.0717
Median, phi	3.8013	3.8011	3.8011	3.8011
Std Deviation, in	0.0022	0.0145	0.0088	0.0097
Std Deviation, mm	0.0561	0.3726	0.2268	0.2480
Std Deviation, phi	4.1548	1.4244	2.1407	2.0114
Skewness	0.3630	1.3786	0.8802	0.5987
Kurtosis	-0.9330	0.3115	0.4506	0.7895
Mode, mm	0.1059			
95% Confidence	0.0598			
Limits, mm	0.0818			
Variance, mm2	0.0032			
Coef. of Variance, %	79.27			

Percentiles [volume, %]	Particle Diameter [in]	[mm]	[phi]
5	0.0065	0.1672	2.5800
10	0.0057	0.1474	2.7620
16	0.0051	0.1317	2.9249
25	0.0044	0.1140	3.1332
50	0.0028	0.0717	3.8011
75	0.0005	0.0122	6.3574
84	0.0003	0.0068	7.2064
90	0.0002	0.0041	7.9372
95	0.0001	0.0023	8.7907

Figure 6-1-1 (cont'd)

Western Atlas International
A Litton Dresser Company

CORE LABORATORIES

Company	GBRN	Depth	7893.8	File Number	57161-11412A
Well	OCS-G 2115 No. A-20, S/T	Field	Eugene Island Block 330	Date	2-Dec-93
Parish	Offshore	State	Louisiana	Analysts	Ligon

Laser Particle Size Analysis

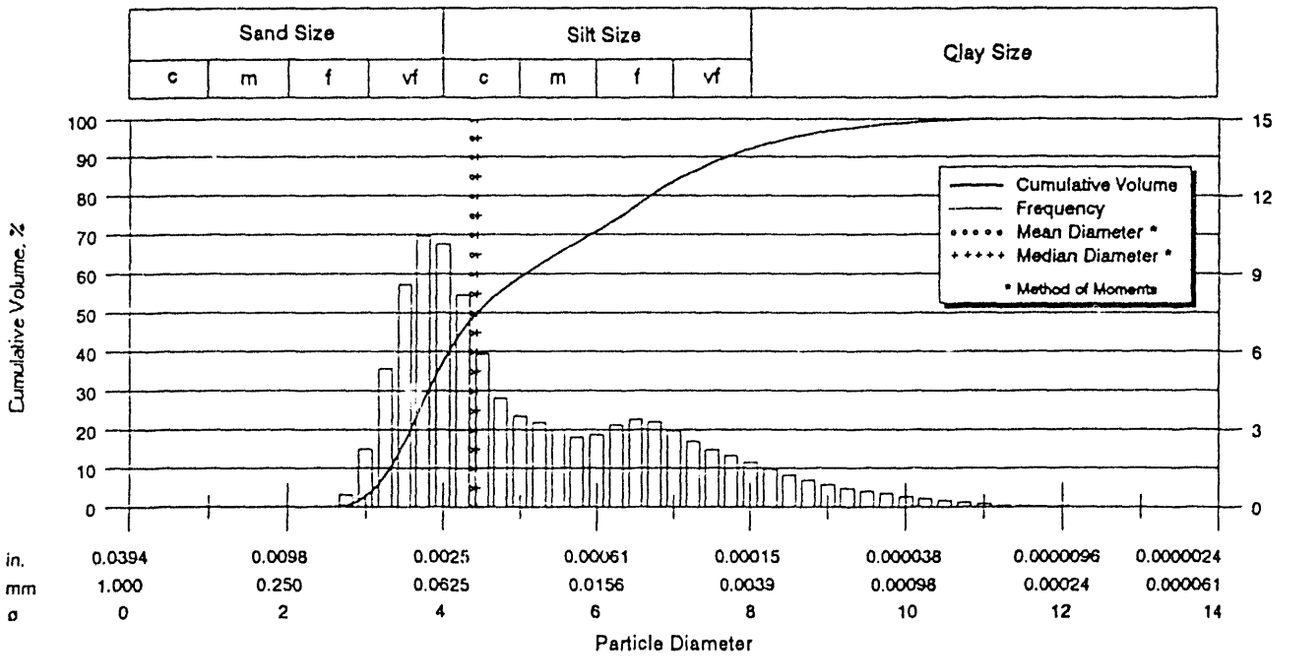

Particle Size Distribution

	[U.S. Sieve]	Diameter [in]	[mm]	[phi]	Volume, % [Inc.]	[Cum.]
Coarse Sand	20	0.0331	0.84	0.25	0.00	0.00
	25	0.0280	0.71	0.50	0.00	0.00
	30	0.0232	0.59	0.75	0.00	0.00
	35	0.0197	0.50	1.00	0.00	0.00
Medium Sand	40	0.0165	0.42	1.25	0.00	0.00
	45	0.0138	0.35	1.50	0.00	0.00
	50	0.0118	0.30	1.75	0.00	0.00
	60	0.0098	0.25	2.00	0.00	0.00
Fine Sand	70	0.0083	0.210	2.25	0.00	0.00
	80	0.0070	0.177	2.50	0.00	0.00
	100	0.0059	0.149	2.75	0.47	0.47
	120	0.0049	0.125	3.00	2.23	2.70
Very Fine Sand	140	0.0041	0.105	3.25	5.34	8.04
	170	0.0035	0.088	3.50	8.60	16.64
	200	0.0029	0.074	3.75	10.47	27.11
	230	0.0025	0.063	4.00	10.14	37.25
Silt	270	0.0021	0.053	4.25	8.21	45.46
	325	0.0017	0.044	4.50	5.89	51.35
	400	0.0015	0.037	4.75	4.23	55.58
	450	0.0012	0.031	5.00	3.52	59.10
	500	0.0010	0.025	5.32	4.16	63.26
	635	0.0008	0.020	5.64	3.66	66.92
		0.00061	0.0156	6.00	3.97	70.89
		0.00031	0.0078	7.00	12.82	83.71
		0.00015	0.0039	8.00	8.46	92.17
Clay		0.000079	0.0020	9.00	4.59	96.76
		0.000039	0.00098	10.0	2.21	98.97
		0.000019	0.00049	11.0	0.84	99.81
		0.0000094	0.00024	12.0	0.17	99.98
		0.0000047	0.00012	13.0	0.02	100.00
		0.0000039	0.00010	13.3	0.00	100.00

Sorting Statistics

Parameter	[Moment]	[Trask]	[Inman]	[Folk]
Mean, in	0.0019	0.0012	0.0010	0.0012
Mean, mm	0.0487	0.0310	0.0262	0.0316
Mean, phi	4.3587	5.0117	5.2553	4.9820
Median, in	0.0018	0.0018	0.0018	0.0018
Median, mm	0.0462	0.0462	0.0462	0.0462
Median, phi	4.4350	4.4352	4.4352	4.4352
Std Deviation, in	0.0015	0.0158	0.0114	0.0120
Std Deviation, mm	0.0373	0.4042	0.2929	0.3069
Std Deviation, phi	4.7455	1.3067	1.7714	1.7039
Skewness	0.4760	1.1896	0.7865	0.4894
Kurtosis	-0.7230	0.2995	0.5243	0.8449
Mode, mm	0.0736			
95% Confidence	0.0414			
Limits, mm	0.0561			
Variance, mm2	0.0014			
Coef. of Variance, %	76.50			

Percentiles [volume, %]	Particle Diameter [in]	[mm]	[phi]
5	0.0045	0.1144	3.1282
10	0.0039	0.1003	3.3182
16	0.0035	0.0894	3.4839
25	0.0030	0.0768	3.7020
50	0.0018	0.0462	4.4352
75	0.0005	0.0125	6.3215
84	0.0003	0.0077	7.0267
90	0.0002	0.0048	7.6908
95	0.0001	0.0027	8.5286

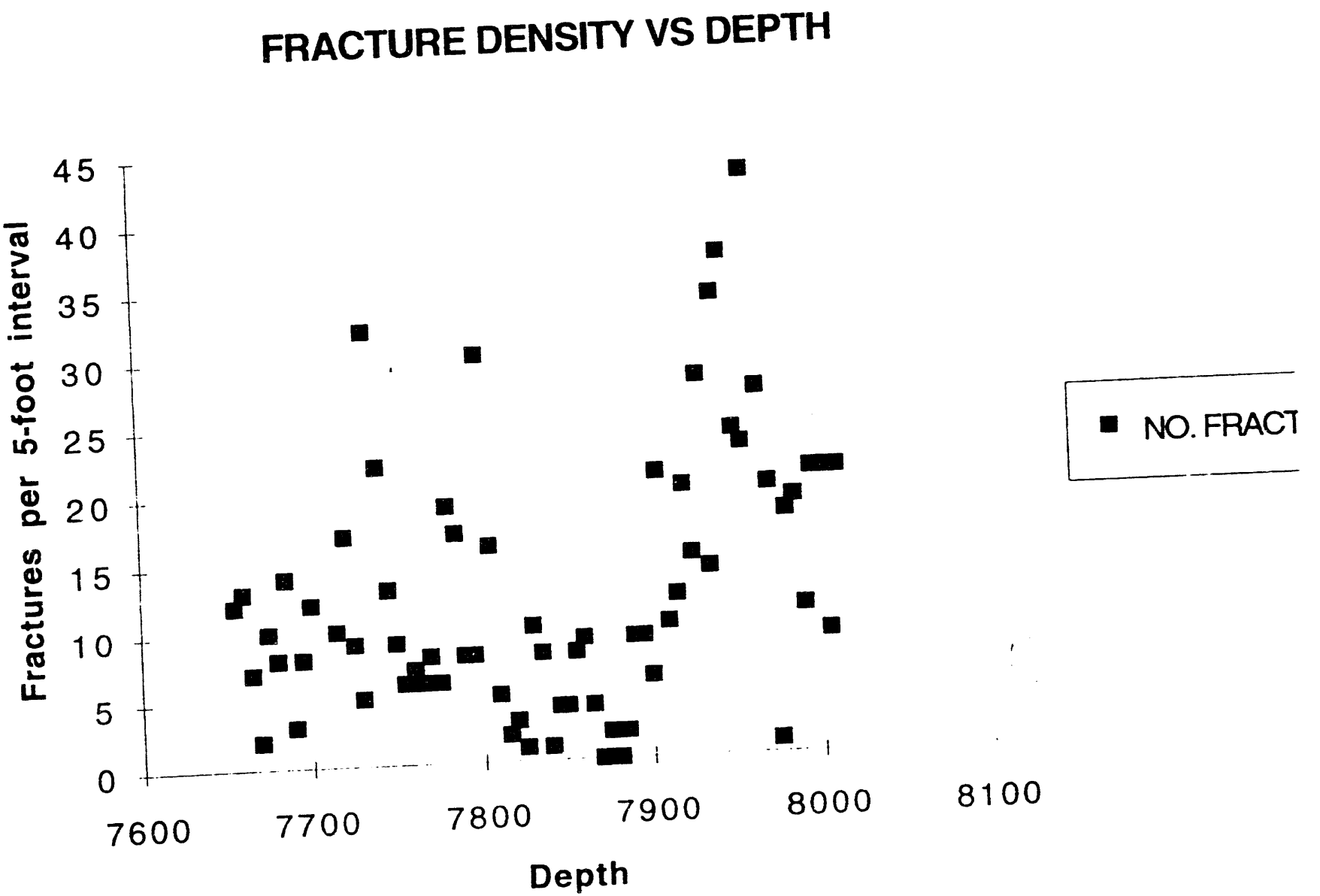
FRACTURE DENSITY VS DEPTH
Fractures per 5-foot interval
45
40
35
30
25
20
15
10
5
0
7600
7700
7800
7900
8000
8100
Depth
NO. FRACT

Phase I Progress Report, Subtask 6.2, Organic Geochemistry.
For period: December 1993 to June 30, 1994
From: Jean Whelan, Woods Hole Oceanographic Institution
Date Report: April 1, 1994.

OBJECTIVES:

Task 6.2.a. Organic geochemistry, hydrous pyrolysis:

1) Hydrous pyrolysis of rocks containing Type III kerogen - Gulf Coast or similar Rocks, completion of experiments for:
   a) Gulf Coast Cretaceous Eutaw Shale
   b) Carbonate Smackover shale, Gulf Coast
   c) Monterey Shale, an organic and organic sulfur-rich, low iron rock containing Type II-S kerogen
   d) Middle Valley Hydrothermal sediments, for which we have very good downhole temperature measurements for calibration of the degree of kerogen maturation and gas generation in EI-330.

Task 6.2.b. Organic geochemistry, Organic chemistry, Organic petrography, 13C isotopes to trace migration pathways and the degree of sediment heating caused by fluids ascending the Fault:

2) Analysis of biomarkers in Pathfinder oils via high resolution gas chromatography mass spectrometry (HRGCMS) at Woods Hole. This objective has been modified from our original proposal because we have determined that the Woods Hole HRGCMS has many advantages over the Texas A & M low resolution GCMS instrument originally proposed for the biomarker work.
3) Analyses of oils recovered from Pathfinder well: whole oil gas chromatograms, percentage alkanes:aromatics:asphaltenes; gas and gasoline range hydrocarbon compositional analyses; gas and oil isotopic analyses (GERG Group, Texas A & M).
4) Analyze bitumens and kerogens from core samples obtained from the Pathfinder well for evidence of degree of heating near *vs* away from faults; analysis of similarities between sediment bitumens and oils allowing migration pathways to be traced.
5) Analyses of 50 oils collected from the resampling of EI wells in Dec of 1993. These oils are from intervals previously studied in the GERG Phase IV oil correlation study so that changes over time can be followed. In addition, replicates taken 4 days apart from the same interval were analyzed in order to determine short term variability of the overall sampling and analytical scheme. To date, whole oil gas chromatograms and gasoline range hydrocarbon compositional analyses have been completed by the GERG group. By completion of the project data will be collected for: whole oil gas chromatograms, percentage alkanes:aromatics:asphaltenes; gas and gasoline range hydrocarbon compositional analyses; and gas and oil isotopic analyses.

6) The oils in Part 5 will also be subjected to biomarker analysis via HRGCMS at Woods Hole. Samples are in hand and will be analyzed this summer.

7) Identification of collaborators for work on Pathfinder Well samples. Preliminary results of Dr. Martin Schoell of Chevron on the analysis of gases from the pathfinder well are reported. Other collaborators who have been identified are described.

8) Analysis of carboxylic acids from reservoir brines have been completed.

9) Cores have been obtained for vitrinite reflectance analysis in the Pathfinder A-20ST well below the red fault. Sidewall core samples have been obtained for these analyses just above and through the red fault zone, which is also the pressure transition zone. The first suite of vitrinite reflectance measurements on these samples will be carried out during April of 1994.

Task 6.2.c. Organic geochemistry, Modeling and technology transfer:

10) The start of the WHOI and Texas A & M subcontracts were unavoidably delayed until Dec of 1993. Therefore, some of the Phase I geochemical tasks will be postponed until Phase II of the project, as described below.

11) A Sun Sparc 10 work station has been installed at Woods Hole which will facilitate collaboration with other institutions involved in the project. AVS, Mosaic, and Gopher programs have been installed and activated. Hypermedia will be installed in mid-April of 1994. Two excellent people have been identified at Woods Hole who will aid in establishing an active computer interface between Woods Hole and the other GBRN institutions involved in this project. The overall goals of the computer interface are: a) to place organic geochemical data into computer models and into a geological and geophysical context in the Eugene Island oil and gas field.

12) Collection, storage, and cataloging of gas, oil, core, and sidewall core samples for organic geochemistry from Pathfinder well.

Summary of Technical Progress

1) Hydrous pyrolysis, rocks containing Type III kerogen - Gulf Coast or similar Rocks These measurements, which were obtained from high temperature laboratory experiments which allow sampling "on-line" without cooling the reaction vessel, will allow us to test the viability of methane solubilization of oil as an oil migration mechanism for EI-330. In addition, activation energies for gas and oil generation are being obtained which will allow a realistic estimation of gas and oil generation depths. Initial results will be reported in an oral presentation at the AAPG in Denver in June, 1994.

Since the source rock for the Eugene Island oils is unknown and too deep to drill, we have carried out experiments on several different rocks which we believe, based on biomarker data discussed below, may be similar to the actual source rocks. To date, results have been completed for:

a) Gulf Coast Cretaceous Eutaw Shale Gas evolution results are shown in Table 1. Activation energies, estimated via the distributed activation energy methods of Burnham and Braun (1985) and Burnham, et al. (1987), for methane and carbon dioxide evolution were found to be 69 - 74 & 60 kcal/mole, respectively. A second smaller CO2 peak was also apparent with an activation energy of 40 kcal/mole.

b) Carbonate Smackover shale, Gulf Coast Based on biomarker evidence, the Eugene Island oils are closest in composition to the on-shore Smackover Type I oils, as described by Sofer, 1990 (see section 2 below). Therefore, an immature and relatively low sulfur and low TOC (1 %) Smackover rock was subjected to hydrous pyrolysis. Preliminary results are shown in Table 2. Surprisingly, gas yields were much lower from this carbonate-rich sediment than from the Eutaw or Monterey shales.

c) Monterey Shale, an organic rich (20% TOC) and organic sulfur-rich low iron rock. The biomarker patterns and high abundance of benzothiophenes in the Eugene Island Oils suggest a marine sulfur-containing source rock, possibly phosphate rich and from an anoxic environment. The carbonate-rich Smackover, recovered from on-shore Louisiana cores, constitutes such a rock. Alternatively, a marine siliceous organic and sulfur-rich, low iron containing rock such as the Monterey Shale, would also produce oils with very similar biomarker characteristics (Peters and Moldowan, 1993). This type of rock has not been described for the Gulf Coast. However, since the source rock for the Eugene Island oils is unknown and too deep to drill, a rock similar to the Monterey is a possibility on the basis of the biomarker evidence. Therefore, hydrous pyrolysis was run on a sample of the Monterey to determine if oil and gas compositions similar to those observed for Eugene Island gases and oils could be produced. The results obtained so far are shown in Table 3.

Surprisingly, this oil-prone rock yielded more gas at lower temperature than any other rock analyzed to date. Very high yields of both carbon dioxide and methane were generated from both acid-treated and non-acid treated samples starting at very low maturities, so that all of the gas appears to be evolving from the kerogen rather than mineral matter starting at relatively low temperatures. Gas evolution is substantial even in experiments conducted as low as 125°C in the laboratory, not much higher than temperatures which actually occur within the oil window. This temperature is much too low for cracking of oil to gas to be occurring. Therefore, we conclude that this gas is being generated during early thermal breakdown of the sulfur-rich kerogen. If similar kerogens occurred, even in narrow bands, within Gulf Coast rocks, substantial gas for oil solubilization would be generated at relatively low temperatures.

d) Middle Valley Hydrothermal sediments, for which we have very good downhole temperature measurements, for calibration of degree of kerogen maturation and gas generation in EI-330. Organic lean sediments were recovered from the Middle Valley hydrothermal area at the Northern end of the Juan de Fuca Ridge in the Northeastern Pacific off the coast of British Columbia. These sediments, which have very poor oil source rock quality (0.5 to 1% Type III gas-prone kerogen), are very similar to those in the Gulf Coast Eutaw shale (see part a above). Because of this similarity and the excellent set of downhole temperature measurements which are also available, the Middle Valley hydrothermal sediments provide an excellent calibration between laboratory and geological paleotemperatures and kinetics. A summary of laboratory hydrous pyrolysis results obtained to date are shown in Table 4.

Hydrous pyrolysis results for generation of saturated C1-C3 gases at temperatures from 225°C to 375°C show that at the highest temperatures, methane continues to increase, while ethane and propane begin to decrease. The activation energy for methane evolution agreed well with those found for the Eutaw shale (66 to 74 kcal/mole) suggesting that clay-rich type III kerogens from diverse areas may have similar energetics with respect to gas evolution.

We are in the process of deciding whether or not hydrous pyrolysis experiments should be carried out on either the Cretaceous Tuscaloosa or Wilcox shales in the next phase of the project. EI oils are missing several characteristic biomarkers of these oils so that both appear to be significant contributors to the Eugene Island oils. The biomarker evidence to date requires a more marine and probably anoxic depositional facies for the Eugene Island oils.

We also have an immature sample of the Sparta formation which will be subjected to hydrous pyrolysis in the next phase of the project. A review of the literature includes one report of biomarkers in an oil from the Sparta formation which appear to have many features in common with the Eugene Island oils.

2) Analysis of biomarkers in GBRN Pathfinder oils via high resolution gas chromatography mass spectrometry (HRGCMS) at Woods Hole. In our last quarterly report, we reported tests with

several "standard" EI oils representing specific reservoir sands at a single location using the Woods Hole HRGCMS instrument for biomarker identification and quantitation. It was found that whole oils could be analyzed without any prior clean up, so that the analyses were fast and reproducible as well as less labor intensive, and more specific with respect to both identification and quantification of biomarkers than previous analyses on the low resolution GCMS (LRGCMS) at GERG. LRGCMS requires oil separation into aliphatic, aromatic, and polar fractions which can cause artifacts in both compound identification and quantitation. HRGCMS eliminates this problem as well as allowing interferences between peaks to be minimized, so that in a single run of whole oil, most peaks for hopanes (for example) can be unambiguously assigned and quantitated. Therefore, we have reached an agreement with GERG that all future biomarker GCMS work required by this project will be run by HRGCMS at Woods Hole rather than via LRGCMS at GERG, as originally proposed.

Future organic geochemical analyses of oils and bitumens will be split between Texas A & M and Woods Hole by having GERG characterize oils with regard to n- and iso-alkane distribution, percentages of alkanes:aromatics:polar compounds, oil isotopic compositions, gas and gasoline range hydrocarbon compositions, and 13C isotopes of methane, ethane and propane as originally proposed. However, all GCMS analyses for biomarkers in oils and bitumens will be carried out on the high resolution GCMS instrument at Woods Hole. A specific schedule of number and types of analyses and where they are to be run is included in the Project Evaluation Report accompanying this report.

We have now analyzed about half of the oils collected from the GBRN Pathfinder well via HRGCMS, as shown in Table 5. To date, HRGCMS data have been completed on:

i) for a series of "standard" EI-330 reservoir samples discussed in previous reports and in Whelan, et al, (manuscript attached).

ii) for the samples shown in Table 5, including samples from the GBRN pathfinder well (labeled "GBRN") as well as samples collected from other wells and depths by Lorraine Eglinton in December 1993 when she was on the rig.

Some of the results of HRGCMS analyses completed to date are shown in Figs 1, 4, and 6-13. Complete HRGCMS data for these samples as well as the other 50 resampled EI oils described under part 5 below will be completed in Phase II of this project; results will be available later this year.

All of the EI oils in Table 5 examined to date appear to be identical via their HRGCMS biomarker and aromatic hydrocarbon patterns. For example, mass scans for the tri and pentacyclic terpanes (m/z=191.1794, Fig 1) for a "standard" oils from the MG reservoir (see Whelan, et al in press; manuscript attached), one of the Pathfinder oils (GBRN-8, an oil water mixture), and the bottom hole oil from the Pathfinder drill stem test are almost identical. These patterns are also very similar to the least mature Smackover oils from Mississippi and Alabama

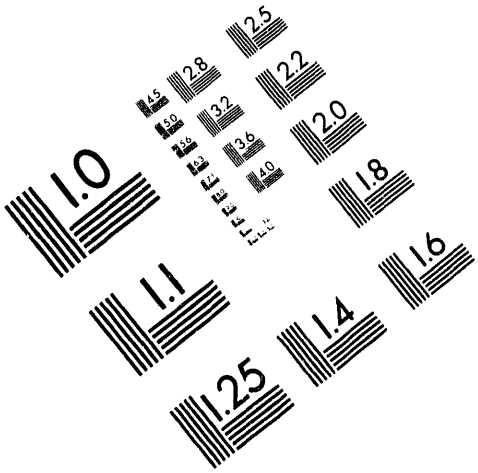

Association for Information and Image Management
1100 Wayne Avenue, Suite 1100
Silver Spring, Maryland 20910
301/587-8202

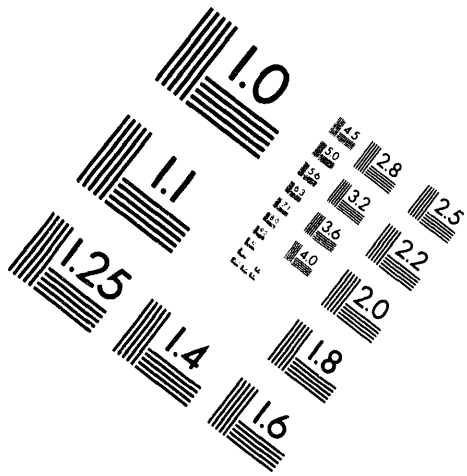

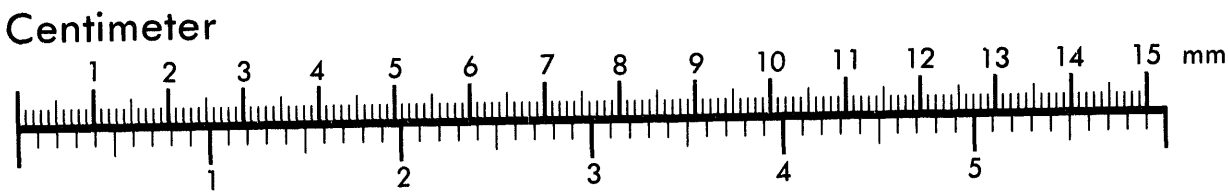

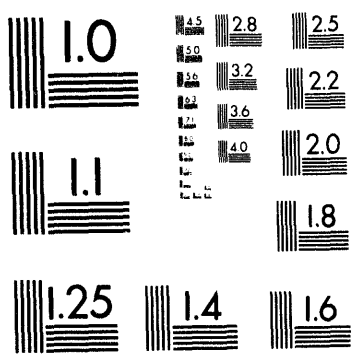

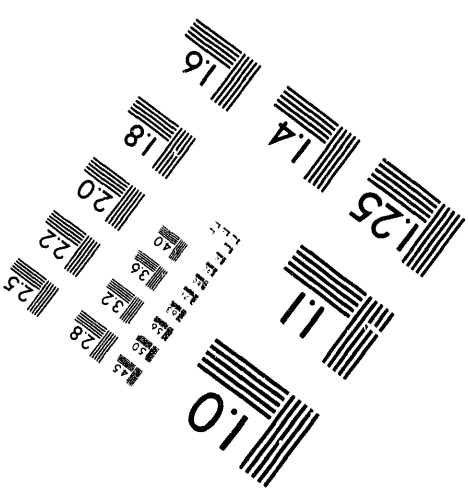

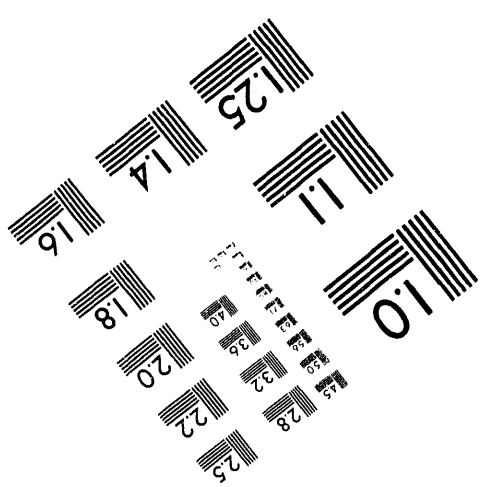

MANUFACTURED TO AIIM STANDARDS
BY APPLIED IMAGE, INC.

3 of 3

described by Sofer, 1990 (Fig 2). The distinctive feature in Figs 1 and 2 are: 1) the C31-C35 extended hopanes (peaks J through M'), characteristic of marine, possibly anoxic, depositional conditions; 2) peak S (T330) along with peaks a through d2 in approximately the relative intensities shown, possibly indicative of carbonate-phosphate rich rocks (Sofer, 1990); and 3) the absence of oleanane (peak O in Fig 3), a biomarker characteristic of terrigenous angiosperm higher plant input. Also missing in both Figs 1 and 2, but not in Fig 3, is an unknown C30 nonhopanoid terpane (X-C30) characteristic of the Tuscaloosa oil family. Gammacerane, often diagnostic of high salinity marine and nonmarine depositional environments, is also absent; however, Peters and Moldowen (1993) caution that the absence of gammacerane cannot be used to deduce that high salinity conditions were not present.

Oleanane, gammacerane, and the X-C30 terpane are all present in representative Cretaceous Wilcox and Tuscaloosa oils (Fig 3, data from Wenger, et al., 1990). The m/z 191 patterns for both the Wilcox and Tuscaloosa oils also appear to be generally much more complex than those for the Smackover oils in Fig 2. The absence of oleanane shows that either the Eugene Island oils are sourced from a sediments having little or no terrigenous organic input or from sediments deposited prior to the Cretaceous when higher plants evolved.

Oils sourced from evaporitic or marine carbonate-clastic sources deposited under anoxic conditions often show C31-C35 extended hopanoids with the C35 peaks (M and M' in Figures 1-3) being enhanced over the C34 peaks (L and L'), as is seen for the Type I and Type II Smackover oils at the bottom of Fig 3. Peters and Moldowen (1993) interpret high C35 hopane concentrations as being diagnostic of highly reducing marine conditions during deposition. However, this feature is often variable within a specific oil family, as shown for the Alabama and Mississippi Smackover oils in Fig 3 and discussed in Sofer, 1990. Sofer also describes a diagnostic patterns of the smaller tricyclic patterns which were used to distinguish different families of oils and differences in depositional conditions.

The Eugene Island tricyclic terpane patterns (Fig 1) most closely resemble those from the Mississippi oils in Fig 2, particularly No 72. The similarity is most noticeable in the relative intensities of peaks P through T including T330 in Figs 1 and 2. Sofer (1990) proposes that the tricyclic terpane pattern of oil No. 72 in Fig 2 is typical of oils sourced from carbonate-phosphate rich rocks.

Steranes mass scans should also be identical for oils with identical sources. Typical sterane HRGCMS mass scans of m/z=217.1956, m/z=218.2028, and m/z=259.2418 for the EI-330 oils, the same oils as in Fig 1, are shown in Fig 4. Comparison LRGCMS mass scans for steranes, m/z=217, for representative Wilcox, Tuscaloosa, and Smackover oils are shown in Fig 5 (data from Wenger et al., 1990).

The sterane mass chromatograms for Eugene Island oils examined to date are virtually identical, as shown in representative examples in Fig 4. The EI mass chromatograms in Fig 4

most closely resemble those from the Smackover in Fig 5, particularly the relative intensities of peaks a and b, with respect to the rest of the mass chromatogram. The Type I Smackover and the sample from the W. Nancy field in Fig 5 are most similar to the m/z 217 pattern in Fig 4. In contrast, the Wilcox, Tuscaloosa, and Type II Smackover samples in Fig 5 all have relatively stronger a and b peaks.

Oils are often classified according to their distribution of C27:C28: C29 regular steranes, as shown for the "standard" EI oils described in Whelan et el. (manuscript attached) in Fig 6a. The ternary diagram shows that EI-330 oils from each of the standard reservoirs group together, including the condensate from the JD reservoir, implying that they all constitute one oil family coming from the same or very similar source facies (see Peters and Moldowen, 1993, for a recent review). Similarly, EI oils collected by L. Eglinton from other EI wells and intervals in Dec 1993 fall in the same area of the ternary diagram (Fig 6b). We are in the process of obtaining similar data for the GBRN oils collected from the Pathfinder well. On the basis of the similarity of the sterane mass chromatograms examined to date (Fig 4), it is anticipated that the Pathfinder oils will fall in the same area of the ternary diagrams as shown in Fig 6a.

Depositional environments proposed to be representative of various assemblages of C27:C28:C29 steranes are indicated in Fig 6a and b. These assignments are controversial (Peters and Moldowan, 1993). However, there is general agreement that an increase in C29 and a decrease in C27 steranes often occurs in going from a more terrigenous to a more marine source facies.

Ternary plots of C1:C2:C3 naphthalenes have been used to show biodegradation in oils (Rowland, 1990). Such a plot for the standard Eugene Island "standard" reservoir oils is shown in Fig 7a and for other EI oils collected by Lorraine Eglinton in Dec 1993 (see Table 5) in Fig 7b. Interestingly, for the "standard" Eugene Island oils shown in Fig 7a, the JD condensate shows the least biodegradation, while the shallowest HB and GA oils show the most, even though the effect appears to be minimal for both. The GA and HB are the shallowest, coolest reservoirs where n-alkane patterns also showed extensive biodegradation (Whelan, et al., in press, manuscript attached). In the case of the JD condensate, the lightest C1 and C2 components are enriched (Fig 7a), as would be expected in a migrating condensate. The other EI samples in Fig 7b fall in the same range as the "standard" samples in Fig 7a, suggesting that these samples, which cover a range of physical states (i.e., oils, oil-water mixtures, emulsions, heavy oils, condensates, etc.) have not been subjected to significant biodegradation.

Mass scans of aromatic compounds in the EI oils can also be used to show similarities and differences in compositions, sources, and maturities. For example, Fig 8 shows alkyl naphthalene mass scans (m/z=142 + 156 + 170) for "standard" EI reservoir samples, including the shallowest (GA), the deepest (OI) and mid-depth condensate (JD). Patterns for the GA and OI reservoirs (Fig 8) are virtually superimposible and also identical to those for the HB, KE, LF,

and MG reservoirs (not shown). The JD condensate shows similar patterns in lower molecular weight compounds (to the left of Fig 8) but with relative concentrations of higher molecular weight compounds dropping off. Similar patterns can be seen for the alkyl benzothiophenes (m/z=134 + 148 + 162 + 176; Fig 9), the alkyl dibenzothiophenes (m/z=184 + 198 + 212; Fig 10), and the phenanthrenes (m/z=178 + 192 + 206 +220; Fig 11). The relatively high concentrations of benzothiophenes and dibenzothiophenes (Figs 9 and 10) are characteristic of the EI oils. In other cases, relatively high concentrations of these compounds are typical of marine, anoxic, sulfur-rich source rocks (Hughes, 1884; Hughes, et al., 1985; Kennicutt, et al., 1992; Peters and Moldowan, 1993), such as the Gulf Coast Smackover and Flexure Trend oils and the California Monterey oils.

Oil biomarkers and aromatic compounds can also be used to deduce the maturity of the oil source rock at the time of oil maturation and expulsion. Several oil maturation parameters have been determined for the EI oils from the HRGCMS data, as shown in Table 6 and in Figs 12 and 13 for the "standard" EI wells and for nearby intervals (Table 5).

All of the biomarker and aromatic hydrocarbon maturation parameters measured to date are consistent with this oil having been generated and expelled approximately from the beginning to the middle of the oil generation window, equivalent to a vitrinite reflectance, Ro, of about 0.75 to 0.8% (Table 6), depending on the exact type of kerogen present. All of these maturation ratios are very constant, although small variations, if they occur, tend to be present in the JD condensate and in the shallower GA and HB reservoirs influenced most by biodegradation and water washing (Whelan, et al, in press; manuscript attached). The biomarker maturation values from the Pathfinder well, including the bottom hole flow-test oil, labeled "drill stem", are also very constant and the same as those for the deeper "standard" EI reservoir oils from the KE, LF, MG, and OI reservoirs.

The discussion above suggests that all of the Eugene Island oils were generated from sediments of approximately the same depth and maturity. However, other ratios can be used to delineate small differences in maturity. For example, Fig 12 shows one example using two triaromatic sterane ratios against each other. According to this plot, there appears to be a general increase in oil maturity with increasing reservoir depth, with the exception of the JD condensate.

The 22R/(22S+22R) homohopane ratios are shown for the EI standard reservoir and the GBRN Pathfinder oils in Table 6. The values are very constant, 0.58 to 0.60, representing an equilibrium value which falls in the range of 0.57 to 0.62 (MacKenzie, 1984; Marzi and Rullkotter, 1992; and Peters and Moldowan, 1993 p 226). This ratio, which is typically measured on the C31 and C32 homologs, was determined here for the C31 homohopanes (see definition in Table 6). A ratio of 0.5-0.54 would represent oils from rocks just barely entering the oil window. With increasing maturity, the ratio increases to the maximum equilibrium value of 0.57-0.6 and then either remains constant or decreases slightly with higher thermal stress.

Thus, the values observed here for the Eugene Island oils are approximately consistent with the calculated vitrinite reflectances (Rcs) computed from the methylphenanthrenes, being indicative of oil expelled from a rock undergoing early to peak oil generation in the maturity range of Ro 0.7 to 0.8%.

The sterane 20S/(20S+20R) ethyl cholestane ratios, also shown in Table 6, show somewhat more variability. The EI standard reservoir values are in the range of 0.41 to 0.49, while the GBRN oils span almost the same range, 0.42 to 0.47. The equilibrium value for this ratio is the maximum of 0.55 which occurs just at the beginning of the oil window. Further maturation then causes a decrease to values in the range between 0.35 and 0.45 (Marzi & Rullkotter, 1992). To be consistent with the other maturation indicators, the sterane 20S/(20S+20R) values measured here indicate that the EI samples would fall in the higher maturity range where the 20S/(20S+20R) values have begun to fall.

Peters and Moldowan (1993) consider the hopane ratios to be a more reliable indicator of the onset of oil generation than these sterane ratios. However, the values for both parameters measured here are consistent with the EI oils being sourced and expelled from rocks approaching the peak of maximum oil generation.

2a. Carbazole and heterocyclic organic nitrogen compounds - analysis by HRGCMS

Because of the ease with which the HRGCMS analyses can be run on whole oils, we propose to add an additional task to our phase II work. As discussed above, the biomarkers for the EI oils are all very similar. Thus, we propose to examine a specific set of compounds which have been found to be very useful in delineating oil migration pathways under similar circumstances in other oil reservoirs. The specific compounds to be examined are heterocyclic nitrogen compounds, in particular pyrolic nitrogen species (carbazoles) which were shown by Li et al (1992), Dorban et al. (1984) to be very useful in tracing North Sea oil primary migration and secondary migration pathways where conventional biomarkers suggested uniformity. If these results are successful, these procedures would be extended to analyze carbazoles in polar bitumen fractions which will be recovered from the frozen Pathfinder core sections and the frozen sidewall cores from the red fault zone.

3) Analyses of oils recovered from Pathfinder well: whole oil gas chromatograms, percentage alkanes:aromatics:asphaltenes; gas and gasoline range hydrocarbon compositional analyses; gas and oil isotopic analyses (data from GERG Group, Texas A & M). Compositions of oils recovered from the GBRN Pathfinder well in comparison to "standard" EI reservoir oils are shown in Figs 14-19 and Table 7 (labeled as GBRN oils) and summarized in Table 8. These analyses from the Pathfinder well, in comparison to similar data from surrounding wells, will allow us to trace migration pathways and any abnormalities in sediment or oil and gas heating caused by fluid flow from depth.

Whole oil chromatograms of the GBRN oils (Fig 14) are most similar to those of the deeper KE through OI standard oils in Fig 15. Condensates, such as found in the JD reservoir in Fig 15, or biodegraded and obviously remigrated oils, such as found in the GA and HB reservoirs (Fig 15) and discussed in Whelan, et al., in press (manuscript attached) are not observed among the GBRN samples collected from the Pathfinder well. Thus, the remigrated n-alkanes observed in the GA and HB reservoirs, diagnostic of remigrated fluids, are not obviously present in the GBRN samples examined in this initial work. The next phase of the project will concentrate on examining these oils further for these processes which may be obscured by the background oil patterns.

Ratios of the branched hydrocarbons, pristane/phytane (Pr/Ph), have been used by various laboratories to show oil maturation, anoxicity of depositional source, and terrigenous to marine source inputs. In reviewing the existing literature, Peters and Moldowen (1993) concluded that Pr/Ph values less than 1, especially if accompanied by high amounts of the hopane, gammacerane, are diagnostic of an anoxic high salinity source facies. Likewise, high Pr/Ph values, > 1.5, are typical of oxic depositional facies. Unfortunately, most of the EI values fall in between, in the range of 1 to 1.5, values which the same authors conclude cannot be used to define source facies. The EI data shown in Fig 16, which represents all of the GERG EI Phase IV oil correlation data base, shows a large spread in Pr/Ph ratios, typical of very anoxic to highly oxic depositional environments.

Some of the spread for the EI samples in Fig 16 may be attributable to sampling and analytical variability or to changing oil compositions in the reservoirs, as proposed in Whelan, et al. (in press; manuscript attached). Values from EI platforms A, B, and C all fall in a much tighter range of 1.2 to 1.5, when these same wells and intervals were resampled in Dec 1993, as indicated in Fig 16. Pr/Ph values for the GBRN oils show an even tighter range of 1.18±0.06 for eight GBRN oil emulsions (labeled as 05 GBRN in Tables 7 and 8) and 1.19±0.08 for the GBRN oil-water mixtures (labeled as 06 GBRN in Table 8). These values are identical to other EI oils in Table 8, consistent with all the EI oils belonging to a single oil family, as concluded previously from the biomarkers. However, the Pr/Ph value of about 1.1-1.2 falls in the range where no conclusions can be drawn about the oxic vs anoxic nature of the source facies, based on this parameter alone. Similar GERG Phase IV data for South Marsh Island-128 oils, just to the north and west, are shown in Fig 16 for comparison.

Odd even ratios (OER) for n-alkane chain lengths for EI and SMI oils are shown in Fig 17. Immature oils tend to have high OERs (i.e., a predominance of odd carbon chain lengths) while mature oils have no even or odd carbon length predominance, producing OER values of around 1. Marine oils from anoxic evaporitic sources often show an even carbon predominance in the C24 to C26 range, producing OER values of less than 1. For the EI-330 Phase IV oils, most of the OER values are in the range 0 to 1.5, suggesting a significant contribution from

mature and marine, possibly with some contribution from evaporitic, oils. In contrast the phase IV SMI-128 oils all fall in a very tight range just at or a little below 1, typical of mature oils.

OER values for Pathfinder GBRN oils as well as oils resampled from Phase IV intervals in Dec of 1993 are also shown in Fig 17 and Table 8. Values from the resampled oils, as well as the GBRN oils, all fall in a fairly narrow range between 0.8 and 1.2, diagnostic of mature oils.

Carbon preference indices for n-alkanes larger than nC23 are also shown in Tables 7 and 8 . Values higher than 1 are diagnostic of the presence of immature oils with some odd carbon (higher plant wax) input (Peters and Moldowen, 1993). EI 330 oils from the GBRN well all have a CPR of > 1, consistent with some contribution from immature terrigenous oils. However, it should not be concluded from this data that terrigenous sourced oils predominate since interference from higher plants from shallower reservoirs can artificially elevate this CPI value because the higher molecular weight n-alkanes tend to be selectively preserved by most alteration processes (i.e., biodegradation, water washing, oil expulsion.)

The ratio of nC3 plus nC4 to nC17 was used in Whelan et al. (in press; manuscript attached) to represent ratios of wet gas to oil, respectively. Many of the EI Phase IV oils studied by the GERG group show high proportions for this ratio (Fig 18; Whelan, et al in press). However, the GBRN oils from the Pathfinder well all show very low values, even lower than those for the oils resampled from other Platform A wells in Dec of 1993.

It was previously argued that high wet gas to oil ratios may be diagnostic of recent hydrocarbon reinjection into a reservoir, since the lighter hydrocarbons are also more prone to escape from a reservoir undergoing leakage (Whelan, et al., manuscript attached). In addition, in any well undergoing active biodegradation which produces "humpane" type baselines, such as those observed for the GA and HB reservoirs in Fig 15, it would be expected that n-C3 and nC4 should also be absent since these low molecular weight compound are easily and preferentially lost by biodegradation, as well as by a number of processes, including water washing and evaporative fractionation (Thompson, 1983; 1987; 1988). Therefore, high (nC3+nC4)/nC17 ratios are consistent with recent oil migration or remigration into a specific reservoir.

Low (nC3+nC4)/nC17 ratios for the GBRN 05 and GBRN 06 oils (Fig 18) suggest no significant remigration or recent hydrocarbon injection into these Pathfinder well intervals. The GBRN (nC3+nC4)/nC17 ratios tend to be very low, similar to the bulk of oils measured previously in SMI-128, where remigration is not thought to be occurring (Whelan, et al, manuscript attached). In contrast, the values for all of the A platform wells resampled in 1993 show a somewhat broader spread of higher values, suggestive of the presence of slightly higher proportions of wet gas in several intervals.

These data do not support any active hydrocarbon injection having recently taken place for the Pathfinder GBRN oils shown in Fig 18 and Tables 7 and 8. However, in a significant number of the other EI-330 oils shown in Fig 18, high (nC3+nC4)/nC17 ratios are observed,

consistent with some contribution from preferential light hydrocarbon injection and which, possibly, derive from episodic dynamic injection.

Ratios of nC9 to nC19, a typical gasoline range hydrocarbon to a typical oil hydrocarbon, show trends very similar to those of (nC3+nC4)/nC17 ratios (Fig 19; Tables 7 and 8). The GERG Phase IV EI samples show a broader range of nC9/nC19 values than the SMI-128 samples. The GBRN Pathfinder samples show much lower values (Fig 19). Also indicated on Fig 19 are the ranges of values for EI oils resampled in Dec 1993 from the EI A, B, and C platforms. As with the Pr/Ph and (nC3+nC4)/nC17 ratios, the nC9/nC19 ratios in the more recently collected samples tend to cover a smaller range of values.

Ratios of C7 hydrocarbons, especially F (n-heptane to methylcyclohexane) and B (toluene to n-heptane) have been used to delineate relative amounts of evaporative fractionation, maturation, water washing, and biodegradation which have affected oils (Thompson, 1983, 1987, 1988). These processes are indicated by the arrows in Fig 20. Previously, it was found that EI oils tend to have abnormally high F values not consistent with their maturities as determined from ethane versus propane d13C values (Whelan, et al., in press; manuscript attached). Because other processes shown in Fig 20 could be ruled out as the cause of the high F values, it was postulated that recent injection of condensate from an evaporative fractionation event may be the cause of the relatively high F values observed in the LF, MG, NH, some of the OI oils, and especially in the JD condensates.

F versus B values for the GBRN oils fall in the same region as for the LF oils (Figure 20 and Table 8). The range of values for all of the oils resampled from Platform A in Dec of 1993 are also shown. All of these F versus B values fall in the same range as the previous data, signifying no significant overall change since the previous (1988) sampling. However, individual wells and intervals do show changes over time (Fig 21). Wet gas and gasoline range hydrocarbons compositions (C4 to C8) from a specific interval and depth sampled in 1984, 1988, and most recently in Dec of 1993 (labeled as 1994 in Fig 21c) are shown in Fig 21a-c. Changes are noticeable, particularly in the ratios of light (C3-C5) to heavier (C7-C8) components, with a higher proportion of lighter components being present in 1994. Ratios of B, F, H (a maturity ratio based on the ratio n-heptane to the sum of branched and cyclo to n-alkanes, Thompson, 1979; 1983), and I (ratio of branched C7 compounds to the sum of cyclic C7 dimethylcyclopentanes) also show changes over the 6 year period.

During the resampling in December 1993, a test was made of the reproducibility of sampling and GC analyses of pairs of samples taken from the same well and interval several days apart (Table 9). The reproducibility is excellent, which gives us increased confidence that the compositional differences shown in Figs 21a-c are real and represent real changes occurring in the wells over time.

During drilling of the pathfinder well, gas samples were obtained by Martin Schoell using a new gas sampler which is currently being used extensively at Chevron. Initial structural and isotopic compositions for these gases as shown in Figure 22. The results are very surprising - the core gas methane collected from throughout the Pathfinder well contains a significant biogenic component, which increases with increasing depth.

To explain these initial gas data, we propose that this gas represents predominantly biogenic methane generated in organic rich sediments at much shallower depth which was then carried down and buried. Mixing is occurring with more thermogenic gas entering the sediments though faults, particularly the Red Fault, above the top of the Pathfinder well, so that the gas becomes more thermogenic in approaching the red fault/pressure transition zone just above the depth where the Pathfinder well coring began. Thus, $d^{13}C$ values for methane are heavier and more thermogenic at the top than at the bottom of the Pathfinder well.

The $d^{13}C$ methane values for the Pathfinder well show little or no thermogenic methane coming from depth and mixing upward in the cored interval. This hypothesis will be tested in Phase II of the project by examining isotopic and molecular compositions of sorbed gases in frozen sidewall cores from intervals within and adjacent to the fault zone, in comparison to other intervals adjacent and away from smaller faults throughout deeper intervals of the Pathfinder well. Core samples have already been collected and frozen for this purpose (Table 10).

4) Analyze bitumens and kerogens from excellent core sample set obtained from the Pathfinder well (see below) for evidence of degree of heating near vs away from various faults; analysis of similarities between sediment bitumens and oils allowing tracing of migration pathways. Cores have been collected for this purpose (Table 10). These analyses will be carried out during the remainder of Phase I and during Phase II of the project.

5) Analyses of oils collected from resampling of EI wells in Dec of 1993 via whole oil gas chromatograms, percentage alkanes:aromatics:asphaltenes; gas and gasoline range hydrocarbon compositional analyses; gas and oil isotopic analyses (GERG Group, Texas A & M). . Oils were collected from the same wells and intervals previously studied in the GERG Phase IV oil correlation study:

About 45 EI oils were resampled in December 1993 by the GERG group. These oils represent intervals previously studied in the GERG Phase IV oil correlation study. To date, whole oil gas chromatograms and gasoline range hydrocarbon compositional analyses have been completed, as summarized in Figs 15 to 21, Tables 7 & 8 and discussed under part 3 above. Percentage alkanes:aromatics:asphaltenes and gas and oil isotopic analyses will be carried out on these oils according to the schedule shown in Table 10.

6) Analysis of biomarkers in same wells as in Part 5 via high resolution gas chromatography mass spectrometry (HRGCMS) at Woods Hole. Samples are in hand but have not yet been analyzed. Current plans are to carry out these analyses during the summer of 1994 (see proposed schedule

in Table 10) after we have had a chance to more fully examine the first sample suite described under part 2 above, and to more fully automate the HRGCMS data output.

7) Identification of collaborators for work on Pathfinder Well samples. To date, the following have been identified for specific analyses:

a) Dr. Martin Schoell of Chevron who has collected gases from the Pathfinder well and analyzed them for chemical and isotopic composition (see part 3 above). He is anxious to work with us on sorbed core gases, as well, and to collaborate in finding reasonable interpretations of the puzzling Pathfinder well gas data.

b) Dr. Bissada at Texaco has offered to run compound specific isotopic analyses on some oils. This procedure has been used very successfully to fingerprint oils in other reservoir areas. Dr. Martin Schoell of Chevron is also very interested in collaborating in this work.

c) Conoco has offered to run routine pyrolysis, total carbon, and total organic carbons on core samples. They have also offered to run any needed analyses on oils which they do routinely

d) Dr Ben Law at USGS in Denver is planning to run vitrinite reflectance measurements on kerogens from cuttings, including those through the fault zone above the Pathfinder well.

f) We have been receiving oil samples from surrounding reservoir areas which oil companies are interested in having us compare to the EI-330 oils.

g) A calibration of the $d^{13}C$ scale for methane vs ethane vs propane is planned using gas samples collected by Martin Schoell. So far, identified participants in this calibration study using Pathfinder well, Middle Valley, and hydrous pyrolysis gas samples are Drs. Melody Rooney and George Claypool of Mobile and Dr Martin Schoell of Chevron. We are working on also getting participation from Dr Alan James of Exxon and Dr Michael Whitaker of University of Victoria.

In addition, Dr. Melody Rooney from Mobil visited us at Woods Hole and is interested in collaboration on calculation of gas generation temperatures as deduced from a combination of gas carbon isotopic data, downhole temperature measurements, and hydrous pyrolysis results from Middle Valley sediments. This calibration will provide a calibration of temperature for modeling fluid flow processes in Eugene Island sediments. In addition, it may shed light on an interesting general question with regard to gas generation - must all of the hydrogen required be derived from organic carbon, or can part of it come from water? : The model of gas generation currently used by Mobile assumes all of the needed hydrogen comes from kerogen. However, Dr. Jeffrey Seewald in our laboratory has submitted a paper to Nature which demonstrates that, at least in the laboratory, water may also provide a source of hydrogen for gas generation. If this phenomena can be demonstrated in nature as well, gas generation models now in common use by oil companies will have to be modified. The results are very important because they relate directly to how much and at what depth various gases can be generated.

h) Wallace Dow and John Castano of DGSI, an organic geochemical oil service company, are anxious to apply new techniques of determining gasoline range hydrocarbon maturities to our samples. A pilot program involving a few samples will be carried out. Additional funding from sources other than DoE will be sought if initial result look promising.

i) Sylvie Charpeny and Rose Bassilakis from Advanced Fuel Research in E. Hartford, Ct. are interested in helping us with pyrolysis analyses which can be used to show migration pathways. In addition, they are working on a project to build a chemical structural model of Type III kerogen during maturation. When complete, this model can be used to gain a better understanding of the energetics of Eugene Island oil generation and cracking, relevant to estimating amounts of oil and gas available at specific depths to drive specific processes in the Eugene Island reservoirs.

8) Analysis carboxylic acids from reservoir brines. Dr Jeffrey Seewald at Woods Hole has analyzed carboxylic acids in EI oil field brines collected by Dr Lynn Walter during Dec 1993. Results obtained on an ion chromatograph are shown in Table 11. It was possible to detect small amounts of dicarboxylic acids in some samples (i.e., oxalic and succinic acids). However, our preliminary conclusions are that the amounts are so small that it is difficult to see how these species could be playing a significant role in mineral alteration, as proposed in numerous publications from (e.g., MacGowan, D.B., and R.C. Surdam, 1990).

9) Vitrinite reflectance analyses.

Vitrinite reflectance values have been found to be considerably higher for samples within the Red Fault zone than in sections further away (Fig 23). In future work, this work will be extended to sidewall cores from within and adjacent to the red fault zone, as well as to core sections obtained from A-20 well near to and further away from smaller fractures (Table 10). Samples are in hand for these analyses, which will be started during April and completed during the summer of 1994. These include frozen core samples from the Pathfinder A-20 well below the red fault as well as frozen sidewall core samples from just above and through the red fault zone, which is also the pressure transition zone.

Using recent vitrinite reflectance data from EI reservoirs collected from Pennzoil, the estimated maturation line for Eugene island can be redrawn as shown in Fig 24 (Whelan, et al., manuscript attached). Note that a point has been added at 14000 ft, which strongly suggests a lower maturity gradient for this well than estimated previously. However, even this maturity gradient may be too steep - the deepest vitrinite reflectance value on this curve actually comes from South Marsh Island, rather than Eugene Island. Maturities tend to become generally lower in moving south and east at a specific depth in this area. Therefore, it is remotely possible that the deep Cretaceous and Jurassic sediments underlying EI-330 may have only recently been within or passed through the oil/gas window. We will work with other scientists at Penn State, Lamont, LSU, and Cornell to test this possibility during Phase II of this project.

10) Postponement of some Phase I work until Phase II. The WHOI and Texas A & M subcontracts were not successfully put in place until Dec of 1993. Therefore, some of the Phase I geochemical tasks will be postponed until Phase II of the project. The specific tasks fitting this category, which are described in detail above, are:

a) completion of vitrinite reflectance measurements

b) core bitumen and gas analyses

c) completion of analyses of biomarkers and isotopes on resampled Eugene Island oils

d) radioiodine measurements on EI fluids (Dr Udo Fehn, Univ Rochester)

e) measurement proportions of n-alkane:aromatics:polar compounds in oils and bitumens via iatroscan (Woods Hole) and HPLC (GERG) (needed to trace migration pathways)

A schedule for carrying out these analyses and other tasks in this project during the remainder of Phase I and in Phase II is shown in Table 10.

11) Sun Sparc 10 work station has been installed at Woods Hole. AVS, Mosaic, and Gopher programs have been installed and activated. Hypermedia will be installed and tested by the GBRN geochemists during April of 1994. Two excellent people have been identified at Woods Hole who will aid in establishing an active computer interface between Woods Hole and the other GBRN institutions using these and other programs.

12) Collection, storage, and cataloging of gas, oil, core, and sidewall core samples for organic geochemistry from Pathfinder well is complete, as described above. The number and types of samples available for the various analyses and a schedule for carrying out specific analyses is shown in Table 10.

References:

Braun, R.L. & A.K. Burnham (1987) Analysis of chemical reaction kinetics using a distribution of activation energies and simpler models, Energy & Fuels, v. 1, pp 153-161.

Braun, R.L. and A.K. Burnham (1990) Mathematical model of oil generation, degradation, and expulsion. Energy & Fuels, v.4, pp 132-146.

Burnham, A.K. and R.L. Braun (1985) General kinetic model of oil shale pyrolysis. In Situ, v. 9, pp 1-23.

Burnham, A.K., R.L. Braun, H.R. Gregg, and A.M Samoun (1987). Comparison of methods for measuring kerogen pyrolysis rates and fitting kinetic parameters, Energy and Fuels, v. 1, pp 451-458.

Dorban, M., J.M. Schmitter, P. Garrigues, I. Ignatiadis, M. Edward, P. Arpino, G. Guiochon (1984). Distribution of carbazole derivatives in petroleum. Org. Geochem. v. 7, pp 111-120.

Hughes, W.B. (1984) Use of thiophenic organosulfur compounds in characterizing crude oils derived from carbonate versus siliciclastic sources. In: J.G. Palacas, ed., Petroleum Geochemistry and Source Rock Potential of Carbonate Rocks. , Amer Assoc of Petro Geologists, Studies in Geology 18, pp 181-196.

Hughes, W.B., A.G. Holba, D.E. Miller, and J.S. Richardson (1985) Geochemistry of greater Ekofisk cride oils. In: B.M. Thomas, ed., Geochemistry in Exploration of the Norwegian Shelf, Graham and Trotman, pp 75-92.

Kennicutt II, M.C., T.J. McDonald, P.A. Comet, G.J. Denoux, and J.M. Brooks (1992) The origins of petroleum in the northern Gulf of Mexico, Geochim Cosmochim Acta, v. 56. , pp 1259-1280.

Li, M., S.R. Larter, D. Stoddart and M. Bjoroy (1992). Practical liquid chromatographic separation schemes for pyrolic and pyridimic nitrogen, aromatic hetercycle fractions from crude oil suitable for rapid characterization of geochemical samples. Anal. Chem., v 64, pp 1337-1344.

MacGowan, D.B., and R.C. Surdam (1990) Importance of organic-inorganic reactions to modeling water-rock interactions during porgrassive clastic diagenesis. In: Chemical Modeling of Aqueous Systems, II. American Chemical Society Special Publications, Chapt 38, pp 494-507.

Mackenzie (1984) Applications of biological markers in petroleum geochemistry. In: Advances in Petroleum Geochemistry, v. 1, J. Brooks & D.H. Welte, eds, Academic Press, London, pp 115-214.

Marzi, R. and Rullkotter, J. (1992) Qualitative and quantitative evolution and kinetics of biological biomarker transformations - laboratory experiments and application to the Michigan Basin. In: J.M Moldowen, P. Albrecht, and R.P. Philp, eds, Prentice Hall, Englewood Cliffs, N.J., pp 18-41.

Peters, K.E. and Moldowan, J.M, (1993) The Biomarker Guide: Interpreting Molecular Fossils in Petroleum and Ancient Sediments. Prentice Hall, Englewood Cliffs, NJ

Radke, M., Welte, D.H., and Willsch, H. (1986) Maturity parameters based on aromatic hydrocarbons: Influence of organic matter type. Org Geochem. v.10, pp 51-63.

Rowland, S.J. (1990) Production of acyclic isoprenoid hydrocarbons by laboratory maturation of methanogenic bacteria. Organic Geochemistry, v.15, pp 9-16.

Rowland, S.J., R. Alexander, R.I. Kagi, D.M. Jones, and A.G. Douglas (1986). Microbial degradation of aromatic components of crude oils: A comparison of laboratory and field observations. Org. Geochem., v 9, no. 4, pp 153-161.

Sofer, Z. (1990) The geochemistry of oils in the Jurassic Smackover Trend of the Gulf Coast States, U.S.A. In: D.Schumacher and B.F. Perkins, eds, Gulf Coast Oils and Gases. Proceedings of the ninth annual Research Conference, SEPM, pp 31-36.

Ten Haven, H.L. (1988) Organic and inorganic geochemical aspects of Mediterranean Late Quaternary sapropels and Messinian evaporitic deposits. Geologica Ultraaiectina, No 46, pp131-170,

Thompson, K.F.M. (1979) Light hydrocarbons in subsurface sediments. Geochim. Cosmochim. Acta, v. 43, pp 657-672.

Thompson, K.F.M. (1983) Classification and thermal history of petroleum based on light hydrocarbons. Geochim. Cosmochim. Acta, v.47, pp 303-316.

Thompson, K.F.M. (1987) Fractionated aromatic petroleums and the generation of gas-condensates. Org. Geochem.. v.11, pp 573-590.

Thompson, K.F.M. (1988) Gas-condensate migration and oil fractionation in deltaic systems, Marine and Petroleum Geology, v. 5, pp 237-246.

Thompson, K.F.M. (1990). Contrasting characteristics attributed to migration in petroleums reservoired in clastic and carbonate sequences in the Gulf of Mexico region. Petroleum Migration Symposium, 1989 Special Publication, Geological Society of London.

Wenger, L.M., R. Sassen, and D. Schumacher (1990). Molecular characteristics of Smackover, Tuscaloosa and Wilcox-Reservoired oils in the Eastern Gulf Coast. In: D.Schumacher and B.F. Perkins, eds, Gulf Coast Oils and Gases. Proceedings of the ninth annual Research Conference, SEPM, pp. 37-57.

Figures:

Figure 1: Comparison of biomarkers, tri- and pentacyclic triterpanes (m/z =191.1794) via HRGCMS: for MG-12, A-20 reference oil; a representative sample of oil-water sample collected during drilling of Pathfinder well (GBRN-8); and oil collected from flow test at bottom of pathfinder well (A-20, Drill stem test oil).

Figure 2: Reference biomarker tri- and pentacyclic triterpanes, m/z=191, Smackover oils, from Sofer, 1990.

Figure 3: Reference biomarker tri- and pentacyclic triterpanes, m/z=191, comparison Wilcox, Tuscaloosa, Smackover, and other miscellaneous oils from Louisiana Gulf Coast (data from Wenger, et al., 1990.)

Figure 4: Biomarkers, Sterane HRGCMS patterns, m/z = 217; 218; and 259, EI oils: a) Standard oil from MG-12 reservoir; b) representative oil from drilling of pathfinder well, GBRN-8, and c) oil collected from flow test at bottom of pathfinder well (A-20, drill stem test oil).

Figure 5: Reference biomarkers, steranes, m/z = 217, oils from Wilcox, Tuscaloosa, Smackover, and miscellaneous Gulf Coast reservoirs.

Figure 6: Distribution of regular steranes in EI oils: a) standard reservoirs and b) miscellaneous other reservoirs, shown in Table 5.

Figure 7: Distribution of C1:C2:C3 naphthalenes: a) standard EI oils and b) oils from miscellaneous other reservoirs.

Figure 8: Comparison, HRGCMS, alkyl naphthalenes (m/z = 142 + 156 +170) from EI standard oils, GA, OI, and JD reservoirs in comparison with representative samples collected from the Pathfinder well, GBRN-8 and drill stem test oil as described in Table 5.

Figure 9:Comparison, HRGCMS, alkyl benzothiophenes (m/z = 134 + 148 + 162 + 176) from EI standard oils, GA, OI, and JD reservoirs in comparison with representative samples collected from the Pathfinder well, GBRN-8 and drill stem test oil as described in Table 5.

Figure 10: Comparison, HRGCMS, alkyl dibenzothiophenes (m/z = 184 + 198 + 212) from EI standard oils, GA, OI, and JD reservoirs in comparison with representative samples collected from the Pathfinder well, GBRN-8 and drill stem test oil as described in Table 5.

Figure 11: Comparison, HRGCMS, alkyl phenanthrenes and methylphenanthrenes (m/z = 178 + 192 + 206 + 220) from EI standard oils, GA, OI, and JD reservoirs in comparison with representative samples collected from the Pathfinder well, GBRN-8 and drill stem test oil as described in Table 5.

Figure 12: Eugene Island oils, standard reservoirs, relative maturities via triaromatic ratios.

Figure 13: Calculated reflectance values for miscellaneous EI oils using methylphenanthrene index 1 (MPI1) as defined by Radke et al., 1986.

Figure 14: Eugene Island-330 Whole oil gas chromatograms - GBRN oils collected from pathfinder A-20 well

Figure 15: Eugene Island-330 Whole oil gas chromatograms - typical oils from each reservoir

Figure 16: Eugene Island-330, oil composition, pristane/phytane (Pr/Ph) ratios, comparison GBRN Pathfinder well data to GERG oil correlation study. Data for other oils from other wells resampled from A platform in Dec, 1993, are also shown.

Figure 17: Eugene Island-330, oil composition, odd/even n-alkane ratios, comparison GBRN Pathfinder well data to GERG oil correlation study. Data for other oils from other wells resampled from A platform in Dec, 1993, are also shown.

Figure 18: Eugene Island-330, wet gas to oil ratio, (nC3+nC4)/nC17, comparison GBRN Pathfinder well data to GERG oil correlation study. Data for other oils from other wells resampled from A platform in Dec, 1993, are also shown.

Figure 19: Eugene Island-330, nC9/nC19 (representative of gasoline/oil), comparison GBRN Pathfinder well data to GERG oil correlation study. Data for other oils from other wells resampled from A platform in Dec, 1993, are also shown.

Figure 20: Eugene Island, C7 hydrocarbon ratios. Position of newly collected GBRN samples and new resamplings of A platform (December, 1993) are also superimposed.

Figure 21: Comparison of gasoline range hydrocarbons, EI-330, A-14A well, oil from OI-1-2 interval, samples from: a) 1984, b)1988, and c) 1994.

Figure 22: Pathfinder well, methane and ethane $\delta^{13}C$ values, from Dr Martin Schoell, Chevron: a) $\delta^{13}C$ methane as function of depth; b) $\delta^{13}C$ methane versus ethane showing gas maturities in Pathfinder well.

Figure 23: Vitrinite reflectance, sediments within Fault A versus sediments away from fault.

Figure 24: Revised estimate burial history of EI-330 (dashed line) with additional point at 14000 ft. Note that the deepest vitrinite reflectance value comes from South Marsh Island-128 and, therefore, is probably higher than the maturity at comparable depth for EI-330.

Tables

Table 1: Eutaw Shale hydrous pyrolysis results

Table 2: Smackover hydrous pyrolysis results

Table 3: Monterey Shale hydrous pyrolysis results

Table 4: Middle Valley hydrous pyrolysis results

Table 5: Eugene Island oils for which HRGCMS data for biomarkers are complete, including GBRN Pathfinder well.

Table 6: Summary oil maturation data for EI standard wells and oils collected from GBRN Pathfinder well.

Table 7: Eugene Island oils, n-alkanes and gas compositions, including those for GBRN Pathfinder well. All intervals sampled or resampled in December, 1994

Table 8: Summary EI oils, n-alkanes and gas compositions for GBRN Pathfinder well other intervals in other wells sampled or resampled in December, 1993.

Table 9: Reproducibility of C7 hydrocarbon ratios

Table 10: Number and types of samples available for GBRN organic geochemical work at Woods Hole and elsewhere and schedule of proposed analyses.

Table 11: Eugene Island, carboxylic acids, reservoir brines

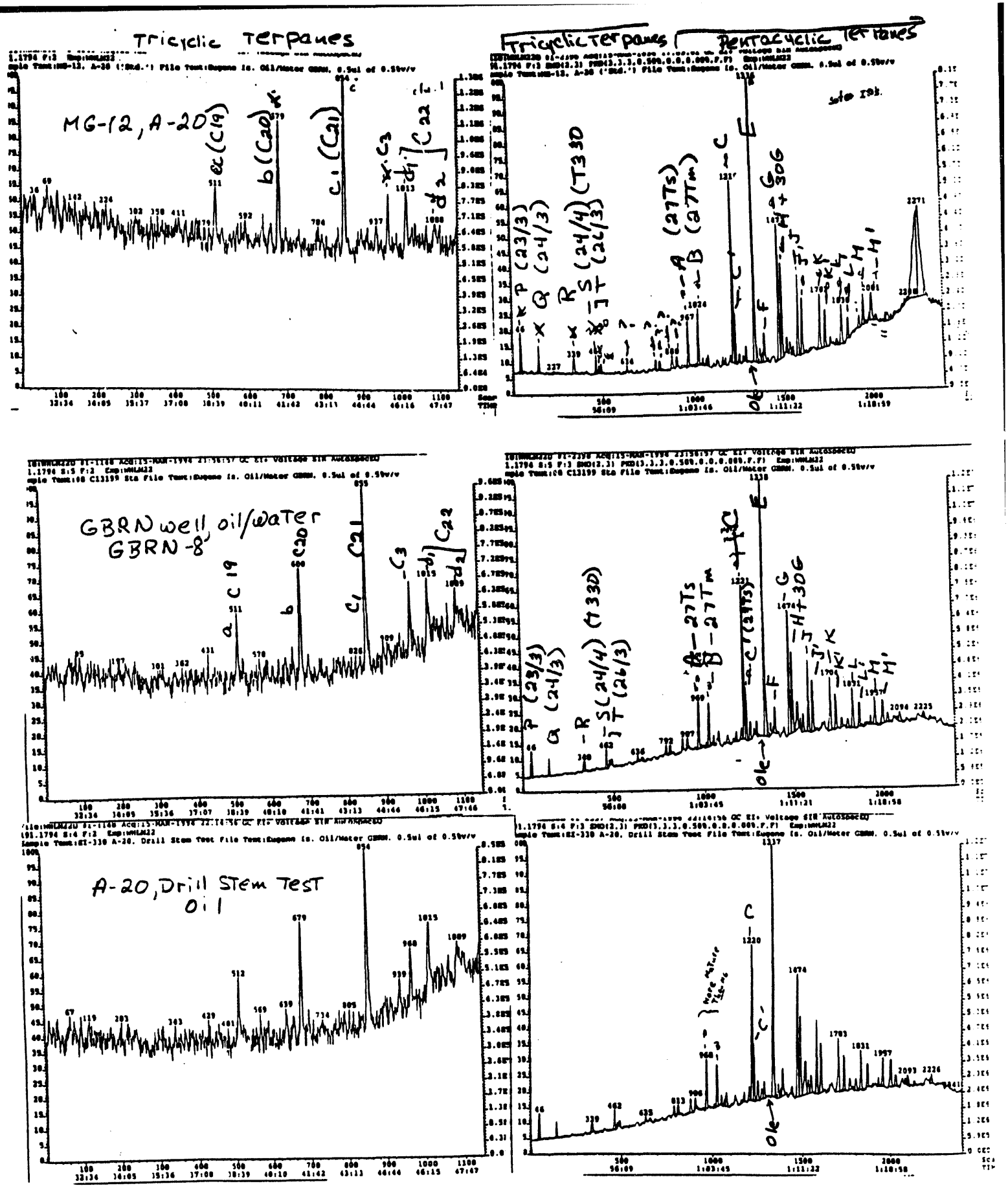

Figure 1: Comparison of biomarkers, tri- and pentacyclic triterpanes (m/z =191.1794) via HRGCMS: for MG-12, A-20 reference oil; a representative sample of oil-water sample collected during drilling of Pathfinder well (GBRN-8); and oil collected from flow test at bottom of pathfinder well (A-20, Drill stem test oil).

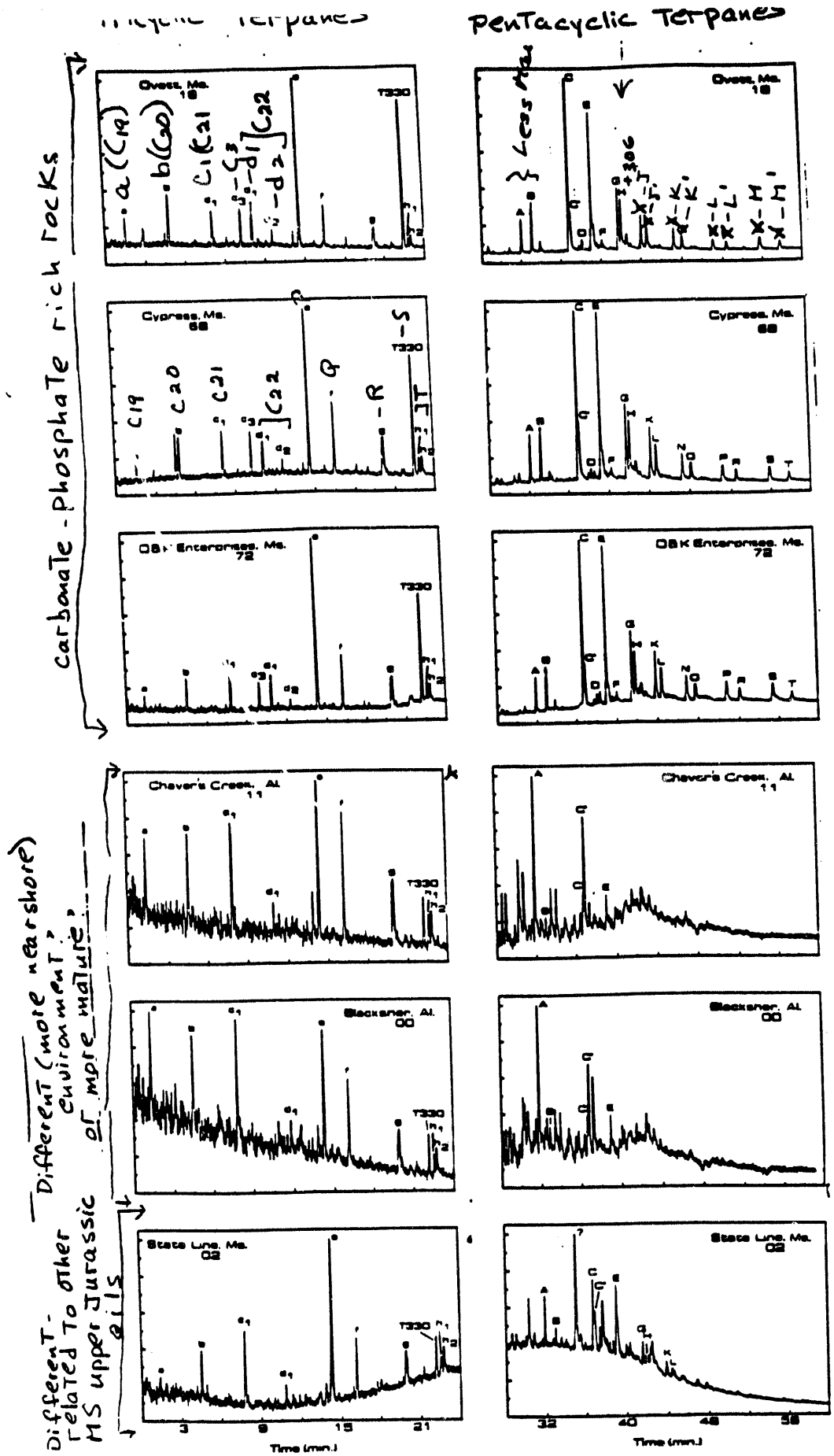

Figure 2: Reference biomarker tri- and pentacyclic triterpanes, m/z=191, Smackover oils, from Sofer, 1990.

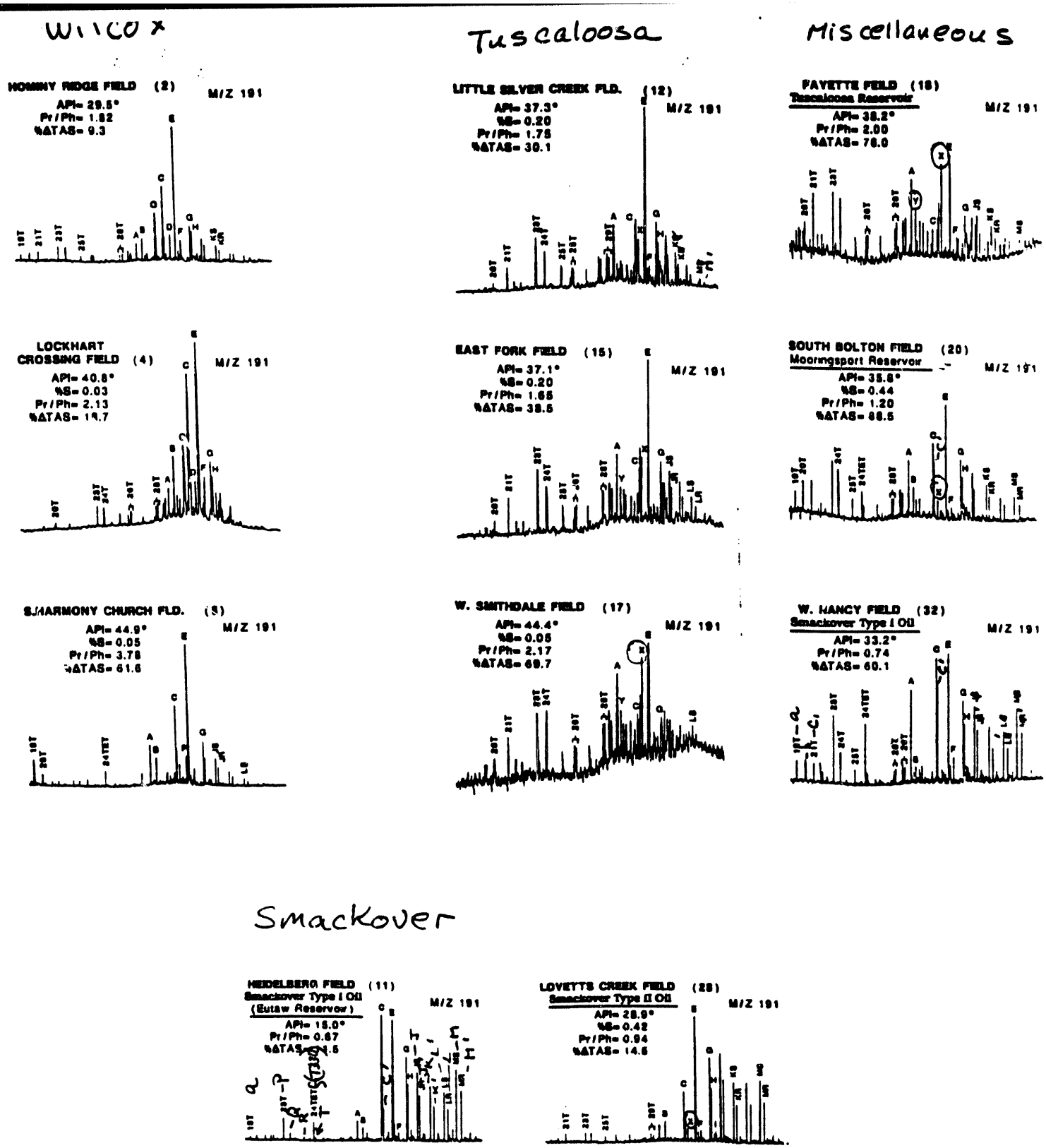

Figure 3: Reference biomarker tri- and pentacyclic triterpanes, m/z=191, comparison Wilcox, Tuscaloosa, Smackover, and other miscellaneous oils from Louisiana Gulf Coast (data from Wenger, et al., 1990.)

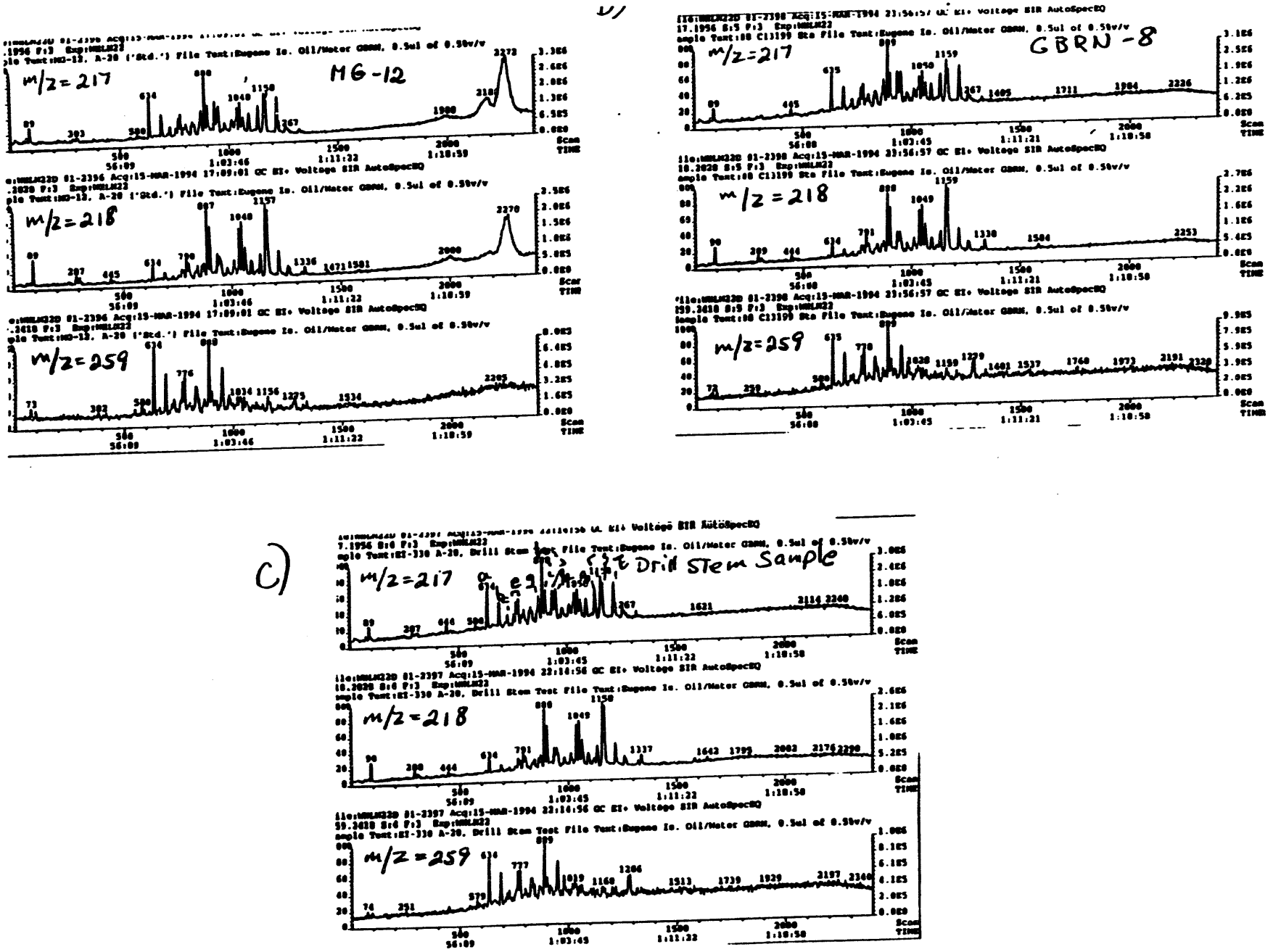

Figure 4: Biomarkers, Sterane HRGCMS patterns, m/z = 217; 218; and 259, EI oils: a) Standard oil from MG-12 reservoir; b) representative oil from drilling of pathfinder well, GBRN-8. and c) oil collected from flow test at bottom of pathfinder well (A-20, drill stem test oil).

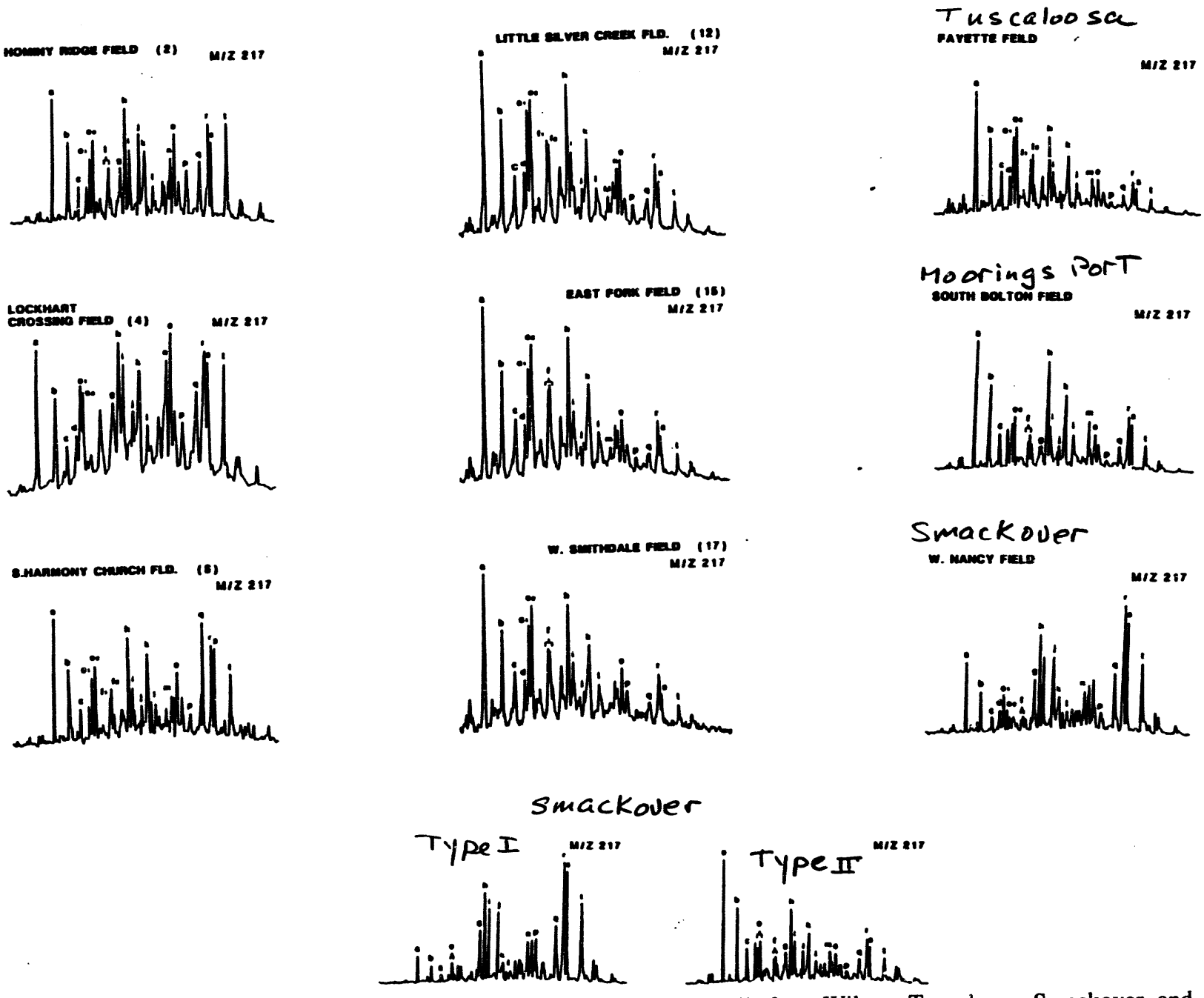

Figure 5: Reference biomarkers, steranes, m/z = 217, oils from Wilcox, Tuscaloosa, Smackover, and miscellaneous Gulf Coast reservoirs.

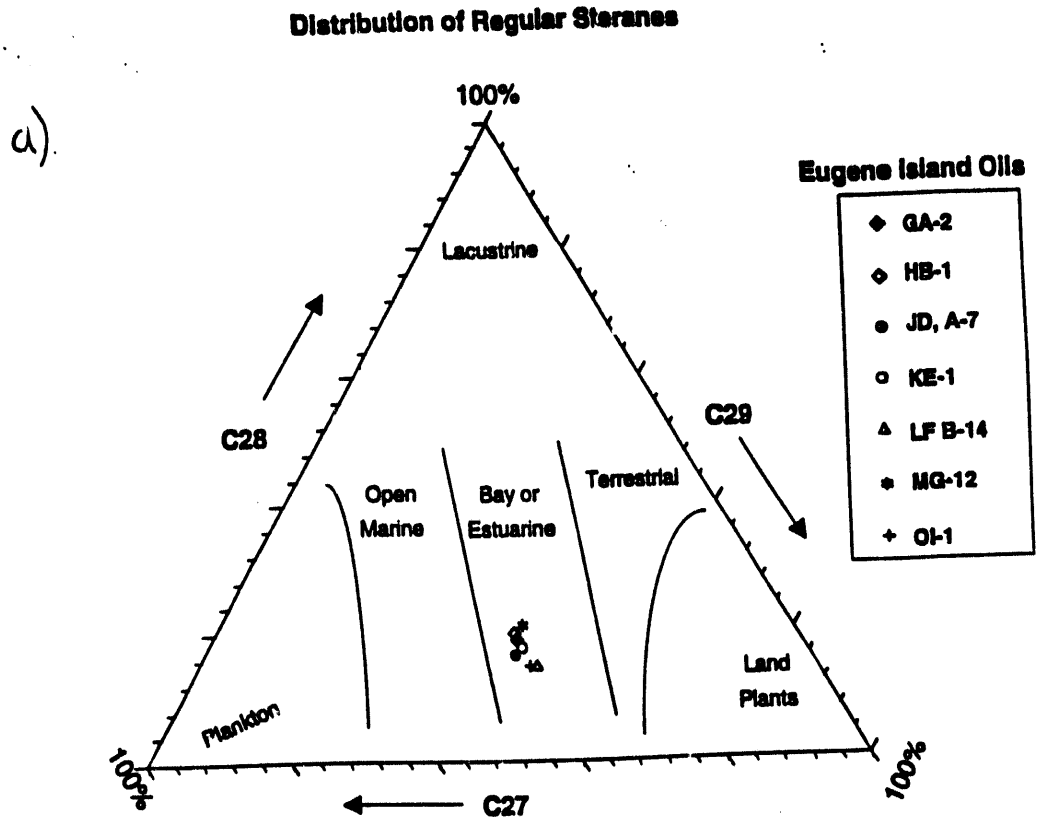

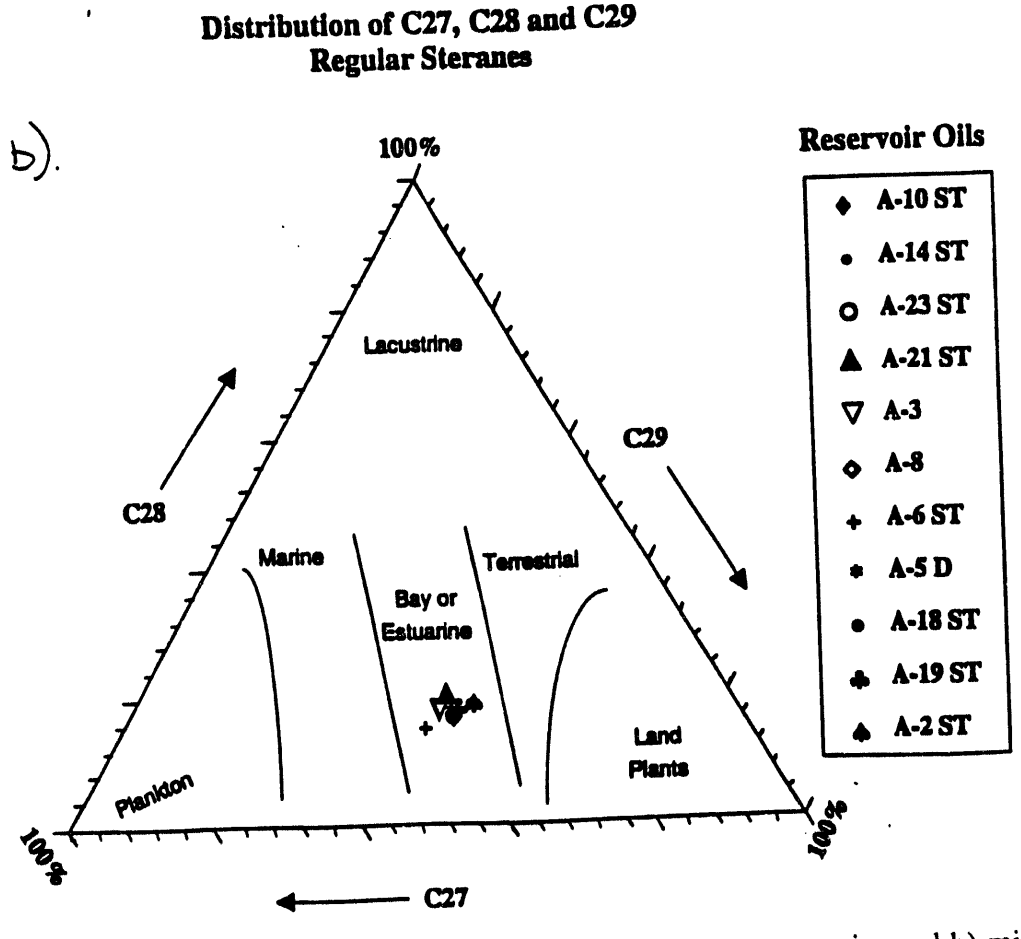

Figure 6: Distribution of regular steranes in EI oils: a) standard reservoirs and b) miscellaneous other reservoirs, shown in Table 5.

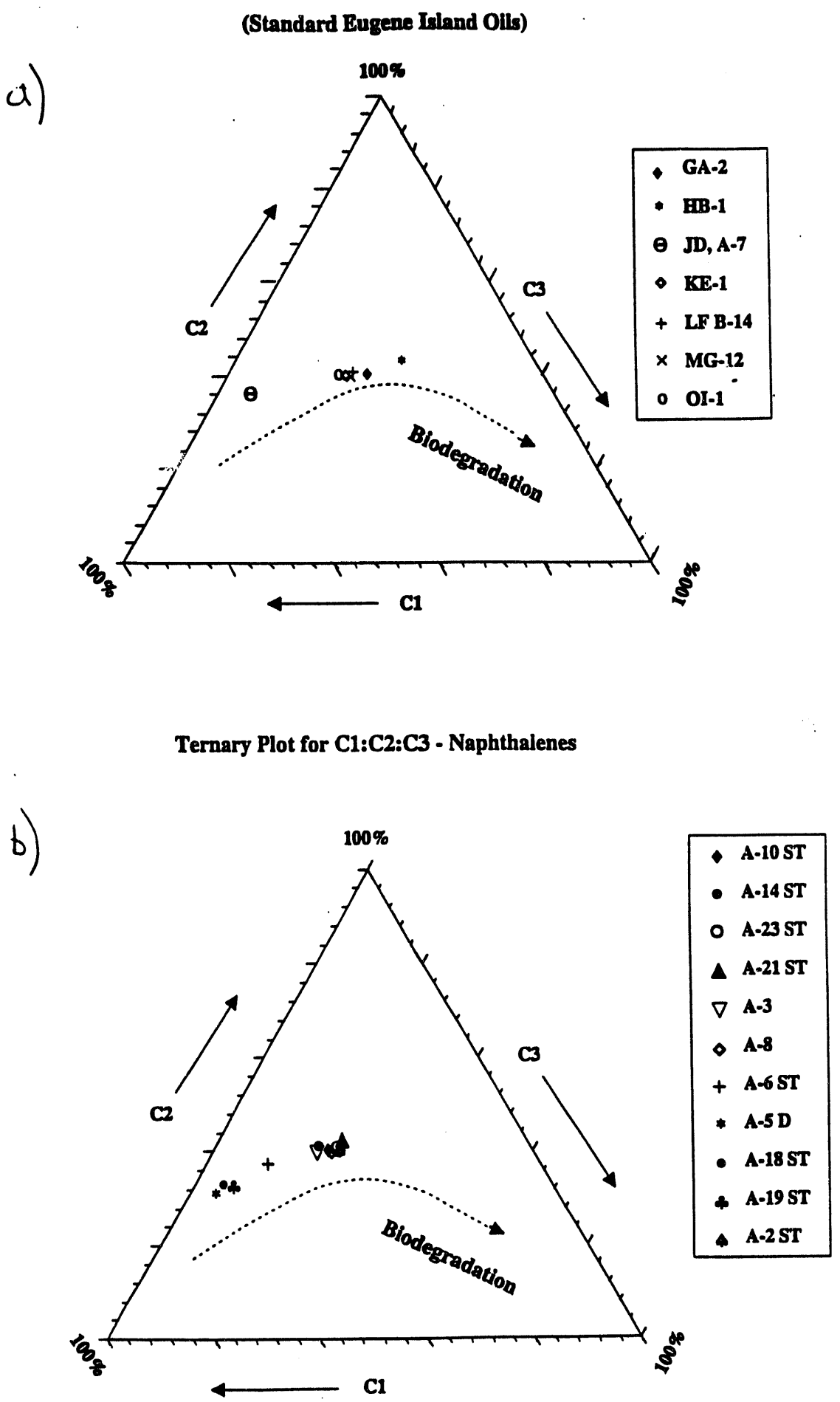

Figure 7: Distribution of C1:C2:C3 naphthalenes: a) standard EI oils and b) oils from miscellaneous other reservoirs.

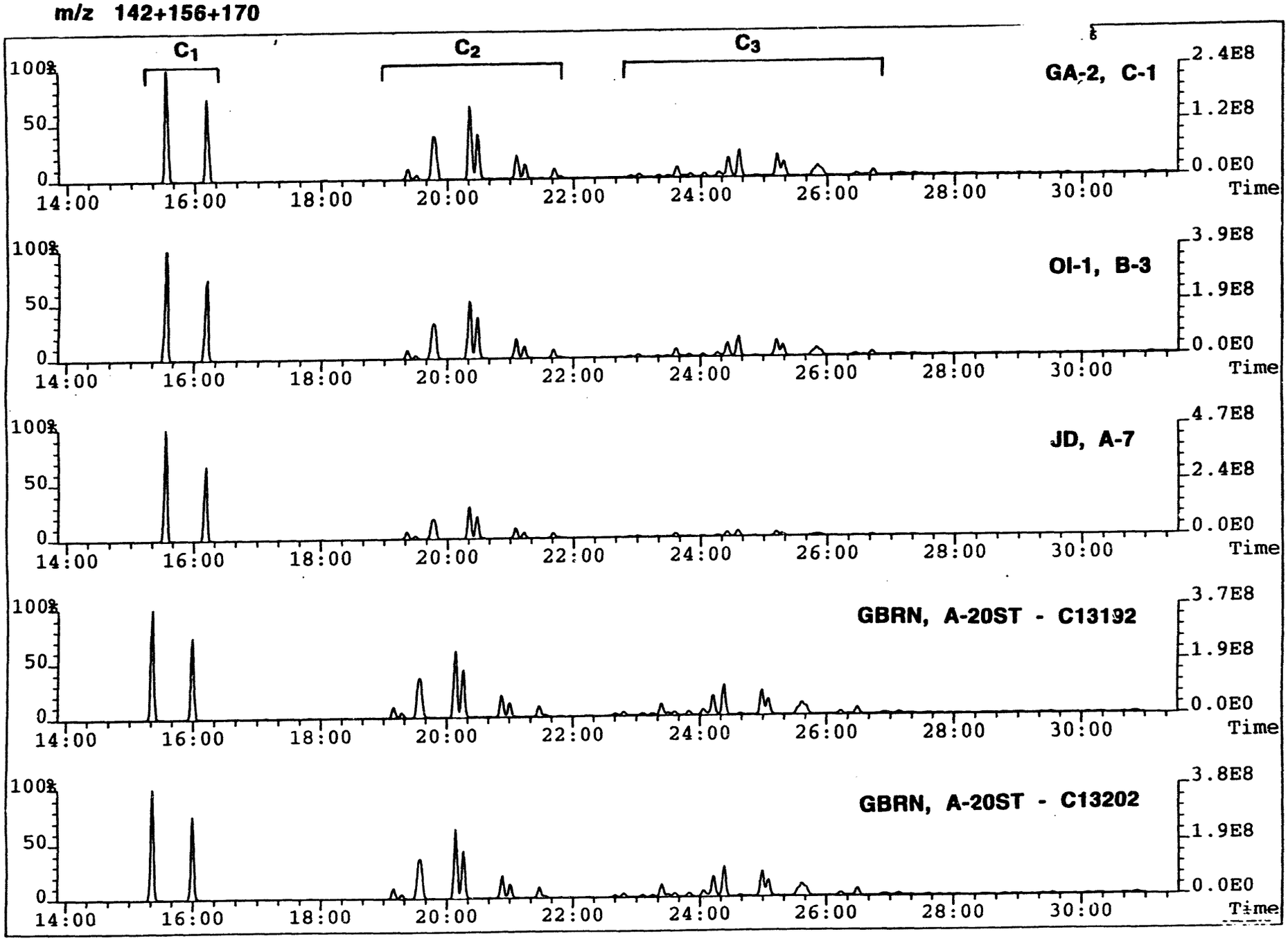

Figure 8: Comparison, HRGCMS, alkyl naphthalenes (m/z = 142 + 156 +170) from EI standard oils, GA, OI, and JD reservoirs in comparison with representative samples collected from the Pathfinder well, GBRN-8 and drill stem test oil as described in Table 5.

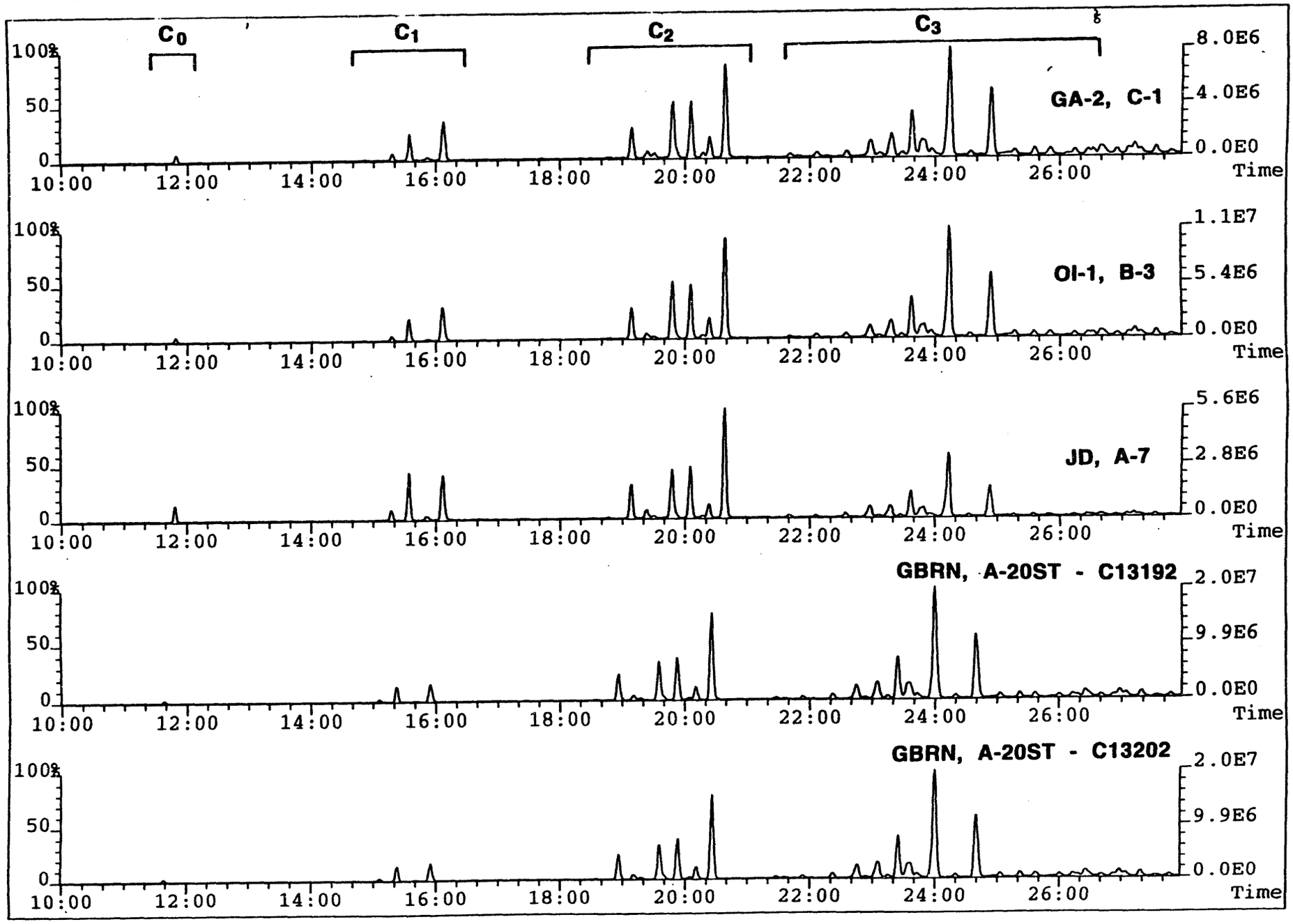

Figure 9:Comparison, HRGCMS, alkyl benzothiophenes (m/z = 134 + 148 + 162 + 176) from EI standard oils, GA, OI, and JD reservoirs in comparison with representative samples collected from the Pathfinder well, GBRN-8 and drill stem test oil as described in Table 5.

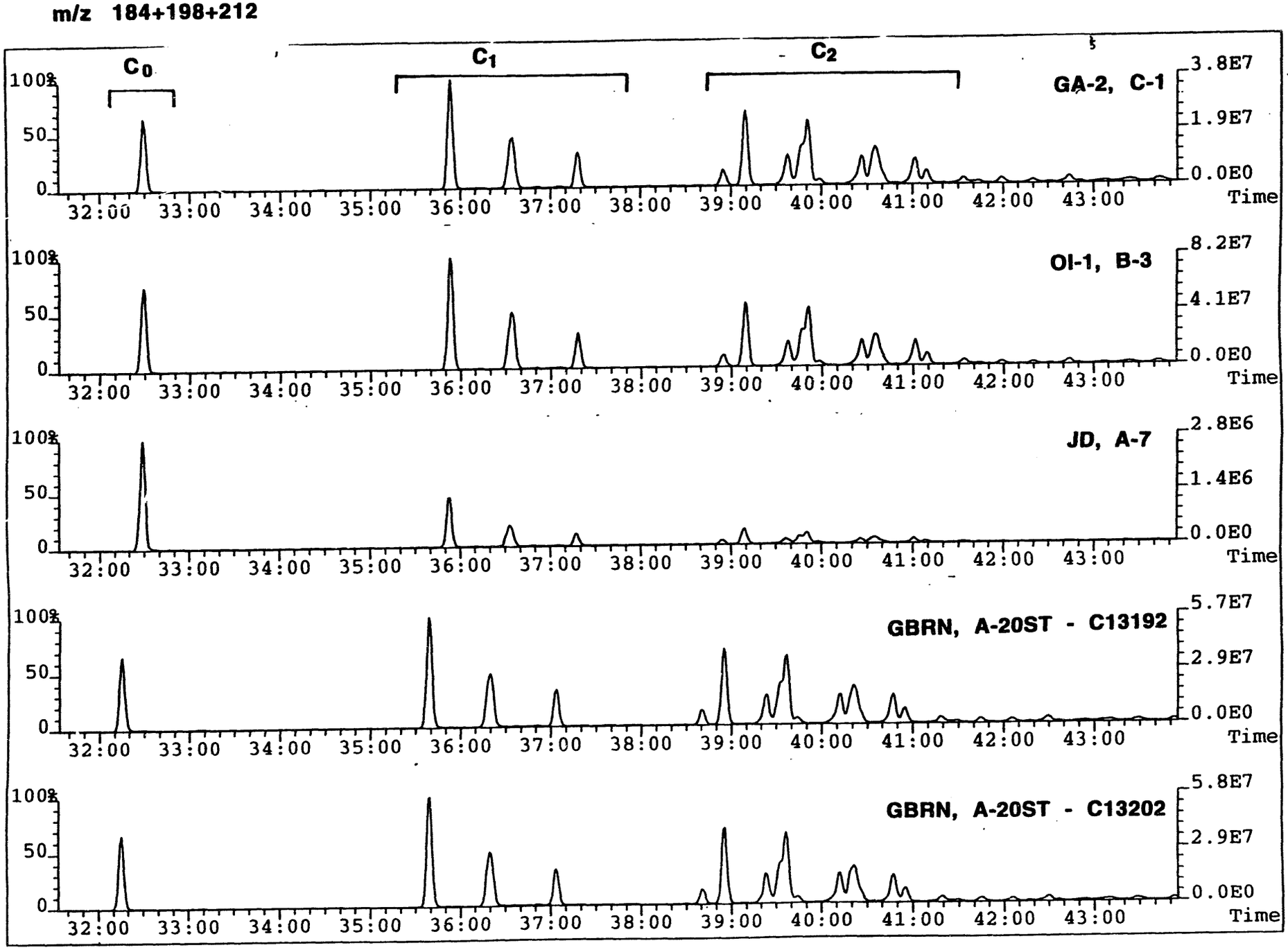

Figure 10: Comparison, HRGCMS, alkyl dibenzothiophenes (m/z = 184 + 198 + 212) from EI standard oils, GA, OI, and JD reservoirs in comparison with representative samples collected from the Pathfinder well, GBRN-8 and drill stem test oil as described in Table 5.

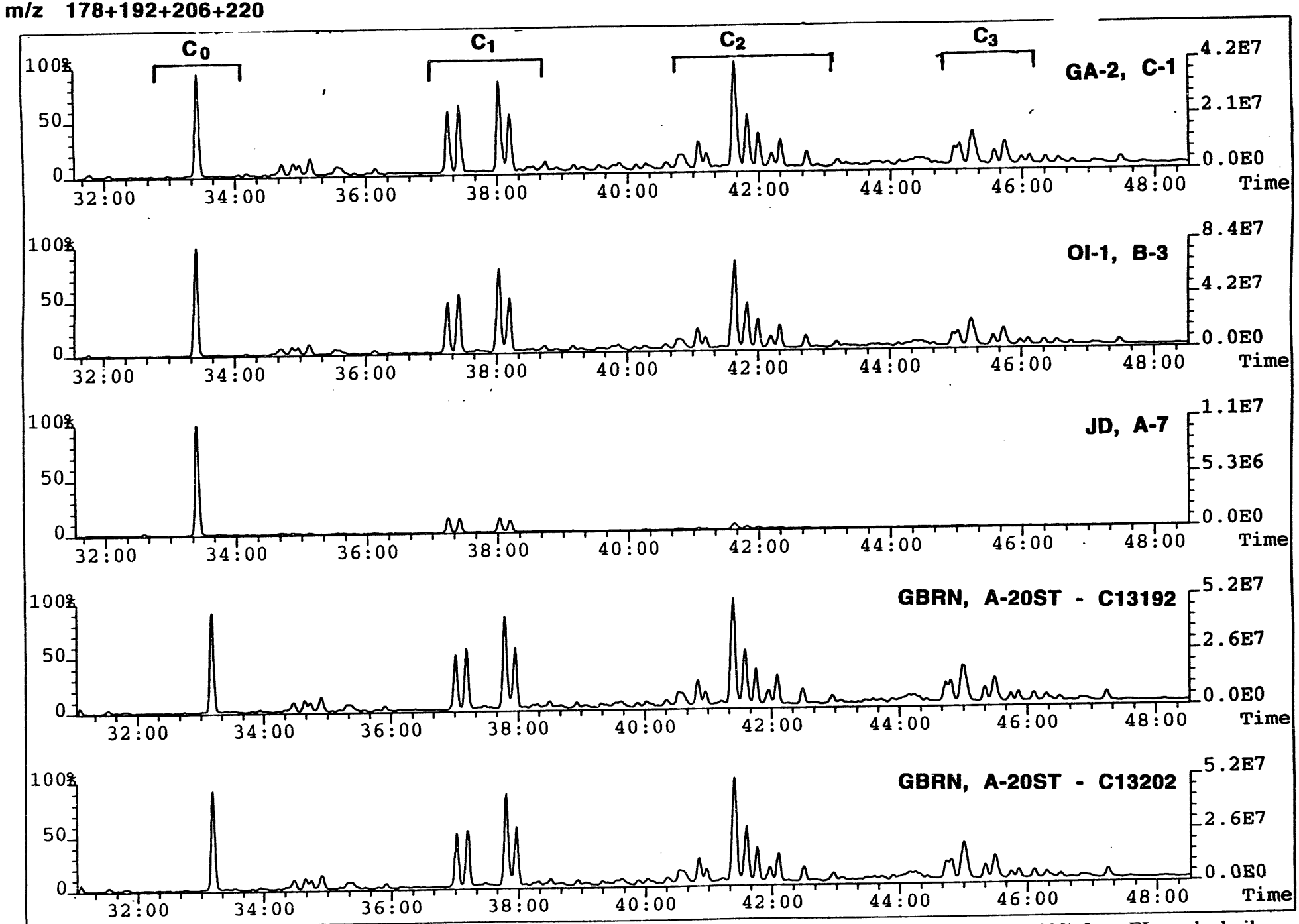

Figure 11: Comparison, HRGCMS, alkyl phenanthrenes and methylphenanthrenes (m/z = 178 + 192 + 206 + 220) from EI standard oils, GA, OI, and JD reservoirs in comparison with representative samples collected from the Pathfinder well, GBRN-8 and drill stem test oil as described in Table 5

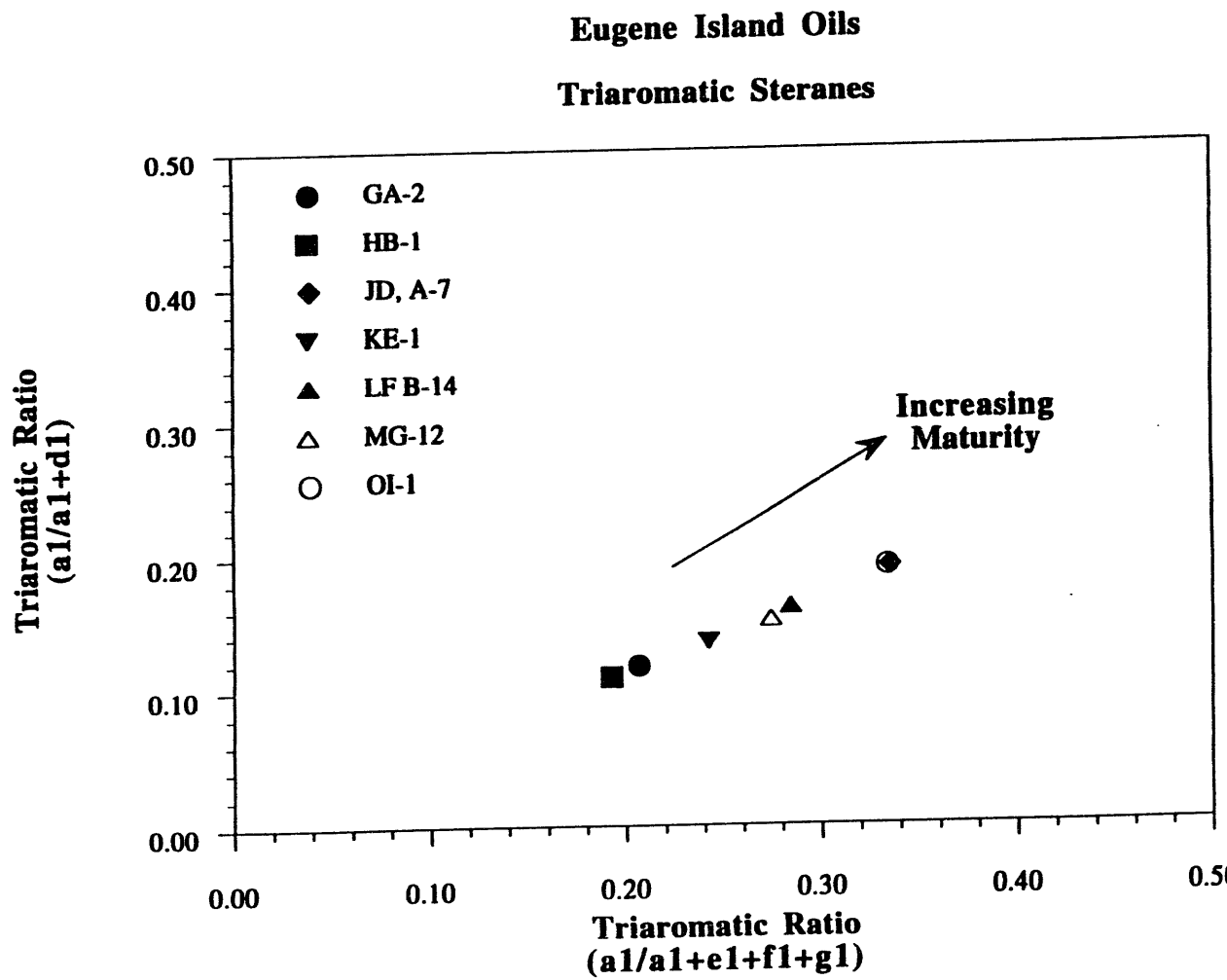

Figure 12: Eugene Island oils, standard reservoirs, relative maturities via triaromatic ratios.

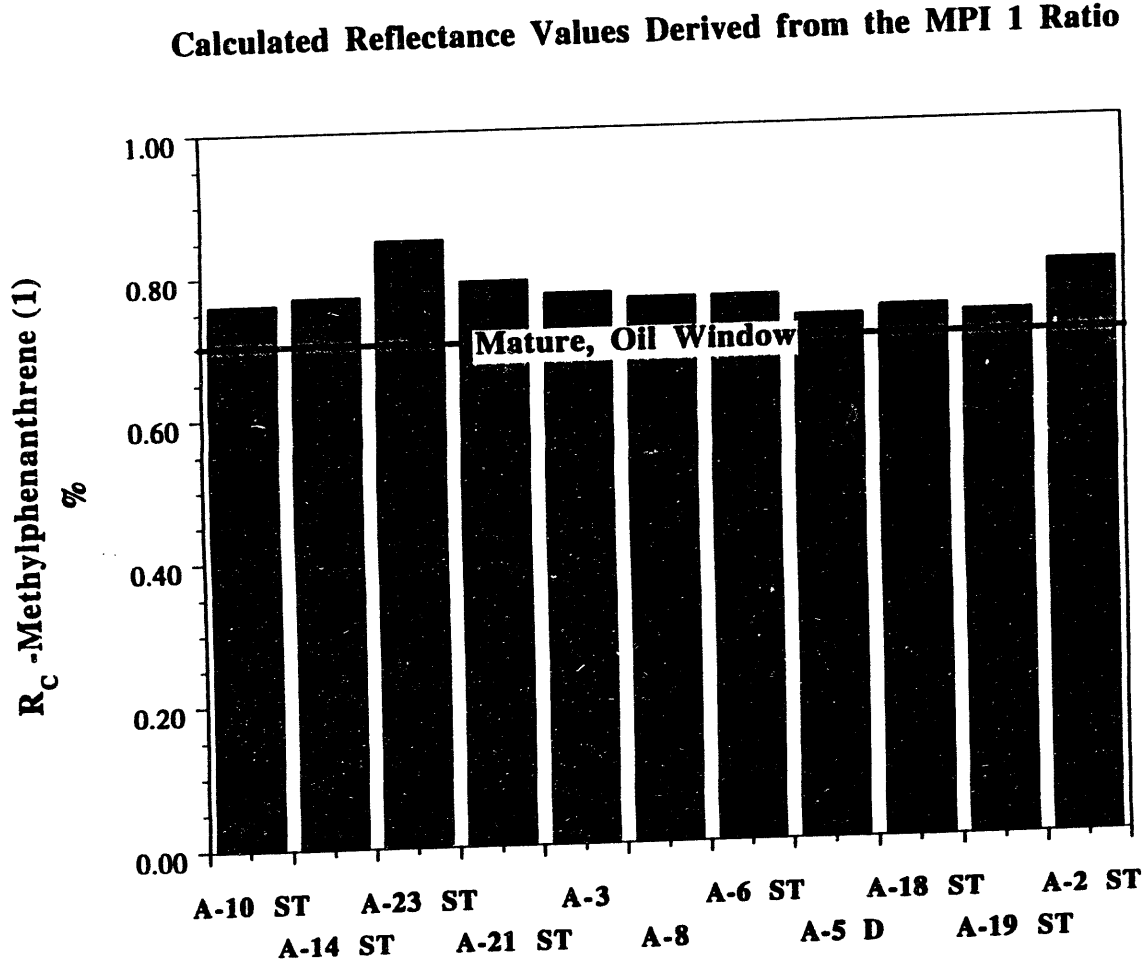

Figure 13: Calculated reflectance values for miscellaneous EI oils using methylphenanthrene index 1 (MPI1) as defined by Radke et al., 1986.

Figure 14: Eugene Island-330 Whole oil gas chromatograms - GBRN oils collected from pathfinder A-20 well

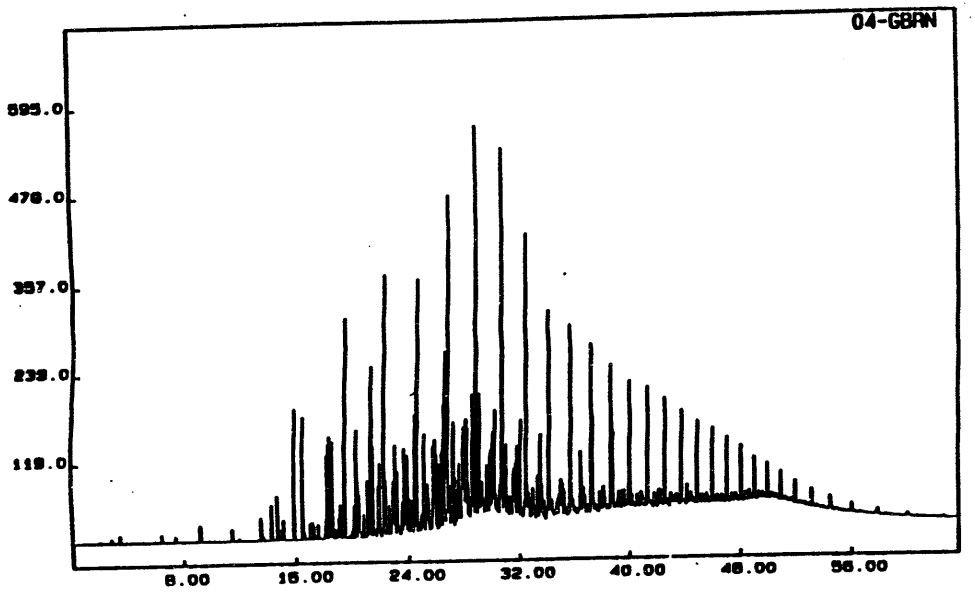

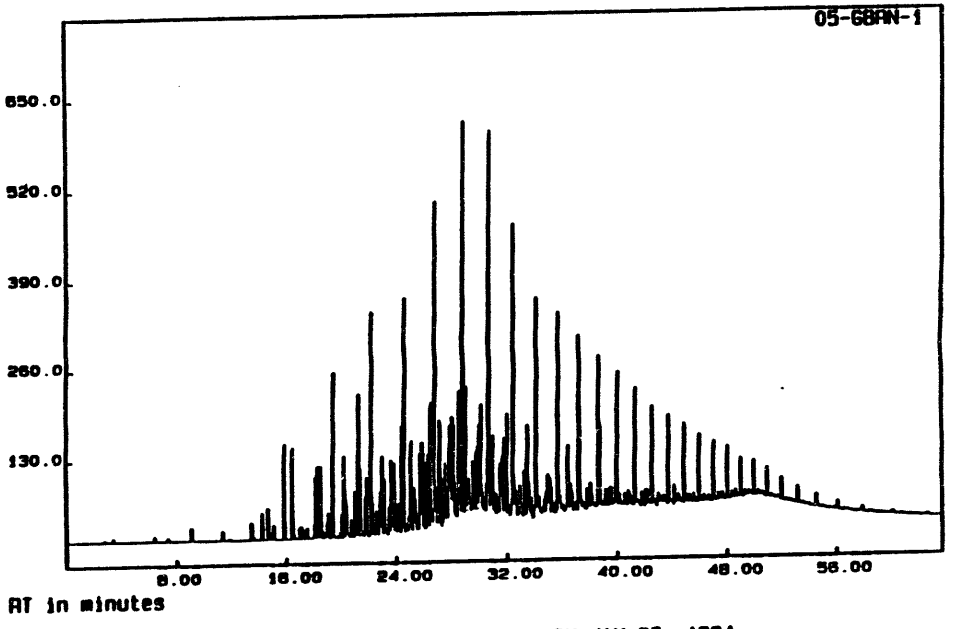

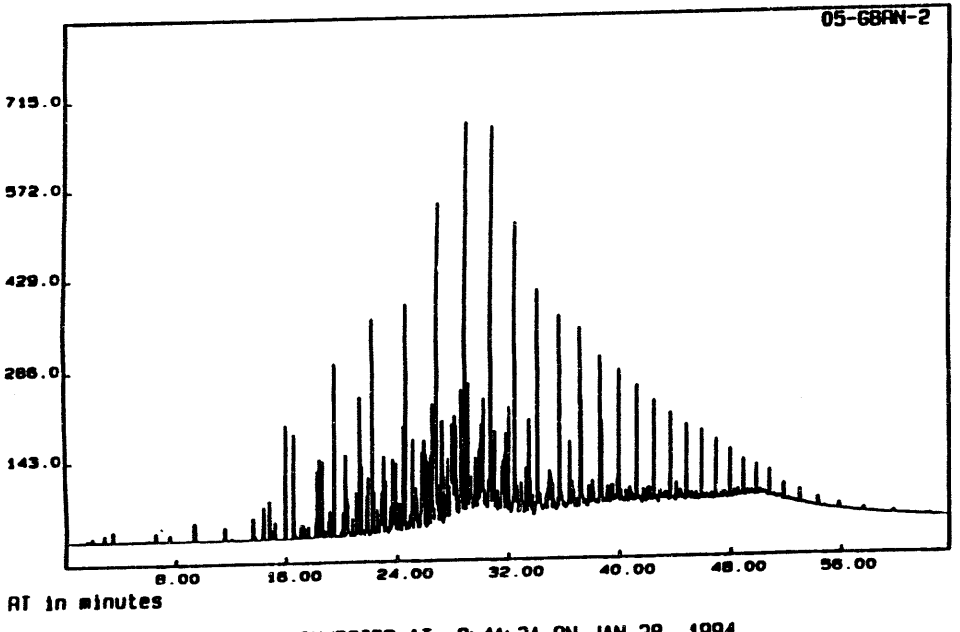

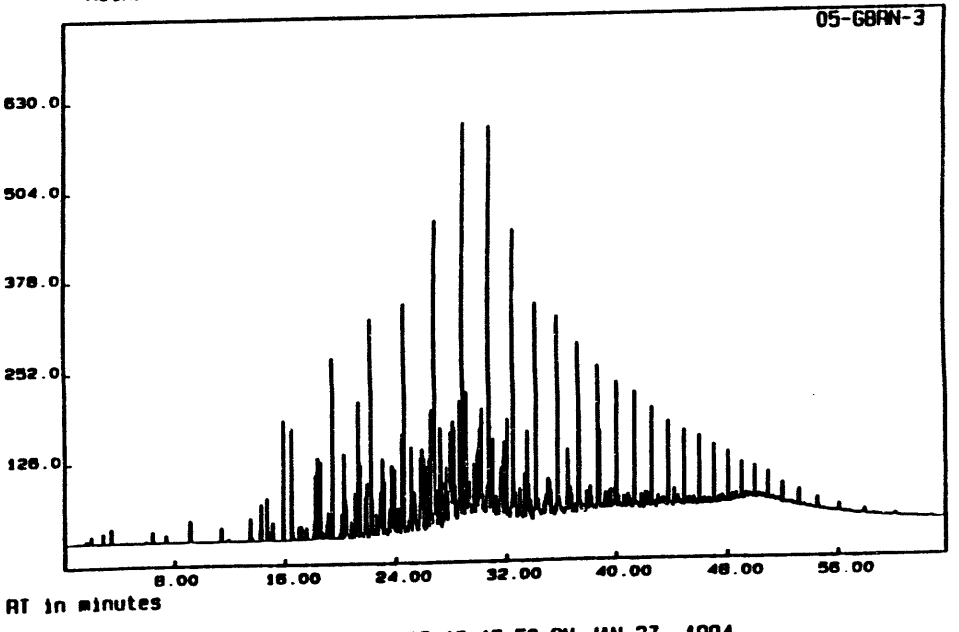

Figure 14 (Cont.)

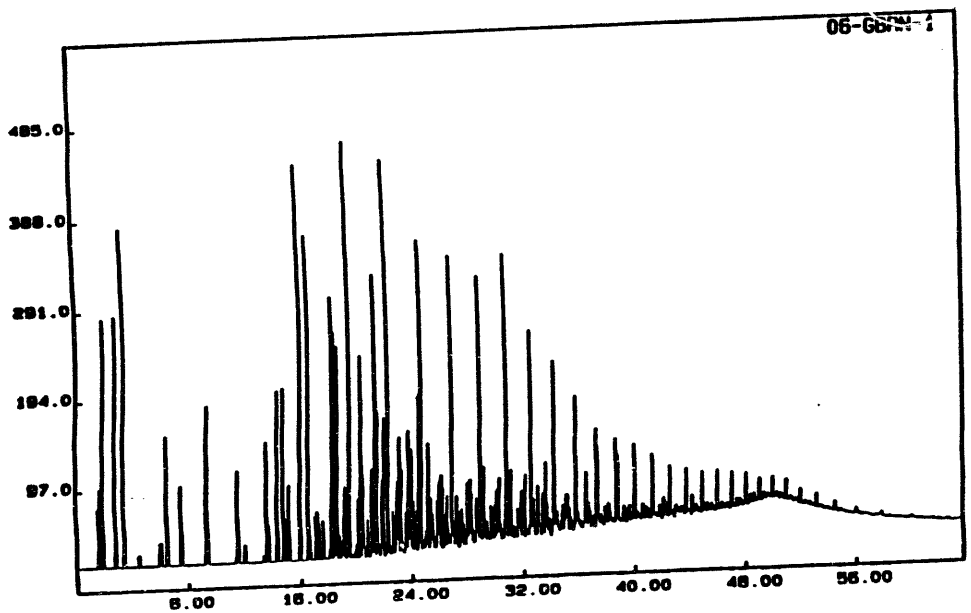

SAMPLE: 06GBRN-1 INJECTED AT 23:48:46 ON JAN 26, 1994
Meth: TOTOIL RAW: CS3192. Proc: CS3192.prc

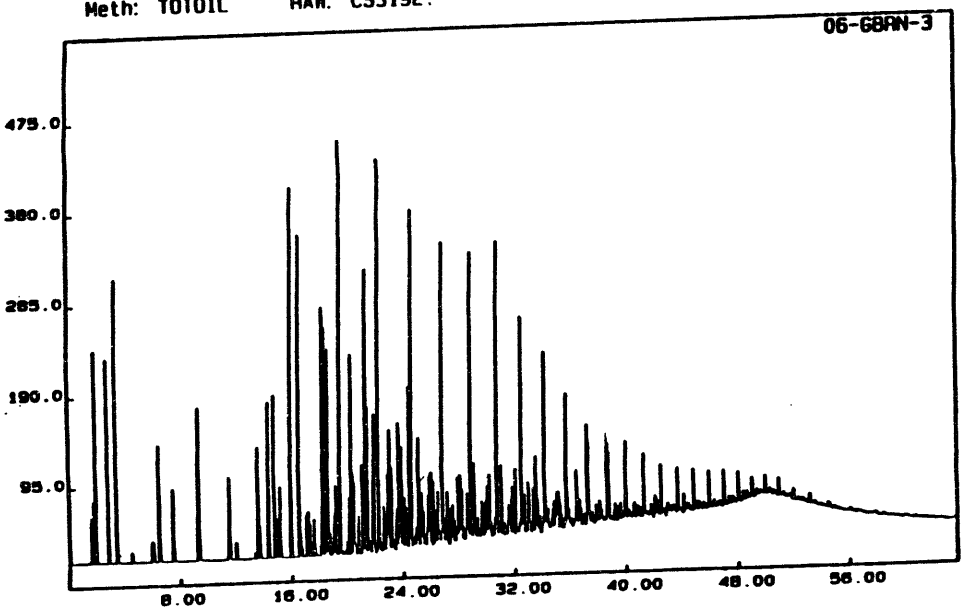

SAMPLE: 06GBRN-3 INJECTED AT 2:26:33 ON JAN 27, 1994
Meth: TOTOIL RAW: CS3194. Proc: CS3194.prc

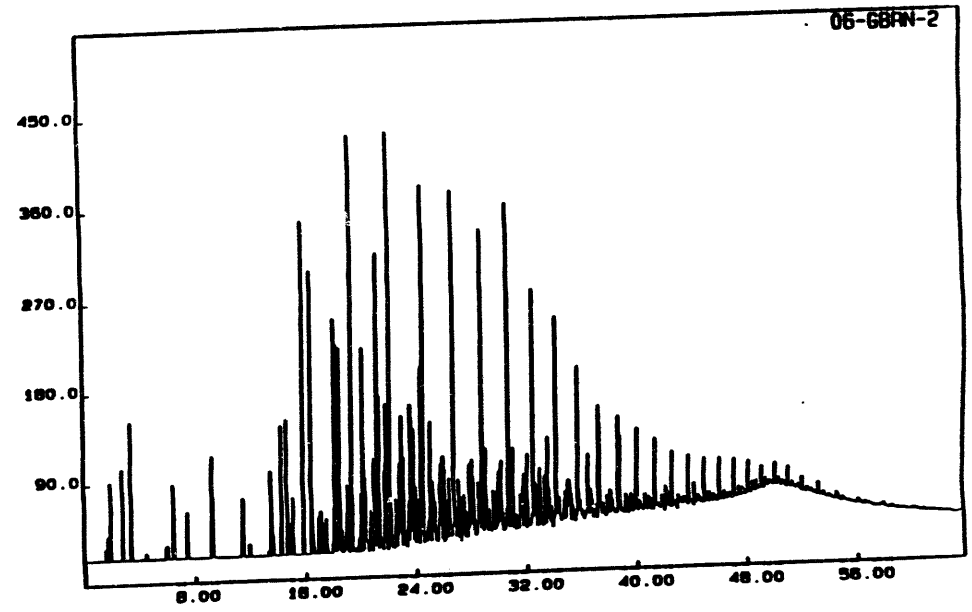

SAMPLE: 06GBRN-2 INJECTED AT 1:07:37 ON JAN 27, 1994
Meth: TOTOIL RAW: CS3193. Proc: CS3193.prc

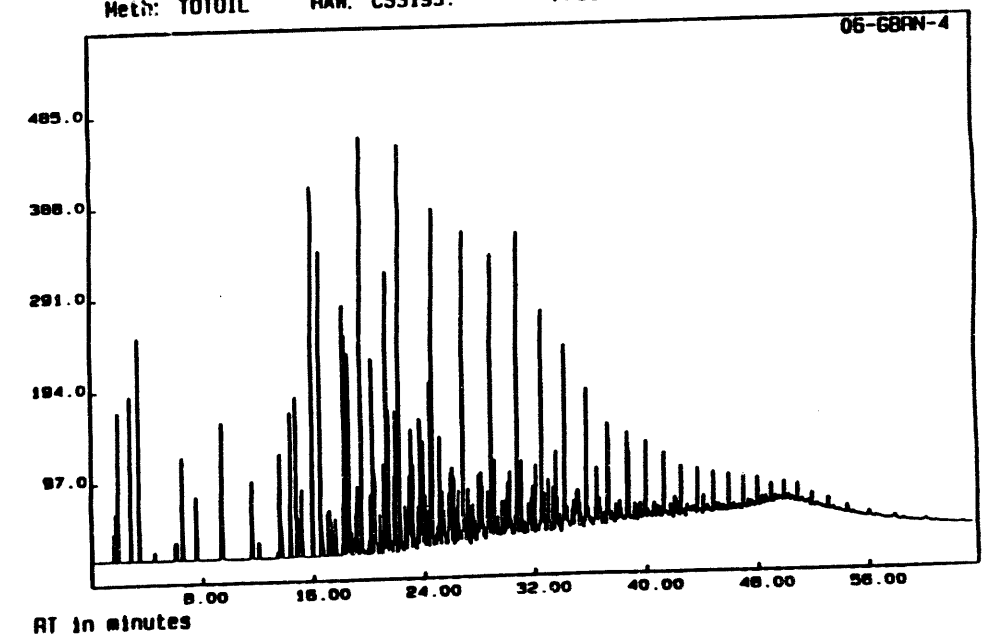

SAMPLE: 06GBRN-4 INJECTED AT 19:52:32 ON JAN 26, 1994
Meth: TOTOIL RAW: CS3195. Proc: CS3195.prc

Figure 14 (Cont.)

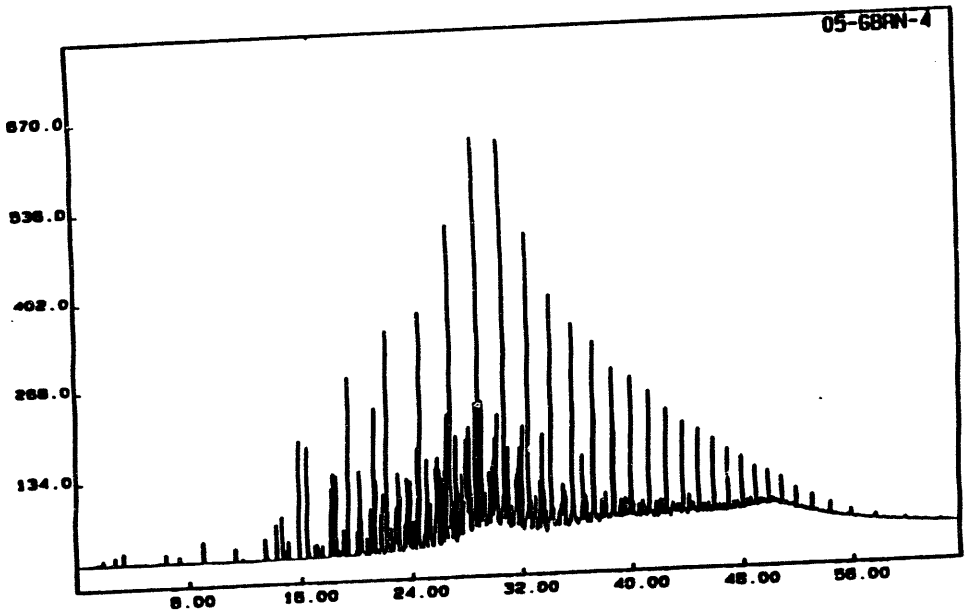

SAMPLE: 05GBRN-4 INJECTED AT 10:59:13 ON JAN 28, 1994
Meth: TOTOIL RAW: CS3188. Proc: CS3188.prc

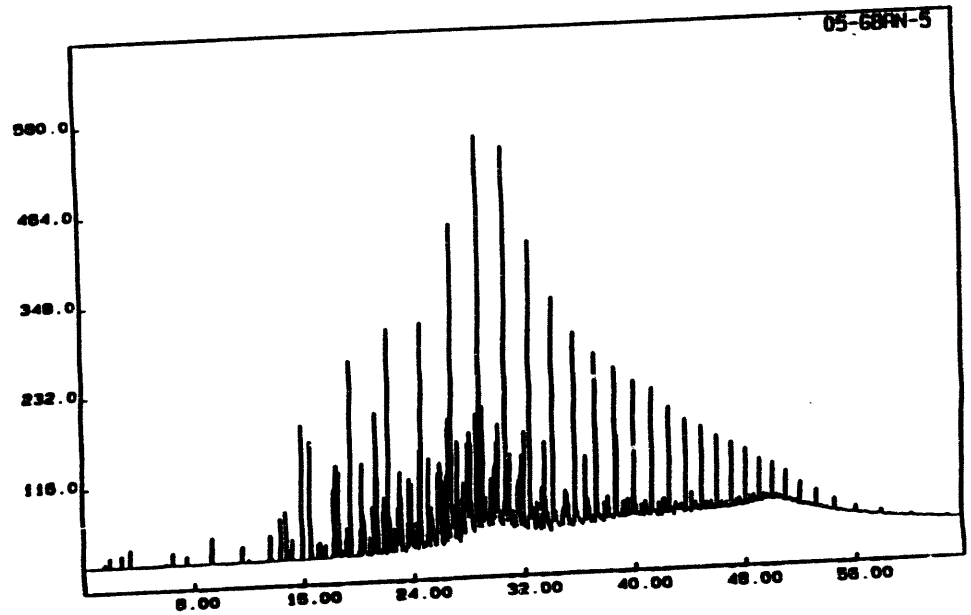

SAMPLE: 05GBRN-5 INJECTED AT 3:45:23 ON JAN 27, 1994
Meth: TOTOIL RAW: CS3189. Proc: CS3189.prc

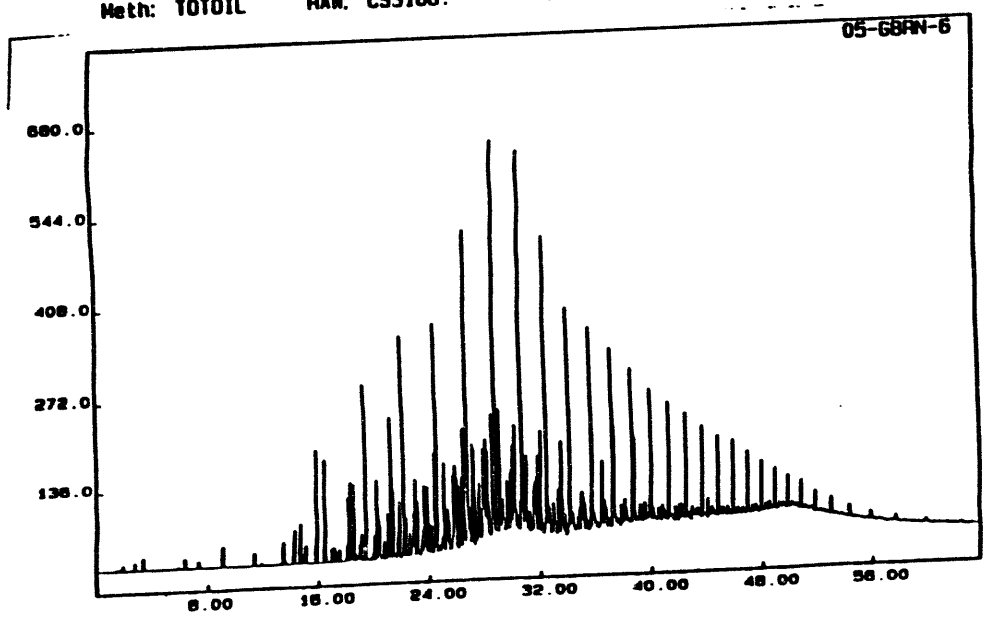

SAMPLE: 05GBRN-6 INJECTED AT 17:35:14 ON JAN 27, 1994
Meth: TOTOIL RAW: CS3190. Proc: CS3190.prc

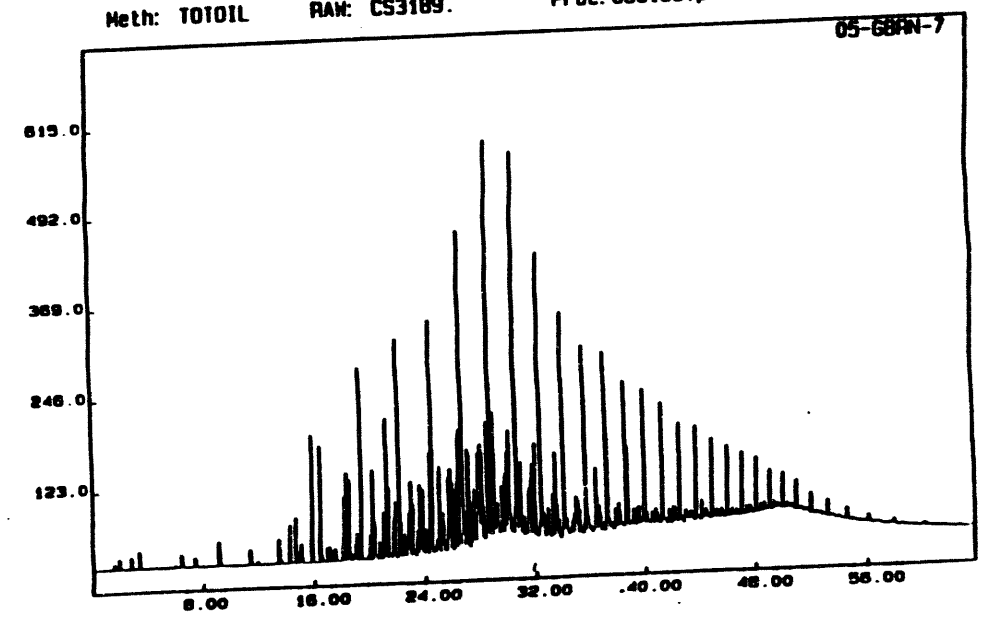

SAMPLE: 05GBRN-7 INJECTED AT 22:30:03 ON JAN 26, 1994
Meth: TOTOIL RAW: CS3191. Proc: CS3191.prc

Figure 14 (Cont.)

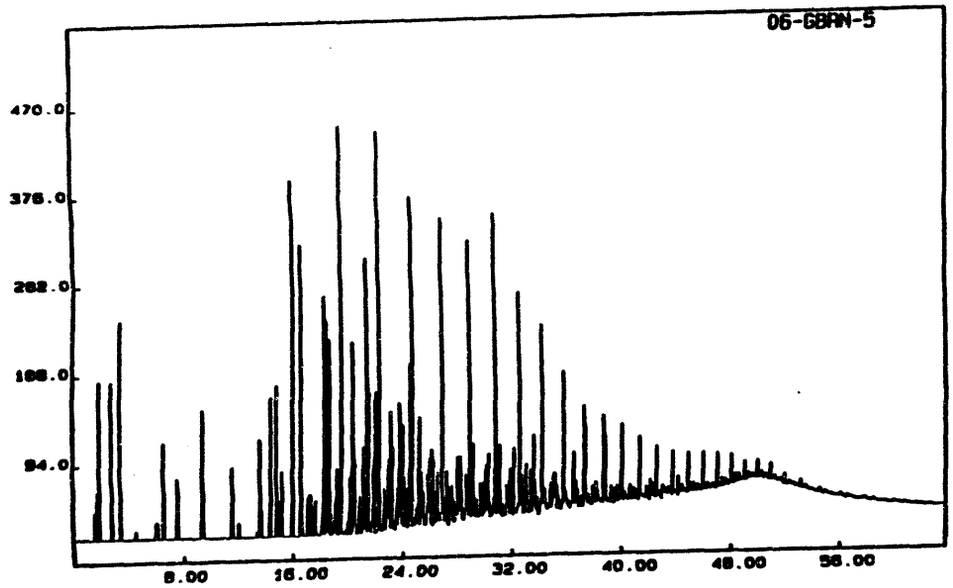

SAMPLE: 06GBRN-5 INJECTED AT 21:11:20 ON JAN 26, 1994
Meth: TOTOIL RAW: CS3196. Proc: CS3196.prc

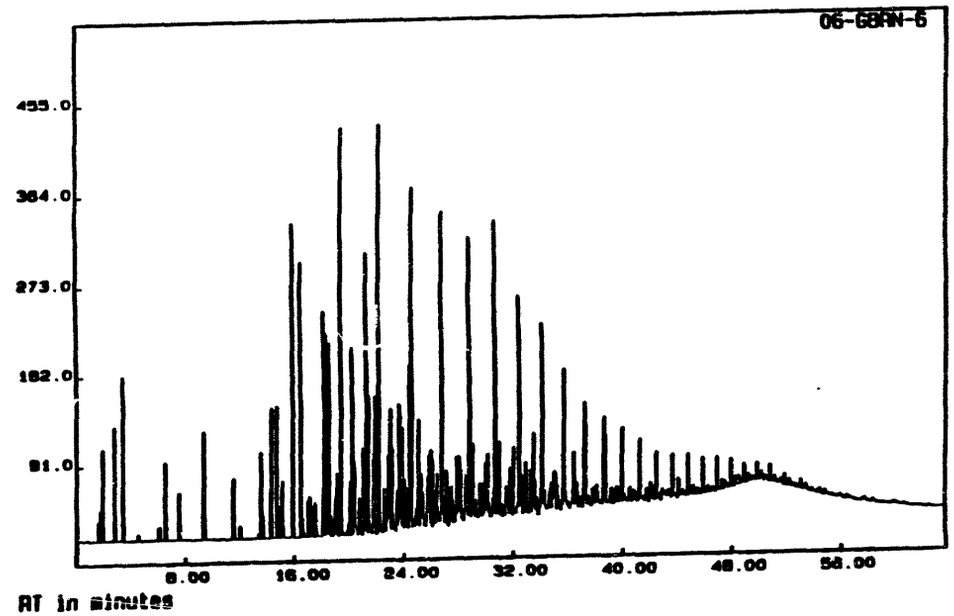

SAMPLE: 06-GBRN-6 INJECTED AT 15:17:30 ON JAN 25, 1994
Meth: TOTOIL RAW: CS3197. Proc: CS3197.prc

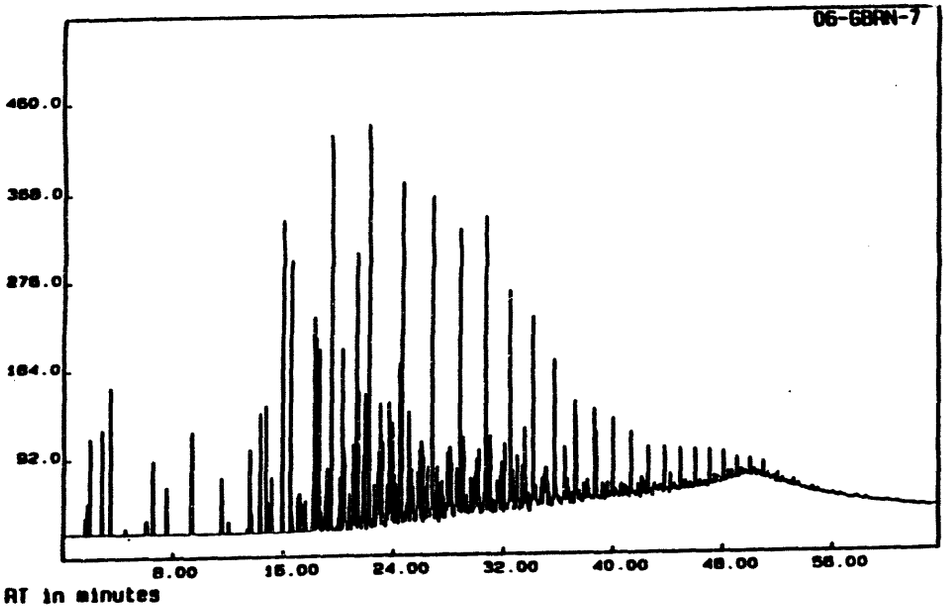

SAMPLE: 06-GBRN-7 INJECTED AT 16:35:48 ON JAN 25, 1994
Meth: TOTOIL RAW: CS3198. Proc: CS3198.prc

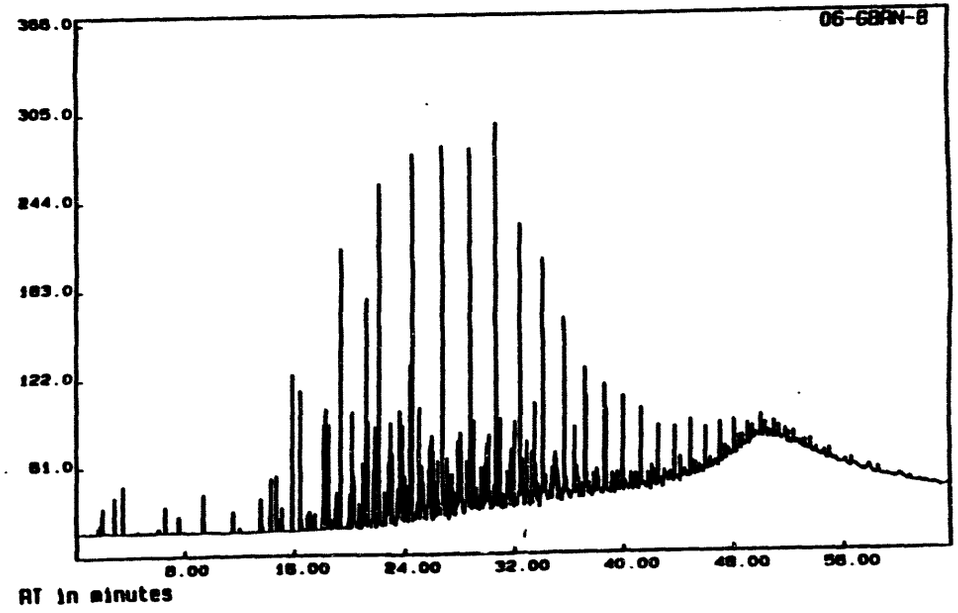

SAMPLE: 06-GBRN-8 INJECTED AT 17:54:14 ON JAN 25, 1994
Meth: TOTOIL RAW: CS3199. Proc: CS3199.prc

Figure 14 (Cont.)

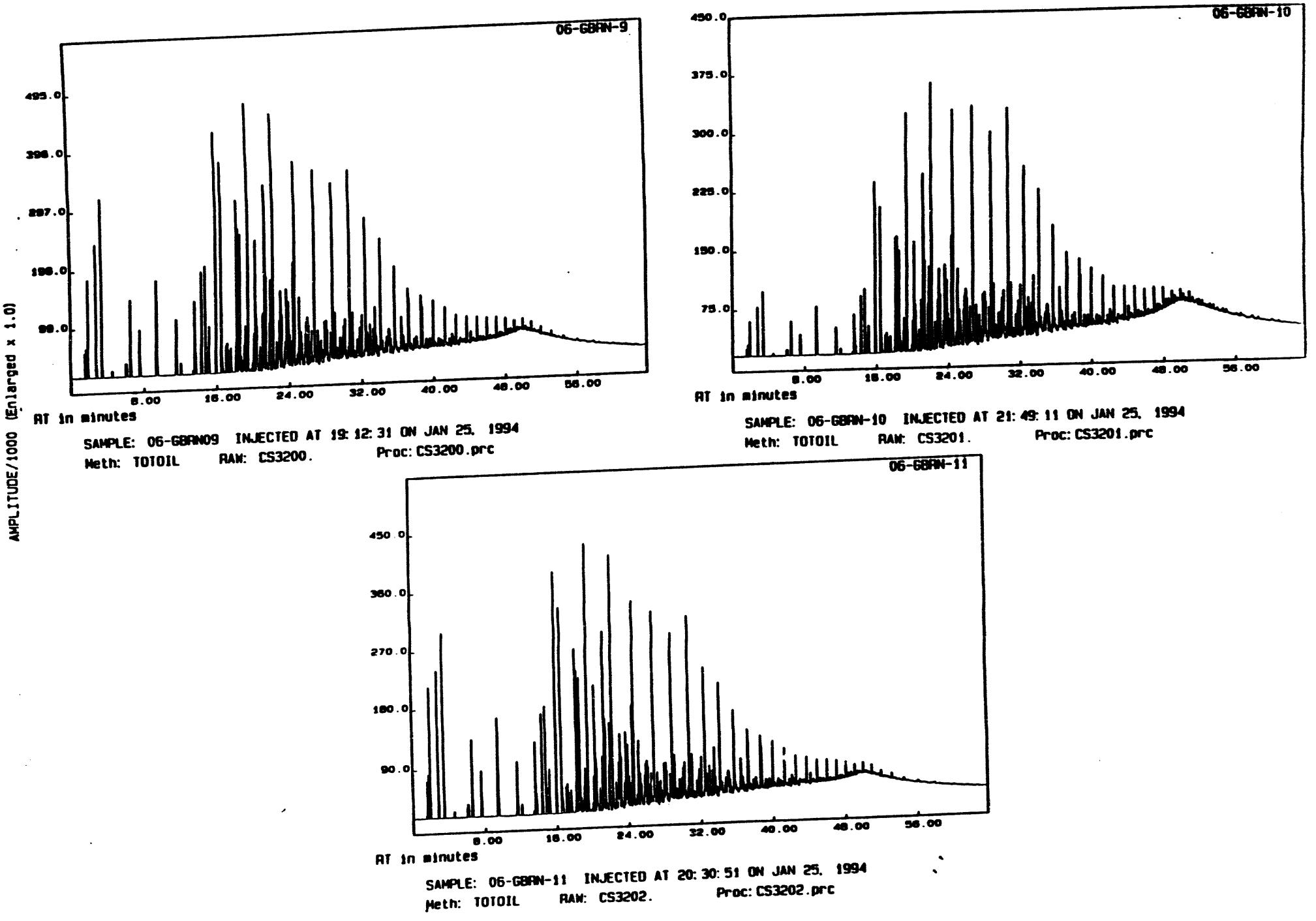

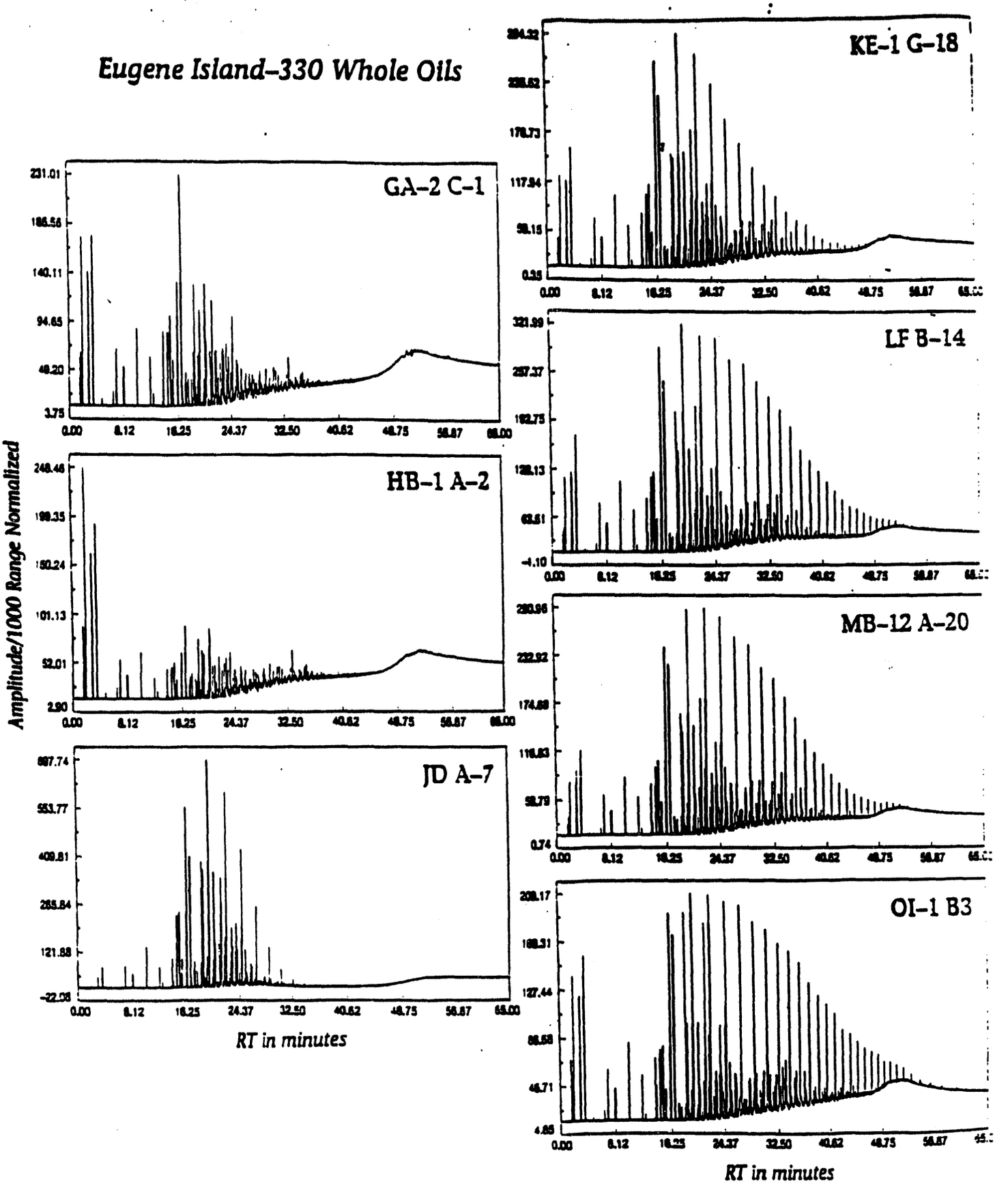

Figure 15: Eugene Island-330 Whole oil gas chromatograms - typical oils from each reservoir

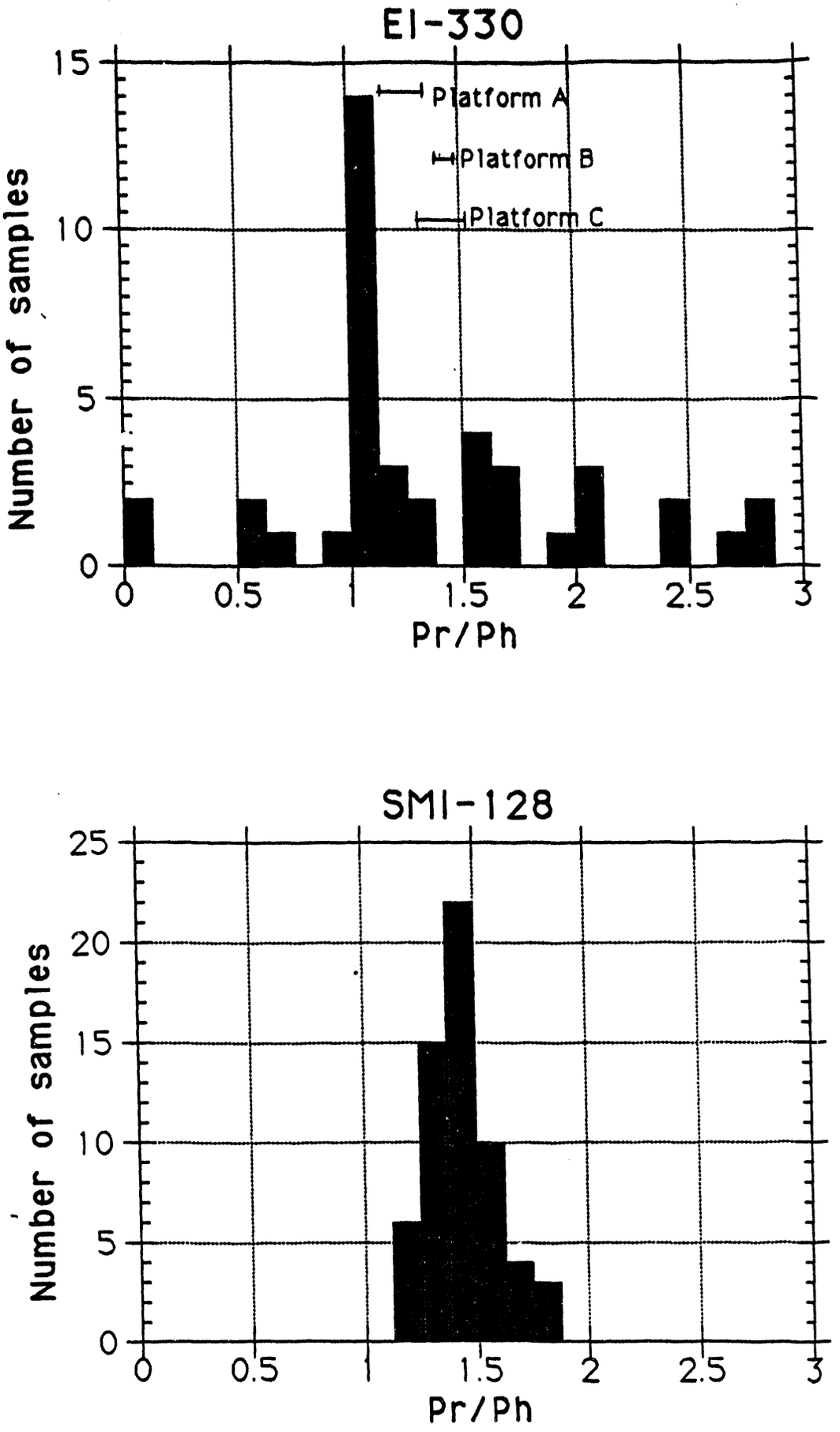

Figure 16: Eugene Island-330, oil composition, pristane/phytane (Pr/Ph) ratios, comparison GBRN Pathfinder well data to GERG oil correlation study. Data for other oils from other wells resampled from A platform in Dec, 1993, are also shown.

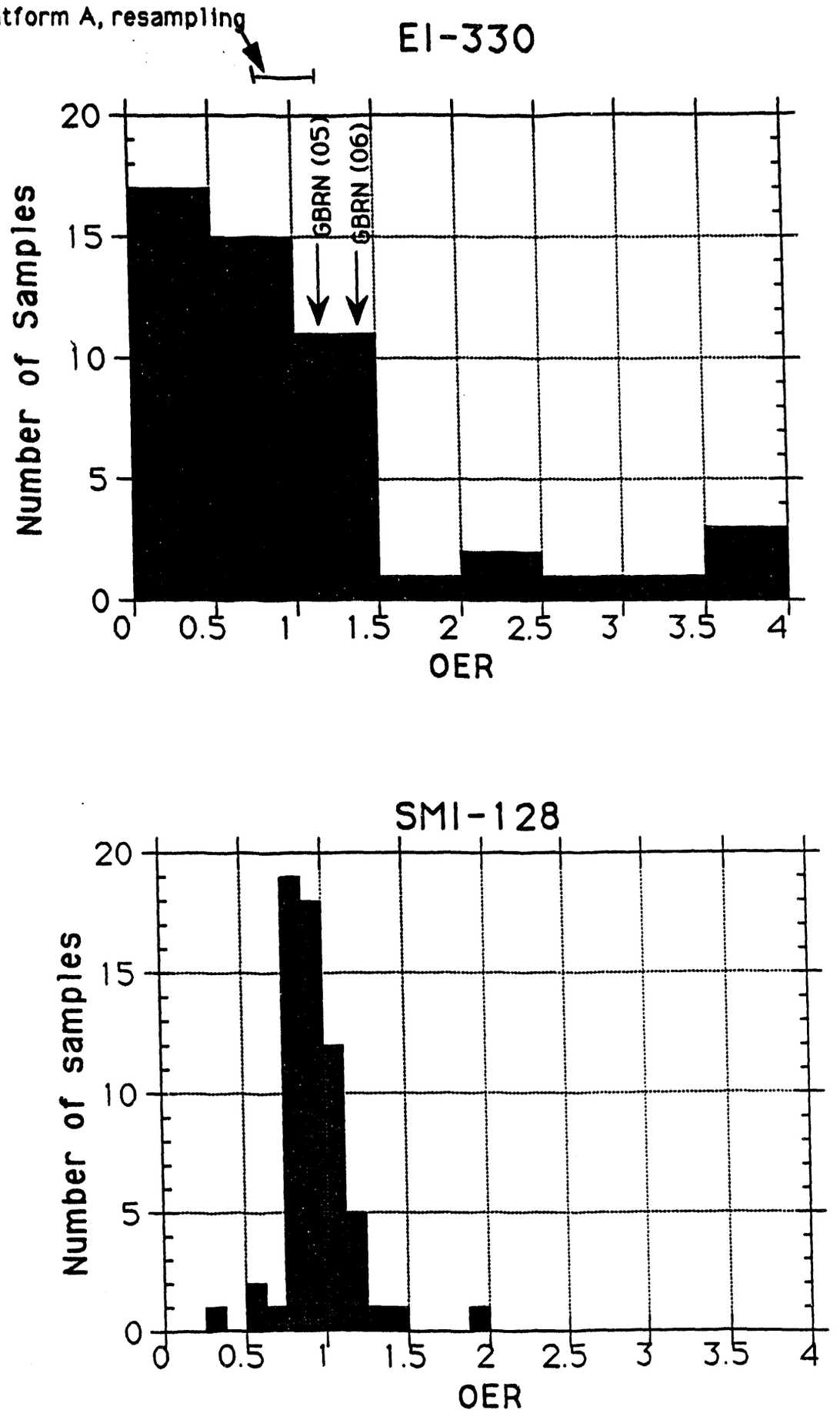

Figure 17: Eugene Island-330, oil composition, odd/even n-alkane ratios, comparison GBRN Pathfinder well data to GERG oil correlation study. Data for other oils from other wells resampled from A platform in Dec, 1993, are also shown.

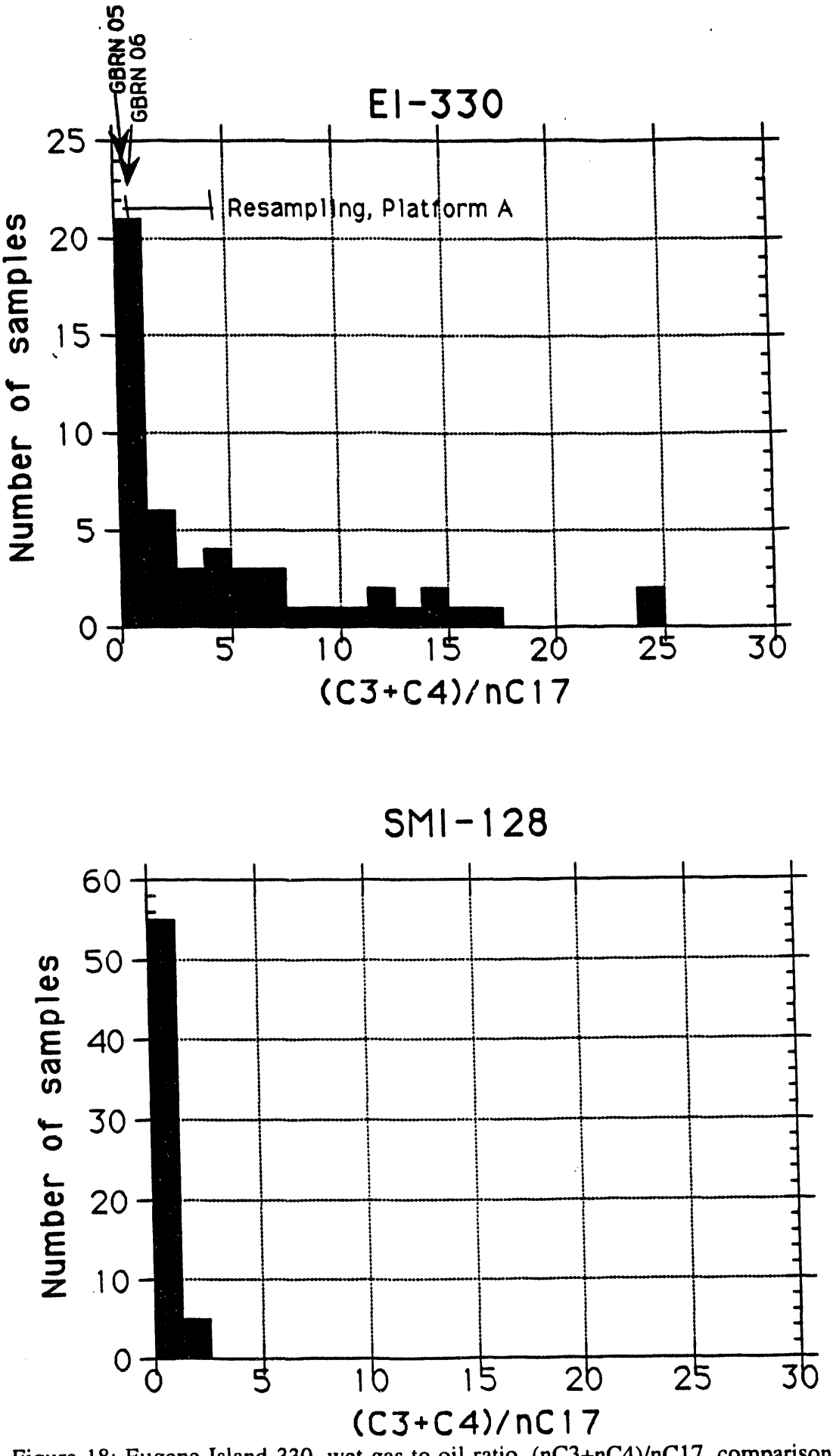

Figure 18: Eugene Island-330, wet gas to oil ratio, (nC3+nC4)/nC17, comparison GBRN Pathfinder well data to GERG oil correlation study. Data for other oils from other wells resampled from A platform in Dec, 1993, are also shown.

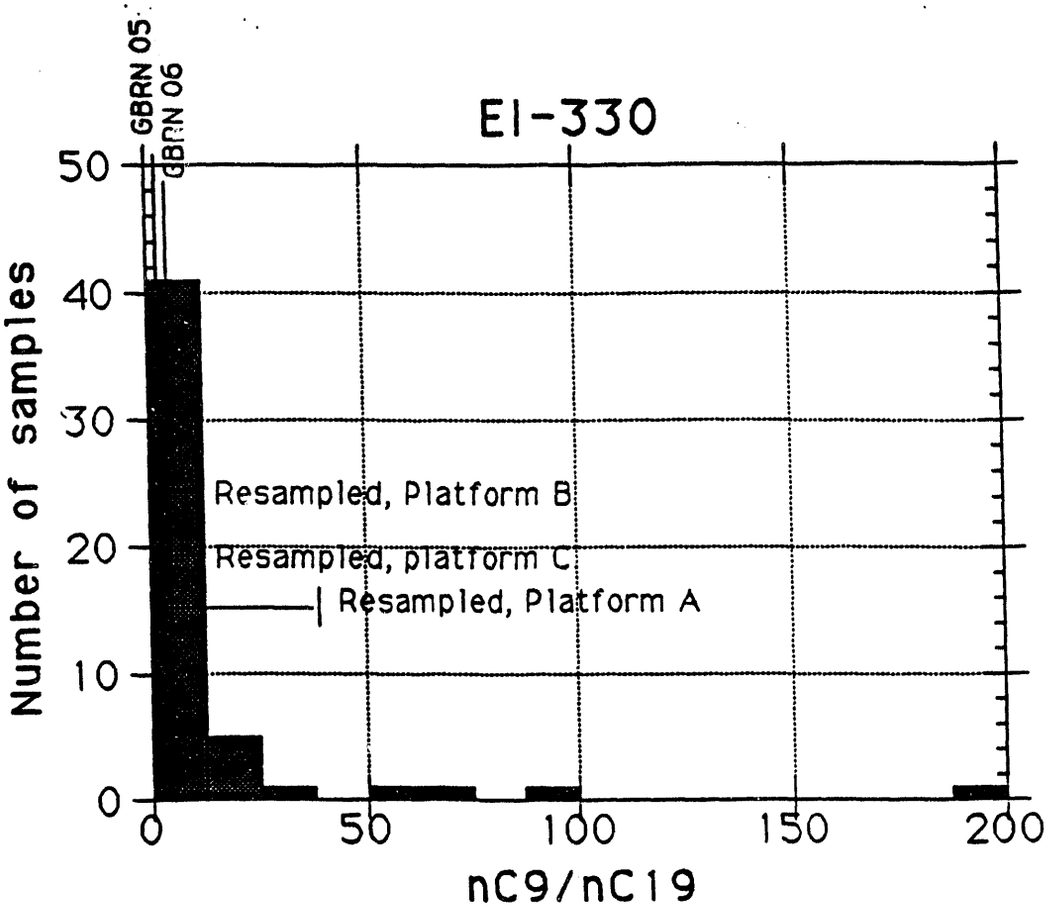

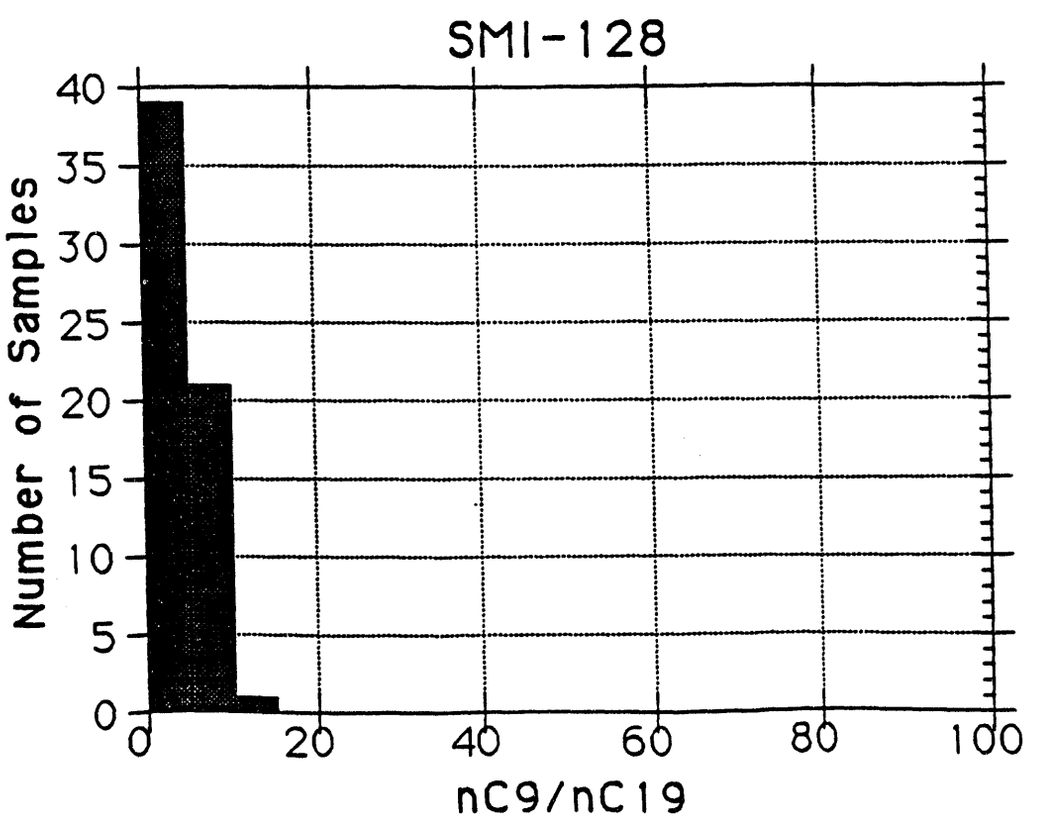

Figure 19: Eugene Island-330, nC9/nC19 (representative of gasoline/oil), comparison GBRN Pathfinder well data to GERG oil correlation study. Data for other oils from other wells resampled from A platform in Dec, 1993, are also shown.

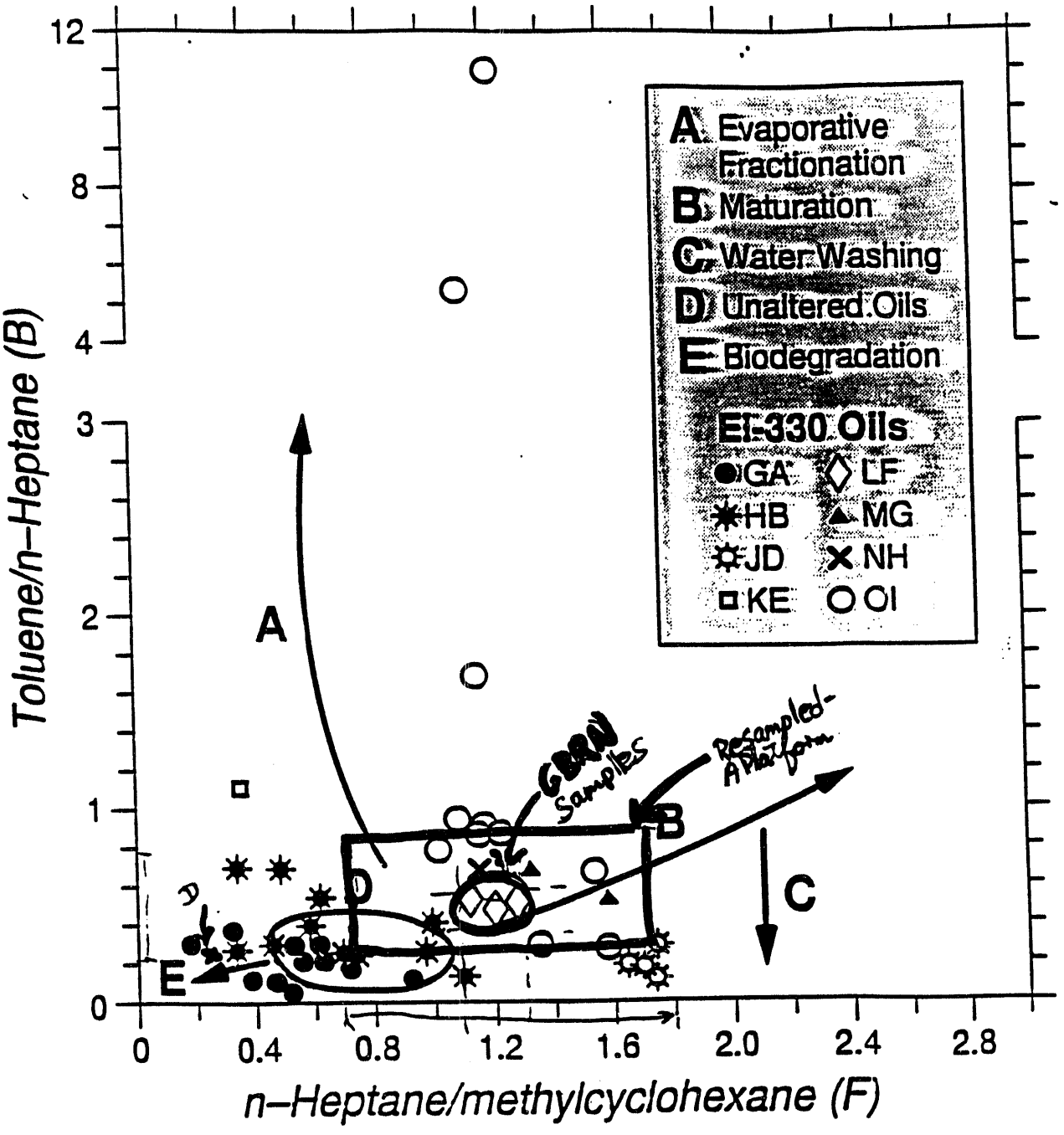

Figure 20: Eugene Island, C7 hydrocarbon ratios. Position of newly collected GBRN samples and new resamplings of A platform (December, 1993) are also superimposed.

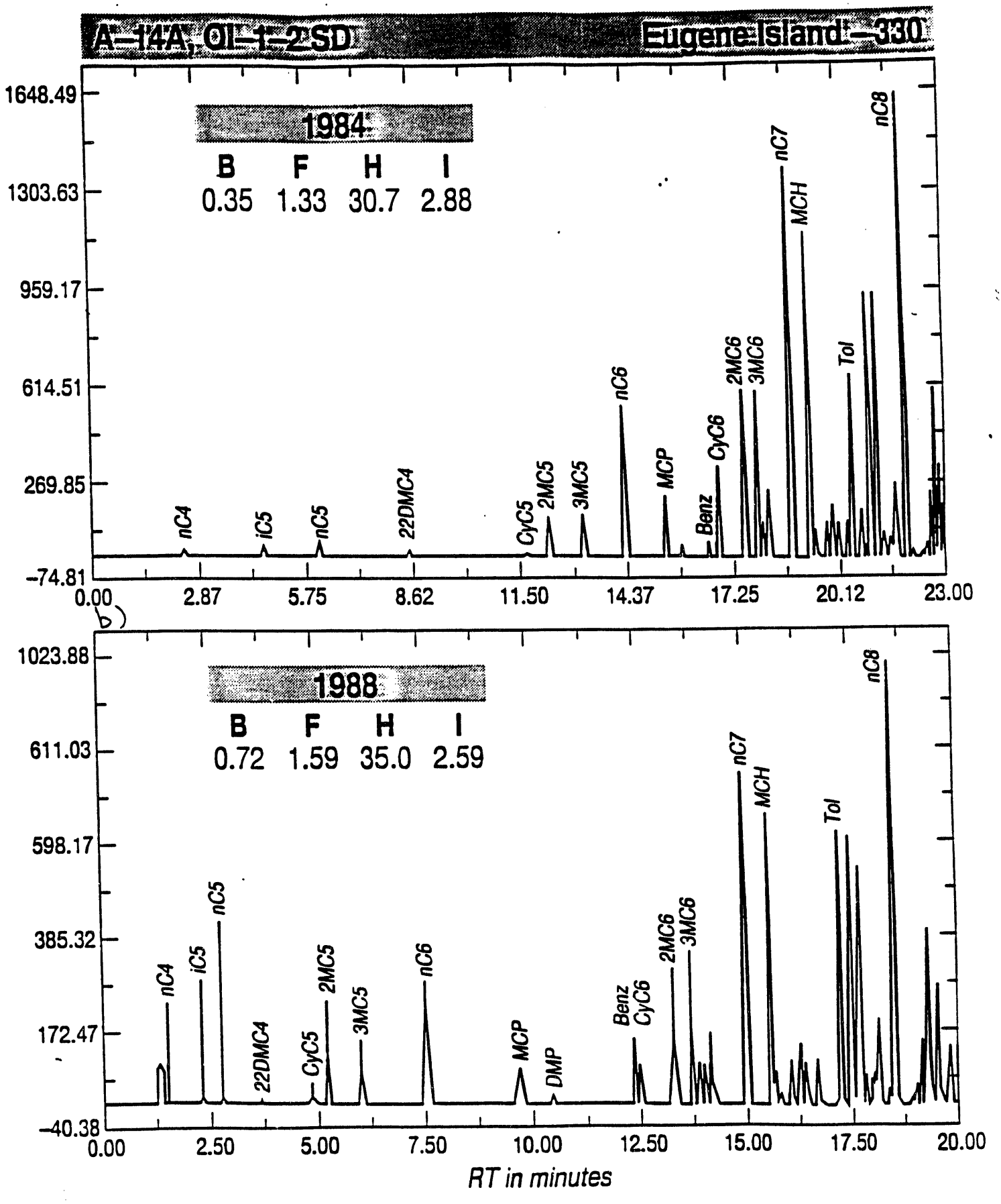

Figure 21: Comparison of gasoline range hydrocarbons, EI-330, A-14A well, oil from OI-1-2 interval, samples from: a) 1984, b)1988, and c) 1994.

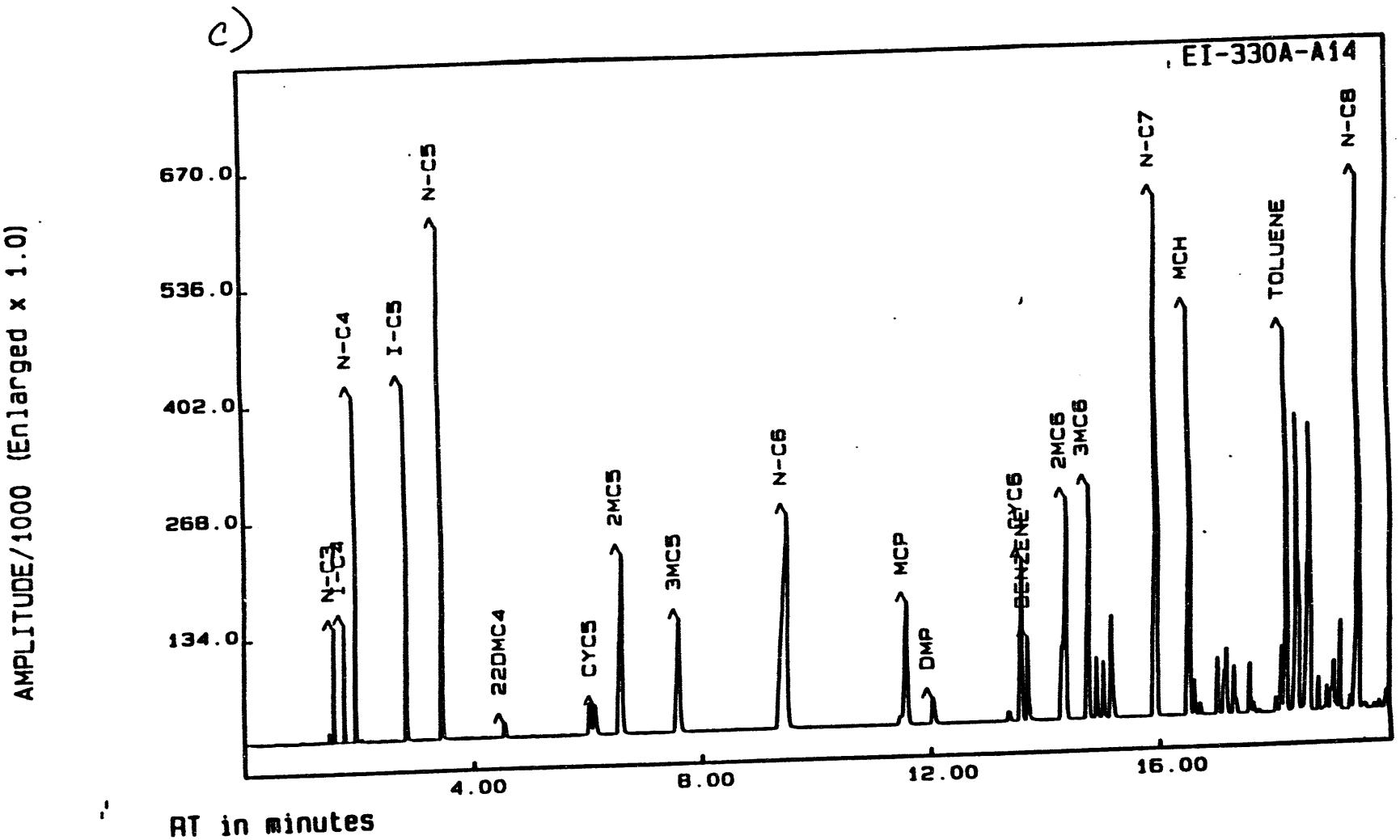

Figure 21 (Cont.)

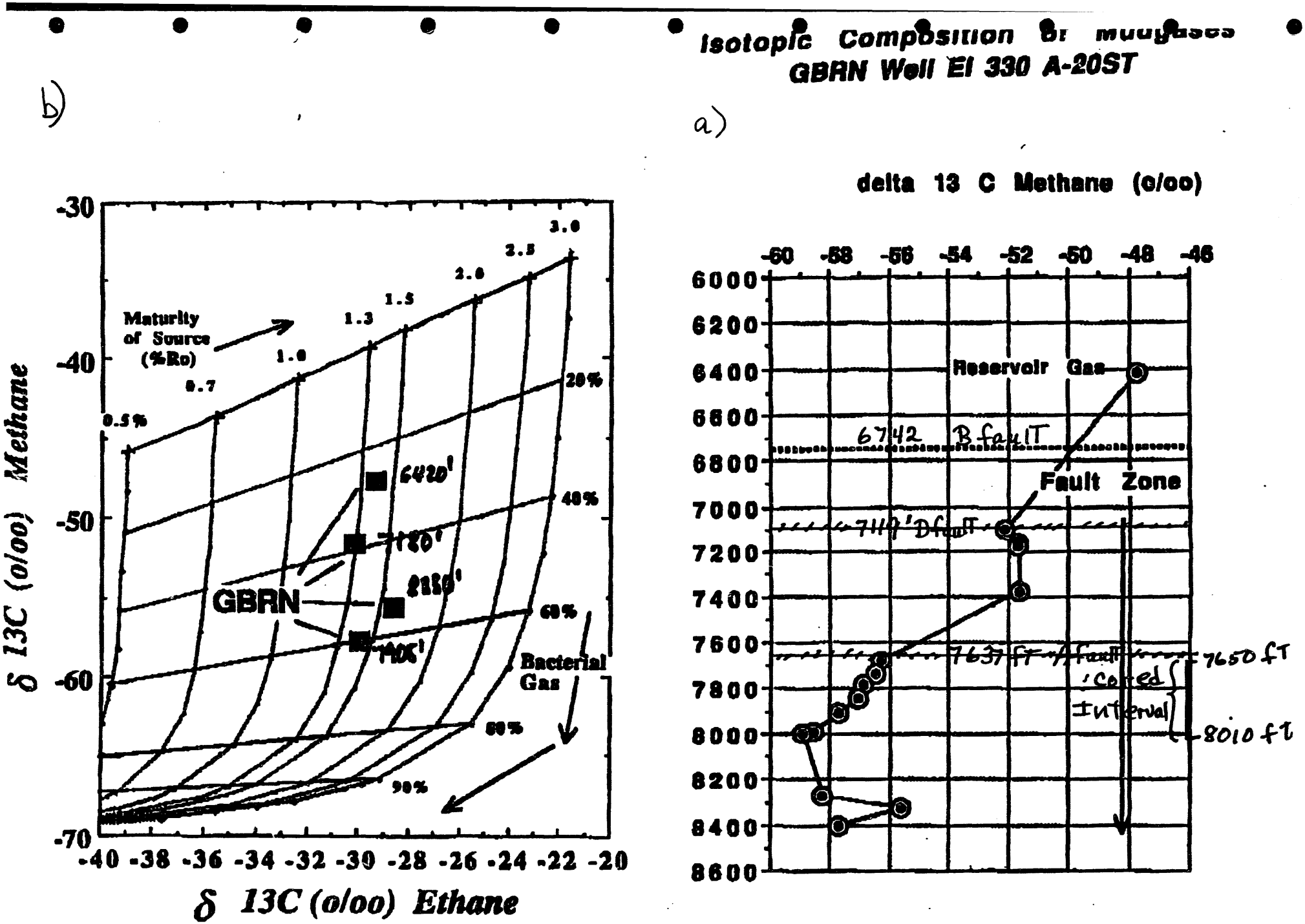

Figure 22: Pathfinder well, methane and ethane $\delta^{13}C$ values, from Dr Martin Schoell, Chevron: a) $\delta^{13}C$ methane as function of depth; b) $\delta^{13}C$ methane versus ethane showing gas maturities in Pathfinder well.

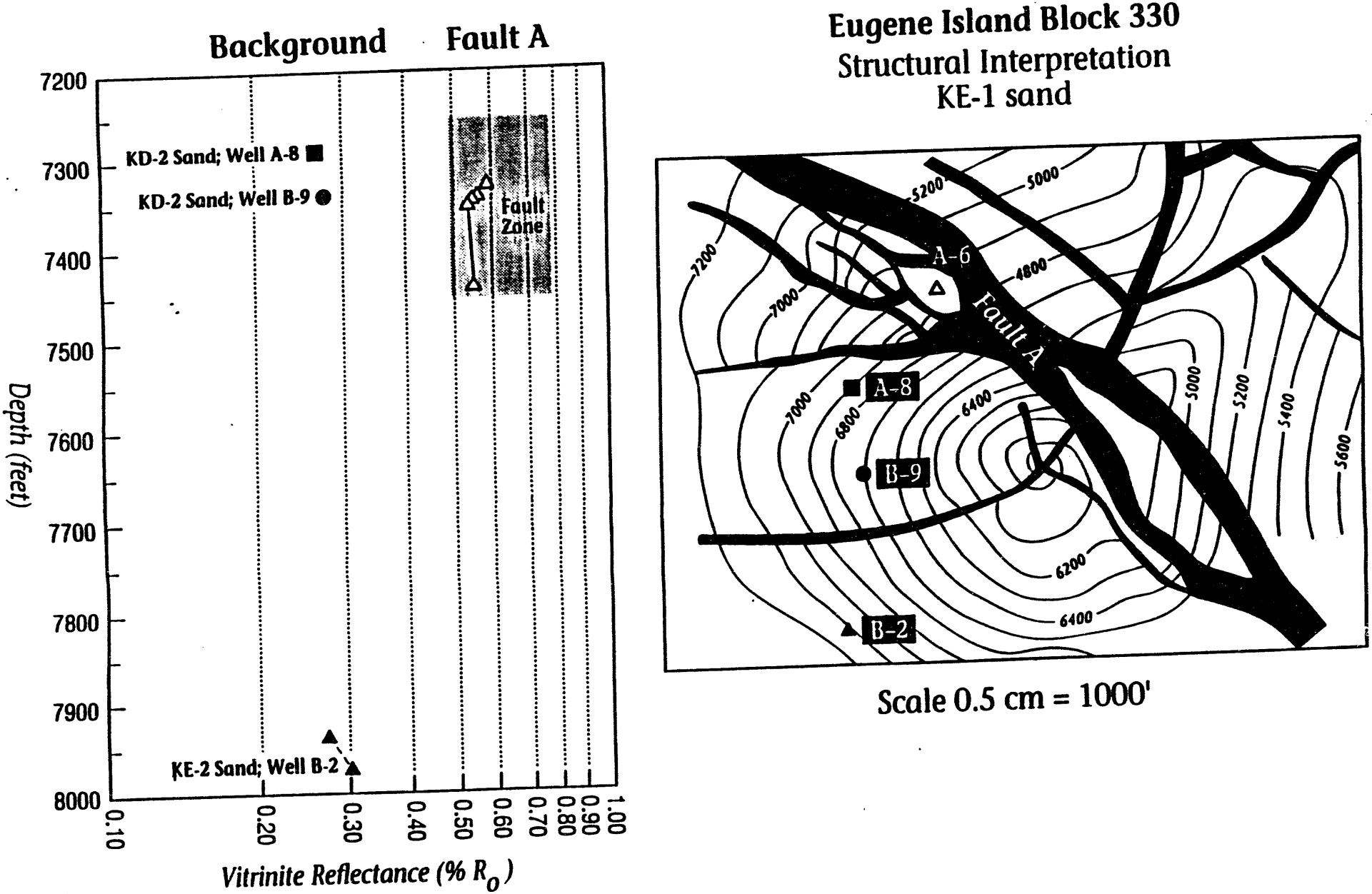

Figure 23: Vitrinite reflectance, sediments within Fault A versus sediments away from fault.

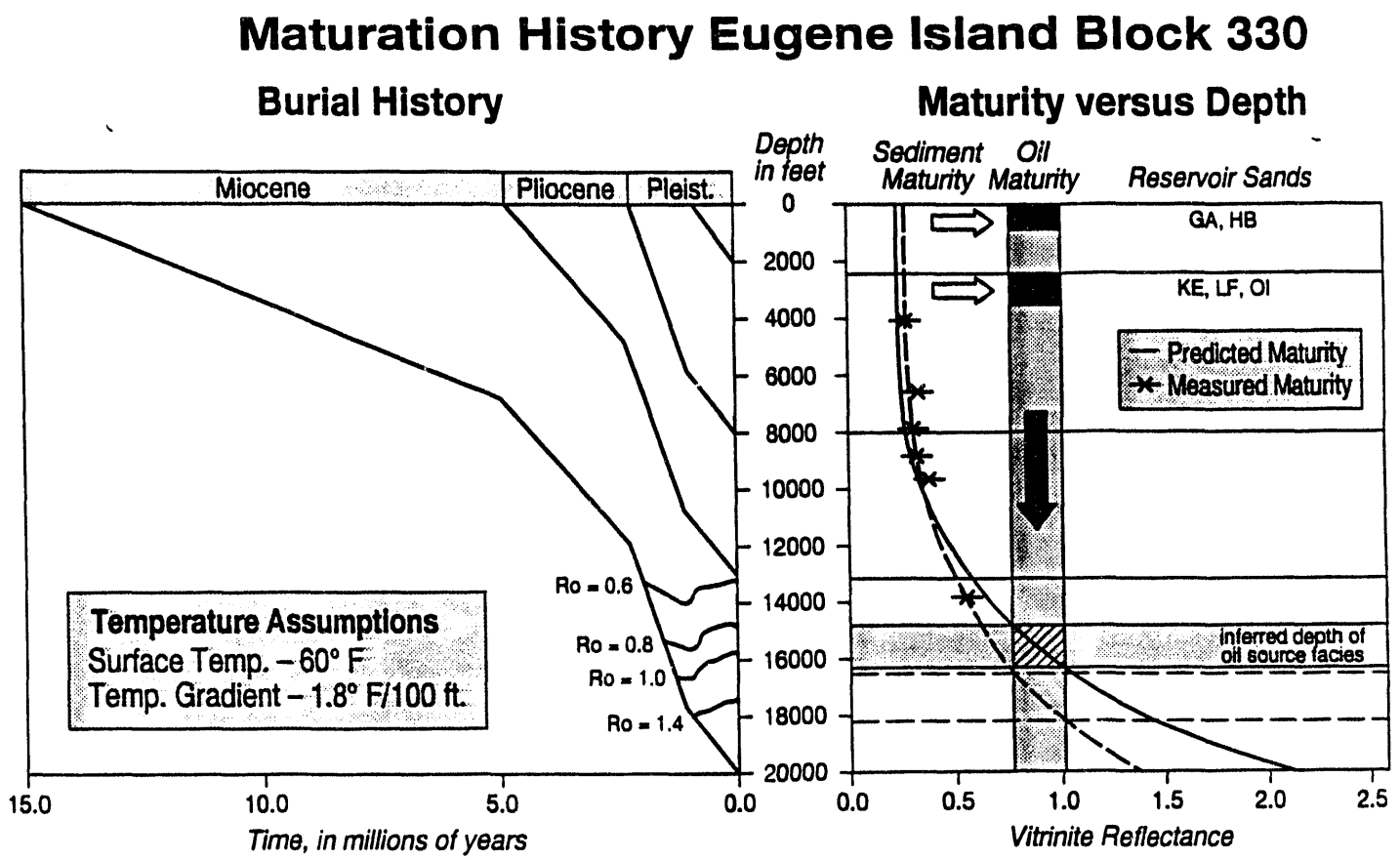

Figure 24: Revised estimate burial history of EI-330 (dashed line) with additional point at 14000 ft. Note that the deepest vitrinite reflectance value comes from South Marsh Island-128 and, therefore, is probably higher than the maturity at comparable depth for EI-330.

Table 1: Eutaw Shale Hydrous Pyrolysis Results*

Time hrs.	Temp. °C	Pressure (Bars)	CO_2 µg/gRock	CH_4 µg/gRock	C_2H_4 µg/gRock	C_2H_6 µg/gRock	C_3H_6 µg/gRock	C_3H_8 µg/gRock
0.0	25	350	0.00	0.00	0.00	0.00	0.00	0.00
22.0	224	350	515.48	0.56	0.07	0.09	0.05	0.13
146.5	224	350	464.44	0.78	0.08	0.12	0.05	0.16
286.0	224	350	470.28	0.96	0.09	0.17	0.05	0.21
287.5	275	350	-	-	-	-	-	-
335.0	275	350	582.56	2.78	0.30	0.91	0.28	0.90
381.0	275	350	572.58	3.06	0.28	0.95	0.28	0.85
383.5	325	350	-	-	-	-	-	-
455.5	324	350	778.96	28.34	0.73	18.42	2.05	13.72
501.5	324	350	-	-	-	-	-	-
596.5	324	350	818.35	38.30	0.64	27.79	2.45	23.28
1009.8	325	350	-	-	-	-	-	-
2136.0	324	350	-	-	-	-	-	-
2325.3	325	350	1012.86	107.90	0.50	72.41	2.05	58.79
2326.5	360	350	-	-	-	-	-	-
2474.0	360	350	1068.20	135.91	0.70	75.21	2.93	75.35
2713.5	360	350	1278.55	159.02	0.64	79.22	2.61	75.77
3218.0	360	350	-	-	-	-	-	-
5042.0	360	350	1888.18	227.08	0.55	101.85	2.13	83.92

*TOC (wt. %): 1.53

Table 2: Smackover Hydrous Pyrolysis Results*

Sample	hrs	T °C	Pressure (bars)	CO2 ug/g Sed	CH4 ug/gSed	C2H4 ug/gSed	C2H6 ug/gSed	C3H6 ug/gSed	C3H8 ug/gSed
SM2-25/125*-350** (Acid treated)									
	0	25	---	0	0	0	0	0	0
	20.1	17.8	370	9	0.013	0	0	0	0
	51	125	311	46	0.052	0.0069	0.008	0.004	0.034
	171	125	406	90	0.052	0.0053	0.012	0.005	0.061
SM1-175*-350** (Acid treated)									
	0	25	----	0	0	0	0	0	0
	24.3	174	378	217	0.085	0.0165	0.0147	0.017	0.038
	72.3	174	344	282	0.105	0.0209	0.02	0.021	,041
	167	174	378	317	0.113	0.019	0.019	0.022	0.042
SM3-325*350** (acid Treated)									
	0	25	-	0	0	0	0	0	0
	25.4	322.7	365	397	7.47	1.21	3.24	1.28	2.59
	69.7	323.6	411	442	13.3	1.54	6.6	1.68	4.52
	170.8	323.7	384	330	10.5	1.02	5.56	1.38	3.74

*TOC (wt %): 1

Table 3: Monterey Shale Hydrous Pyrolysis Results*

Sample	hrs	T °C	Pressure (bars)	CO2 ug/g Sed	CH4 ug/gSed	C2H4 ug/gSed	C2H6 ug/gSed	C3H6 ug/gSed	C3H8 ug/gSed
MS4-25/125*-350* (Acid treated)									
	0	25	---	0	0	0	0	0	0
	8	*17.8*	375	826	0.023	0.013	0	0	0
	71.5	125	113	3322	0.45	0.052	0.034	0.102	0.017
	194	125	180	6010	1.19	0.04	0.085	0.135	0.038
MSE3-175* 350 (acid treated)**									
	0	25	----	0	0	0	0	0	0
	24.4	174	381	8373	6.1	0.01	0.43	0.58	0.23
	72.4	174	340	11110	12.1	0.013	0.88	0.69	0.5
	168	174	373	13335	19.3	0.016	1.32	0.86	0.78
MSE3-175*350 (acid Treated)**									
	0	25	---	0	0	0	0	0	0
	26.4	174	381	8372	6.1	0.29	0.43	0.58	0.23
	74.2	174	340	11110	12.1	0.37	0.88	0.69	0.5
	170	174	373	13335	19.3	0.45	1.32	0.86	0.78
MSE1-225*-350 (Non-acid treated)**									
	0	25	---	0	0	0	0	0	0
	21.3	225	343	18302	77.1	7.38	7.38	7.64	4.42
	71.7	224	338	20180	109	11.5	11.5	7.53	6.87
	167	224	333	21589	148	16.9	16.9	6.92	10.3
MSE2-275*-350 (Non-acid treated)**									
	0	25	---	0	0	0	0	0	0
	22.5	274	344	18885	279	13.7	68.3	18.1	84.9
	70.3	274	349	24048	464	9.9	145	14.6	180
	165	274	356	25832	598	8.6	219	29.7	160
MSE5-325*350 (acid treated)**									
	0	25	---	0	0	0	0	0	0
	23.9	323	374.15	34005	1071	31.4	637.41	63.76	272
	70.6	323	390.61	34933	1420	11.1	1091.4	472.6	391
	286	224	380.95	14662	500	7.25	357.21	126.2	134

TOC (wt %): 20

Table 4: Middle Valley Hydrous Pyrolysis Results

Sample	hrs	T °C	$C0_2$ µg/gSed	CH_4 µg/gSed	C_2H_6 µg/gSed	C_3H_8 µg/gSed	i-C_4H_{10} µg/gSed	n-C_4H_{10} µg/gSed
MV6-375*-350-10#**								
0	0	20	-	0.00	-	-	-	-
1	48	375	6493.13	122.86	28.07	21.26	1.39	6.55
2	143	375	6780.15	150.78	30.87	19.50	0.35	4.95
3	338	375	7080.98	179.00	31.89	18.09	0.27	3.49
4A	697	375.4	-	-	-	-	-	-
4B	720	374.8	6282.49	190.95	30.39	15.11	0.26	2.69
MV1-325-350-10								
0	0	20	-	-	-	-	-	-
1	46	325	4383.51	66.89	17.88	8.35	3.49	1.80
2	141	325	4747.82	81.33	20.36	11.81	5.61	4.29
3	336	325	4961.84	90.00	22.43	14.20	6.50	5.97
4	722	326	5113.85	94.06	23.10	15.66	5.89	6.51
MV5-325-350-4								
0	0	20	-	-	-	-	-	-
1	45.8	325	4340.72	48.42	10.03	6.53	2.47	2.16
2	147	325	4379.19	61.54	13.13	8.48	4.92	3.45
3	336	325.8	4621.06	69.91	15.33	10.74	5.72	4.98
4A	699	325.2	-	-	-	-	-	-
4B	720	325.3	4167.55	79.09	17.24	11.98	6.24	5.48
5	1509	325.4	4505.83	83.06	18.80	12.74	6.50	5.52
MV7-325-350-80								
0	0	20	-	0.00	-	-	-	-
1	45	324	4537.22	71.98	23.47	9.29	2.04	1.34
2A,B	144	324.2	5503.96	112.38	29.06	15.54	2.80	2.67
3	336	324.2	5801.26	111.45	30.42	17.83	2.88	4.10
4	721	324.8	6760.90	120.41	31.47	18.90	2.68	4.25
MV2-275-350-10								
0	0	20						
1	50.4	275	3811.14	4.39	0.91	0.76	0.25	0.19
2	146	275	4193.83	8.49	1.96	1.51	0.55	0.37
3	341	275	4184.31	12.25	2.89	2.06	0.87	0.49
4	722	275	4231.42	15.11	3.53	2.54	1.16	0.67
MV4-275-350 5								
0	0	20						
1	45.8	274	3744.59	5.93	1.00	0.92	0.28	0.29
2	142	274	3934.33	9.76	1.91	1.61	0.54	0.53
3	333	275	4111.43	13.61	2.77	2.42	0.84	0.79
4	719	275	4037.03	16.04	3.35	3.00	1.16	1.11
MV3-225-350-10								
0	0	20						
1	47	224	3982.61	1.04	0.13	0.11	-	0.00
2	144	224	4107.15	1.50	0.20	0.18	-	0.00
3	334	225	4311.06	1.98	0.28	0.26	-	0.00
4	721	225	4196.74	2.47	0.36	0.34	-	0.08

* Temp (°C) ** Pressure(Bars) # Water:Rock Ratio

Table 5: **Eugene Island oils for which HRGCMS data are complete**

Platform	Well	Reservoir	Depth of flowing zone (m) (Top)	(Bottom)
330A	C1	GA-2	1131	
	G-18	KE-1	2017	
	B-3	OI-1	2134	
	A-7	JD	1981	
	A-2	HB-1	1463	
	B-14	LF	2164	
	A-10 ST	?	?	
	A-12	LF	7346	7376
	A-14 ST	OI	8576	8650
	A-23 ST	QI4	7450	7514
	A-21 ST	NH	8676	8722
	A-3	QI1	8309	8309
	A-8 ST	KE	?	
	A-6 ST	KE	7104	7150
	A-5D	JD	6661	6732
	A-18	?	?	
	A-19 ST	JD1	7258	7278
	A-2 ST	OI5	7677	7671
	A-11 ST	JD	6978	6990
	A-7 ST	HB1	6594	6606
Pathfinder well (A-20):				
	06 GBRN-1			
	06 GBRN-2			
	06 GBRN-3			
	06 GBRN-7			
	06 GBRN-8			
	06 GBRN-11			
	A-20 Drill Stem			

Table 6: Comparison of biomarker maturity parameters GBRN pathfinder oils in comparison to EI-330 standard reservoir oils (measurements via HRGCMS).*

Parameter:	Reservoir: Standard reservoir oils: GA	HB	JD	KE	LF	MG	OI	GBRN Pathfinder oils: GBRN 1	GBRN 2	GBRN 3	GBRN 7	GBRN 8	GBRN 11	Drill stem GBRN A-20
methyl phenanthrenes:														
MPI1	0.74	0.70	0.33	0.65	0.64	0.63	0.66	0.65	0.65	0.65	0.64	0.64	0.65	0.66
MPI2	0.72	0.69	0.33	0.64	0.61	0.62	0.62	0.63	0.63	0.63	0.62	0.63	0.63	0.64
Rc	0.84	0.82	0.60	0.79	0.79	0.78	0.79	0.79	0.79	0.79	0.78	0.79	0.79	0.80
Hopanes: 22S/(22S+22R)	0.58	0.59	0.59	0.58	0.59	0.59	0.59	0.58	0.59	0.59	0.60	0.60	0.59	0.60
Steranes: 20S/(20S+20R)	0.41	0.43	0.41	0.43	0.49	0.44	0.44	0.44	0.45	0.43	0.42	0.47	0.45	0.44

*notes: Abbreviations are:
MPI1 = methylphenanthrene index 1=1.5*(2MP+3MP)/(P+1MP+9MP) (Radke,)
MPI2 = 3*(2MP)/(P+1MP+9MP)
Rc=0.6MPI+0.4 for Ro<1.35%
P = phenanthrene
22S = 29aaaS (or 29(S)-24-ethyl-5a(H), 14a(H), 17a(H)-cholestane)
22R= 29aaaR (or 29(R)- 24-ethyl-5a(H), 14a(H), 17a(H)-cholestane)
20S = 31abS 17a(H), 21b(H), 22(S)-homohopane
20R = 31abR 17a(H), 21b(H), 22(R)-homohopane

Table 7: Eugene Island oils on which analysis n-alkanes and gases complete on resampled well (Data from GERG,Texas A & M)

Platform	Well	Sample (Date collected)	Depth (m)	Sample type	Aromaticity B	Paraffinicity F
330A	A1B			Fluid	0.24	1.83
	A2ST			Fluid	0.64	1.2
	A3			Fluid	0.64	1.51
	A5			Fluid	0.38	1.78
	A6ST			Fluid	0.27	1.59
	A7ST			Fluid	nd	0.68
	A8ST			Fluid	0.66	1.24
	A10ST			Fluid	0.7	1.25
	A11D			Fluid	0.37	1.53
	A14			Fluid	0.6	1.48
	A19ST			Fluid	0.31	1.74
	A21			Fluid	0.41	1.59
	A23-1			Fluid	0.58	1.26
	A23-2			Fluid	0.58	1.26
	A20	04 GBRN		Oil-water	0.36	1.09
	A20	05 GBRN-1		Oil-Emulsion	0.36	1.08
	A20	05 GBRN-2			0.33	1.1
	A20	05 GBRN-3		Oil-Emulsion	0.37	1.16
	A20	05 GBRN-4		Oil-Emulsion	0.35	1.12
	A20	05 GBRN-5		Oil-Emulsion	0.36	1.17
	A20	05 GBRN-6		Oil-Emulsion	0.35	1.13
	A20	05 GBRN-7		Oil-Emulsion	0.35	1.16
			05 GBRN Average		0.35	1.13
			05 GBRN Std Dev		0.01	0.03
	A20	06 GBRN-1		Oil-water	0.55	1.37
	A20	06 GBRN-2		Oil-water	0.47	1.29
	A20	06 GBRN-3		Oil-water	0.52	1.36
	A20	06 GBRN-4		Oil-water	0.54	1.33

	A20	06 GBRN-5		Oil-water	0.51	1.33
	Well	Sample (Date collected)	Depth (m)	Sample type	Baseline Range Ratios Aromaticity B	Paraffinicity F
	A20	06 GBRN-6		Oil-water	0.49	1.29
	A20	06 GBRN-7		Oil-water	0.49	1.27
	A20	06 GBRN-8		Oil-water	0.37	1.15
	A20	06 GBRN-9		Oil-water	0.56	1.34
	A20	06 GBRN-10		Oil-water	0.44	1.23
	A20	06 GBRN-11		Oil-water	0.56	1.35
	A20 ST	Bottom Flow		Oil		
			06 GBRN Average		0.50	1.30
			06 GBRN Stnd Dev		0.06	0.07
330B	B3AST			Fluid	0.27	0.43
	B5ST			Fluid	0.53	1.41
	B6ST			Fluid	0.52	1.45
	B7AST			Fluid	0.55	1.56
	B10ST			Fluid	0.69	1.23
	B11			Fluid	0.77	1.22
	B11D			Fluid	0.7	1.28
	B12D			Fluid	0.78	1.18
330C	C1D	12/16/93		Fluid	0.15	0.53
	C2D	12/16/93		Fluid	0.46	0.86
	C3D	12/16/93		Fluid	0.4	0.7
	C4E	12/16/93		Fluid	0.54	1.06
	C5-1	12/16/93		Fluid	0.15	0.54
	C5-2	12/21/93		Fluid	0.19	0.56
	C7ST-1	12/16/93		Fluid	0.21	0.27
	C7ST-2	12/21/93		Fluid	0.52	0.27

	C9D-1	12/16/93		Fluid	26.61	1.35
Platform	Well	Sample (Date collected)	Depth (m)	Sample type	Aromaticity	Paraffinicity
	C9D-2	12/21/93		Fluid	22.76	1.32
	C10ST-1	12/16/93		Fluid	0.27	0.76
	C10ST-2	12/21/93		Fluid	0.32	0.78
	C11-1	12/16/93		Fluid	0.45	1.11
	C11-2	12/21/93		Fluid	0.44	1.11
	C13D-1	12/16/93		Fluid	0.08	0.9
	C13D-2	12/21/93		Fluid	0.13	0.9
	C14-1	12/16/93		Fluid	0.77	1.18
	C14-2	12/21/93		Fluid	0.78	1.18
	C15-1	12/16/93		Fluid	0.34	1.78
	C15-2	12/21/93		Fluid	0.28	1.74
	C17-1	12/16/93		Fluid	0.45	1.71
	C17-2	12/21/93		Fluid	0.42	1.71
	C18-1	12/16/93		Fluid	0.64	1.26
	C18-2	12/21/93		Fluid	0.64	1.25
	C19-1	12/16/93		Fluid	0.77	1.19
	C19-2	12/21/93		Fluid	0.78	1.18
	C20-1	12/16/93		Fluid	0.1	0.83
	C20-2	12/21/93		Fluid	0.1	0.82

Baseline Range Ratios

Platform	Well	Sample (Date collected)	Depth (m)	Sample type	Baseline Range Ratios Aromaticity	Paraffinicity
	C21-1	12/16/93		Fluid	0.8	1.17
	C21-2	12/21/93		Fluid	0.81	1.17
	C4E	12/21/93		Fluid	0.49	1.12
330D	D2			Fluid	0.22	0.17
316	A4			Fluid	0.43	0.73
	A8			Fluid	0.62	0.55
	A9			Fluid	0.2	0.82
	A10			Fluid	0.85	0.77

Table 7: Eugene Island oils on which analysis n-alkanes and gases complete on resampled well (Data from GERG,Texas A & M)

Platform	Well	High Molecular Weight Ratios					Whole oil chromatograms:			
		OER	CPI >nC23	Pr/Ph	nC9/nC19	nC15/nC25	(C3+C4)/nC17	nC3	nC4	nC17
330A	A1B	nd	nd	nd	nd	nd	nd	0	0	0
	A2ST		1.25	1.21	3.04	5.2	1.36	1	2.8	2.8
	A3		1.32	1.26	5.47	4.19	3.17	1.3	4.4	1.8
	A5	nd	nd	nd	nd	nd	nd	0.4	1.3	0
	A6ST	nd	nd	nd	nd	nd	nd	0.5	1.6	0
	A7ST	nd	nd	nd	nd	nd	nd	9.8	18.3	0
	A8ST	1.17	1.42	1.35	6.02	4.87	3.41	1.8	4	1.7
	A10ST	1.11	1.16	1.09	4.58	4.45	1.94	0.6	2.7	1.7
	A11D	nd	2.23	1.04	33.54	7.02	2.00	0.2	1	0.6
	A14	1.07	1.31	1.4	6.71	5.28	1.55	0.6	2.5	2
	A19ST	nd	nd	nd	nd	nd	nd	0.3	1	0
	A21	1.11	1.2	1.23	2.7	3.98	2.74	1.8	5.6	2.7
	A23-1	1.05	1.23	1.21	4.66	4.47	1.46	1.1	2.4	2.4
	A23-2	0.85	1.16	1.16	3.87	4.05	1.12	0.7	2.1	2.5
04 GBRN	A20	1.08	1.31	1.16	1.92	3.21	0.00	0	0	3.6
05 GBRN-1	A20	1.13	1.16	1.19	1.5	3.82	0.00	0	0	3.8
05 GBRN-2	A20	1.11	1.18	1.22	1.5	4.35	0.03	0	0.1	3.9
05 GBRN-3	A20	1.23	1.21	1.1	1.47	4.05	0.03	0	0.1	3.8
05 GBRN-4	A20	1.01	1.14	1.25	1.36	4.21	0.00	0	0	3.9
05 GBRN-5	A20	1.08	1.29	1.25	1.47	3.86	0.03	0	0.1	3.8
05 GBRN-6	A20	1.1	1.17	1.14	1.41	3.58	0.00	0	0	3.8
05 GBRN-7	A20	1.08	1.21	1.13	1.53	3.63	0.03	0	0.1	3.6
		1.10	1.21	1.18	1.52	3.84	0.01			
		0.06	0.06	0.06	0.17	0.37	0.01			
06 GBRN-1	A20	1.12	1.33	1.19	5.36	4.6	1.28	0.4	1.9	1.8
06 GBRN-2	A20	1.21	1.3	1.3	5.18	5.23	0.30	0.1	0.6	2.3
06 GBRN-3	A20	1.18	1.35	1.21	5.79	4.57	1.00	0.3	1.7	2
06 GBRN-4	A20	1.18	1.38	1.28	5.46	4.95	0.70	0.2	1.2	2

06 GBRN-5	A20	1.29	1.32	1.19	4.9	5.14	0.71	0.3	1.2	2.1
Platform	Well	High Molecular Weight Ratios					Whole oil chromatograms:			
		OER	CPI >nC23	Pr/Ph	nC9/nC19	nC15/nC25	(C3+C4)/nC17	nC3	nC4	nC17
06 GBRN-6	A20	1.2	1.31	1.22	5.43	5.09	0.48	0.2	0.8	2.1
06 GBRN-7	A20	1.39	1.24	1.1	5.44	5.3	0.45	0.1	0.8	2
06 GBRN-8	A20	2.48	1.55	1.18	3.59	4.68	0.11	0	0.3	2.7
06 GBRN-9	A20	1.15	1.29	1.28	5.79	4.9	0.84	0.2	1.4	1.9
06 GBRN-10	A20	1.77	1.51	1.07	4.48	4.79	0.26	0.1	0.5	2.3
06 GBRN-11	A20	1.21	1.37	1.05	5.72	4.42	1.29	0.4	1.8	1.7
Bottom Flow	A20 ST									
		1.38	1.36	1.19	5.19	4.88	0.68			
		0.41	0.09	0.08	0.66	0.29	0.40			
330B	B3AST	nd	nd	nd	nd	nd				
	B5ST	1.25	1.53	1.13	5.99	5.74				
	B6ST	1.25	1.19	1.29	5.08	5.6				
	B7AST	1.31	1.33	1.19	7.42	6.49				
	B10ST	1.05	1.2	1.32	2.53	3.01				
	B11	0.94	1.23	1.35	2.17	2.89				
	B11D	1.03	1.18	1.35	2.88	3.51				
	B12D	1.07	1.25	1.27	2.49	3.33				
12/16/93	C1D	nd	nd	nd	nd	nd				
12/16/93	C2D	nd	nd	nd	nd	nd				
12/16/93	C3D	nd	nd	nd	nd	nd				
12/16/93	C4E	nd	nd	1.48	13.58	nd				
12/16/93	C5-1	nd	nd	nd	nd	nd				
12/21/93	C5-2	nd	nd	nd	nd	nd				
12/16/93	C7ST-1	nd	nd	nd	nd	nd				
12/21/93	C7ST-2	nd	nd	nd	nd	nd				

Platform	Well	High Molecular Weight Ratios OER	CPI >nC23	Pr/Ph	nC9/nC19	nC15/nC25	Whole oil chromatograms: (C3+C4)/nC17	nC3	nC4	nC17
12/16/93	C9D-1	1.07	1.12	1.41	1.98	3.01				
12/21/93	C9D-2	0.78	1.04	1.49	1.79	2.48				
12/16/93	C10ST-1	nd	nd	nd	nd	nd				
12/21/93	C10ST-2	nd	nd	nd	nd	nd				
12/16/93	C11-1	1.3	1.25	1.35	6.11	4.77				
12/21/93	C11-2	1.32	1.12	1.4	6.75	4.74				
12/16/93	C13D-1	nd	nd	nd	nd	nd				
12/21/93	C13D-2	nd	nd	nd	nd	nd				
12/16/93	C14-1	1.11	1.23	1.41	2.37	3.24				
12/21/93	C14-2	1.05	1.24	1.38	2.65	3.96				
12/16/93	C15-1	nd	nd	nd	nd	nd				
12/21/93	C15-2	nd	nd	nd	nd	nd				
12/16/93	C17-1	nd	nd	nd	nd	nd				
12/21/93	C17-2	nd	nd	nd	nd	nd				
12/16/93	C18-1	1.07	1.17	1.46	2.74	3.14				
12/21/93	C18-2	1.08	1.25	1.41	3.36	3.49				
12/16/93	C19-1	1	1.17	1.25	2.26	3.42				
12/21/93	C19-2	1.12	1.26	1.54	2.62	3.41				
12/16/93	C20-1	nd	nd	nd	nd	nd				
12/21/93	C20-2	nd	nd	nd	nd	nd				

12/16/93	C21-1	1.07	1.25	1.3	2.3	3.2					
Platform	Well	High Molecular Weight Ratios					Whole oil chromatograms:				
		OER	CPI >nC23	Pr/Ph	nC9/nC19	nC15/nC25	(C3+C4)/nC17	nC3	nC4	nC17	
	C21-2	1.07	1.15	1.38	2.25	3.98					
	C4E	nd	0.98	1.11	9.48	5.22					
330D	D2	nd	nd	nd	nd	nd					
316	A4	nd	nd	1.27	nd	nd					
	A8	nd	nd	1.38	nd	nd					
	A9	nd	nd	nd	nd	nd					
	A10	nd	1.3	1.38	8.74	nd					

Table 8: Selected gasoline and oil ratios, EI resampling, Texas A & M

Platform, Sample	No. Samples	Gasoline ratios B	Gasoline ratios F	Selected oil ratios OER	Selected oil ratios CPI>nC23	Selected oil ratios Pr/Ph	Selected oil ratios nC9/nC19	Selected oil ratios nC15/nC25
330A	33	0.24 to 0.7	0.68 to 1.8 (most 1.2-1.5)	1.17-0.85 (most ≈1)	1.16-2.23 (most 1.2-1.3)	1.16-1.35 (most 1.2)	3-33 (most 4-6)	4-7 (most 4-5)
05 GBRN	8	0.35±0.01	1.13±0.03	1.10±0.06	1.21±0.06	1.18±0.06	1.52±0.17	3.85±0.37
06 GBRN	11	0.50±0.06	1.30±0.07	1.38±0.41	1.36±0.09	1.19±0.08	5.19±0.66	4.88±0.29
330B	8	0.27-0.78 (most>0.5)	0.43-1.56 (most 1.2-1.4)	0.94-1.3 (1-1.2)	1.18-1.53 (1.2-1.3)	1.13-1.35 (1.3)	2.2-7 (2.5)	3-6.5 (3.5)
330C	31	0.1-27 (0.2-0.5)	0.27-1.78	0.8-1.3 (1)	0.98-1.24 (1.2)	1.3-1.5	2.3-9.5 (2.5)	2.5-5 (3-3.5)
330D	1	0.22	0.17	nd	nd	nd	nd	nd
316	4	0.2-0.8	0.55-0.77	nd	nd	nd	nd	nd

Table 9: Reproducibility C7 hyrocarbon ratios

Date collection	12/19/93	12/21/93	12/19/93	12/21/93				
Sample	B	B	F	F				
EI-330A-A23	0.58	0.58	1.26	1.26				
	12/16/93	12/21/93	12/16/93	12/21/93	12/16/93	12/21/93	12/16/93	12/21/93
Date Collection								
Sample	B	B	F	F	H	H	I	I
EI-330C-C5	0.15	0.19	0.54	0.56	16.63	16.31	1.76	1.77
EI-330C-C7ST	0.21	0.52	0.27	0.27	9.42	9.32	1.43	1.46
EI-330-C11	0.45	0.44	1.11	1.11	25.78	25.98	1.8	2.05
EI-330-C13D	0.08	0.13	0.9	0.9	23.01	22.85	2.28	2.31
EI-330-C14	0.77	0.78	1.18	1.18	28.9	28.79	2.19	2.12
EI-330-C15	0.34	0.12	1.78	1.74	37.71	38.07	2.63	2.67
EI-330-C17	0.45	0.42	1.71	1.17	33.83	34.21	2.48	2.66
EI-330-C18	0.64	0.64	1.26	1.25	29.49	29.36	2.2	2.2
EI330-C19	0.77	0.78	1.19	1.18	28.8	28.85	2.22	2.15
EI-330-C20	0.1	0.1	0.83	0.82	21.37	21.1	2.06	2.19
EI-33-C21	0.8	0.81	1.17	1.17	28.96	29.13	2.2	2.17

Table 10: Number and types of samples available for DoE Eugene Island organic geochemical work at Woods Hole and elsewhere.

Sample type	Number Samples	To be used for analysis numbers:* (organization other than WHOI or GERG carrying out analyses)	No. samples (type analyses completed) date	Projected Start date	Projected completion date
Pathfinder well:					
Frozen cores for pyrolysis	34	9	0	Jul-94	Jun-95
Frozen cores (biomarkers & gas)	1	1, 4, 6, & 8	0	Jul-94	6/1/95
Frozen cores (biomarkers and vitrinite)	3	1,4,6-8	0	Jul-94	Jun-95
Frozen cores (sorbed gas and vitrinite)	10	7 & 8	0	Jul-94	Jun-95
Frozen cores (sorbed gas)	14	8	0	Jul-94	Jun-95
Frozen cores (vitrinite)	12	7 & 9	0	Apr-94	Jun-94
gas samples (Chevron bags)	15	2 and 3 (Chevron, Martin Schoell)	15		completed
oils -					
oil emulsions	5	1,2,4,5,6	5 (1,2) ;3 (6)	Feb-94	Dec-94
oil-water mixtures	6	1,2,4,5,6	6 (1,2); 3 (6)	Feb-94	Dec-94
oils	1	1-6	1 (1, 2, and 6)	Feb-94	Dec-94
Red fault and shallower sediments:					
well cuttings	>50	7 (USGS, Denver)	0	?	Oct-95
sidewall cores	33	7 (Woods Hole)	0	Apr-94	Jun-94
thin sections	40	7	0	Jul-94	Dec-94

Table 10: (cont): Number and types of samples available for DoE Eugene Island organic geochemical work at Woods Hole and elsewhere.

Sample type	Number Samples	To be used for analysis numbers:* (organization other than WHOI or GERG carrying out analyses)	No. samples (type analyses completed) date	Projected Start date	Projected completion date
Nearby Eugene Island samples:					
oils (resampled , phase IV oils and gase	50	1-6	50 (1,2)	Mar-94	Jun-95
oils, replicates sampled 5 days apart	11	1-6	11 (1,6)	Mar-94	Jun-95
Nearby oils contributed by oil companies:	20	1,2,4,5,6	20 (6)	Mar-94	Jun-95

* Analyses to be carried out:
1) whole oil gas chromatograms (GERG)
2) gas and gasoline range compositions (GERG)
3) gas compound specific 13C isotopes (GERG)
4) % alkanes:aromatics: asphaltenes (GERG, via HPLC; Woods Hole via Iatroscan)
5) 13C alkanes vs aromatics vs asphaltenes (GERG)
6) Biomarker analyses (HRGCMS, Woods Hole)
7) Vitrinite reflectance and organic petrography (Woods Hole)
8) Sorbed gas analysis (Woods Hole)
9) Pyrolysis & TOC analyses either at Woods Hole or at Conaco. Based on results, selected samples will be subjected to analyses 1-8 above.

Table 11: **Eugene Island, carboxylic acids, reservoir brines**

Concentrations (ppm):

Platform	Well	Cl*	Acetate	Propionate	Formate	Valerate	succinate	oxylate
330C	C2	56000	3.3	0.8	0.77	0	0	1.4
	C6D	103000	2.5	0.3	0.09	0	0	0.4
	C13D	103100	5	0	0.2	0	0	0.4
	C3D	60900	2.1	1	0.09	0	0	0.5
	C20	96600	16.4	0.4	1.5	0	0	0.6
	C7ST	91200	9.5	1	5.99	0	0	0.4
330A	A11ST	63400	129	22.6	2.1	0	17.3	4.2
	A23	64000	289	72.5	5.36	0	6.3	6.5
	A14A	90000	232	75.2	4.86	0	8.8	6.4
	A2	33100	887	127	5.36	0	51.6	7.7
	A6ST	80800	72.6	12.6	1	0	5.7	2.6
316A	A8S	94100	326	58	3.6	0	26.8	8.4
	A10	85400	158	24.5	1.6	0	33.4	8.2
	A9	98100	2.5	0.2	0.2	0	0	2
	A4	90800	38.6	24.3	1	0	0	6.2
330B	B1	97100	21.2	1	13.9	0	0	0.5
	B2ST	55800	11.6	0.3	8.01	0	0	0.6
	B16D	92500	4.9	0.1	2.2	0	0	0.5
	B17D	54600	3.8	0	2	0	0	0.3
	B18D	98600	7.38	0.4	3.2	0	0	0.7
	B9	73700	375	57.9	7.25	0	0	3

* Determined by Lynn Walters at Michigan Tech

DATE
FILMED
7/21/94

END